

THERMODYNAMICS OF ALKANE SOLUTIONS

A thesis presented for the degree of
Doctor of Philosophy
in
Chemical and Process Engineering
in
the University of Canterbury

by
Shen Weiguo
1988

TP
156
M5
W419
1988

ACKNOWLEDGEMENTS

I wish to thank my supervisor, professor A. G. Williamson for his guidance and valuable advice, and for many stimulating discussions during the past three years. I would also like to thank professor R. Battino (Wright State University, U.S.A) and Dr. P. J. McElory for helpful discussions and suggestions.

My thanks are also due to all the technical staff in the Department of Chemical and Process Engineering, especially to Mr. N. W. Foot, Mr. W. M. Earl, and Mr. T. R. Berry, for their kindly and skillful assistance.

I am also indebted to Lanzhou University, The People's Republic of China, for encouragement and financial support, and to the University Grants Committee, New Zealand, for the award of a postgraduate scholarship in 1987.

CONTENTS

SUMMARY	1
CHAPTER 1 INTRODUCTION	3
1-1. Preface	3
1-2. Aims and plan of this work	4
1-3. General thermodynamic relations of mixing	5
CHAPTER 2 REVIEW OF EXPERIMENTAL METHODS FOR DETERMINATION OF EXCESS GIBBS FUNCTION	7
2-1. Introduction	7
2-2. Dynamic methods	7
2-3. Static methods	9
2-4. Dewpoint and bubble point method	17
2-5. McBain balance method	18
2-6. Isopiestic method	18
2-7. Gas chromatographic method	19
2-8. Freezing-point depression method	20
2-9. Light-scattering method	21
2-10. Liquid-liquid equilibrium method	22
CHAPTER 3 DESCRIPTION AND DISCUSSION OF APPARATUS AND EXPERIMENTAL TECHNIQUES	24
3-1. Vacuum lines	24
3-2. Pressure measurement	25
3-3. Thermostat and temperature controller	28
3-4. Temperature measurement	32
3-5. Nitrogen supply	33
3-6. Vapour pressure cell	34
3-7. Manifold of measurement side of Baratron	36
3-8. Degassing	37
3-9. Loading manifold and preparation of mixtures	38

CHAPTER 4	VAPOUR PRESSURES OF PURE COMPOUNDS	
	AND TESTS OF EXPERIMENTAL TECHNIQUES	43
4-1.	Introduction	43
4-2.	Materials	43
4-3.	Vapour pressures of pure components	44
4-4.	Tests of experimental techniques	47
CHAPTER 5	THE REDUCTION OF EXPERIMENTAL DATA	52
5-1.	Review of the methods of P-x data reduction	52
5-2.	Statistical methods in the treatment of experimental data	59
5-3.	The method of data reduction used in this work	70
5-4.	Error analysis	80
CHAPTER 6	THE EXPERIMENTAL RESULTS OF VAPOUR LIQUID EQUILIBRIUM	88
6-1.	General description	88
6-2.	n-hexane + n-hexadecane at 303.15 K	93
6-3.	Binary mixtures	95
6-4.	Ternary mixtures	102
CHAPTER 7	EXCESS VOLUMES OF MIXING	108
7-1.	Review of experimental methods for measurements of excess volumes	108
7-2.	Experimental apparatus and procedure	116
7-3.	Calculation procedure	123
7-4.	Tests of experimental method	125
7-5.	Error analysis	127
7-6.	Experimental results	130

CHAPTER 8	EXCESS ENTHALPIES OF MIXING	139
8-1.	General description of the experimental apparatus and methods	139
8-2.	Experimental operations	141
8-3.	Materials and preparation of pseudo n-dodecane	144
8-4.	Experimental results	146
CHAPTER 9	THEORIES OF MIXTURES OF ALKANES	156
9-1.	Introduction	156
9-2.	The principle of corresponding states	157
9-3.	Lattice model	159
9-4.	Cell model and the number of external degree of freedom	161
9-5.	Flory theory	163
9-6.	The correlation of molecular orientation and thermodynamics of alkane mixtures	165
9-7.	The principle of congruence	167
CHAPTER 10	DISCUSSION OF THE EXPERIMENTAL RESULTS	170
10-1.	Graphical test of the principle of congruence for G^E of binary mixtures	170
10-2.	Graphical test of the principle of congruence for G^E of ternary mixtures	173
10-3.	Null tests	178
10-4.	Analytical test using B-M equation for G^E of binary mixtures	180
10-5.	Analytical test using B-M equation for G^E of ternary mixtures	184
10-6.	Test of the principle of congruence by modified B-M equation	189
10-7.	The significance of g_0	197

10-8. Graphical tests of the principle of the congruence for H ^E , V ^E of pseudo n-alkanes + branched hexanes	200
Chapter 11 SUGGESTIONS FOR THE FURTHER WORK	202
REFERENCES	205
APPENDIX 1	214
APPENDIX 2	215
APPENDIX 3 COMPUTER PROGRAMMES	218
A3-1. DVEC and DVES	218
A3-2. HE	221
A3-3. CHVE	223
A3-4. PVLR2 and PVLR3	226
A3-5. PVLR4	240
A3-6. PVLR5 and PVLR6	245

SUMMARY

An apparatus for static vapour pressure measurements on pure liquids and on binary and ternary mixtures containing one involatile component has been designed and constructed. The apparatus and corresponding experimental techniques have been tested and experimental errors have been discussed.

Measurements have been made of the vapour pressures of binary mixtures of n-hexane + n-hexadecane at 298.15 K and 303.15 K and of binary mixtures of n-hexane + n-octane, n-octane + n-hexadecane, and ternary mixtures of n-hexane + n-octane + n-hexadecane at 298.15 K.

The experimental measurements of pressures (P) vs mole fractions (x) have been fitted to the Redlich-Kister equation by Barker's method to obtain activity coefficients of each component in the liquid phase, the excess Gibbs functions, and the mole fractions in the vapour phase.

The results for n-hexane + n-hexadecane at 303.15 K have been compared with those of previous work (Williamson, 1957) and the agreement is reasonably good.

The excess volumes of n-hexane + benzene, n-dodecane + 2-methylpentane and pseudo n-dodecane prepared from equimolar numbers of n-decane + n-tetradecane + each of four branched hexane isomers at 298.15 K have been obtained from measurements of the densities of pure compounds and mixtures with a vibrating tube densimeter. Two methods for preparation of mixtures of which densities are required to be accurately measured have been designed and compared with each other.

The excess enthalpies of 2-methylpentane with n-dodecane and with each of

three pseudo n-dodecanes prepared from equimolar mixtures of n-decane + n-tetradecane, n-undecane + n-tridecane, and n-octane + n-hexadecane, and the excess enthalpies of equimolar decane + tetradecane mixture with each of the other three branched hexane isomers at 298.15 K have been measured with an isothermal displacement calorimeter.

The experimental results of binary mixtures have been discussed in term of the principle of congruence with Hijmans' graphical method and Bellemans and Mat's analytical formula. New graphical tests of the principle of congruence and a modified Bellemans and Mat equation for ternary mixtures have been developed and applied to the experimental p-x data of ternary systems. The agreement between the experimental values and those predicted by the principle are excellent. The modified Bellemans and Mat equation seems to be more powerful than and preferable to the Redlich-Kister equation for the systems investigated in this work.

CHAPTER 1 INTRODUCTION

1-1 PREFACE

The work involved in this thesis is part of continuing studies in this department of the properties of the binary and multicomponent n-alkanes mixtures.

A number of theories, such as the lattice model (Guggenheim, 1952), the cell model (Prigogine, 1957), and their modifications which allow for vacant lattice sites (Lacombe, 1976; Chai, 1987), Flory's model (1964; 1965;), and Patterson's theory (Lam et al, 1974) have been developed to interpret the properties of mixture of liquid r-mer molecules.

Tests of these theoretical treatments have stimulated the experimental work in this area. Extensive investigations of excess molar enthalpies (H^E), excess molar volumes (V^E) excess molar heat capacities at constant pressure (C_p^E), and dV^E/dT and a few determinations of molar Gibbs functions (G^E) of alkane mixtures have been made. With the development of more precise experimental techniques, the effects of isomers of hydrocarbons recently have attracted the attentions of many authors. (Fenby et al., 1980; Hamam and Benson, 1984a; 1984b; 1986; Barbe and Patterson, 1980; Ott et al., 1980; Zheng, 1984; Kimura et al., 1983).

The comparison of theories and experimental results showed that the theories are still far from successful quantitative expressions of the properties of liquid mixtures of r-mer molecules, therefore as pointed by Fenby et al. (1980), more work, both experimental and theoretical, is clearly needed.

The empirical principle of congruence proposed by Bronsted and Koefoed (1946), on the other hand, affords one of the simplest correlations of the properties of mixtures of homologous series independent of any theoretical model. This principle has been successfully applied to predict the excess molar enthalpies, and excess molar volumes of binary and multicomponent systems (Koh and Williamson, 1980; Lim and Williamson, 1980, Looi et al., 1974). A few applications of the principle to binary vapour-liquid equilibrium also have been made by Bronsted and Koefoed (1946), Bellemans and Mat (1963).

The principle of congruence is closely related to the modern theories of mixtures of r-mer molecules. Longuet-Higgins (1953) gave an interpretation of the principle of congruence in term of a statistical theory. Hijmans and Holleman (Holleman, 1963; Hijmans and Holleman, 1965) extended the principle of corresponding states to n-alkane mixtures by incorporating the principle of congruence. Orwoll and Flory (1967) pointed out the departure of his model from the strict conformity with the principle of congruence. Hutchings and Van Hook (1985) stated that many modern theories are in fact congruence theories.

It can be properly said that the examination of the applicability of the principle of congruence and its potential extension opens up a fertile area for both experimental and theoretical studies.

1-2 AIMS AND PLAN OF THIS WORK

The aims of this work are:

1. To accumulate more thermodynamic data on alkane mixtures including branched isomers.
2. To investigate the applicability of the principle of congruence to the vapour-liquid equilibrium of binary and ternary mixtures.
3. To investigate the applicability of the principle of congruence to ternary mixtures obtained by mixing a pseudo n-alkane with n-hexane isomers.

Therefore, we shall attempt

1. to develop an apparatus and techniques for precise measurements of vapour-liquid equilibrium of binary and ternary mixtures by the static method,
2. to test the apparatus and the experimental techniques,
3. to measure the vapour-liquid equilibrium of binary systems: n-hexane + n-hexadecane, n-hexane + n-octane, n-octane + n-hexadecane, and a ternary system: n-hexane + n-octane + n-hexadecane,
4. to derive the activity coefficients and excess molar Gibbs functions from the vapour pressure measurements by adequate data treatments,
5. to discuss, as far as possible, the applicability of the principle of congruence in the prediction of vapour-liquid equilibrium of binary and ternary systems by both graphical and analytical methods,

6. to measure the excess molar enthalpies and excess molar volumes of mixtures of pseudo n-alkanes + hexane isomers, and to test the potential extension of the principle of congruence to the ternary mixtures with a branched alkane as one component.

1-3 GENERAL THERMODYNAMIC RELATIONS OF MIXING

In this section, we shall list the thermodynamic relations which will be useful in later chapters. The derivations of these relations can be found in Van Ness' book "Classical Thermodynamics of Non-electrolyte solutions" (1964).

The molar functions of mixing are defined by

$$\Delta X_m = X_m(T, p, x) - \sum_i x_i X_{i,m}(T, p) \quad \text{..... (1-3.1)}$$

where X_m denotes any molar quantity of a mixture such as the molar Gibbs function (G_m), molar entropy (S_m), molar enthalpy (H_m), molar volume (V_m) or chemical potential (μ_i), i denotes the i th component, $X_{i,m}$ denotes the molar quantity of the i th pure component. An excess molar property is defined as the difference between the actual property and the property which one would obtain for an ideal solution:

$$G^E = \Delta G_m - RT \sum_i x_i \ln x_i = RT \sum_i x_i \ln \gamma_i \quad \text{..... (1-3.2)}$$

$$S^E = -(\partial G^E / \partial T)_{p, x} = -R \sum_i x_i \ln \gamma_i - RT \sum_i x_i (\partial \ln \gamma_i / \partial T)_{p, x} \quad \text{..... (1-3.3)}$$

$$H^E = \Delta H_m \quad \text{..... (1-3.4)}$$

$$V^E = \Delta V_m \quad \text{..... (1-3.5)}$$

$$\mu_i^E = \left(\partial G^E / \partial n_i \right)_{T, P, n_j \neq i} = RT \ln \gamma_i \quad \text{..... (1-3.6A)}$$

and

$$\mu_i^E = \left[G^E - \sum_{k \neq i} x_k \left(\frac{\partial G^E}{\partial x_k} \right)_{x_{L \neq k, i}} \right] \quad \text{..... (1-3.6B)}$$

where G^E , S^E , H^E , V^E are excess molar Gibbs function, entropy, enthalpy,

volume, respectively; μ_i^E is excess chemical potential, γ_i is the activity coefficient, R is the gas constant.

The Virial equation truncated after the second term may be written as

$$pV_m/RT = 1 + B/V_m \quad \text{..... (1-3.7)}$$

where V_m is molar volume, p is pressure and B is the second Virial coefficient.

For an n -component mixture, B in equation (1-3.7) may be written as

$$B = \sum_i \sum_j y_i y_j B_{ij} \quad \text{..... (1-3.8)}$$

where B_{ij} ($i \neq j$) is the interaction second Virial coefficient. The activity coefficient

of the i th component in a gas mixture (γ_i^v) may be expressed as

$$\ln \gamma_i^v = (P/2RT) \sum_j \sum_k y_j y_k (2\delta_{ji} - \delta_{jk}) \quad \text{..... (1-3.9)}$$

$$\delta_{ji} = 2B_{ji} - B_{ii} - B_{jj} \quad \text{..... (1-3.10)}$$

where y is the mole fraction of a gas mixture, summations are taken for all j and

k . The criteria of vapour-liquid equilibrium may be written as:

$$\gamma_i^l x_i f_i^l = \gamma_i^v y_i f_i^v \quad \text{..... (1-3.11)}$$

where l, v denotes the liquid and vapour phase, respectively. f_i is the fugacity of vapour or liquid phase. At constant temperature, the relation between f_i and pressure may be expressed by

$$d \ln f_i = (V_{i,m}/RT) dP \quad \text{..... (1-3.12)}$$

With eq. (1-3.11), (1-3.12), and (1-3.8), the activity of the i th component in the liquid phase may be derived and expressed as:

$$\ln \gamma_i^l = \ln (y_i P / x_i P_i^0) + (B_{ii} - V_{i,m}^l) (P - P_i^0) / RT + \ln \gamma_i^v \quad \text{..... (1-3.13)}$$

CHAPTER 2 REVIEW OF EXPERIMENTAL METHODS FOR DETERMINATION OF EXCESS GIBBS FUNCTION

2-1. INTRODUCTION

The excess Gibbs function unlike excess enthalpies and excess volumes, cannot be measured directly, and usually it is derived from vapour-liquid equilibrium measurements (VLE). A survey of the measurements of VLE was presented by Abbott (1986) recently.

In VLE experiments, simultaneous measurements of total vapour pressure p , mole fraction y in the vapour phase and mole fraction x in the liquid phase at fixed temperature, or any two of these, are made by either a dynamic or a static method. When a complete VLE data set including x , y , p , T is measured, the activity coefficients obtained from this set data must satisfy the Gibbs-Duhem equation:

$$\sum_i x_i d \ln \gamma_i = -(H^E/RT^2) dT + (V^E/RT) dp \quad \text{.....} \quad (2-1.1)$$

Therefore equation (2-1.1) and its integrated form can be used as a thermodynamic consistency test (or so called internal test) for a set of experimental data. There is a vast literature on this test and the recent work of Dohnal and Fenclova (1985) is representative of the efforts in this area. The Gibbs-Duhem equation may instead be incorporated as a constraint on the activity coefficients, in which case the number of variables to be measured in a complete VLE data set may be reduced by one.

G^E also can be determined from the experimental results of gas-liquid chromatography and from isopiestic measurements, the McBain balance method, freezing temperature determination, light scattering and liquid-liquid equilibrium. All these methods have been reviewed by Williamson (1975) and Marsh (1978).

2-2. DYNAMIC METHODS

The dynamic circulation methods and apparatus have been summarized by Hala et al. (1967), and Malanowski (1982a). The common principle of this

method is shown in figure 2-1. The mixture is boiled in a boiler A, and the vapours pass through the condenser B. After complete condensation, the condensate is collected in receiver C and returns in a controlled manner to A for recirculation. This recirculation lasts for a period of time, and a steady state is attained when the compositions of both A and C remain invariant with time. The compositions in A and C are then determined and the temperature and pressure are recorded simultaneously. It was proved (Hala et al., 1967) that the compositions of the liquid phases in the receiver and the composition of the evolved vapour must be identical provided there is no entrainment of droplets of boiling liquid. However, it is possible that the vapour leaving A is not in continuous thermodynamic equilibrium with the boiling liquid due to the superheating of liquid and partial condensation of vapour and this is difficult to check. The other drawbacks of the dynamic circulation methods are the difficulties in minimization of pressure fluctuation and determination of the true value of equilibrium temperature and the mole fractions in the vapour phase.

Nevertheless, the search for well-designed dynamic circulation methods which can produce VLE data as good as a static method still continues. The modified Swietoslowski ebulliometer developed by Rogalski and Malanowski (1980) is an example of the well-design modern dynamic circulation apparatus and is shown in figure 2-2. The liquid is boiled in an electrically heated container H1, from which a continuous stream of vapour and overheated liquid was delivered into an equilibrium chamber E via Cottrell pump in the tube W. The liquid and vapour stream separate in the equilibrium chamber. The liquid drains into a mixing chamber A and the vapour passes into the condenser C, from which the vapour condensate flows through a drop counter K and container S1 to the mixing chamber A. The contents of the mixing chamber then return to H1, completing the cycle. The vapour and liquid samples are withdrawn through septa from S1 and S2 respectively, using hypodermic gas-tight syringes and the compositions of both phases are determined by measurements of refractive index or density. A simpler apparatus for total pressure and overall composition at fixed temperature rather than a complete x , y , p , T data set was also developed by Rosalski and Malanowski (1980), in which, instead of S1 and S2, a container was placed between the equilibrium chamber E

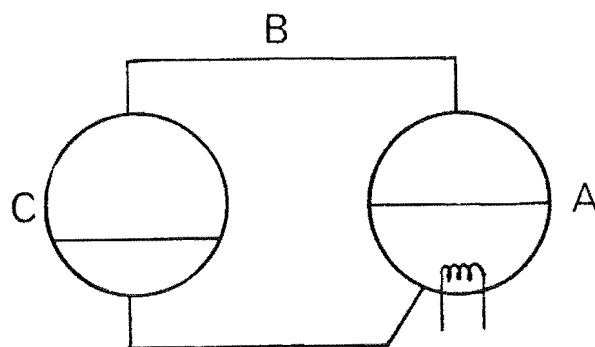


Figure 2-1 Principle of Recirculation still. A, boiler; B, condenser, c, receiver

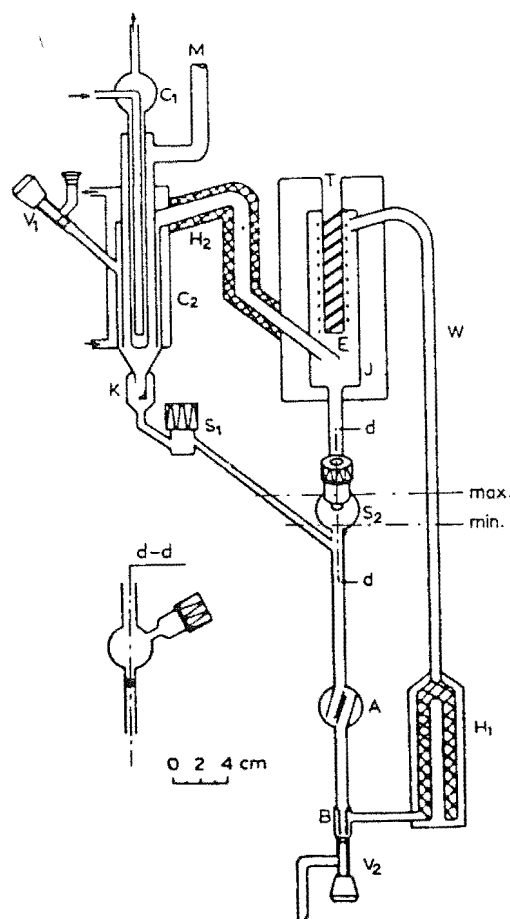


Figure 2-2 Modified Ebulliometer. H1, Heated container; A,B, mixing containers; K, drop counter; C1, C2, condensers; E, equilibrium chamber; V1, valve for introducing samples; V2, valve for removing liquid from ebulliometer; M, to the manostat; I, vacuum jacket; H2, heater for preventing partial condensation of vapour; S1, device for withdrawal of vapour condensate sample through septum; S2, for withdrawal of liquid sample.

and mixing chamber A. The composition of the liquid phase was calculated from overall compositions via a materials balance and the equilibrium equations by means of an iterative method. This method was used by Gierycz et al (1985) to determine VLE for 13 binary systems containing N-methylpyrrolidone as a common component at 21 isotherms.

Since difficulty was encountered when the circulation stills were used for measuring equilibrium data in systems with limited miscibility in the liquid phase various flow methods have been developed. In the flow methods, a steady stream of boiling liquid or preheated vapour with constant and known composition is fed into an equilibrium cell. The liquid and vapour phase are then separated and analysed. A detailed discussion of this method has been presented by Hala et al. (1967).

2-3. STATIC METHODS

A static method offers many advantages in vapour-liquid equilibrium measurement, as compared with most dynamic methods. It makes possible operation over a wider temperature range, allows measurements on systems whose components differ highly in volatility and may eliminate analyses of the composition of vapour phase which produces the largest experimental uncertainties.

In recent years, great attention was paid to static methods since adequate calculation procedures and computer facilities became available for evaluation of VLE from total vapour pressure data. The methods and related formulae for the evaluation will be discussed in chapter 5.

The total-pressure approach has some disadvantages. The activity coefficient is related to a slope property. When we obtain γ_i by the total pressure method, the P , T , and x values have to be measured with great precision and a sufficient number of points have to be measured to provide correct dp/dx over the entire composition range. Since small amounts of gas dissolved in the liquids can render the measured vapour pressures of mixtures inaccurate, the method requires thorough degassing of the substances which constitute the mixture. The procedures of filling components into the equilibrium cell and the

determination of the composition of liquid phase also give rise some difficulties. As a price paid for elimination of the phase analyses, the accuracy of the experimental results cannot be explored with an internal consistency test, although, Olson (1983) has used the Gibbs-Helmholtz equation to test the consistency of p-T-x data measured at several temperatures.

2-3.1 DEGASSING TECHNIQUES

Degassing is merely the removal of highly volatile components from a relatively involatile liquid, but the difficulty is that the volatile components are present in small amounts and their concentration must be reduced to near zero. Almost every serious reseacher has developed his own technique for degassing, recognizing the importance of this factor in obtaining reliable data.

A rapid and efficient degassing technique was developed by Bell (1968) and is shown in figure 2-3. A sample of 40 ml of liquid is filled in a detachable cell. With coolant in the finger, the system is continuously evacuated. It was claimed that one cycle, (about from 1 to 2 hr) was sufficient to completely degass aqueous systems and pure hydrocarbons; and less than 5% of the sample was lost in the degassing procedure. Bell's degassing units may be directly connected to a vapour pressure apparatus (Tomlins and Marsh, 1976).

Battino (1971) reported an apparatus, which was capable of handling liquid samples of the order 500 cm³ and degassed rapidly. Battino's apparatus is shown in Figure 2-4. The apparatus is fabricated from a standard 2-liter heavy wall filtering flask with tubulation. A 20 cm long condenser, C, is added at the tubulation end of the filter flask and a thermocouple gauge, TC, served as a pressure indicator. The sample is added into the flask until the layer of liquid in the flask is 4 cm deep, then the stirrer is turned on and the speed of stirring is increased slowly. For a volatile liquid, with stopcocks S1, S2 and S3 closed, the system is pumped down to its base pressure (5-10 μ), stopcock S4 is closed and S3 opened for 2-3 seconds. After waiting 1 minute for the vapour to freeze out, the pressure is read and stopcock S4 is opened to pump down the trap section. The procedure is repeated. When the pressure reaches the base pressure of system for

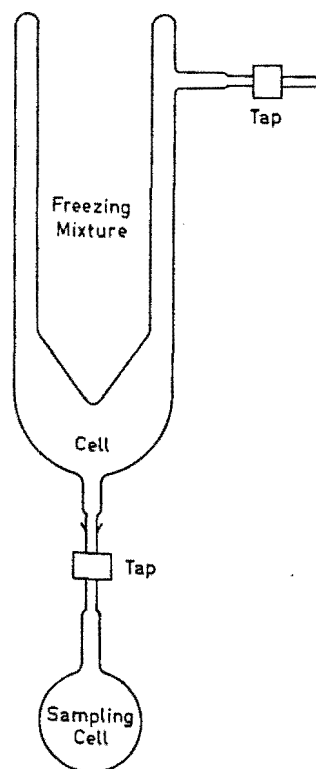


Figure 2-3 Bell's Degassing Apparatus.

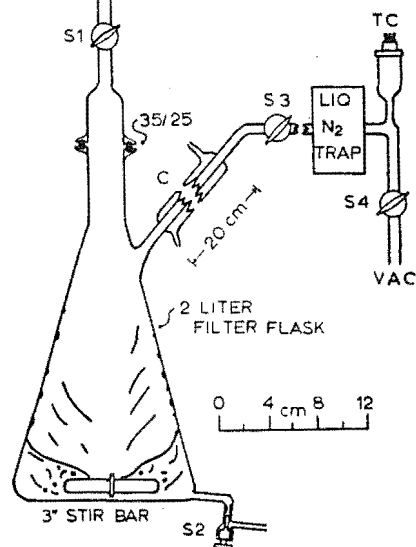


Figure 2-4 Battino's Degassing Apparatus.

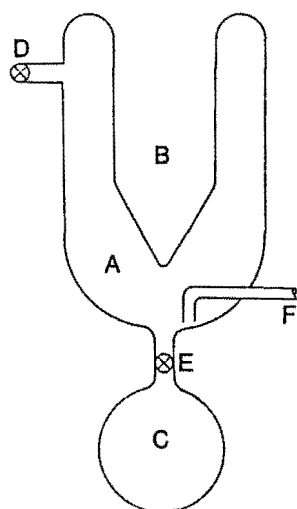


Figure 2-5 Gibbs and Van Ness's Degassing Apparatus: A, reflux chamber; B, cold finger; C, liquid-storage bulb; D, vacuum stopcock; E, teflon needle valve; F, port to piston-injector.

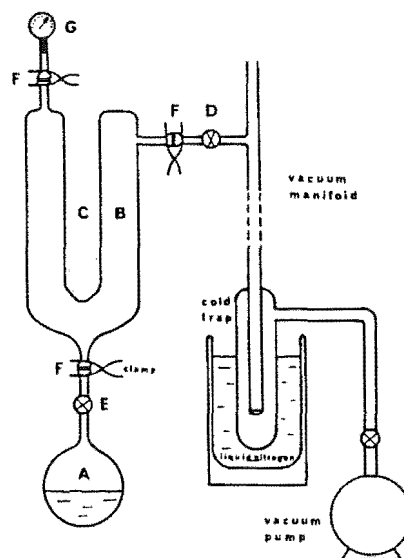


Figure 2-6 Ronc's Degassing Apparatus.

two successive trials, the liquid is considered degassed. For a involatile liquid, with S3, S4 opened, the entire system is pumped on for 2 minutes. S4 is closed and the pressure is read after 1 minute. The procedure is repeated until the base pressure is attained. The degassed liquid is transferred via S2 to another vessel under exclusion of the atmosphere.

Gibbs' apparatus (1972) is shown in figure 2-5. The sample to be degassed is added into bulb C. With tap E closed, A is evacuated through D. The cold finger B is filled with ice+water. With tap E open, heat is gently applied to C until the liquid refluxes. Heating is then removed, E closed, and A evacuated. This sequence is repeated several times and is then followed by a vacuum sublimation using either liquid nitrogen or dry ice in B. The system is pumped continuously during the sublimation. The rate of sublimation is controlled by needle valve E. With E closed, the thawed liquid is withdrawn through F into the VLE apparatus.

Ronc and Ratcliff (1976) stated that Bell's method had some drawbacks: the consumption of liquid nitrogen was large; the continuous presence of an operator was necessary to maintain the level above the point where the crystal mantle starts melting; the quantity that could be degassed was limited by the size of cold finger, since the crystal mantle grew to a limiting size and further condensate then dropped back into flask A. Another degassing process, which is shown in figure 2-6, was designed by Ronc and Ratcliff (1976). Flask A is loaded with 250 to 300 ml of liquid and then connected to vacuum briefly to remove the air and its attendant water vapour. E is then closed and the liquid sample frozen by submerging the flask in liquid nitrogen for about one hour. The coolant is removed and the material left to melt with the flask open to vacuum. Many bubbles could be observed rising to surface. After melting had been complete (about half an hour), the procedure is repeated until no bubbles could be observed. Usually, three or four cycles are sufficient. When degassing is complete, with E tightly closed, flask A is removed from the degassing apparatus and installed in the main VLE apparatus.

Van Ness and Abbott (1978) developed yet another rapid degassing technique. The apparatus is shown in figure 2-7. The liquid to be degassed is introduced into the still pot, A, through stopcock 1. After connection of still pot to the rectifying column B by an "O"-ring joint and with cooling water flowing in the condenser C

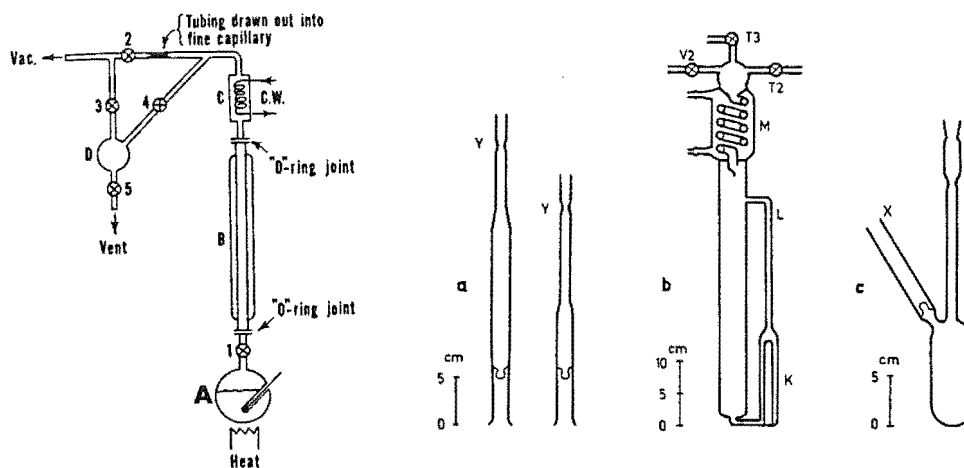


Figure 2-7 Van Ness and Abbott's Degassing Apparatus: A: still pot; B, rectifying column; D, surge vessel.

Figure 2-8 Accessories for Transfer and Degassing in Karel Aim's Apparatus:

a, ampoules; b, apparatus for degassing of volatile liquid; c, storage ampoules for involatile liquid.

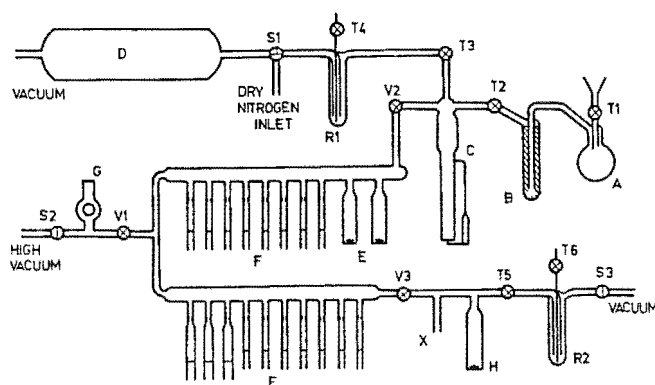


Figure 2-9 Assembly for Degassing in Karel Aim's Apparatus:

A, storage flask; B, molecular sieve; C, apparatus for degassing of volatile liquid; d, vacuum container; E, fingers with stirrers; F, ampoules; G, Penning gauge; H, degassing finger for involatile liquid; X, point to seal on storage ampoule; R, cold traps; S, glass stopcocks; T, teflon taps; V, bellows valves.

the entire apparatus is evacuated through stopcocks 3 and 4. These stopcocks then are closed and with stopcock 2 opened, heat is applied very gradually to the still pot from a heating mantle so as to bring the column to operation at some level below flooding. The upper opening of the condenser leads to a vacuum system through a fine capillary with a diameter of about 0.1 mm and a length of 0.5 cm, which is the key to successful operation of the apparatus. Generally, 24 hr was more than enough for degassing common chemicals. Termination of the process is accomplished by removing the heating mantle from the still pot, allowing the liquid to drain from the column into the still pot, and closing stopcock 5. The still pot is disconnected, and attached into the VLE apparatus.

Aim (1978) found the methods used by Bell, Battino and Ronc did not succeed in degassing benzene and cyclohexane. He reported a method for both volatile and involatile components, which is shown in figure 2-8 and 2-9. Volatile components are degassed in C of figure 2-9 (more clearly shown in figure 2-8) and involatile component in finger H. With T3 closed, 200-400 cm³ of liquid to be degassed is introduced into flask A via valve T1. A coolant with a temperature of 8-10° C is circulated through condenser M, yielding a sufficient pressure drop for slow distillation of liquid from the flask, by way of molecular sieve, into the apparatus. After stopping the cooling and closing T2, the heater K is switched on, the liquid then is, by gentle heating (8-12w), forced to circulate vigorously and is sprayed by the Cottrell Pump L on to the opposite wall of the apparatus. After 10-20 min, the vapour phase is exhausted by opening T3 to vacuum for 5 seconds. This procedure should be repeated until the material is completely degassed. For involatile components, the storage ampoule (see C in figure 2-8) is connected to X in figure 2-9. T5 is closed, the ampoule break seal opened and liquid is distilled overnight to the finger H. Degassing is then achieved in finger H by continuous pumping out of the vapour phase for at least 2-5 h, while the liquid is vigorously stirred and the space between V3 and T5 is warmed by a 50° C air stream.

Maher and Smith (1979) degassed pure liquids and mixtures in equilibrium cells without changing the mole fraction appreciably by successive freezing-evacuation -thawing. After freezing, the cells were evacuated to

remove the gases above solids. The manifold and cells were then swung over and lowered into an oven where they were heated above the highest freezing temperature to release gas trapped when the liquid were frozen. After the impurity gases had achieved a new equilibrium distribution between vapour and liquid in each cell, the cell contents were quickly frozen again and the cycle was repeated until the residual pressure was less than 10μ of mercury. Usually, seven to nine cycles are required with each taking about 1 hr.

Tamir et al (1981) degassed the pure material by pumping the cell filled with the liquid to be degassed at room temperature until $1/3$ of the material was evaporated.

2-3.2 THE EXPERIMENTAL TECHNIQUES OF STATIC VAPOUR PRESSURE METHODS

The experimental techniques of static methods for VLE measurement before 1976 have been summarized by Williamson (1975), and Marsh (1976). Apart from degassing, the main technical problems in the static method are sampling and accurate pressure measurement. A successive-distillation loading method was described in detail by McGlashan and Williamson (1961). The degassed samples were distilled into cells or ampoules with break seals and weighed, and transferred into the equilibrium cell. The mole fraction in the liquid was then calculated. This method was a little time consuming, especially for involatile samples and the operator had to make sure that there was no appreciable loss of sample during the transfer from ampoules to equilibrium cell.

Gibbs and Van Ness (1972) developed a method of sampling which involved volumetric metering of degassed liquids directly into the evacuated cell from piston injectors. The piston injector was a commercial 100 cm^3 capacity liquid metering pump capable of operating under vacuum conditions. The displacement volume could be read to 0.01 cm^3 . The piston kept liquid under a pressure of above 500 kpa, determined by an accurate break point torque wrench, for preventing bubbles from forming in the injector. The problem of how to correct the density of liquid under higher pressure was inherent in this method. Tomlins and Marsh (1976) constructed a loading system using a similar

principle. The piston injector, capacity 20 cm^3 and graduated to 0.001 cm^3 was immersed in the thermostat. It was driven by a motor through a clutch which was designed to slip when the pressure on the liquid was slightly above 100 kpa.

The technique of metering a known volume of liquid was adapted to ternary systems merely by adding a third injector (Dieisi et al., 1978) and also was applied to systems which form two liquid phases (Loehe et al., 1983).

The method of volumetric metering had considerable advantage of speed, but the mole fraction determined by this method was not as accurate as with the method of transferring the known masses of degassed liquid. Both of the methods need a correction for the amount of volatile components in the vapour phase and therefore the vapour space must not be excessive.

The third procedure of sampling was developed by Rogers and Prausnitz (1970). In their apparatus, the compositions of both phases were able to be analysed.

The total vapour pressures can be measured by either one manometer or two manometers in the static VLE measurements. McGlashan and Williamson (1961) measured pressure by an external manometer and a cut-off manometer. The external manometer recorded the pressure of nitrogen which was used to balance the vapour pressure to be measured in the equilibrium cell and the cut-off recorded the pressure difference between the nitrogen and the vapour in the cell. The vapour pressure was the sum of the pressures on the two manometers. Measuring the pressure primarily on the external manometer increased the complexity of the apparatus and the number of operations and measurements required for a simple pressure determination. Marsh (1968) used an apparatus containing an internal manometer only, but a tall thermostat had to be constructed and the space above the mixture was larger. In order to eliminate the difficulties associated with the reaction of some materials with the mercury in the manometer, Watson et al. (1968) used a capacitance deflection indicator as a mechanical cut-off. Tomlins and Marsh (1976) used a nulling manometer instead of the mercury cut-off. The difference of pressures on the nulling device was kept to less than 0.7 pa by using a pressure controller to stabilize the nitrogen pressure. Singh and Benson (1968), and Gibbs and Van Ness (1972) measured vapour pressure by using quartz spiral pressure gauges. Smith and Robinson (1970) connected the equilibrium cell to an

absolute-pressure transducer immersed in the thermostat.

For a binary system, if only one component is volatile and its vapour pressure is known accurately, the differential method may be used to determine VLE. The differences of vapour pressures, Δp , between pure volatile component and mixtures with known-compositions are measured by a mercury cut-off or any other differential pressure gauge. The activity coefficient of liquid phase at the given composition x_1 may be calculated (neglecting gas imperfections) by:

$$\ln \gamma_1 = \ln [(p_1^0 - \Delta p) / p_1^0 x_1] \quad \text{..... (2-3.1)}$$

Since the term of $\Delta p / p_1^0$ is much less temperature dependent than the vapour pressures themselves, the error of $\ln \gamma_1$ due to temperature fluctuation from one pressure measurement to another is much reduced compared with a set of direct pressure measurements. The work of Kershaw and Malcolm (1968) is representative of this method.

In the past decade, a numerous experimental data were produced by the static method based on the techniques described above and some modifications of static apparatus also have been made.

Ronc and Ratcliff (1976) improved Van Ness's apparatus. Figures 2-10 and 2-11 show their designs. The cell is made from a standard end piece of 2" glass tubing. The temperature is measured by a thermometer in a stainless steel housing placed inside the cell. The magnetic stirrer is driven by a turbine-powered magnetic drive H. The pressure rise in the cell due to leakage is less than 0.10 mmHg per week. The pressure is measured by a temperature-compensated absolute pressure transducer TR accurate to ± 0.01 mmHg, without the upper temperature limitation which existed in the earlier Van Ness design. The Clausius-Clapeyron equation is used to correct the measured pressure when the equilibrium temperature differs from the desired value. The bath temperature is controlled to ± 0.005 K and the absolute temperature measurement inside the cell is better than ± 0.005 K. The mole fractions are determined from the volumes and the densities of injected components, and are accurate to ± 0.0002 .

Several improvements over previous designs were made by Mentzer et al. (1982): Their cell was constructed from stainless steel instead of glass, with a

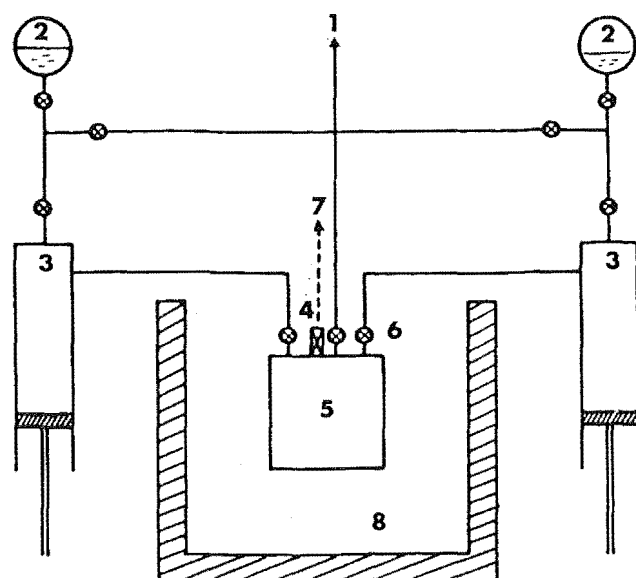


Figure 2-10 Ronc's Apparatus: Schematic Diagram
 1: to vacuum system, 2: flasks containing pure liquids,
 3: injectors, 4: transducer, 5: cell, 6: valves, 7:
 electrical output, 8: constant temperature bath.

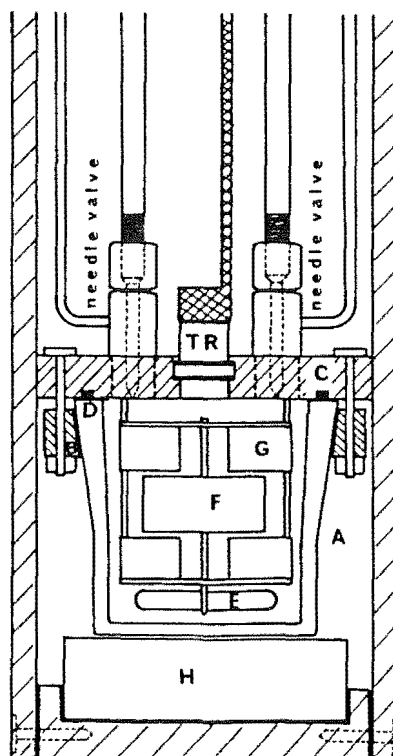


Figure 2-11 Ronc's apparatus: Equilibrium
 Cell. A, cell; C, cell lid; D, Viton "o" ring;
 E, teflon-coated magnet; F, teflon paddle; G, teflon baffles;
 H, turbine-powered magnetic drive.

copper gasket providing a leak-tight seal between the body of the cell and the lid. Pure degassed liquids entered through the sides of cell rather than the top, to ensure good mixing.

Maher and Smith (1979) described a new multicell apparatus for measurements of total pressure, with which three isotherms usually were measured in a 5-day run. A diagram of their apparatus is shown in figure 2-12. Fifteen small cells (approximately 25 cm³ each) are loaded with two pure components and thirteen intermediate binary mixtures. The cells are loaded by adding the desired amounts of liquid to each cell and weighing after each addition. After loading the 15 cells are attached via Cajon Ultra-Torr fitting (for glass cells) or Cajon VCO fitting (for metal cells) to 15 bellows valves mounted in a ring and connected to a common low-volume manifold. The liquid bath temperature can be maintained within ± 0.003 K of the set temperature. The accuracy of absolute temperature measurement is ± 0.03 K. A Datametric model 531 pressure transducer is used for the nulling device in the air bath. The vapour pressure on one side of the diaphragm is balanced with nitrogen gas on the other side. The pressure of nitrogen is measured with a Datametric model 572 transducer mounted outside the apparatus. The accuracy of the pressure measurement is about 0.1% of the measured value. The liquid mole fraction is determined to ± 0.0005 . The P-x isotherm is obtained by sequentially opening each cell to the transducer. Isotherms at other temperature are obtained by repeating the pressure measurements at other bath temperature. Since a period of 5 days is need to complete a experimental run a leak-tight connection is required for each cell and for each connection to the ring. Since 1979, a very large number of VLE data have been measured by Smiths' group on this multicell apparatus.

Ampoule-transfer techniques are still used in some new VLE apparatus. A schematic diagram of the major components of the static apparatus designed by Aim (1978) is shown in figure 2-13. The equilibrium cell is a 5 cm diameter, flat-bottomed cylindrical glass vessel. The total volume of the cell including that of the pressure gauge Bourdon helical tube and the interconnecting tube K is determined with liquid cyclohexane. Mixing of liquid in the cell is achieved with a glass-coated iron bar I and magnetic drive J. Valves V1 to V3 are bellows

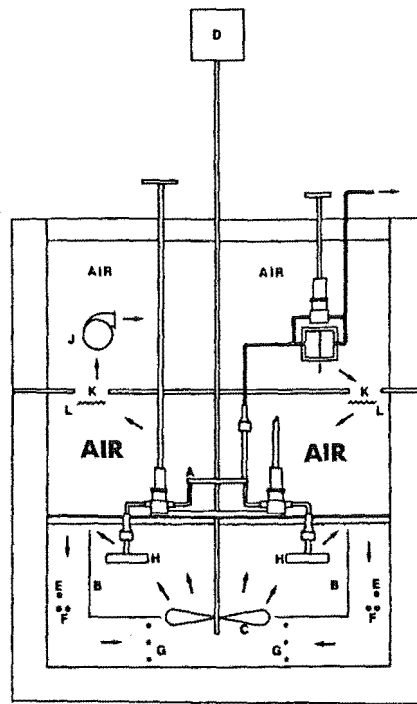


Figure 2-12 Maher's Apparatus.

A, manifold assembly; B, baffled tank;
 C, impeller; D, impeller motor; E, auxiliary
 heater; F, auxiliary cooling coils; G, control
 heater; H, cells; I, nulling transducer;
 J, air bath blower; K, openings
 for air flow; L, air bath heaters.

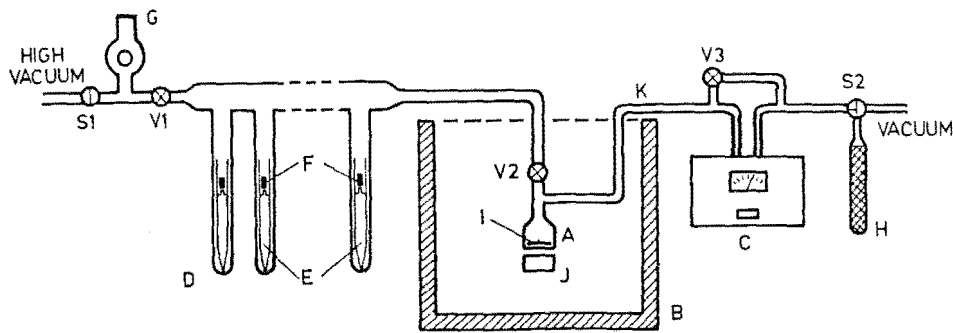


Figure 2-13 Aim's Apparatus.

A, equilibrium cell; B, thermostat; C, pressure
 gauge; D, ampoule holders; E, ampoules; F, nickel
 cylinders; G, penning gauge head; H, finger with
 active carbon; I, magnetic stirrer; J, magnetic drive;
 K, interconnecting line; S1, S2, vacuum glass
 stopcocks; V1 to V3, vacuum bellows valves.

valves. The cell is put in a two-stage bath. The internal bath has no heating of its own and is stirred by a heat insulated propeller. The temperature stability in the bath and the accuracy of the absolute temperature measurement are ± 0.002 K. The vapour pressure was measured with a Texas instruments fused quartz Bourdon tube precision pressure gauge. The accuracy of vapour pressure measurement is estimated to be $\pm 0.015\%$ of the measured value.

Weclawski and Bylicki (1983), constructed a static apparatus for rapid and precise VLE measurements based on McGlashan and Williamson's design (1961). Owing to the symmetrical construction of the oil bath and to efficient heat exchange, good temperature and pressure stabilities were obtained. The use of greaseless valves in the loading manifold facilitated the loading operations and eliminated absorption of materials in grease.

Some new designs allowing analysis of compositions also have been developed in last decade. Tamir (1981) designed a simple apparatus based on an isoteniscope, which is suitable for determination of the vapour composition. With these apparatus, VLE of the ternary system of acetone + chloroform + methanol at 50°C was measured. Very recently, a new VLE apparatus for fast determination of pressure, temperature, the mole fractions of both liquid and vapour phases has been developed by Laugier and Richon (1986). Microsamples of vapour and liquid phases are withdrawn and conducted by a carrier gas directly to a gas chromatograph where analyses are performed. The operation of this apparatus was very simple and no significant experimental difficulty is involved in measurements in the critical region. The equilibrium cell and the flow diagram of the apparatus are shown in figure 2-14 and 2-15.

2-4 DEWPOINT AND BUBBLE POINT METHOD

The principle of the dewpoint and bubble point method for measurement of VLE is illustrated in figure 2-16. For an overall constant composition, the pressure and volume of the system are slowly altered to traverse along the line GCAF, while the temperature is constant. The dewpoint and bubble-point on the phase boundaries are determined by the discontinuities of the P-V isotherm at points C and A.

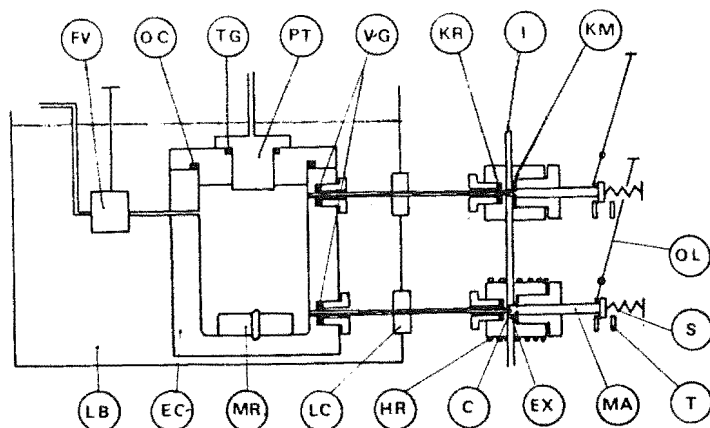


Figure 2-14 Equilibrium cell of Laugier and Richon's apparatus. B: buffer, C: capillary, EC: equilibrium cell, EX: expansion chamber, FV: feeding valve, HR: heating resistance, I: carrier gas inlet, KG: kalrez gasket, KM: kalrez membrane, KR: kalrez O ring, LB: liquid bath, LC: leakproof connection, MA: movable axis, MI: metallic injector, MR: magnetic rod, O: carrier gas outlet, OL: operating lever, OC: cell O ring, PT: pressure transducer, S: helicoidal spring, T: thrust, TG: Teflon gasket, and VG: Viton gasket.

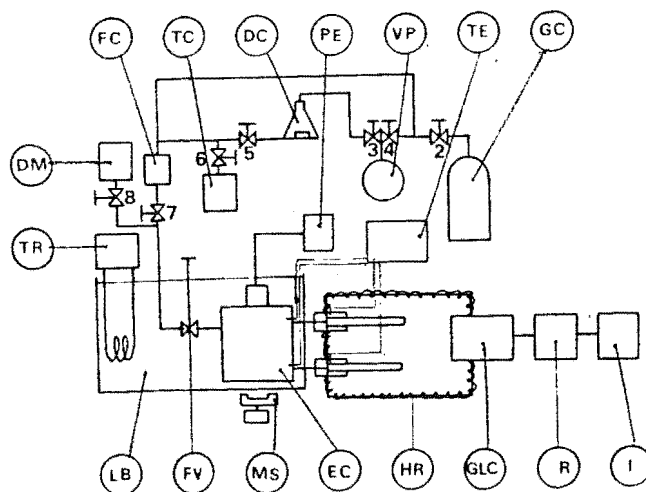
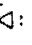


Figure 2-15 Flow diagram of Laugier and Richon's apparatus DC: degassing cell, DM: digital manometer (HEISE), EC: equilibrium cell, FC: feeding cell, FV: feeding valve, GC: gas cylinder, GLC: gas liquid chromatograph, HR: heating resistance, I: integrator, LB: liquid bath, MS: magnetic stirrer, PE: pressure electronic display, R: recorder, TC: thermal compressor, TE: thermal regulator, VP: vacuum pump, and : shut-off valve AUTOCLAVE ENGINEERS.

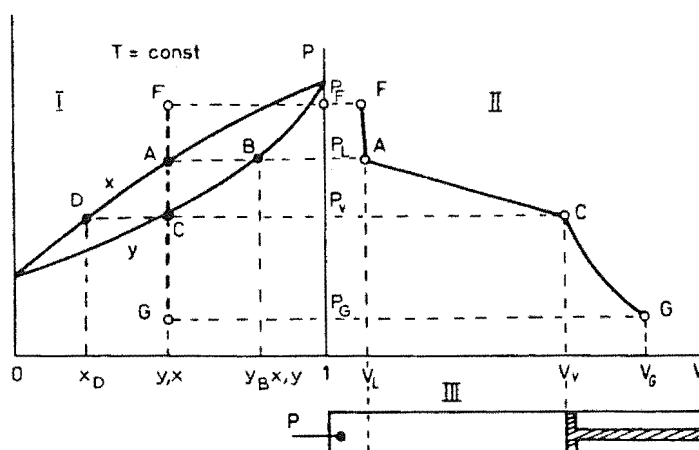


Figure 2-16 Principles of dew- and bubble-point method. (I) Phase diagram showing change of state of sample in piston-cylinder assembly (III), from liquid of composition x through bubble point A and dew point C into vapour of the same composition ($y = x$). (II) Corresponding decompression chart showing determination of liquid volume V_L and vapour volume V_v at the bubble point A and dew point C, respectively.

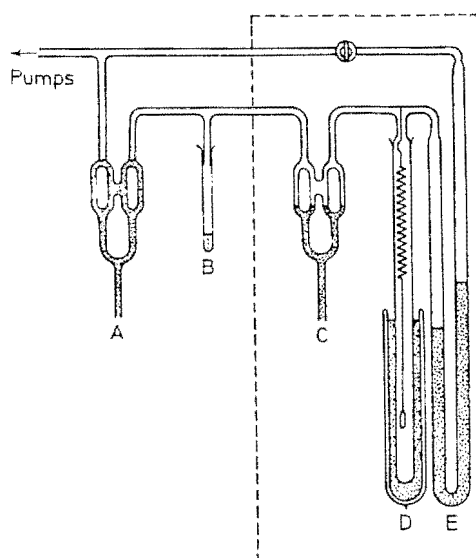


Figure 2-17 The McBain balance apparatus of Ashworth and Everett : A and C are mercury float valves. B is the volatile component, D is the quartz spiral and E is the manometer.

A calculational method for determination of the excess Gibbs function based on the observation of dewpoints and bubble points for a binary system without a knowledge of the composition in each phase was described by Dixon and McGlashan (1965).

The experimental techniques for high-pressure VLE measurements have been reviewed by Schneider (1975), Young (1978), and Eubank et al. (1980). The application of this method in the pressure region not exceeding 10 Mpa has also been summarized by Malanowski (1982b).

2-5 MCBAIN BALANCE METHOD

If one component in a binary mixtures is volatile, the VLE behaviour may be investigated by the technique originally developed by McBain (1926) for gas-solid adsorption. As an example, the apparatus of Ashworth and Everett (1960) is shown in figure 2-17. A weighed quantity of involatile component is placed on the pan of a quartz spring balance D and thoroughly degassed. The volatile component is then introduced from B into the vessel containing the spring balance D. When the system reaches equilibrium, the amount of volatile component dissolved in the liquid phase and hence the liquid composition are determined from the extension of the spring. The vapour pressure is measured on a manometer E attached to the equilibrium vessel.

2-6 ISOPIESTIC METHOD

The isopiestic method can be used to determine the Gibbs excess function provided only one component is volatile. A solution which contains the same volatile component but different involatile components and which has a known variation of vapour pressures with the composition is chosen as a reference. The mixture to be investigated and the reference solution are then placed in dishes on a metal block in airtight enclosure. The volatile component distills between the two solutions until the equilibrium is reached. Samples of the two solutions are analysed, and the properties of the mixture to be investigated are established by comparison with that of the reference solution. An apparatus suitable for

measurements with organic mixtures was described by Harris and Dunlop (1967).

2-7 GAS CHROMATOGRAPHIC METHOD

The static method is usually very time consuming and when it is used for the study of a system with only one volatile component the experimental errors at low concentrations are much greater than at higher concentrations. More rapid and accurate measurements of the activity coefficient of a volatile component at infinite dilution in an involatile component have been made by gas chromatography. The theory and experimental techniques for this method have been reviewed by Letcher (1978) and Conder and Young (1979).

When a volatile solute is injected on to a involatile stationary phase spread along a column, it is necessary to pass a volume of inert gas V_R (the retention volume) along the column to move this zone of solute from the inlet to the outlet. This retention volume includes a mobile phase (gas) holdup volume V_M . The net retention volume V_N which is related to the interaction between molecules of solute and stationary phase is defined by

$$V_N = V_R - V_M \quad \text{..... (2-7.1)}$$

The activity coefficient of volatile component at infinite dilution is related to the measured V_N by the equation (Conder and Young, 1979)

$$\ln V_N = [\ln (nRT/\gamma^\infty p_1^0) - (B_{11} - V_1^0) p_1^0/RT] + [(2B_{12} - V_1^\infty)/RT] p_0 J_3^4 \quad \text{..... (2-7.2)}$$

$$\text{where, } J_3^4 = 3 [(p_i/p_0)^4 - 1]/4 [(p_i/p_0)^4 - 1] \quad \text{..... (2-7.3)}$$

and p_i and p_0 are column inlet and outlet pressures, respectively; B_{11} is second virial coefficient of solute; B_{12} is the mixed second virial coefficient of carrier gas and solute; V_1^0 and V_1^∞ are molar volume of solute and partial molar volume of solution at infinite dilution in the stationary liquid, respectively; p_1^0 is the saturated vapour pressure of solute; n is mole number of stationary liquid. The activity coefficient of solute at infinite dilution and the mixed second virial coefficient B_{12} may be obtained simultaneously by a set of measurements of retention volumes vs the pressures and by extrapolation to zero pressure.

The apparatus and experimental operations for obtaining thermodynamic

data from gas chromatography have been described by a number authors (Cruickshank, 1966; Young, 1968; Conder, 1968). A flow diagram of an apparatus is shown in figure 2-18. The quantity of stationary liquid phase on the column is 1 to 5 g determined by weighing within $\pm 1\text{mg}$ and checks should be continually made to ensure that no significant loss of stationary liquid occurred during experiments. The temperature should be controlled within 0.2 K. The pressure usually is varied from 200 kpa to 1000 kpa and measured within $\pm 2\text{ kpa}$.

This method also has been extended to finite concentrations (Conder and Purnell, 1969).

2-8 FREEZING- POINT DEPRESSION METHOD

The freezing -point depression method has been used to obtain excess Gibbs functions in many aqueous solutions and some organic liquids. Although few precise measurements have been made in organic systems, for certain favourable solvents which have low enthalpy of freezing and hence large cryoscopic constants, this method is far superior to vapour-pressure measurements for obtaining excess Gibbs functions in the dilute region. A disadvantage of the method was the possibility of the solid phase being a solid solution.

The recommended experimental apparatus (Marsh, 1978) for this method is an isothermal dilution calorimeter such as the apparatus designed by Stokes et al (1969;1974). The experimental procedure is summarized as follows:

Degassed pure solvent is injected with a syringe into the calorimeter and held over mercury to remove the vapour space. The calorimeter is placed in a thermostat controlled at about 0.5 K below the freezing temperature of the solvent. With continuous stirring, the solvent is supercooled and the freezing of solvent is shown by the reversal of the time-temperature recording determined by a thermistor in the calorimeter. The thermostat temperature is raised to follow the rise of the calorimeter temperature until solid + liquid equilibrium was established and then the thermostat is adjusted within 0.01 K of the freezing temperature. A steady current of 4 mA is passed through a 100 Ω heater in the calorimeter and the time-temperature was recorded. On complete melting, there

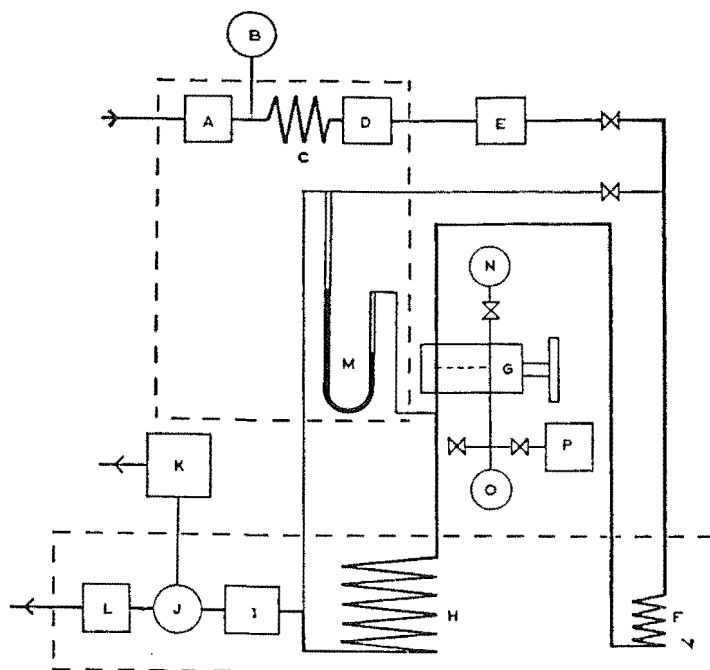


Figure 2-18 Medium-high-pressure g.l.c. apparatus. (A) Pressure regulator; (B) pressure gauge; (C) conditioning coil; (D) soap-film flow meter; (E) drying trap; (F) conditioning coil; (G) sample injector; (H) column; (I) control valve; (J) splitter; (K) needle valve; (L) detector and recorder; (M) manometer; (N) solute vapour reservoir; (O) pressure gauge; (P) vacuum pump
The heavy dotted lines refer to thermostatted regions

is a rapid linear increase in temperature. The freezing temperature of solvent is determined from the two linear portions of the recorded time-temperature curves.

The freezing points of mixtures are determined immediately following the determination of the freezing point of pure solvent. The calorimeter is heated to approximately 0.05 K above the value obtained for the solvent and the degassed solute is added into the calorimeter. The thermostat temperature is again lowered and the freezing curve is determined as before. The temperature is then raised to 0.05 K above the freezing temperature of solvent and further injection of solute is made for next measurement.

The solution of air in solvent can have a marked effect on the freezing point (0.17 K difference between degassed cyclohexane and air saturated cyclohexane), and the variation of solubility of air in the solvent during an experiment could make a marked error in measurement of the depression of freezing point.

The depression of freezing point is defined by

$$\theta = T_f^0 - T_f \quad \text{..... (2-8.1)}$$

where T_f^0 and T_f are the freezing temperatures of pure solvent and mixture, respectively. The activity coefficient of solvent is given by

$$\ln \gamma_1 = \Delta H_1^0 \theta / R (T_f^0)^2 + (\Delta H_1^0 / R T_f^0 - \Delta C_{p1}^0 / 2R) (\theta / T_f^0)^2 \\ - \ln (1-x) - \Delta H^m \theta / R (T_f^0)^2 \quad \text{..... (2-8.2)}$$

where γ_1 is the activity coefficient of solvent; ΔH_1^0 is the enthalpy of melting of pure solvent; ΔC_{p1}^0 is the difference in heat capacity of solid and liquid solvent; and ΔH^m is the partial molar excess enthalpy of solvent. The activity coefficient of solute may be obtained by integration of the Gibbs-Duhem equation by either graphical or numerical methods.

2-9 LIGHT-SCATTERING METHOD

Light-scattering measurements have been widely used in obtaining activity

coefficient and hence excess Gibbs functions. Kerker described the basic theory and summarized the practical applications of light scattering in his book "The Scattering of Light" (1969).

According to the statistical-thermodynamics description, a liquid is not uniform in the microscopic point of view, some properties of the liquid in a given small volume fluctuate from the macroscopic or average values. These fluctuations cause light scattering. The total Rayleigh scattering of pure liquid is the sum of isotropic, R_{is} and anisotropic scattering, R_{an} . In a pure liquid the former is contributed by the density fluctuation, R_d ; the later is contributed by orientation fluctuation of anisotropic molecules. For binary mixtures, there are additional contributions to isotropic scattering due to fluctuations in concentration, R_c , and the cross term due to dependence of density and concentration fluctuations, R' . Let R_{id} be the R_c of an ideal solution, which can be calculated from a knowledge of the density, concentration and partial derivative of refractive index with respect to mole fraction of mixture. The measured total Rayleigh scattering can be separated into R_{is} and R_{an} and theoretical value of R_d and R' are computed, R_c then is obtained by the difference, $R_{is} - R_d - R'$ and the function $(1 - R_{id}/R_c)$ is computed for each composition. Activity coefficients can be obtained by numerical integration of

$$\ln \gamma_1 = \int_0^{x_2} \left(\frac{1}{x_1} \right) [1 - (R_{id} / R_c)] dx_2 \quad \dots\dots\dots (2-9.1)$$

$$\ln \gamma_2 = \int_0^{x_1} \left(\frac{1}{x_2} \right) [1 - (R_{id} / R_c)] dx_1 \quad \dots\dots\dots (2-9.2)$$

Myers and Clever (1970) have described the experimental and calculational procedures of this method. This method has limited applications because the error in determination of excess Gibbs function is as large as 40 J mol⁻¹.

2-10 LIQUID-LIQUID EQUILIBRIUM METHOD

The molar excess Gibbs function of a partial miscible mixtures may be

determined from the data on liquid-liquid equilibria, i.e: the mole fractions (x_i) in liquid phases being equilibrium with each other at fixed temperature and pressure.

A detailed discussion of determination of mole fraction in each liquid phase has been made by Alder (1959) and Sorensen et al (1979a) and a review of the correlation of liquid-liquid equilibrium data were given by Sorensen (1979b).

The isoactivity criterion may be used to describe the liquid-liquid equilibrium calculation:

$$x_i^A \gamma_i^A = x_i^B \gamma_i^B \quad \text{..... (2-10.1)}$$

where superscript A, B represent the phases A and B. γ_i is the activity coefficient of the i th component in the liquid phase, and may be expressed as the function of x_i with a few parameters by some models such as Margules, Redlich-Kister equations. The parameters (c) can be determined by minimizing the objective function [F(c)]:

$$F(c) = \sum_k \sum_i [x_{ik}^A \gamma_{ik}^A (x_{ik}^A, c) - x_{ik}^B \gamma_{ik}^B (x_{ik}^B, c)]^2 \quad \text{..... (2-10.2)}$$

$i = 1, 2, \dots, N$ (components)

$k = 1, 2, \dots, M$ (tie lines)

For binary data at fixed temperature and pressure, there are two independent measurements : x_1^A and x_1^B . This enables the determination of a maximum of two parameters from one binary tie line. However, a ternary liquid-liquid equilibrium data set gives a number of tie lines at fixed temperature and pressure. If the number of tie lines is M, a maximum of 3M parameters can be determined from the data set. The activity coefficients of components in liquid phases hence the excess molar Gibbs function may be calculated from the model equation and the optimal parameters.

CHAPTER 3 DESCRIPTION AND DISCUSSION OF APPARATUS AND EXPERIMENTAL TECHNIQUES

A line diagram of the experimental apparatus for measurements of vapour pressures of pure components and mixtures is shown in figure 3-1. The various parts of the apparatus and of techniques are described and discussed in the following sections.

3-1 VACUUM LINES

The vacuum lines were made either of "pyrex" glass tubes 0.5 cm in diameter (thin lines in figure 3-1) or copper tubes 0.4 cm in diameter (thick lines in figure 3-1). Glass-to-metal joints (stainless steel for vapour pressure cells, kovar for the others) were used to join the glass tubes and metallic tubes together .

Ground-glass valves (G) were used in the main vacuum manifold and in the vacuum line for evacuation of the nitrogen supply manifold. "Young" teflon taps (Y) were used in those glass lines which needed to be grease-free. Valve Y2 isolated the degassing manifold (5) from the other parts of the apparatus and Y10,Y11,and Y6 separated the loading manifold, pressure measurement manifold, and the main vacuum manifold, respectively.

Metallic valves were mounted in the metallic lines either with Swagelok fittings or by welding. Three bellows sealed "Nupro" valves (N) [model SS-4H] were welded in those regions where high vacuum needed to be held for a long term after the vacuum line had been isolated. Four "Whitey" ball valves (W) [model B-43S4] and a "Nupro" fine metering valve (F) were mounted in the nitrogen supply manifold to provide a fine adjustment of the nitrogen gas pressure. Valve W4 separated the "Baratron" gauge from the rest of the apparatus.

The experimental system was evacuated by a mercury diffusion pump [Edwards model IM2] (4) backed by a two-stage rotary pump [Edwards, model 2. S.20] (1). The pressure in the vacuum systems was checked with a thermocouple vacuum gauge [Edwards model Tc1] (11) between 3 and 10^{-3}

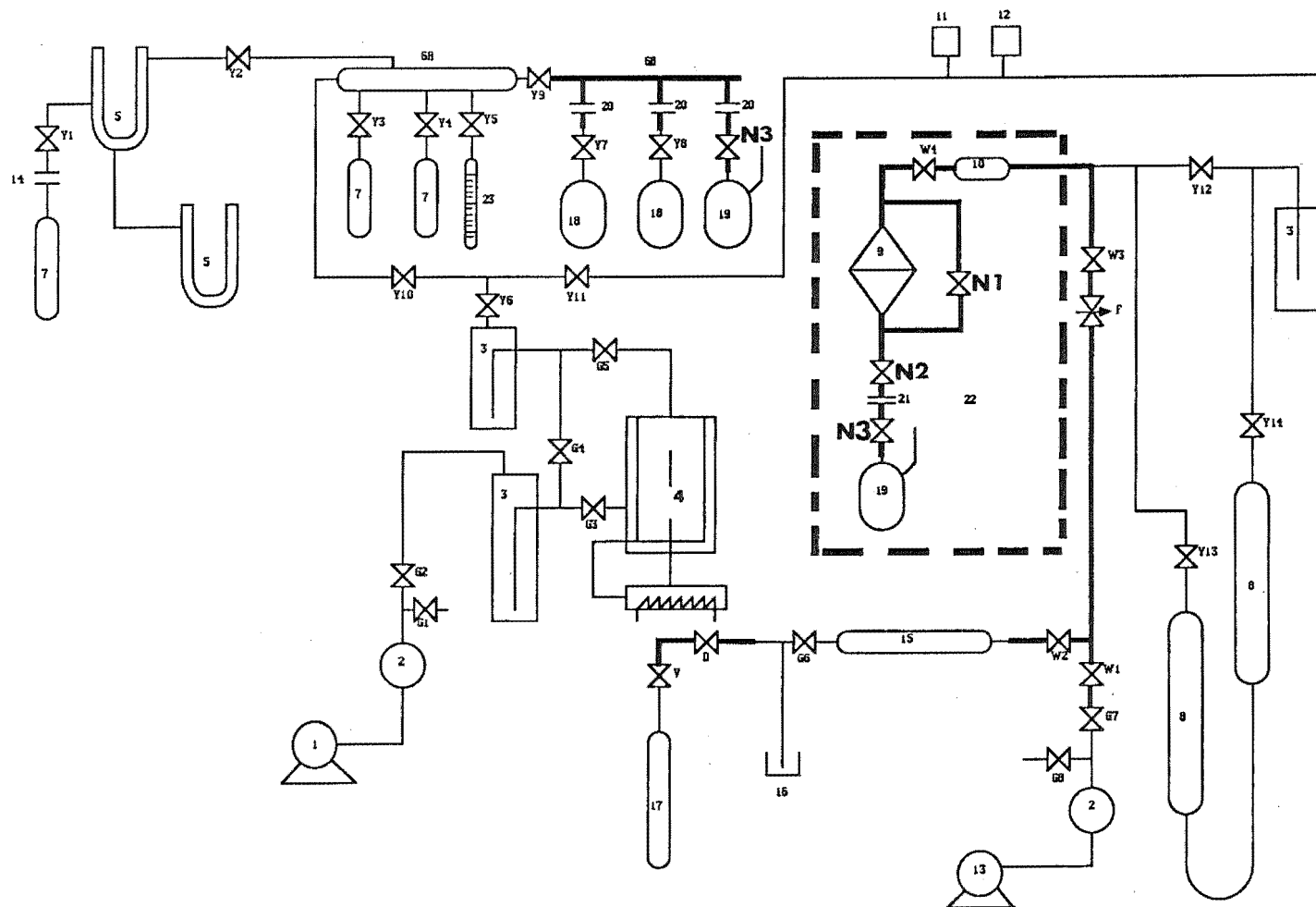


FIGURE 3-1 VACUUM LINES

Key to Figure 3-1

- (1) Two-stage vacuum pump.
- (2) 1000 cm³ glass globes.
- (3) Liquid nitrogen cold traps.
- (4) Mercury diffusion pump.
- (5) Degassing manifold.
- (6A) Loading manifold made of glass tube.
- (6B) loading and degassing manifold made of stainless steel tube.
- (7) Glass storage sample ampoules.
- (8) Mercury-in-glass manometer.
- (9) Baratron pressure gauge.
- (10) Stainless steel vessel of about 1000 cm³ capacity.
- (11) Thermocouple vacuum gauge.
- (12) Penning Gauge head.
- (13) One-stage vacuum pump.
- (14) "Soveril" teflon joint.
- (15) Dry silica gel tube.
- (16) Mercury safty valve.
- (17) Dry oxygen-free nitrogen supply cylinder.
- (18) Glass cells with approximately 15 cm³ capacity.
- (19) vapour pressure cells.
- (20) "Cajon" fittings.
- (21) "Cajon" fitting.
- (22) Air bath.
- (23) pipette.

F: "Nupro" fine metering valve.

D: Needle valve.

V: Nitrogen supply regulator.

G1-G8: Ground glass vacuum valves.

Y1-Y14: "Young" teflon taps.

W1-W4: "Whitey" ball valves.

N1-N3: "Nupro" stainless steel bellow valves.

— : Glass tubes.

—

— : Copper tubes.

mbar and with a penning vacuum gauge [Edwards model 8] (12) between 10^{-2} and 10^{-7} mbar. The cold traps were immersed in liquid nitrogen to remove the vapours of the vacuum pump oil and the mercury in the system. The cold trap placed between Y11 and Y12 was grease free. The whole experimental system could be evacuated to 10^{-6} mbar.

3-2 PRESSURE MEASUREMENT

The vapour pressure measurement system is simply indicated in figure 3-2. The pressure of nitrogen gas used to balance the pressure of sample vapour in the vapour pressure cell was measured by a mercury-in-glass manometer. The pressure difference between nitrogen gas and sample vapour was measured by a "Baratron" differential diaphragm gauge.

The vapour pressure P at the surface of the liquid in the vapour pressure cell was the sum of the hydrostatic pressures and the pressure difference of the both sides of the "Baratron" gauge:

$$P = P_{hg} + P_B + \Delta P_1 + \Delta P_2 \quad \dots\dots\dots (3-2.1)$$

let $h' =$ the value of h_1 when $h_{hg} = 0$, then

$$h_1 = h' - h_{hg}/2 \quad \dots\dots\dots (3-2.2)$$

$$\Delta P_1 = \rho_1 h_1 g \quad \dots\dots\dots (3-2.3)$$

where, ρ_1 is the density of nitrogen, $P_{hg} = \rho_{hg} g h_{hg}$, g is the acceleration of gravity, and

$$\rho_1 = M_1 P_{hg} / (RT_1) = M_1 \rho_{hg} g h_{hg} / (RT_1) \quad \dots\dots\dots (3-2.4)$$

where, M_1 and ρ_{hg} are the molar mass of nitrogen gas and the density of mercury, respectively. Combining eqs. (3-2.2), (3-2.3) and (3-2.4) gives:

$$\Delta P_1 = M_1 (h' - h_{hg}/2) \rho_{hg} h_{hg} g^2 / (RT_1) \quad \dots\dots\dots (3-2.5)$$

Similarly for ΔP_2 , $\rho_2 = M_2 \rho_{hg} h_{hg} g / (RT_2)$, therefore

$$\Delta P_2 = \rho_2 h_2 g = h_2 M_2 \rho_{hg} h_{hg} g^2 / (RT_2) \quad \dots\dots\dots (3-2.6)$$

The subscript 2 in eq. (3-2.6) refers to the vapour of the sample in the vapour pressure cell.

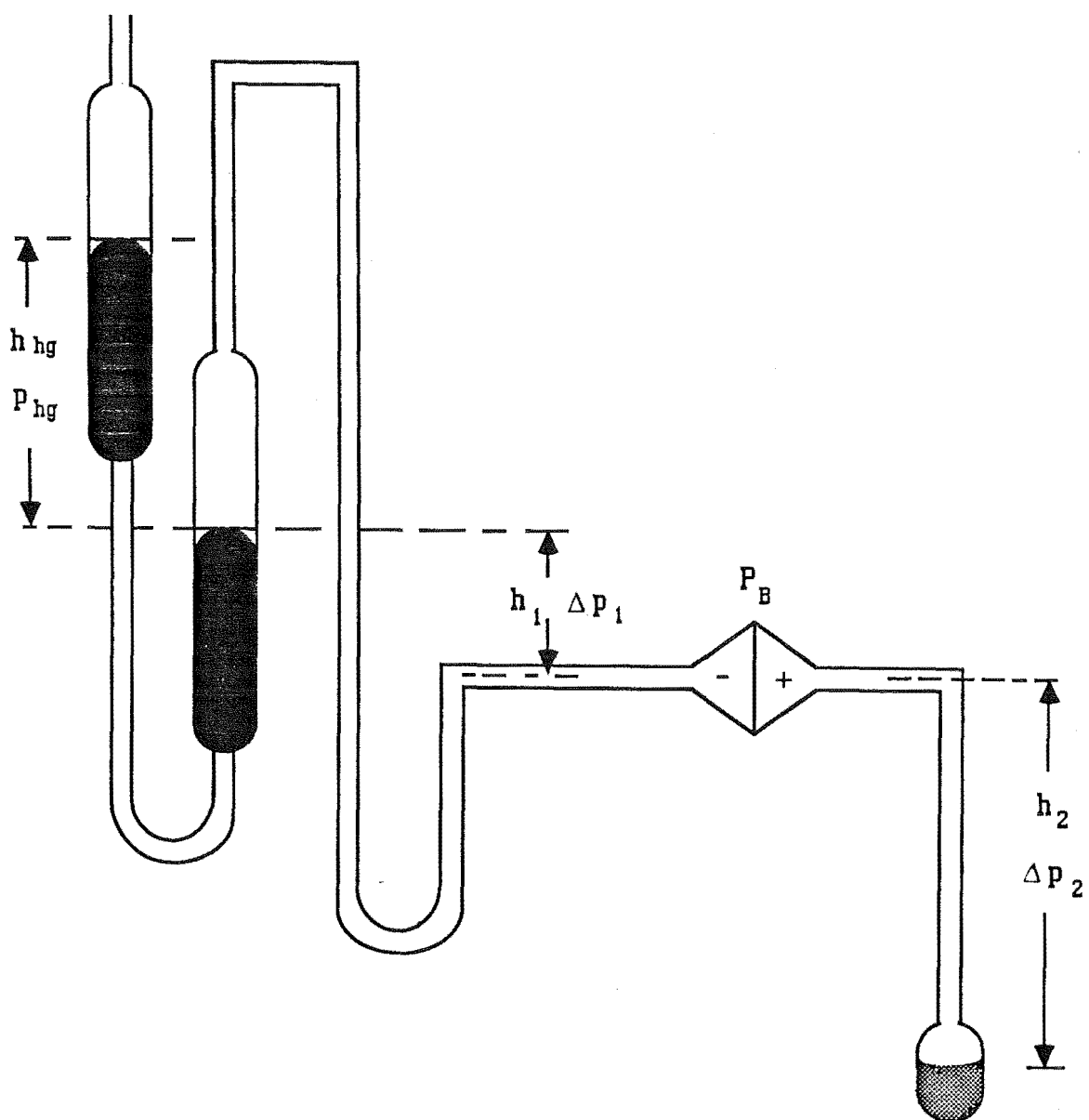


Figure 3-2 PRESSURE MEASUREMENT

because $\partial \Delta P_1 / \partial h_{hg} = M_1 (h' - h_{hg}) \rho_{hg} g^2 / (RT_1)$, and $\partial^2 \Delta P_1 / \partial h_{hg}^2 < 0$, ΔP_1 reaches its maximum value at $h_{hg} = h'$, and $\text{Max } \Delta P_1 = M_1 h'^2 \rho_{hg} g^2 / (2RT_1)$.

In our experiments, $h' = 0.16$ m, $\text{Max } h_{hg} = 0.19$ m, $M_1 = 28 \times 10^{-3}$ kg mol⁻¹, $M_2 = 86 \times 10^{-3}$ kg mol⁻¹, $\rho_{hg} = 13.6 \times 10^3$ kg m⁻³, $h_2 = 0.35$ m, and $g = 9.8$ m s⁻². The maximum ΔP_1 is 0.2 pa. The maximum ΔP_2 was about 3 pa, and the error in estimation of ΔP_2 , mainly due to the error of estimation of h_2 , is less than 10% of the value, that is less than 0.3 pa.

The mercury-in glass manometer was constructed from 20 mm bore glass tubing. The manometer was totally enclosed in a box insulated with polystyrene. Two 10 cm wide plate glass window were fixed at the front and back of the box. the temperature inside of the box was measured with a 0-50 °C glass thermometer which could be read to ± 0.1 °C. The long term fluctuation in the box was usually less than ± 0.5 K.

Two fluorescent tubes were mounted outside of the box behind the rear window, and there were only two narrow gaps on the rear window to allow light to pass through. The beams then passed through brass tubes attached to brass shields. The brass shields were fixed round the manometer tubes to eliminate stray light from the regions of the menisci. The shields were adjusted from outside of the box by two handles through a mechanical device, so that the narrow bands of light passed between the bottom of the shields and mercury surface. The menisci then appeared in the telescope of the cathetometer as sharp shadows. The apparent position of the mercury surface was independent on the position of the shield as long as the gap between the bottom of shield and the mercury surface was less than about 0.25 mm.

The mercury levels in the manometer were measured with a one metre precision Tool and Instrument Co cathetometer with a sealed incremental length measuring system [Heidenhain model LS 903] installed on its bar. The difference of the heights of mercury levels was read out by a Bidirectional counter [Heidenhain, model VR 2100] within ± 0.002 mm.

The manometer and cathetometer were mounted to the rigid steel frame,

which was fixed to the concrete wall and the floor. The cathetometer was set in the front of the mercury-in-glass manometer. The bar of the cathetometer was set at such position that the two manometer tubes were coaxial with it. This avoided the need for change of focus of the telescope between the two measurements of the mercury levels in the two manometer tubes. Both of the cathetometer and the manometer were carefully levelled.

The telescope was levelled before each measurement. The spirit level on the telescope could be set to within ± 0.2 division, and experiments showed that a change of angle of one division on the spirit level of the telescope caused a change in reading of height of 0.05 mm. The error in pressure measurement due to incorrect levelling could be as large as ± 0.01 mmHg or ± 1.3 pa. The reproducibility of sets of measurements of the same menisci height agreed to within ± 0.015 mm. Some error could be caused from uncertainty in sighting of the position of the menisci with telescope.

The vacuum side of the manometer was continuously evacuated during measurements, and pressure was calculated by

$$P = \rho_{\text{hg}} h_{\text{hg}} g \quad \text{..... (3-2.7)}$$

The value of g ($=980.48 \text{ cm s}^{-1}$) was provided by Christchurch Meteorological Service. The densities of mercury at various temperature were given by Brown and Lane (1976). The uncertainty in pressure measurement due to the measurement of the temperature in the manometer box was less than 2×10^{-3} mmHg or 0.3 pa.

The pressure difference between the nitrogen gas and the vapour sample under measurement was measured with a Baratron sensor head [MKS, model 315 BD] a conditioner [type 270 B] and a 0–10 v d.v.m. The MKS company provided the calibration with a quoted accuracy of $\pm 0.08\%$ reading. It is necessary to raise the temperature of the Baratron to 0.5–1 K above the liquid in the vapour pressure cell in order to prevent condensation of vapour in the Baratron. The Baratron was therefore enclosed in a box insulated with glass wool. As a heating element, a piece of about 2 M nichrome wire was wound on to the body of the Baratron. The differences of temperatures in the box and in the air bath was adjusted by the voltage across the heating element, through a dc power supply [Redfern, model 51 A], and measured by a copper vs constantan

thermocouple. The zero drift during each experiment period was less than 3×10^{-3} mmHg or 0.4 pa.

The Baratron was calibrated against the mercury manometer before the experiments. The calibration procedure is described as follows:

A glass globe, instead of the vapour pressure cell, with about 1000 cm³ capacity was attached to the pressure measurement side of the Baratron through a Cajon fitting (21). With N1 open, both sides of the Baratron were evacuated to 10^{-5} mbar. The null position and full scale of the Baratron were adjusted after the temperature in the air thermostat was stable. The zero then was set up. The valve Y12 was closed and then nitrogen gas expanded through W2, F, W3, W4, N1 into the both sides of the Baratron. Valve N1 was then slowly closed. The pressure of nitrogen gas was adjusted again so that the pressure difference indicated in the display unit was 0.000 v (or 0.000 mmHg) and then the pressure of nitrogen gas was measured with the mercury manometer. The reference side of the Baratron was evacuated. The pressure indicated on the display unit was recorded after the reference side was pumped to 10^{-5} mbar. The calibration was carried on in the region of 0–2.2 mmHg and is shown in figure 3-3. The Δp in figure 3-3 is $P_{\text{baratron}} - P_{\text{manometer}}$. No observable difference was found between calibrations at 298.15 K and 303.15 K.

The pressure of nitrogen gas was always adjusted so that the pressure difference between the sides of Baratron was less than 0.5 mmHg for each measurement in our experiments. The error due to this calibration, Baratron zero drift and the uncertainty of measurement with Baratron is believed to be less than 0.005 mmHg or 0.7 pa. Therefore the total uncertainty in pressure measurement was about ± 0.02 mmHg or 2.7 pa.

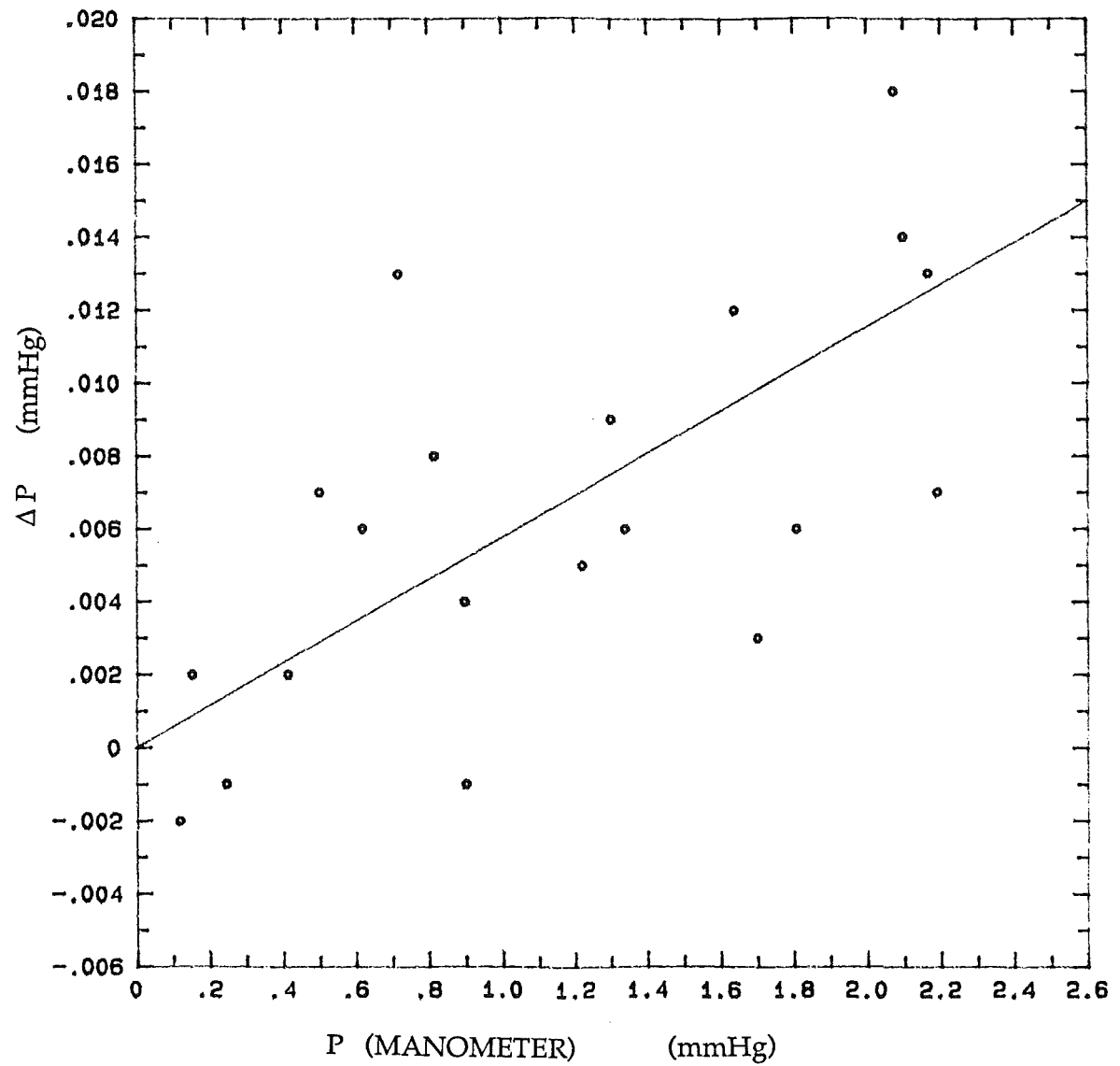
3-3 THERMOSTAT AND TEMPERATURE CONTROLLER

DESIGN AND CONSTRUCTION OF THE AIR BATH

An air bath used in previous work was redesigned and rebuilt to improve the temperature stability which was required for accurate VLE measurements.

A diagram of the air bath is shown in figure 3-4. The dimensions of the bath

FIGURE 3-3 CALIBRATION OF BARATRON VS MANOMETER



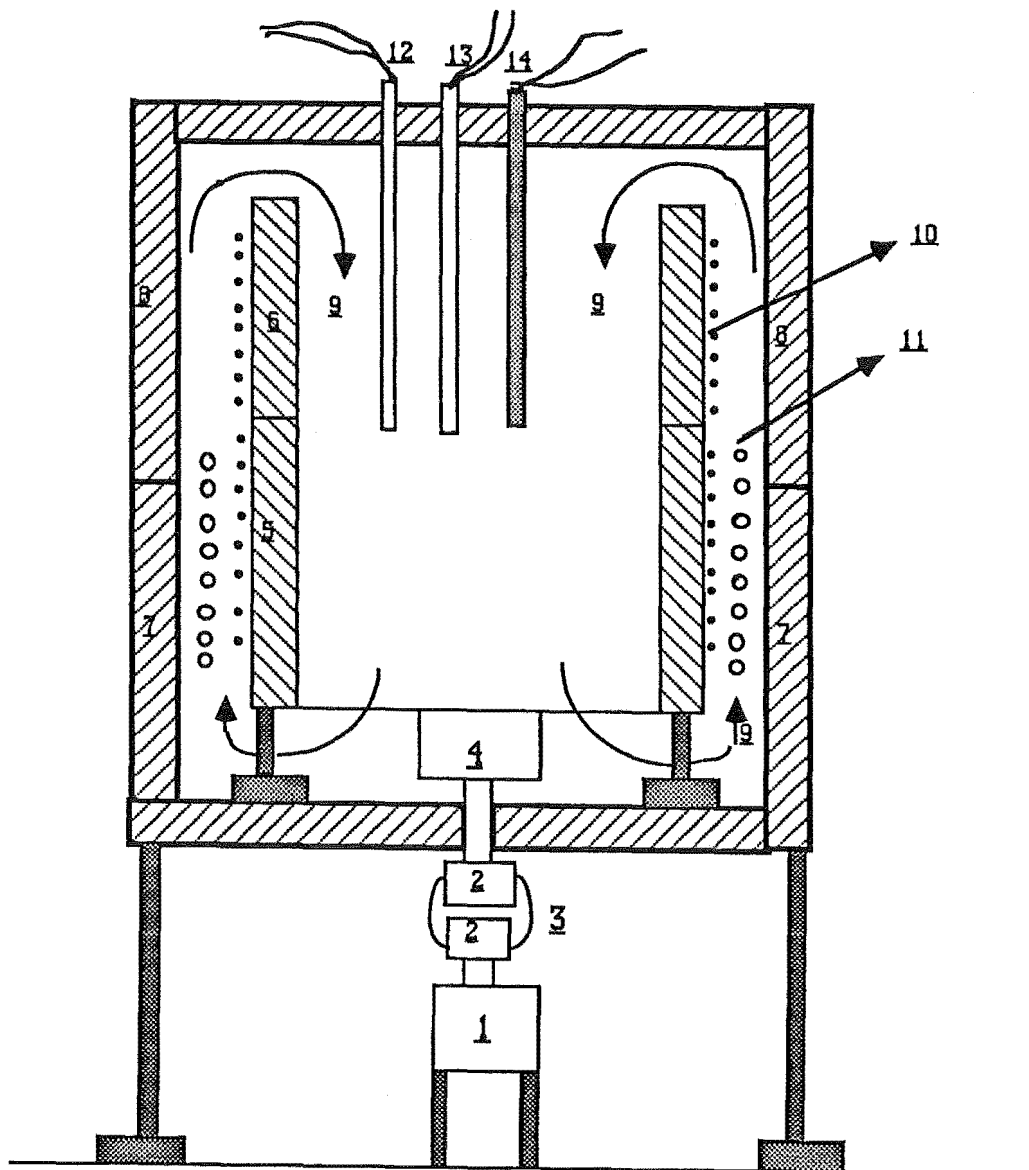


FIGURE 3-4 AIR BATH

Key to Figure 3-4

1. A.F.I. single phase 1/4 Hp electric motor.
2. Stainless steel cylinders.
3. Flexible coupling.
4. Centrifugal fan with a capacity $300 \text{ ft}^3 \text{ min}^{-1}$.
5. Bottom section of baffle box.
6. Top section of baffle box.
7. Air bath wall (bottom section).
8. Air bath wall (top section).
9. Direction of the air flow set up by the fan.
10. Heating elements.
11. cooling water tube
- 12,13. Glass tubs with thermistors immersed in transformer oil.
14. platinum resistance thermometer probe.

were 90 cm \times 90 cm \times 105 cm. It was constructed 50 cm above the floor, on a rigid frame affixed to the floor. The walls of the bath were made of a 7.5 cm layer of polystyrene foam thermal insulation, covered on either side by aluminium sheet. The edges of the walls were covered by "Hardy Therm" asbestos board. The detachable parts of the walls had silicone rubber seals on the surface to ensure an airtight fit.

The working space in which the instrument was installed was separated by a "baffle box". The "baffle box" was of 61 cm \times 61 cm \times 68 cm, with open top, 7 cm from the walls of the bath. The walls of the baffle box were 7.5 cm thick metal foiled polystyrene foam. The box had two sections: the top and the bottom. The bottom part was fixed to the main body of bath and the top was detachable to provide an access to the apparatus.

The air in the bath was vigorously circulated by a fan in the direction shown by the arrows in Figure 3-4. The fan is a centrifugal blower with a capacity of 300 ft³ min⁻¹ installed inside the bath and driven by an AEI single-phase 1/4 HP electric motor, via a shaft through the base of the air bath. The temperature in the air bath remained 14 K higher than room temperature with the fan on and no other heating. The room temperature was airconditioned at 21 ± 2 °C.

In order to design the heating elements and the water circulated cooler, two sets of observations were made: (1) the temperature in the air bath vs the energy supplied for heating the air bath, and (2) the temperature in air bath vs the time after 100 watts heater was switched on. The results are shown in figure 3-5, and figure 3-6. In these figures, ΔT is the temperature difference between air bath and room. An intercept of about -32 watts was obtained by extrapolating the straight line in figure 3-5, which was the energy produced by the fan. According to the figure 3-6, a 100 watts heater could maintain the temperature in air bath at about 60 °C, and the heat capacity of the air bath was estimated (see appendix 1) and was about 23 kJ K⁻¹. An auxiliary heater of about 200 watts are required in order to heat the air bath to a given temperature within 1 hour. Therefore two 100 watts light bulbs were fixed in the air bath for quick heating.

Twenty pieces of Nichrome Wire were wound around the outside of each baffle sections. Ten of them constituted a half of the base heating element, the rest was a half of the intermittent heating element. They were interleaved with

FIGURE 3-5 ΔT VS W IN AIR BATH

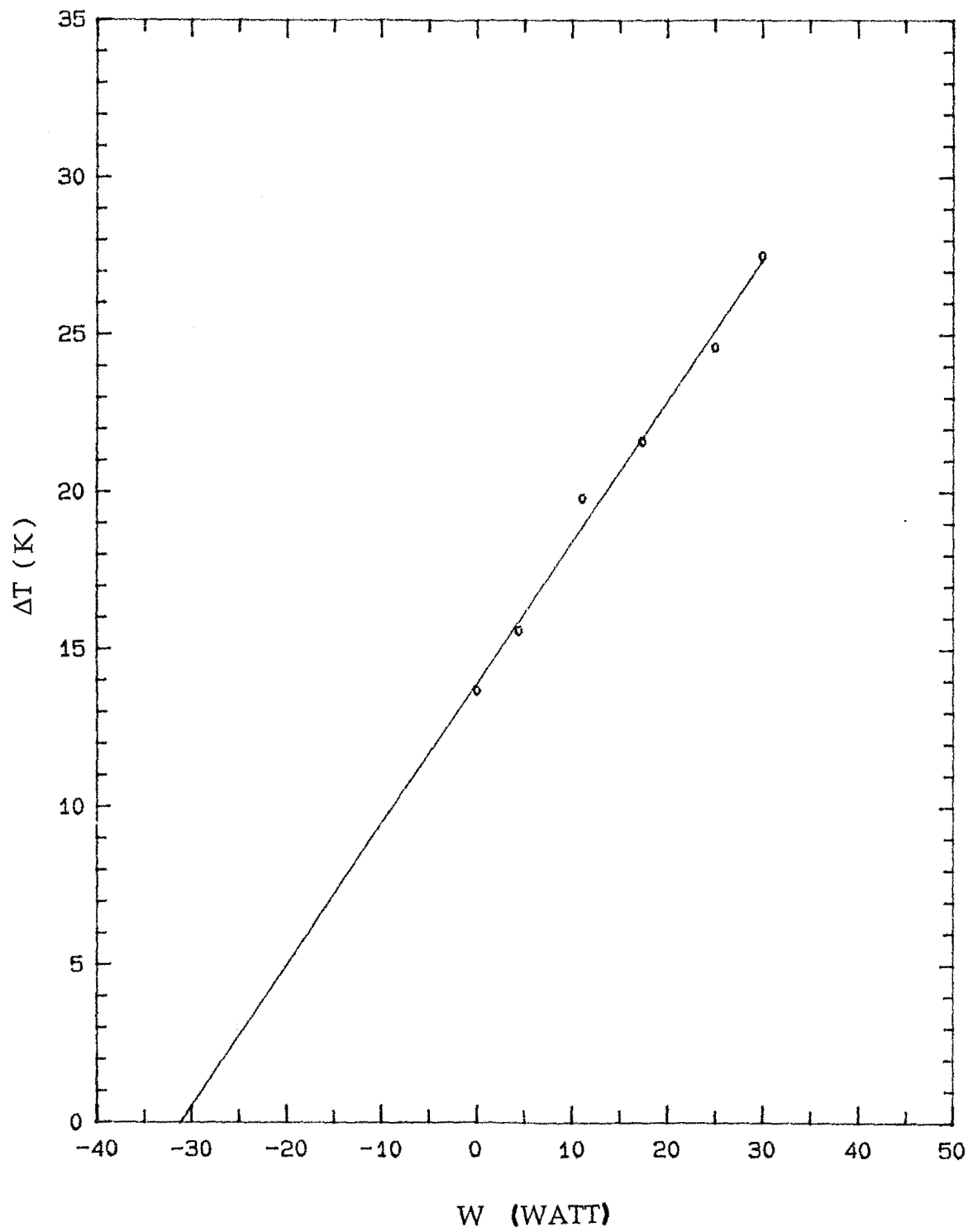
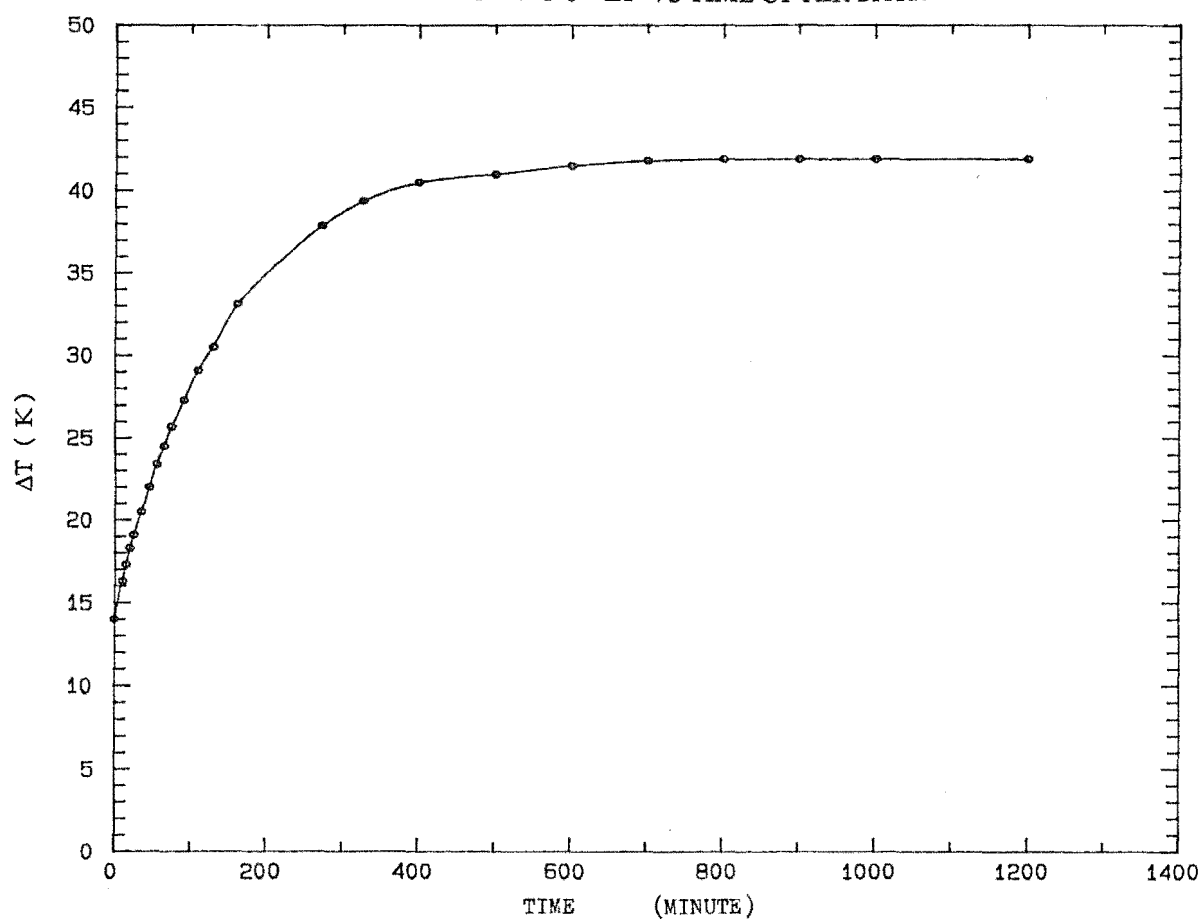


FIGURE 3-6 ΔT VS TIME OF AIR BATH



each other. Each piece of wire was 8.5 m long and was coiled round a 4.7 mm former and stretched out to be 2.5 m long (the circumference of the baffle box). The resistance of each length was approximately 50 ohms. Each ten lengths for each half element in each section were linked in parallel, and the resistance of each block (a half heating element) was 5 ohms. Two blocks of bottom and top sections then were linked in series. The total resistance for each heating element was 10 ohms (see Figure 3-7).

For safety reasons, two transformers were used to reduce the voltage of supply to below 32 v. The maximum energy dissipation for each heating element was 100 watts. With these arrangements, the two elements evenly covered the outside of the baffle boxes to provided a good heat transfer area and an even temperature field inside of the baffle box.

A 15 m long copper tube 0.95 cm in diameter wound around the bottom baffle box was used as a cooler to take the energy of about 32 watts away. The cooling water was circulated by a pump from the cooling water bath.

COOLING WATER BATH

Experiment showed that a temperature change of 0.2 K in the cooling water bath (at 21 °C) caused a temperature change of 0.004 K in the air bath. To provide a temperature stability of ± 0.002 K in the air bath a temperature stability of, at least, about 0.1 K in the cooling water bath should be achieved. The dimensions of the cooling water bath were 30cm x40cm x30 cm and it was insulated with polystyrene foam. A 100 kw heater was used as a heating element. A stirrer was used to produce a vigorous stirring in water bath, and a 5.5 m long, 0.6 cm in diameter coiled copper tube was fixed in the the water bath through which tap water was running . It was used as a cooler in water bath to maintain the temperature in water bath about 2 K lower than room temperature. Two glass tube with 10 k thermistor immersed in transformer oil were put in the water bath. One of the thermistors was used with a temperature controller and the other do record temperature stability. An SCR proportional temperature controller was used to control the temperature in the water bath within ± 0.05 K for both short and long term.

The effect of the set temperature of cooling water bath in the range from 19 °C to 24 °C and the effect of the flow rate of cooling water (at 21°C) in the range of

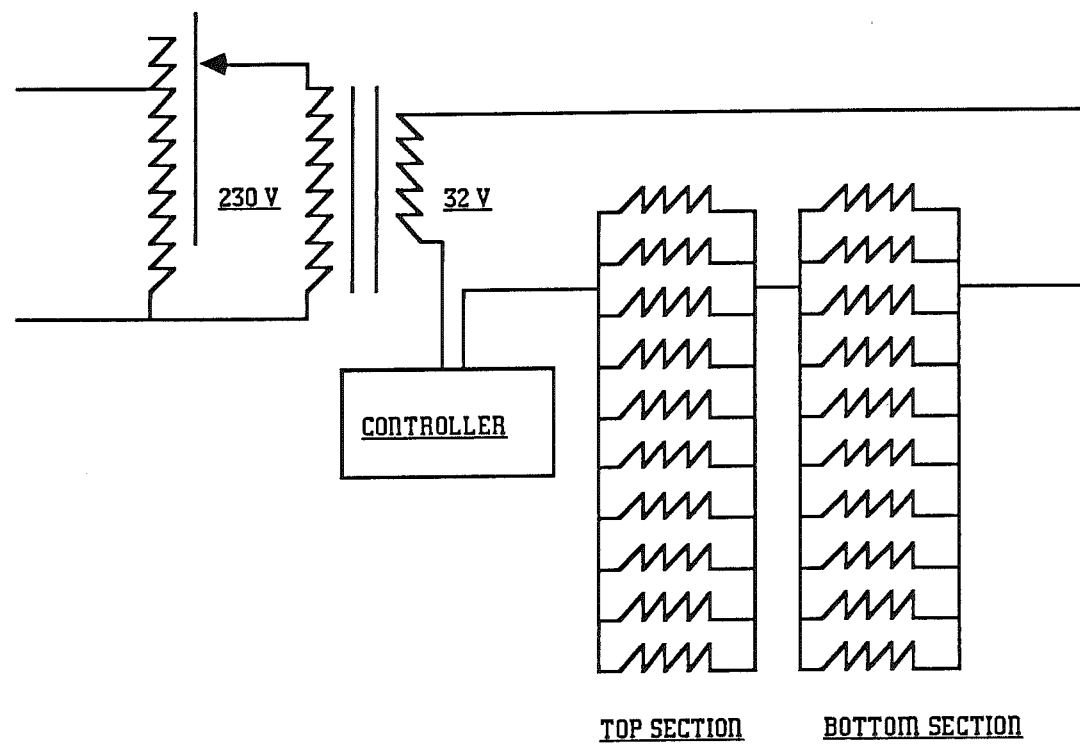


FIGURE 3-7 HEATING ELEMENTS

from $150 \text{ cm}^3 \text{ min}^{-1}$ to $250 \text{ cm}^3 \text{ min}^{-1}$ on the stability of air bath were examined and no observable changes in stability of the air bath were noticed.

TEMPERATURE-CONTROL SYSTEM

The temperature stability in the air bath was maintained by a temperature-control system, which was developed by the department of chemical and process engineering, University of Canterbury. The control system consisted of an on/off controller and an integrating unit. The on/off control was used to control the power delivered to the "intermittent" heating element through a solid state relay, and was adjustable in steps of 1% of the output across the heating element. The adjustment was achieved by adjustment of the fraction of 100 cycles for which the current was supplied to the load in any 2 second period while the controller was in the ON position. The integrating unit was used to adjust the output across the "base" heating element. This was achieved by using the on/off signal of the first unit to control an accumulating counter which counted up when the first unit was in the ON position, and DOWN when the first unit was in the OFF position. A further fine adjustment of the outputs across the two heating elements was achieved by adjustment of the supply voltage in the range of 0-32 volt through two "Variac" autotransformer. The function of the controller system is depicted in figure 3-8.

TEST OF STABILITY AND UNIFORMITY OF TEMPERATURE IN AIR BATH

The air bath was tested at the set temperatures of 298.15 K, 303.15 K, 308.15 K, and 323.15 K. The temperature shift in the air bath in long term was recorded by a chart recorder [servo corder SR 6312] through a null detector [Leeds & Northrup, model CAT 9834], a dc-bridge and a thermistor. The short time temperature fluctuation was recorded by the chart recorder and monitored with a platinum resistance thermometer and a AC bridge [ASL, Model F26] with a resolution of 0.00025 K in temperature measurement. The temperature shift in long term and the temperature fluctuation in short term were less than ± 0.002 K. The temperature differences between several points in the working space in which the vapour pressure cell was to be placed were measured with the platinum resistance thermometer and the ASL Bridge. The temperature gradient in this space was less than 0.002 K. Figure 3-9 shows the temperature stability in

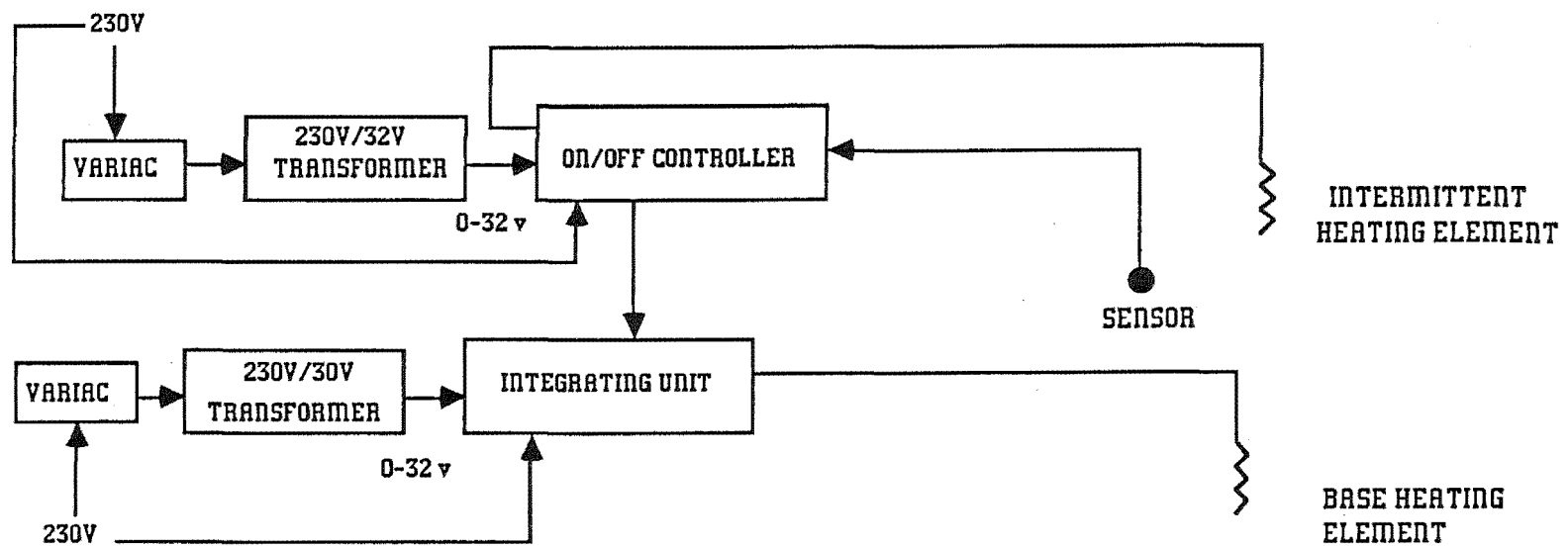
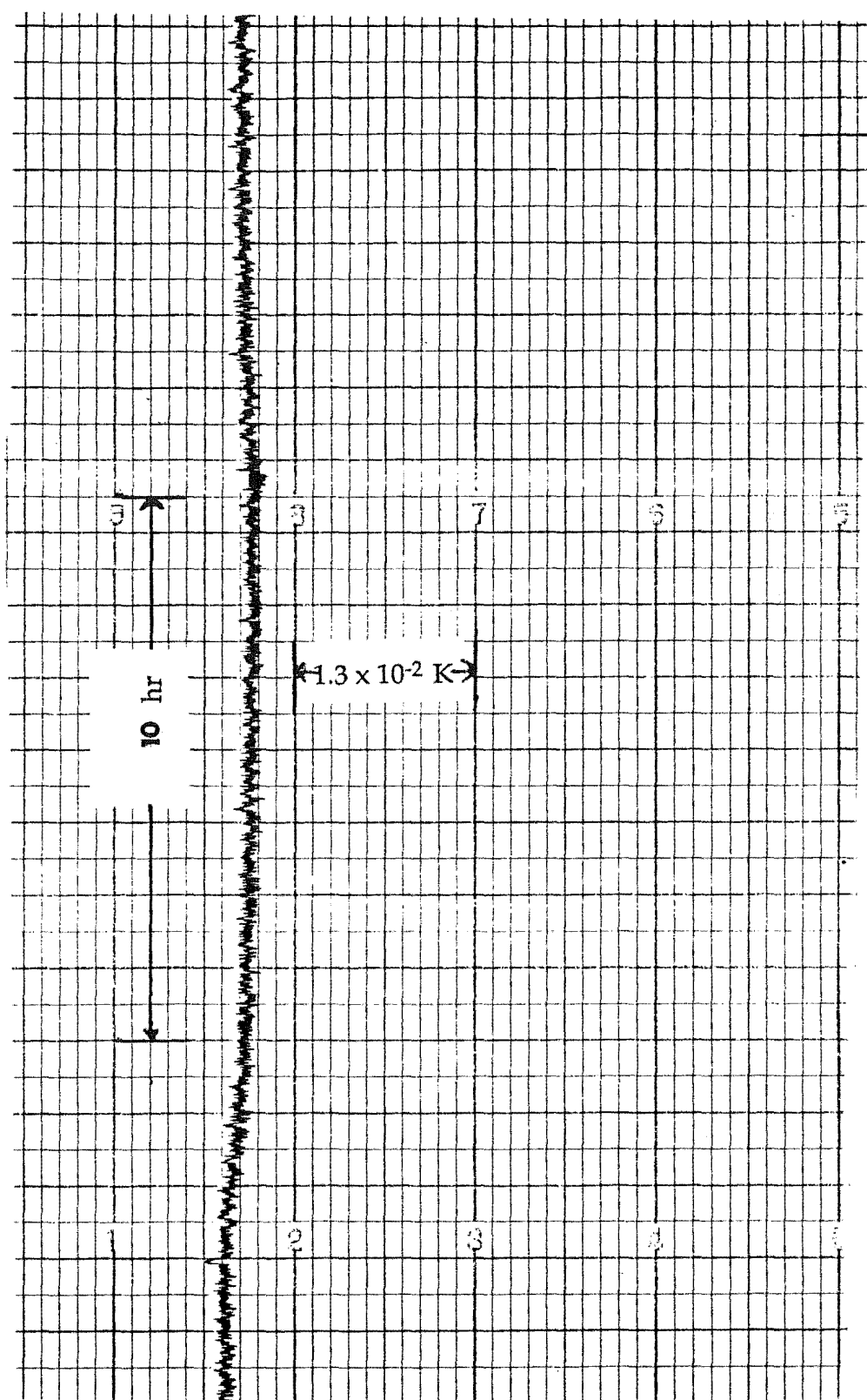


FIGURE 3-8 TEMPERATURE CONTROLLER

FIGURE 3-9 STABILITY OF TEMPERATURE IN AIR BATH



the air bath at 298.15 K.

3-4 TEMPERATURE MEASUREMENT

The temperature in the air bath was measured by a platinum resistance thermometer [Rosemount, model WS104HL, serial No 240] and a precision ac bridge [Rosemount, model VIF 51A-150 or ASL , model F26]. This thermometer was recalibrated by the physical and engineering laboratory, DSIR, NZ. in June, 1985, and checked in this laboratory in November, 1985, and November, 1986. The resistances of this probe at ice point and the boiling point of distilled water are listed in table 3-1. The ice point was carefully established in a Dewar flask, having equilibrium between crushed ice and air-saturated distilled water. The boiling point was established in a hypsometer (Nicholas and White, 1982) and the temperature of the boiling point of water at given pressure was calculated by the Clapeyron-Clausius equation:

$$\ln(p_2/p_1)=\Delta H_v/R (1/T_1-1/T_2) \quad \dots\dots\dots (3-4.1)$$

where, ΔH_v = latent heat of vaporization of water,

$$T_1= 373.15 \text{ K,}$$

$$R= 8.3144,$$

$$P_1= 101325 \text{ pa,}$$

$$P_2= \text{given pressure,}$$

$$T_2= \text{the temperature of boiling point at given pressure.}$$

Table 3-1 The Resistances of Platinum Thermometer (Ω)

	0 °C (Ice point)	99.61 °C (boiling point at 99932 pa)
first check	25.520	
second check	25.519	35.496
reported by DSIR	25.520	35.496

3-5 NITROGEN SUPPLY

The oxygen-free dry nitrogen, which was used to balance the vapour pressure in the vapour pressure cell was supplied by New Zealand Industrial Gases Ltd. The nitrogen gas was taken from the high pressure cylinder and passed via a regulator (V) and a needle control valve (D) into a drying tube packed with dry silica gel. A mercury safety valve (16) was connected between the supply and the rest of the apparatus to guard against over-pressure above one atmosphere. The dried nitrogen then bled through W2, F, and W3 into the Baratron reference side and manometer nitrogen side.

A vacuum pump was used in the nitrogen supply manifold in order to pump out the nitrogen gas without disturbing the main vacuum system. The nitrogen pressure was easily adjusted by valves W1, W2, F, W3. A stainless steel vessel with about 1000 cm³ in volume was connected between W4 and the nitrogen supply line and fixed in the air bath. All the tubes between the W3, Y12, the mercury manometer box, and the air bath were well insulated. With these arrangements the fluctuation of the nitrogen pressure due to the fluctuation of room temperature between two measurements of heights of two mercury levels was less than 10⁻³ mmHg .

3-6 VAPOUR PRESSURE CELL

The vapour pressure cell is shown in figure 3-10. It is 17.5 cm high and about 20 cm³ in internal volume. The cell consists of a "Cajon" fitting, a Nupro valve [model SS-4H], a stainless steel-to-glass joint and a glass cell with a branch tube for loading involatile component and cleaning. All the metal parts were welded together. A stirring bar made of a piece of kovar coated by compatible glass was put in the glass cell before it was joined to the stainless steel-to-glass joint. The stirring bar was actuated by a magnet powered by an electric motor placed in the air bath. There were three seal marks on the branch tube. With N3 closed, the internal volumes of the cell (V_c) up to the three marks were calibrated with distilled water to ± 0.02 cm³. The seal at a mark on the branch tube could result in an error of ± 0.03 cm³ in the internal volume. Thus the total uncertainty in the internal volume of the vapour pressure cell was about ± 0.05 cm³ which could cause an error of $\pm 10^{-4}$ g in calculation of the weight of air filled in the vapour pressure cell. The cell could be used for three measurements before a piece of glass tube with another three marks was joined to the cell and the internal volume was calibrated again. The internal volume of the cell was checked by weighing the evacuated cell and the air-filled cell. The results are shown in table 3-2. In the table, W_e and W_a are the weights of evacuated cell and air-filled cell, respectively, ρ_a is the density of air, V_c is the internal volume of the cell and $\Delta W = W_a - W_e$.

Table 3-2

W_e (g)	W_a (g)	ΔW (g)	$\rho_a V_c$ (g)
169.0901	169.1112	0.0211	0.0210
169.9863	169.9647	0.0216	0.0216
170.3189	170.2985	0.0204	0.0206

The external volume of the cell was calibrated as follows: A beaker contained

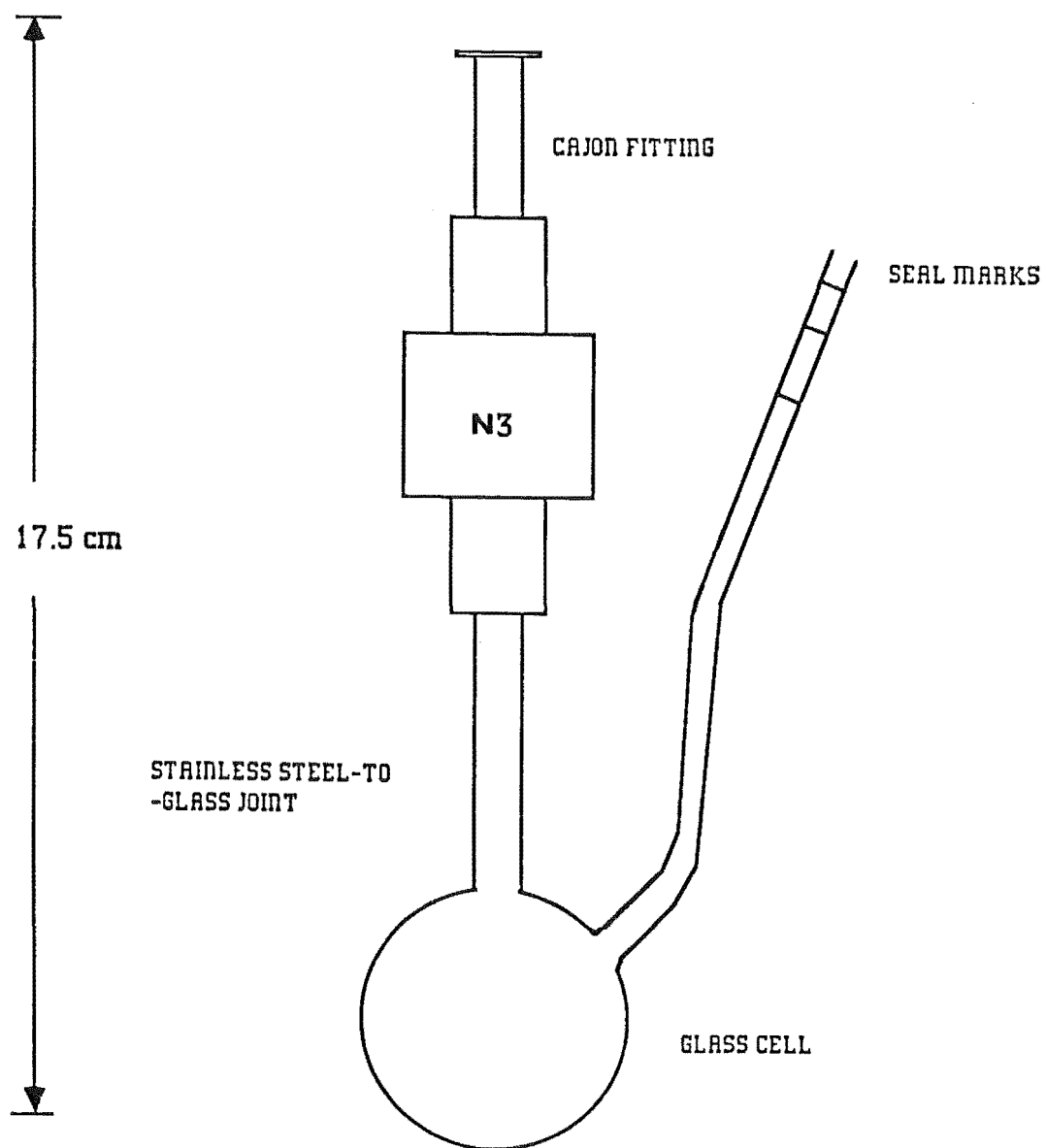


FIGURE 3-10 VAPOUR PRESSURE CELL

distilled water was placed on a balance and the weight was recorded. The cell hung by a piece of thin string was then immersed in the water without touching the beaker. The weight on the balance then recorded again, and the external volume V_s is equal to $\Delta w / \rho_{\text{water}}$ where ρ_{water} is the density of the water and Δw is the difference between the two weighings. The error in determination of the external volume of the cell was estimated by several repeats and was about 2 % of the volume. Because the external volume was used for the buoyancy correction when the empty cell and the cell filled with sample were weighed and the mole fraction was determined, we checked it by weighing the evacuated cell at various densities of the air. The basic equation for determination of the true mass of the cell (empty or filled with sample) with buoyancy correction is:

$$M_s - V_s \rho_a = M_w - V_w \rho_a = M_w (1 - \rho_a / \rho_w) \quad \text{..... (3-6.1)}$$

where M_s = the true mass of the cell, V_s = the external volume of the cell, M_w = the true mass of the weights, V_w = the volume of the weights, ρ_w = the density of the weights.

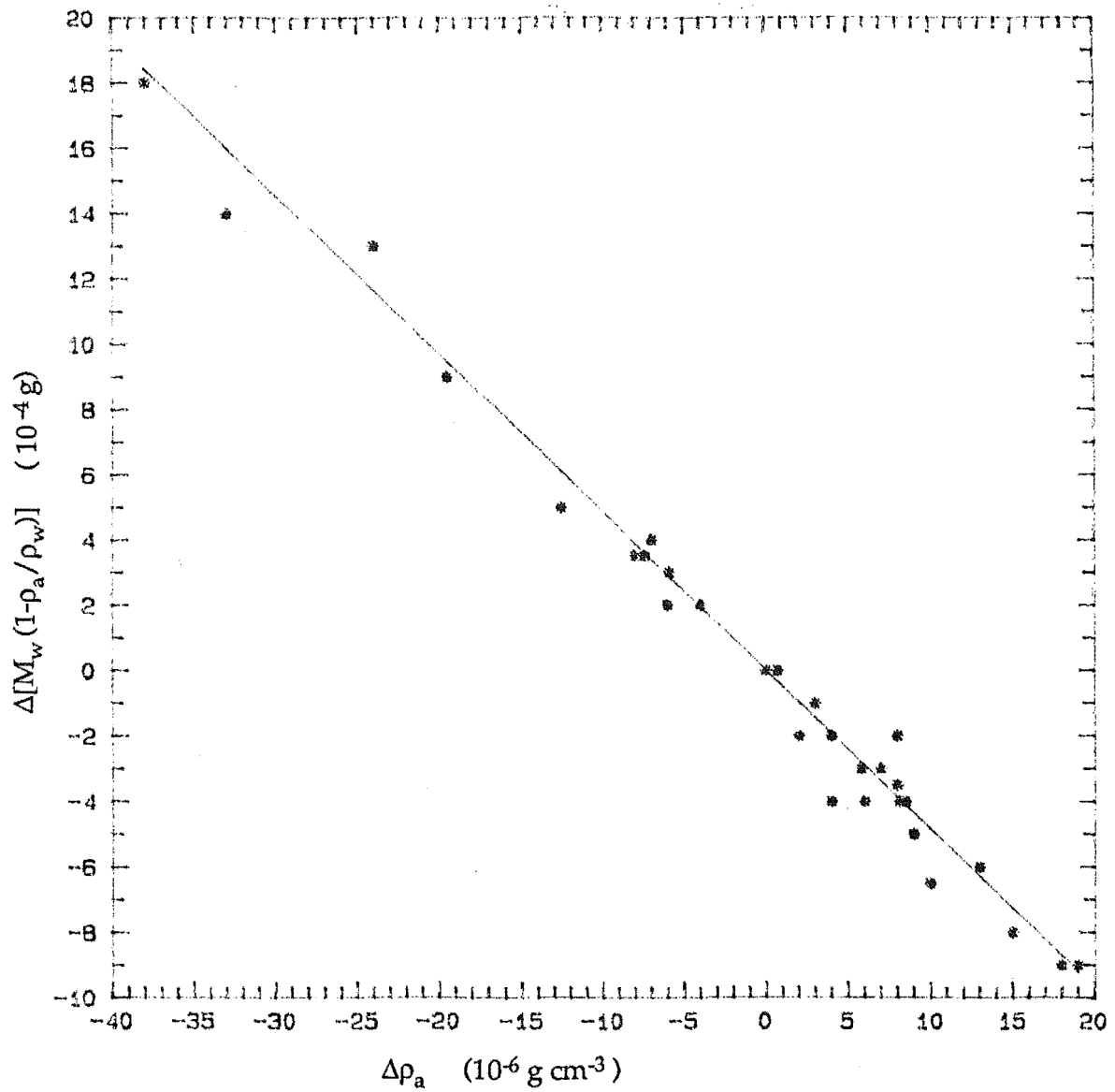
The difference of $M_w (1 - \rho_a / \rho_w)$ for each of two balances is

$$\Delta [M_w (1 - \rho_a / \rho_w)] = - V_s \Delta \rho_a \quad \text{..... (3-6.2)}$$

A straight line through the origin and the external volume of the cell was obtained when the left term in eq. (3-6.2) was drawn vs $\Delta \rho_a$. The results deduced by the method of least squares are shown in the figure 3-11. The discrepancy of the external volumes from the two methods described was about 5 % of the value.

A leak-test of the vapour pressure cell was carried on before it was used in measurements. The clean cell was degassed for one day, then the valve N3 was closed and it was taken off from the vacuum line and laid in air for 7-10 days before it was attached back to the pressure measuring side of the Baratron through a "Cajon" fitting (21). With valve N1 opened the both sides of the Baratron were evacuated to 10^{-5} mbar. The Baratron Zero was set up before valve N1 was closed. Valve N3 was then opened and the Baratron showed the pressure in the cell. The leak-rate was found to be less than 10^{-5} mmHg/hr or 1.33×10^{-3} pa/hr. Because the measurements with a cell never took more than 7 days, the

FIGURE 3-11 BUOYANCY CORRECTION



error due to leakage of air into the vapour pressure cell was less than 0.002 mmhg or 0.3 pa.

3-7 MANIFOLD OF MEASUREMENT SIDE OF BARATRON

The manifold on the measurement side of the Baratron was constructed of two "Nupro" valves (N1, N2), two "Cajon" fittings, and a stainless steel tee pipe. All the parts were welded together. These two "Nupro" valves and a "Whitey" ball valve W4 connected on the reference side of the Baratron were mounted on a rigid steel frame. The frame was fixed in the air bath. These three valves were controlled from outside the air bath. One of the "Cajon" fittings, with a mating half, was connected to the measurement port of the Baratron which was fitted with a Cajon 4VCR fitting and a mating half. The other mating half was welded at the open end of the manifold for connecting the vapour pressure cell. The mating half on the side of the vapour pressure cell was fitted with a split nut, which could be taken off from the cell to allow the cell to be weighed on the balance with a weighing range of 200 g. The valve N2 was always closed before the vapour pressure cell was detached, and opened to allow the section between N2 and N3 to be evacuated after the cell was connected to the manifold. The section had been continuously evacuated for at least 2 hours for degassing before valve N3 was opened. Experiment showed that the pressure in the cell increased due to leaking and, mainly, degassing at the rate of 2×10^{-4} mmHg/hr. The total time when the valve N3 was opened for a series of measurements in a sealed cell was less than 40 hours. It caused a maximum error of about 0.01 mmHg or 1.3 pa in pressure measurement. Therefore the total maximum uncertainty in pressure measurement is 4 pa and the probable uncertainty is 2.8 pa.

The volume of the section between N1, N3, and the diaphragm of the Baratron, V_x , was calibrated as follows:

Both sides of the Baratron were evacuated after an empty vapour pressure cell was connected to the measurement manifold. The null position, the full scale, and the zero of the Baratron were adjusted and set up after the temperature of the air bath achieved a steady state. The valve Y12 was closed and the nitrogen expanded into both sides of the Baratron. Valve N1 then was closed. The air bath was opened to allow valve N3 to be slowly closed before the air bath was closed

again. The pressure in the cell (P_c^1) was measured with the mercury manometer and the Baratron after thermal equilibrium had been achieved in the air bath. Valve N1 was opened and the section to be calibrated then was evacuated and zero of Baratron was set up again. Valve N1 was closed and the air bath was opened once more to allow N3 to be opened and the nitrogen to be expand into the section to be calibrated. The pressure in the section and cell (P_{c+x}^1) was then recorded after the air bath reached steady state. This procedure was repeated several times and a series of values of P_c^n and P_{c+x}^n were obtained. Taking the nitrogen gas as an ideal gas in the pressure range involved in the calibration, we have the equation:

$$V_c/(V_c+V_x) = P_{c+x}^n / P_c^n \quad \dots\dots\dots (3-7.1)$$

where V_c is the internal volume of the vapour pressure cell and n refers to the n th measurement.

Rearrangement of eq. (3-7.1) gives

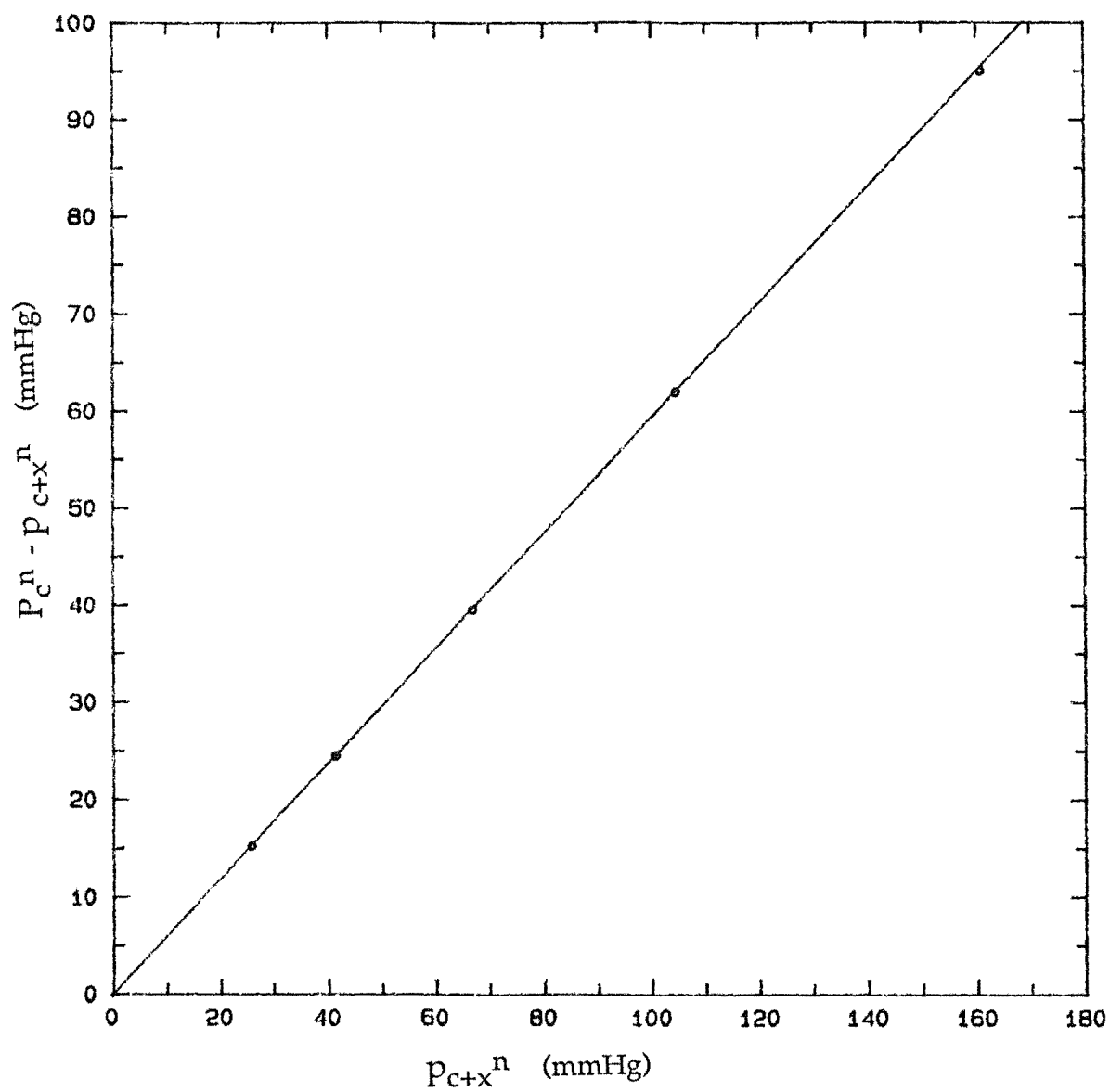
$$P_c^n - P_{c+x}^n = P_{c+x}^n V_x / V_c \quad \dots\dots\dots (3-7.2)$$

A straight line through the origin can be obtained by plotting the left term in eq.(3-7.2) against P_{c+x}^n and the slope of the line is equal to V_x/V_c . The straight line deduced by the method of least squares are shown in the figure 3-12. V_x was calculated from the ratio of V_x and V_c and the value of V_c , that was 10.13 cm^3 . The uncertainty due to this calibration was estimated by three repeats and was 0.03 cm^3 . With the addition of an error of 0.02 cm^3 due to the uncertainty in the volume of the vapour pressure cell the total uncertainty in this volume was about 0.05 cm^3 , and caused a negligible uncertainty in mole fraction of volatile component in liquid phase.

3-8 DEGASSING

The volatile components were degassed in the degassing manifold [(5) in figure

FIGURE 3-12 CALIBRATION OF VAPOUR SPACE



3-1], which is similar to the design of Bell et al. (1968). The degassing unit was evacuated to 10^{-5} mbar and degassed overnight. The sample ampoule filled with volatile component to be degassed was connected to the degassing unit by a teflon joint (14) ["soveril"; type SVC 15]. Taps Y1 and Y2 then were opened. A small quantity of volatile component was boiled off by cautious reduction of the pressure in the ampoule. Liquid nitrogen was then placed in the cold finger of the degasser. The frozen liquid slowly sublimed onto the cold surface of the compartment. During sublimation the system was pumped continuously. This vacuum sublimation was carried for three times before the degassed liquid was distilled into a storage ampoule (7) cooled by liquid nitrogen. The material in the storage ampoule was degassed further by the following procedure: Y3 or Y4 was opened after Y10, Y9, Y2 were closed. Heat was gently applied to the storage ampoule for a few seconds and a small quantity of material was distilled into the space of 6A. Y3 or Y4 was then closed and Y9, Y7 or Y8 were opened to allow the small quantity to be transferred into a glass cell (18) cooled by liquid nitrogen. Then the space was evacuated to 10^{-5} mbar. This procedure was repeated for six times. The efficiency of the degassing procedure was shown by the constancy of the vapour pressure measurements made after successive small amounts of material had been distilled out of the cell during the measurements described in chapter 4. The vapour pressure of the degassed component which had been in the storage ampoule for up to 30 days was measured again. No significant change in pressure was observed.

The involatile component was degassed in the loading manifold. The vapour pressure cell filled with the involatile material was connected to the loading manifold (6B). The magnetic stirrer was turned on so that a strong vortex was formed around the stirring bar. Valve N3 then was slowly opened and the system was pumped at 10^{-5} mbar overnight.

3-9 LOADING MANIFOLD AND PREPARATION OF MIXTURES

The loading manifold consisted of a glass tube (6A) and a stainless steel tube

(6B), joined together through a glass-to-metal joint and separated by tap Y9. Two storage ampoules (7) and a pipette (23) were joined on the glass branch and taps Y3, Y4, Y5 were used to isolate the storage ampoules and the pipette from the glass branch. Three Cajon fittings with female nuts were welded on to the metal branch for the connections of the glass cells and the vapour pressure cells. The glass cell was similar to the vapour pressure cell, but there was a teflon tap, instead of a "Nupro" valve between the glass bulb and the glass-to-metal joint and no glass branch tube on the glass bulb. These glass cells were detachable and easy to clean. In the case that all of the components were volatile, the fluids after measurements were distilled from the vapour pressure cell into a glass cell, and then the glass cell was detached for cleaning. The glass cells also were used for further degassing samples either as described in section 3-7 or by distillations of the sample between the two glass cells before they were distilled into the vapour pressure cell whenever it was necessary. The distillation which is mentioned above and the other places in this section was carried out by cooling with liquid nitrogen the container into which the sample were to be transferred.

The mixtures which consisted of two volatile components were prepared by distillations of two fluids into the vapour pressure cell. The empty clean vapour pressure cell was sealed at a mark on the glass branch tube and connected to the manifold 6B. With valves N3, Y9, Y10 opened, the cell was degassed overnight. Valve N3 was closed, and the cell was detached for weighing. After weighing, the cell was connected back to the loading manifold 6B and the manifold was evacuated to 2×10^{-5} mbar. Valves Y10 and Y9 were closed. With valves Y3 and Y5 opened, an amount of first component 1 was distilled from the storage ampoule into the glass pipette. The amount of component 1 then was adjusted in the pipette by distilling some sample back to storage ampoule or more sample from storage ampoule into the pipette. Valves Y3 and Y5 were closed, and Valves Y9 and Y10 were opened, and the manifold was evacuated to 2×10^{-5} mbar once more. Valve Y10 was closed, and valves Y5, Y9, and N3 were opened. The first component was distilled into the vapour pressure cell. The cell was then detached and weighed after valves Y9 and N3 were closed and the vapour pressure was measured. After the pressure measurement, the cell was immersed in liquid nitrogen for half an hour to condense all the contents on the measurement side of the Baratron into the cell. Valves N2 and N3 were closed

and the cell was detached and weighed to confirm that no loss of the volatile component had been occurred during the measurements. The cell was then attached to the loading manifold and a certain amount of component 2 was adjusted and transferred into the vapour pressure cell as described above to produce the first mixture. After measurement of the vapour pressure of the first mixture, the weight of the cell was checked again and then more component 2 was loaded into the vapour pressure cell to make the second mixture. These operations were continued until the vapour pressure of five mixtures covering about a half of the composition range had been measured. After each loading of the second component, the cell was weighed and the total amount of component 2 instead of the individual additional amount was obtained. This eliminates the accumulated error in weighing.

The procedure for preparation of mixtures which involved an involatile component was as follows: After an empty clean vapour pressure cell was weighed, the involatile component was introduced into the cell by a hypodermic syringe through the branch tube. The cell then was sealed and attached to the loading manifold for degassing. After degassing, valves Y9 and N3 were closed and the cell was detached and weighed and the vapour pressure of the involatile component was measured. The volatile second component was then loaded into the vapour pressure cell to make a series of mixtures in the manner described above.

The ternary mixtures were produced by a series of distillations of the third component into the vapour pressure cell in which a binary mixture had been prepared and its vapour pressure had been measured.

All weighings were done on an electronic analytical balance (Mettler AE 200) with reproducibility of ± 0.1 mg. A silica gel desiccator was kept in the balance case at all times. The cell to be weighed was brought to room temperature, wiped clean with a slightly moist chamois leather cloth and then was placed in the balance case. The balance was calibrated just before the cell was introduced in. Several readings were taken after the cell had been in the balance case for 20 minutes. The temperature in the balance case and the pressure of the atmosphere were recorded for the buoyancy correction. The cell then was removed from the balance pan, and the balance was calibrated again before the cell was weighed once more. Successive weighings usually agreed with their mean to within ± 0.15

mg.

The mass of the component concerned was calculated from

$$M_s = M^f (1 - \rho_a^f / \rho_w) - M^e (1 - \rho_a^e / \rho_w) + (\rho_a^f - \rho_a^e) V_s \dots\dots\dots (3-9.1)$$

where,

M_s = the mass of the component concerned

M^f = the mass of the cell including the component concerned

M^e = the mass of the cell before the component is filled

ρ_a^f, ρ_a^e = the densities of air at the temperatures and the pressures of the weighings

ρ_w = the density of weights which is 8 g cm^{-3}

V_s = external volume of the cell

In determination of the mass of the involatile component, the air-filled empty cell was weighed. The weight of the air (M_a) in the cell, calculated by $M_a = \rho_a V_c$, then was subtracted from the mass of the air-filled empty cell, where V_c is the internal volume of the cell, which was calibrated with distilled water as described in section 3-6.

For the purpose of calculation of the composition of the liquid in the vapour pressure cell, a correction must to make for the amount of volatile component present in the vapour phase. The volume of the vapour phase, V_v which need to be known for this correction was calculated by

$$V_v = V_c + V_x - V_L \dots\dots\dots (3-9.2)$$

The definition and the determination of V_x are given in section 3-7. V_L is the volume of liquid in the cell, and was calculated from the masses and densities of the components at the given temperature. The amount of i th component in the vapour phases in a given experiment was evaluated from

$$n_i = (P_i V_v) / (RT + B_i P_i) \dots\dots\dots (3-9.3)$$

where: P_i = vapour pressure of i th component

V_v = volume of the vapour phase

B_i = second virial coefficient of i th component

R = gas constant

T = absolute temperature

n_i = number of moles of i th component

The mole fraction in the liquid phase was then calculated from the weights of components introduced to the cell corrected as described above for the amounts in the vapour phase. The error in mole fractions will be estimated in chapter 5.

CHAPTER 4 VAPOUR PRESSURES OF PURE COMPOUNDS AND TESTS OF EXPERIMENTAL TECHNIQUES

4-1 INTRODUCTION

The aims of measurements of vapour pressures of pure compounds are :

(1) To compare our measurements of the vapour pressures with published data and use them as a general test of the accuracy of our experimental techniques, of the purity of the components, and of the completeness of degassing.

(2) To test the experimental techniques by examining the reproducibility of vapour pressure measurements.

(3) Examination of the literature shows that inter-laboratory discrepancies in measurements of vapour pressures of pure components from a few Pa to a few tens of Pa. These differences might be due to the errors in measurements of the absolute temperature, the absolute pressure or to sample impurities. Although the individual vapour pressures of a pure compound p^0 and of a mixture p strongly depend on these factors, particularly on temperature, the ratio p/p^0 , which is more closely related to the accuracy in measurement of G^E , is not so dependent. It is therefore important that the vapour pressures of pure components are measured along with the vapour pressures of mixtures and not taken from other sources.

4-2 MATERIALS

The n-hexane was Phillips research grade, 99.99 mol per cent pure, and n-octane and n-hexadecane were from Aldrich, with quoted purities better than 99 per cent. n-octane and n-hexadecane were packaged in bottles with Aldrich sure/seal system. In order to protect these chemicals from exposure to atmospheric moisture or oxygen, a syringe transfer technique described by Lane and Kramer (1977) was used to take samples from the bottles. All the chemicals were dried with 4A molecular sieve and then were distilled into the degassing chamber. The densities of these chemicals were measured with a Mettler DMA60/DMA602 vibrating tube densimeter and are compared with literature values in table 4-1.

Table 4-1 The Density of Chemicals at 298.15 K (g cm^{-3})

Compound	Source			
	This work	(1)	(2)	(3)
n-C6	0.65474	0.65481	0.65484	0.65533
n-C8	0.69841	0.69849	0.69876	0.69876
n-C16	0.76990		0.76994	

- (1) Riddick and Bunger (1970).
 (2) TRC Thermodynamic Tables (1985).
 (3) Hutchings and Hook (1985).

The mercury for the precision manometer was filtered through a sintered filter funnel to remove gross impurities. It was then passed three times in fine droplets through a column 1 m long and 2.5 cm in diameter filled with 13 % nitric acid and three times through 10 % potassium hydroxide, and final three times through distilled water. The mercury then dried in a current of air at 110 °C for at least 2 hours and distilled in vacuum.

4-3 VAPOUR PRESSURES OF PURE COMPONENTS

The vapour pressure of n-hexane at 298.15 K, 303.15 K, 308.15 K, of n-octane at 298.15 K, 303.15 K, and n-hexadecane at 298.15 K, 333.15 K were measured. The time needed to reach equilibrium and the effect of stirring had been examined before the measurements were carried out.

Weclawski and Bylicki (1983) pointed that the thermal steady state in most cases of their experiments was achieved after 2 hrs, and pressure was well stabilized within the next 0.5 hr. Ronc and Ratcliff (1976) found that it usually took 10 to 15 minutes to establish equilibrium in a vapour pressure cell after

each addition of component to form a new mixture. They then stopped the stirrer for an additional 10 to 15 minutes before the pressure was measured. Shen (1981) investigated the time needed to reach equilibrium in VLE experiments and found it was about 2.5 h. Aim (1978) noticed that stirring at 100 rpm was entirely sufficient for homogenization and rapid equilibrium in their experiments and detected an increase of 0.001-0.003 K in temperature in the cell caused by more vigorous stirring.

Our experiments showed that the temperature in the air bath was well stabilized within 1 to 1.5 hr in the temperature range of 298.15 K to 308.15 K and after another 15 to 30 minutes, the pressure in the cell was stable. We switched off the stirrer for 15 minutes before the pressure was measured. A reproducible increase in vapour pressure accompanying the elevation of the steady-state temperature by about 0.007 K due to friction heat by stirring was found. When the pressure in the cell became stable the first measurement was taken. Several pressures were recorded ~~over~~ over a period of at least 2 hrs and an average then was taken as the result of the measurement.

The results are listed and compared with literature values in table 4-2. The vapour pressure of n-hexane measured in this work is in perfect agreement with that recently obtained by Marsh et al (1980a) at 308.15 K, and that obtained by Bell et al. (1968) at 298.15 K. The discrepancies between our measurements and the other literature values varied from 9 to 15 pa. These discrepancies are believed to be caused mainly by absolute temperature measurement, because the agreement of our set temperature with the other authors' could not be expected to be better than ± 0.01 K, which might cause a difference of ± 10 pa in absolute pressure measurement for pure n-hexane. The discrepancies of vapour pressures of n-octane between our and literature values range from 5 to 9 Pa, which cannot be attributed to the different absolute temperature scales. These discrepancies may be due to impurities or to errors in absolute pressure measurement. The excellent agreements of our measurements of n-hexadecane with literature values showed that our technique used for degassing of n-hexadecane is effective.

Table 4-2 Vapour Pressures of Pure Compounds

Compound	Temperature (K)	Pressure (pa)	Source
n-hexane	298.15	20157	this work
		20172	(1)
		20166	(2)
		20153	(3)
	303.15	24933	this work
		24945	(2)
		24947	(4)
	308.15	30567	this work
		30564	(5)
n-octane	298.15	1872	this work
		1867	(1)
		1863	(3)
	303.15	2466	this work
		2460	(2)
n-hexadecane	298.15	0	this work
		0	(4)
	333.15	5	this work
		4	(4)

(1) Riddick and Bunger (1970).

(2) calculated using the Antoine equation and the parameters from (1).

(3) Bell et al. (1968).

(4) Williamson (1957).

(5) Marsh et al. (1980a).

4-4 TESTS OF EXPERIMENTAL TECHNIQUES

A series of measurements of vapour pressures of pure compounds were made in order to test our designed operations.

TEST 1

The degassed n-hexane was transferred from a storage ampoule into the vapour pressure cell. the cell then was detached, weighed, and connected to the measurement side of the Baratron. The vapour pressure was then recorded. The contents in the space of the measurement side of the Baratron were cooled down into the cell with liquid nitrogen. The cell was detached and weighed again before it was connected back to the loading manifold. The contents were distilled into an empty glass cell then distilled back into the vapour pressure cell, and the vapour pressure cell was detached again for weighing and measuring the vapour pressure. The procedure was repeated and the results are shown in table 4-3. No significant change in mass and in vapour pressure due to the transfer were noticed.

TEST 2

The completeness of the degassing and the purities of materials were tested by measurements of vapour pressures after successive small quantities of materials had been distilled out of the cell, and the results listed in table 4-4. These results confirmed the efficiency of our degassing procedure for n-hexane and n-octane.

A slow upward drift in pressure of n-hexadecane due to imperfect degassing was observed by Williamson (1957). Therefore the following test was carried to check the efficiency of the degassing procedure for n-hexadecane. The vapour pressure of n-hexadecane at 298.15 K was measured just after degassing, then valve N3 was closed and the cell was detached. The vapour pressure in the cell was measured again after 10 days. No significant change in vapour pressure was observed.

Table 4-3 Test for Transfer of Sample (n-hexane at 298.15 K)

No of transfer	Pressure (Pa)	Weight (g)	Weight (g)
		before transfer	after transfer
1	20155	169.8862	169.8862
2	20158	169.8865	169.8863
3	20157	169.8864	169.8865
4	20157	169.8862	169.8862

Table 4-4 Test of Completeness Degassing and Purities of Materials (298.15 K)

n-hexane	
Volume in Cell (cm ³)	Pressure (Pa)
2	20157
1.9	20156
1.8	20157
1.4	20157
1	20158
0.9	20156
n-octane	
0.37	1872
0.30	1871
0.14	1872

TEST 3

The measurements of the vapour pressure of n-hexane, n-octane, and n-hexadecane were repeated at various temperatures. The contents in the cell were cooled into the cell from the space of the measurement side of the Baratron with liquid nitrogen and the cell was detached and weighed after each pressure measurement. The results are shown in table 4-5 and table 4-6. No loss of samples during the operations and no hysteresis in pressure measurements due to by raising and lowering temperature were observed.

TEST 4

The vapour pressures of n-hexane and n-octane stored in the storage ampoules for up to 30 days after degassing were measured again and listed in table 4-6. No significant change in vapour pressure was noticed.

A further test was made by measurement of total vapour pressure of the system n-hexane + n-hexadecane at 303.15 K and comparison with literature values and will be described in chapter 6.

Table 4-5 Test of Reproducibility of Pressure Measurements

No	time (day)	Temperature (K)	Pressure (pa)	Weight (g)
n-hexane				
1	1	298.15	20154	169.9863
2	2	298.15	20157	
3	3	298.15	20159	169.9864
4	4	298.15	20153	169.9864
5	5	303.15	24936	169.9866
6	6	303.15	24929	169.9863
7	7	308.15	30567	169.9861
8	8	303.15	24933	
9	9	298.15	20154	169.9862
n-octane				
1	1	303.15	2464	170.0418
2	2	303.15	2468	170.0417
3	3	298.15	1872	170.0419
4	4	298.15	1874	
5	5	298.15	1871	
6	6	298.15	1870	
7	7	303.15	2466	

Table 4-6

No	time (day)	Temperature (K)	Pressure (pa)
n-hexane			
1	1	298.15	20157
2	12	298.15	20152
3	15	298.15	20153
4	30	298.15	20156
n-octane			
1	15	298.15	1872
2	16	303.15	2468
3	30	298.15	1873

CHAPTER 5. THE REDUCTION OF EXPERIMENTAL DATA

5-1 REVIEW OF THE METHODS OF P-X DATA REDUCTION

Several methods have been employed for the calculation of the behaviour of each component in a solution from the total vapour pressure over a composition range of liquid phases (p-X data). Ljunglin and Van Ness (1962) suggested that these methods could be classified into two categories, namely, indirect and direct methods.

5-1.1 INDIRECT METHODS

The indirect methods are the calculation procedures in which the liquid activity coefficients are calculated first by some appropriate means, and subsequently, the vapour compositions are calculated. These methods include those of Barker (1953), Tao (1961), and Mixon-Gumowski-Carpenter (1965).

A BARKER'S METHOD

The first systematic method capable of extracting the best results from given p-x data, with due allowance for vapour phase non-ideality, was described by Barker in 1953. The term Barker's method now is usually used to denote all those reduction methods, which require some analytic expression to give the dependence of excess free energy (G^E) or, more directly, of the activity coefficients (γ_i) of components in liquid phase on liquid compositions. The latter may be derived from the former with the Gibbs-Duhem equation. This method usually is used in the reduction of constant-temperature data because a simplified form of the Gibbs-Duhem equation:

$$d(G^E/RT) = (\ln \gamma_1 - \ln \gamma_2) dx_1 \quad \dots\dots\dots (5-1.1)$$

is less restrictive in the case of constant temperature and leads to a simple expression for $\ln \gamma_i$ depending on the mole fraction of liquid phase only. In equation (5-1.1), R is the gas constant, T is the absolute temperature. The

suitability of an expression of G^E or $\ln \gamma_i$ is important for reducing the experimental data to within their errors. Various equations such as those of Margules (1895), Van Laar (1913), Wilson (1964), Redlich-Kister (1948), Myers-Scott (1963), and Marsh (1977), have been used in this calculation procedure. Plank et al. (1981) and Munjal et al. (1983) compared a number of equations for various systems. The Barker method can be used to test theoretical models and semi-empirical expressions for G^E or $\ln \gamma_i$ by the standard deviations of reduction and some statistical tests. Shen et al. used Barker's method to test a regular associated (1983) and athermal associated model (1981) for systems of some polar solvents + styrene and o-xylene. Nitta and Katayama (1973) used Barker's method to fit p-x data for alcohols + nonpolar substances in a continuous linear association model.

The equation of state used to describe the vapour behaviour affects the results of data reductions. Various equations such as ideal, truncated second virial coefficient, modified Redlich-Kwong (Hamam et al., 1977), Peng-Robinson (1976) equation were used in the data reduction procedure and compared with each other by Plank et al. (1981) and Munjal et al. (1983).

The objective functions and convergence techniques, and the initial value set for the iterative procedure may also affect the results of data reduction.

The computing procedure used for the Barker method requires the input of the vapour pressures of pure components. These were regarded as a physical constant, presumed fixed and known for data taken at constant temperature in previous work. Fabries and Renon (1975) suggested the vapour pressures of pure components be treated as adjustable parameters and Abbott and Van Ness (1977) suggested the vapour pressures of pure components be measured as part of the data of total pressure vs mole fraction and that they be treated in the regression procedure exactly as all the other data points.

The Barker method has been extended to the reduction of p-x data in ternary mixtures. A number of G^E vs x or $\ln \gamma_i$ vs x analytic expressions, such as Wohl, Scatchard, Van Laar, Margules Equations may be extended to ternary mixtures and they are summarized by Hala et al. (1967). A part of the parameters in these equations may be determined by three sets of binary data, and the ternary terms

are then obtained by regression of ternary data. Mcdermott and Ellis (1965) fitted p-x data of the system toluene + n-propanol + 1,2-dichloroethane to the ternary three suffix Margules equation. Abbott et al. (1975) chose an equation similar to that proposed by Wohl (1953) to represent G^E for the ternary system of methanol + chloroform + acetone. Goral et al. (1985) extended the Redlich-Kister equation to ternary mixtures for the same system. In the methods of both Abbott and Goral, three additional parameters were introduced and determined from ternary data, after the "binary" parameters had been obtained from the binary systems. Details of this method of p-x data reduction may be found in sections 5-2, and 5-3.

B. TAO'S METHOD

The basic disadvantage of the Barker approach is the need for the prior assumption of an expression for G^E . This deficiency was recognized by Tao, who presented another indirect method to remove the deficiency.

In the equilibrium of vapour and liquid, the following equation expresses the behaviour of a binary solution:

$$(x_1 p_1^0 / \phi_1 p) (\gamma_1 / \gamma_2) + (x_2 p_2^0 / \phi_2 p) = 1 / \gamma_2 \quad \text{..... (5-1.2)}$$

where ϕ_i is vapour phase activity coefficient of i th component, p_i^0 is the vapour pressure of pure component, and γ_1 and γ_2 are the activity coefficients of the components in the liquid phase. The excess free energy of mixing can be written as:

$$G^E/RT = x_1 \ln \gamma_1 + x_2 \ln \gamma_2 \quad \text{..... (5-1.3)}$$

The Gibbs-Duhem equation for activity coefficients in binary solution (Van Ness, 1964) is

$$\left(\frac{G^E}{RT} \right) \Big|_{x_1''} - \left(\frac{G^E}{RT} \right) \Big|_{x_1'} = \int_{x_1'}^{x_1''} [\ln(\gamma_1 / \gamma_2) + \Gamma] dx_1 \quad \text{..... (5-1.4)}$$

where, $\Gamma = -(\Delta H/RT^2)(\delta T/dx_1)$ for constant pressure data,

$\Gamma = (\Delta V/RT)(\delta p/dx_1)$ for constant temperature data.

$\Delta H, \Delta V$ are the molar integral heat and volume change of mixing respectively.

Assuming small $\Delta x_1 = \epsilon$, $X_1' = (n-1)\epsilon$, $X_1'' = n\epsilon$, the simultaneous equations (5-1.3) and (5-1.4) are solved by the trapezoid integration rule to get another equation for the relationship between γ_1 and γ_2

$$\left(\frac{\gamma_1}{\gamma_2}\right)_{n\epsilon}^{(n-1/2)\epsilon} = \left(1/\gamma_2\right)_{n\epsilon} \left\{ \gamma_1^0 e^{-\epsilon/2} e^{\frac{\epsilon\Gamma_n}{2}} \prod_{k=0}^{n-1} \left[\left(\frac{\gamma_1}{\gamma_2}\right)_{k\epsilon}^{\epsilon} e^{\epsilon\Gamma_k} \right] \right\} \quad \text{..... (5-1.5)}$$

The infinite dilution activity coefficient γ_1^0 in eq. (5-1.5) is obtained from Gautreaux and Coates' equation (Gautreaux and Coates, 1955), with the experimental $(\partial T/\partial x_1)_p$ or $(\partial p/\partial x_1)_T$ at $x_1 = 0$. Combining eq. (5-1.5) and (5-1.2), γ_1/γ_2 , hence γ_1 and γ_2 may be solved by iteration.

Tao's procedure, though indirect, retains the rigour usually associated with the direct method, more precise computation may be carried out conveniently by using smaller Δx_1 in a digital computer. However, this procedure requires input of γ_1^0 which could cause some error in the final results and it appears to be not easy to extend this procedure to ternary systems.

C MIXON-GUMOWSKI-CARPENTER METHOD

Mixon et al. (1965) presented another indirect method that retains the same degree of rigour as Tao's method and the direct method. This method is comparatively easy to generalize to ternary and higher order systems.

Assuming the vapour is an ideal gas, the total vapour pressure P for a system of N components at constant temperature is given by

$$P = \sum_{k=1}^{N-1} x_k P_k^0 \exp \left[Q + \frac{\partial Q}{\partial x_k} - \sum_{i=1}^{N-1} x_i \left(\frac{\partial Q}{\partial x_i} \right) \right] + x_N P_N^0 \exp \left[Q - \sum_{i=1}^{N-1} x_i \left(\frac{\partial Q}{\partial x_i} \right) \right] \quad \text{..... (5-1.6)}$$

where, $Q = G^E/RT$. Equation (5-1.6) can be approximated by its finite difference representation. With lattice interval Δ , $x_i = L\Delta$ and

$$\frac{\partial Q_L}{\partial x_i} = (Q_{L+1} - Q_{L-1})/2\Delta \quad \text{..... (5-1.7)}$$

Equation (5-1.6) becomes

$$p(L) = \sum_{k=1}^{N-1} L_k \Delta P_k^0 \exp \left[Q_L + \frac{Q_{L+1} - Q_{L-1}}{2\Delta} - \sum_{i=1}^{N-1} L_i \Delta \frac{Q_{L+1} - Q_{L-1}}{2\Delta} \right] + L_N \Delta P_N^0 \exp \left[Q_L - \sum_{i=1}^{N-1} L_i \Delta \frac{Q_{L+1} - Q_{L-1}}{2\Delta} \right] \quad \text{..... (5-1.8)}$$

Assuming that one has available the n th estimates of the values of Q , $Q^{(n)}(L)$, at the lattice points. The n th estimated value for vapour pressure, $P^{(n)}(L)$, are calculated from eq. (5-1.8) with the n th estimates of Q appropriately substituted. In general, $P^{(n)}(L)$ will differ from $P(L)$, the experimental vapour pressure, and $Q^{(n)}(L)$ must be incremented to $Q^{(n+1)}(L)$, i.e.,

$$Q^{(n+1)}(L) = Q^{(n)}(L) + q^{(n)}(L) \quad \text{..... (5-1.9)}$$

With Newton's method, an equation related to $q^{(n)}(L)$ can be derived

$$\frac{p^{(n)}(L)}{p(L)} q^{(n)}(L) = 1 - \frac{p^{(n)}(L)}{p(L)} - \sum_{k=1}^{N-1} \left(\frac{p_k^{(n)} - p_k^{id}}{p(L)} \right) \left[\frac{q_{(L+1)}^{(n)} - q_{(L-1)}^{(n)}}{\Delta} \right] \quad \text{..... (5-1.10)}$$

where p_k^{id} is the partial pressure of the k th component in an ideal solution,

$p_k^i = x_k p_k^0$. Equation (5-1.10) can be solved by relaxation techniques.

The Mixon-Gumowski-Carpenter method has been extended to constant pressure data, and non-ideal behaviour of the vapour phase by Nagata and Ohta (1974).

Mixon-Gumowski-Carpenter method needs the p-x values for each lattice point, therefore the smoothed p-x relation needs to be established appropriately before the relaxation procedure starts. Mixon et al. chose ordinary polynomials to fit experimental data. A number of unsuccessful instances of the search for an adequate polynomial representation were found and this handicap was removed by using orthogonal method of curve surface fitting (Nagata and Ohta 1974, Plank et al. 1981).

5-1.2 DIRECT METHOD

The direct method involves calculation of vapour compositions by integration of the coexistence equation, a first-order differential equation derived from the Gibbs-Duhem equation relating phase compositions at equilibrium (Ljunglin and Van Ness, 1962).

The general Gibbs-Duhem equation may be written as:

$$(V/RT)dp + (H^* - H)/RT^2 = X_1 d \ln f_1 - X_2 d \ln f_2 \quad \dots\dots\dots(5-1.11)$$

here, H is the molar enthalpy of the solution, H* is the molar enthalpy of the solution at pressure approaching zero, V is the molar volume of the solution, f_i is the fugacity of component i in solution. Equation (5-1.11) may be used for both liquid and vapour phases and these two resulting equations are easily combined when two phases are at equilibrium. Then the coexistence equation is derived:

$$\Psi dP + \Omega dT = \{(y_1 - x_1) d \ln(\gamma_1^v / \gamma_2^v) + (y_1 - x_1) / [y_1(1 - y_1)]\} dy_1$$

..... (5-1.12)

$$\Psi = (\Delta V^v + X_1 V_1^v + X_2 V_2^v - V^l) / RT, \quad \Omega = -(\Delta H^v + X_1 H_1^v + X_2 H_2^v - H^l) / RT^2$$

where ΔV is the molar volume change of mixing, ΔH is the molar enthalpy of mixing, γ_i is the activity coefficient, x and y are the mole compositions of liquid and vapour phases, the superscripts v and l represent the vapour and liquid

phase, respectively.

Assuming the behaviour of the vapour phase can be described by eq (1-3.7) and (1-3.8) and Let V , instead of V_m used in section 1-3, denote the molar volume, at constant temperature, eq. (5-1. 12) becomes

$$dy_1/dp = [\Psi - (1-2y_1)(y_1-x_1)(\delta_{12}/RT)] / \{[(y_1-x_1)/y_1(1-y_1)] - (y_1-x_1)(2p\delta_{12}/RT)\} \quad \text{..... (5-1.13)}$$

where,

$$\Psi = [(y_1y_2\delta_{12} - V^l + x_1B_{11} + x_2B_{22})/RT] + 1/p \quad \text{..... (5-1.14)}$$

$$\delta_{12} = 2B_{12} - B_{11} - B_{22} \quad \text{.....(5-1.15)}$$

At constant pressure, we have

$$\Omega dT = (y_1 - X_1) d\ln(\gamma_1^v/\gamma_2^v) + (y_1 - X_1) / [y_1(1-y_1)] \quad \text{..... (5-1.16)}$$

Multiplication of eq (5-1.13) by dp/dx_1

$$dy_1/dx_1 = [\Psi - (1-2y_1)(y_1-x_1)(\delta_{12}/RT)] / \{[(y_1-x_1)/y_1(1-y_1)] - (y_1-x_1)(2p\delta_{12}/RT)\} dp/dx_1 \quad \text{..... (5-1.17)}$$

the compositions of vapour are then computed by a numerical integration technique such as the Runge-Kutta method.

As in the Mixon-Gumowski-Carpenter's method, the p - x data need to be fitted before eq. (5-1.17) is integrated. An extension of the spline fit technique was developed by Klaus and Van Ness (1967). The curve obtained by this technique usually gives an excellent representation of the experimental data points and a smooth first derivative.

The direct method is a rigorous one for VLE data reduction, but the numerical integration in this method is often much more troublesome than the other methods. Particularly when the method is applied to ternary systems, the complexities increase from the solution of one first order ordinary differential equation to the simultaneous solution of two first-order partial differential equations.

5-2 STATISTICAL METHODS IN THE TREATMENT OF EXPERIMENTAL DATA

As in Barker's method, in the study on thermodynamics of mixing suitable models of excess functions G^E , H^E , v^E etc are often used to represent the experimental data in order to calculate the value of the thermodynamic properties in the whole range of temperature, pressure, and mole fraction from limited experimental observations. The experimental observations, in fact, almost always have inaccuracies and may be treated as a random sample. Therefore statistical methods have been widely used in the treatment of experimental data.

5-2.1 CURVE FITTING

Assuming that x, y are the properties observed by experiments and y is a function of x we can write

$$y = f(x, c_1, c_2, \dots, c_m) \quad \dots\dots\dots (5-2.1)$$

where c_1, c_2, \dots, c_m are parameters. N sets of observations of x and y may be written as

$$x_1^*, y_1^*; x_2^*, y_2^*; \dots; x_N^*, y_N^*.$$

where $*$ represents the experimental data, and $N > m$.

Curve fitting aims to find the optimal parameters c_1, c_2, \dots, c_m to make the calculated value of y from eq. (5-2.1) as close to that from the measurements as possible. This may be generalized as a optimization procedure to search for a minimum value of a certain objective function:

$$d = d(x_1^*, \dots, x_N^*; y_1^*, \dots, y_N^*; c_1, \dots, c_m)$$

LEAST SQUARES ESTIMATES

Least squares estimates take the sum of $(y_i^o - y_i^*)^2$ of all experimental points as a objective function and let

$$\sum_{i=1}^N (y_i^o - y_i^*)^2 \omega_i = \min \quad \dots\dots\dots (5-2.2)$$

where y_i^0 is calculated from eq. (5-2.1), ω_i is a weighting factor. The conditions which must be satisfied for eq. (5-2.2) are

$$\begin{aligned} \frac{\partial \sum_{i=1}^N (y_i^0 - y_i^*)^2 \omega_i}{\partial c_1} &= \frac{\partial \sum_{i=1}^N (y_i^0 - y_i^*)^2 \omega_i}{\partial c_2} = \\ &\dots\dots\dots = \frac{\partial \sum_{i=1}^N (y_i^0 - y_i^*)^2 \omega_i}{\partial c_m} = 0 \quad \dots\dots (5-2.3) \end{aligned}$$

If all experimental points have the equal weight eq. (5-2.3) becomes

$$\begin{aligned} \frac{\partial \sum_{i=1}^N (y_i^0 - y_i^*)^2}{\partial c_1} &= \frac{\partial \sum_{i=1}^N (y_i^0 - y_i^*)^2}{\partial c_2} = \dots\dots = \\ &= \frac{\partial \sum_{i=1}^N (y_i^0 - y_i^*)^2}{\partial c_m} = 0 \quad \dots\dots (5-2.4) \end{aligned}$$

Calculation of $c_1, c_2, \dots\dots c_m$ now requires the solution of the simultaneous equations (5-2.3), or (5-2.4).

Equation (5-2.2) may be written in matrix form:

$$(Y^* - Y^0)^T W_y (Y^* - Y^0) \Big|_{c=c} = \min \quad \dots\dots (5-2.5)$$

where Y^* , Y , and C are all matrices. W_y is the weight matrix and c is the optimal matrix of c .

$$Y^* = \begin{bmatrix} y_1^* \\ y_2^* \\ \vdots \\ y_N^* \end{bmatrix}, \quad Y^0 = \begin{bmatrix} y_1^0 \\ y_2^0 \\ \vdots \\ y_N^0 \end{bmatrix}, \quad C = \begin{bmatrix} c_1 \\ c_2 \\ \vdots \\ c_m \end{bmatrix} \quad \text{..... (5-2.6)}$$

$$W_y = \begin{bmatrix} \omega_1 & \text{.....} & 0 \\ \vdots & \omega_2 & \vdots \\ 0 & \text{.....} & \omega_N \end{bmatrix} \quad \text{..... (5-2.7)}$$

LINEAR CASE

Let c simply represent c_1, c_2, \dots, c_m , a generalized form of y in this case is

$$y = y(x, c) = y_0(x) + c_1 y_1(x) + c_2 y_2(x) + \dots + c_m y_m(x) \quad \text{..... (5-2.8)}$$

Eq. (5-2.3) may be written in matrix form

$$(F^T W_y F) C = F^T W_y (Y^* - Y^0) \quad \text{..... (5-2.9)}$$

where,

$$\begin{aligned}
 F &= \begin{bmatrix} f_1(x_1) & f_2(x_1) & \dots & f_m(x_1) \\ f_1(x_2) & f_2(x_2) & \dots & f_m(x_2) \\ \vdots & \vdots & & \vdots \\ f_1(x_N) & f_2(x_N) & \dots & f_m(x_N) \end{bmatrix} = \\
 &= \begin{bmatrix} f_{11} & f_{12} & \dots & f_{1m} \\ f_{21} & f_{22} & \dots & f_{2m} \\ \vdots & \vdots & & \vdots \\ f_{N1} & f_{N2} & \dots & f_{Nm} \end{bmatrix} = (f_{ij}) \quad \dots (5-2.10)
 \end{aligned}$$

and $f_{ij} = f_j(x_i) = \partial f(x_i, c) / \partial c_j$. C then may be expressed as

$$C = (F^T W_y F)^{-1} F^T W_y (Y^* - Y^0) \quad \dots (5-2.11)$$

NONLINEAR CASE

The multiple first-order Taylor expansion of $f(x_i, c)$ about c^0 , the initial value or zero-order approximation of c , can be written as

$$y_i = f(x_i, c) = f(x_i, c^{(0)}) + \sum_{j=1}^m (c_j - c_j^{(0)}) \left. \frac{\partial f(x_i, c)}{\partial c_j} \right|_{c_j = c_j^{(0)}} \quad \dots (5-2.12)$$

The first-order approximation of $c^{(1)}$ then is

$$c_j^{(1)} = c_j^{(0)} + \delta_j^{(1)} \quad \dots (5-2.13)$$

Eq. (5-2.13) can also be written in matrix form

$$\mathbf{C}^{(1)} = \mathbf{C}^{(0)} + \delta^{(1)} \quad \text{..... (5-2.14)}$$

The sth-order approximation of \mathbf{C} is

$$\mathbf{C}^{(s+1)} = \mathbf{C}^{(s)} + \delta^{(s+1)} \quad \text{..... (5-2.15)}$$

where δ is a matrix,

$$\delta^{(s+1)} = \begin{bmatrix} \delta^{(s+1)}_1 \\ \delta^{(s+1)}_2 \\ \vdots \\ \delta^{(s+1)}_m \end{bmatrix} \quad \text{..... (5-2.16)}$$

The application of the principle of least squares yields an equation similar to eq. (5-2.11):

$$\delta^{(s+1)} = \left(\mathbf{F}^T \mathbf{W}_y \mathbf{F} \right)^{-1} \mathbf{F}^T \mathbf{W}_y (\mathbf{Y}^* - \mathbf{Y}^0) \Big|_{\mathbf{c}=\mathbf{c}^{(s)}} \quad \text{..... (5-2.17)}$$

With the initial value of $\mathbf{C} = \mathbf{C}^{(0)}$, $\delta^{(1)}$ is calculated by eq. (5-2.17), and $\mathbf{C}^{(1)}$ is then calculated by eq. (5-2.15). This procedure is repeated until the results reach the required accuracy.

The process used in the nonlinear least squares method needs a good initial estimate. The convergence may be very slow or may not occur when a poor initial estimate is input or the normal equations are ill-conditioned. A Modified Newton method and the Gauss- Marquardt method (Anderssen and Osborne, 1969) have been applied to overcome those disadvantages in the standard Newton-Gauss approach.

THE ERROR IN LEAST SQUARES ESTIMATE

According to the principle of propagation of error, the covariance matrix of parameters \mathbf{C} is

$$\mathbf{V}_C = \left[\left(\mathbf{F}^T \mathbf{W}_y \mathbf{F} \right)^{-1} \mathbf{F}^T \mathbf{W}_y \right] \mathbf{V}_y \left[\left(\mathbf{F}^T \mathbf{W}_y \mathbf{F} \right)^{-1} \mathbf{F}^T \mathbf{W}_y \right]^T \quad \text{..... (5-2.18)}$$

where V_y is the covariance matrix.

$$V_y = \begin{bmatrix} \sigma^2(y_1^*) & \text{cov}(y_1^*, y_2^*) & \dots & \text{cov}(y_1^*, y_N^*) \\ \text{cov}(y_1^*, y_2^*) & \sigma^2(y_2^*) & \dots & \text{cov}(y_2^*, y_N^*) \\ \vdots & \vdots & \ddots & \vdots \\ \text{cov}(y_1^*, y_N^*) & \text{cov}(y_2^*, y_N^*) & \dots & \sigma^2(y_N^*) \end{bmatrix}$$

..... (5-2.19)

and $\sigma^2(y_i^*)$ is the variance of the i th experimental observation of y , $\text{cov}(y_i^*, y_j^*)$ is the covariance of the i th and the j th experimental observations of y . Assuming all the experimental points have equal weight, and the accuracy of each measurement is the same with variance σ and independent of the other measurements, then $W_y = E$, the unity matrix, and $V_y = \sigma^2 E$. After some rearrangements Eq. (5-2.18) becomes

$$V_c = (F^T F)^{-1} \sigma^2 \quad \text{..... (5-2.20A)}$$

The covariance matrix of estimated y , V_Y , then is calculated by

$$V_Y = F V_c F^T \quad \text{..... (5-2.20B)}$$

Usually, the diagonal elements in the covariance matrix of V_c and V_Y are regarded as the standard errors in their estimates, σ_c and σ_y . The quantity σ_y is usually smaller than the error in measurement.

Goral and Janaszewski (1977), and Kolasinskan and Oracz (1979) used the covariance matrix to discuss the error in p - x data reduction and the error caused

by vapour nonideality in Barker's method.

OTHER OPTIMAL METHODS

Besides the least squares method, a number of other optimal methods such as the gradient search method, the pattern search method, the complex search method have been used to seek the minimum value of objective functions. Nagahama (1971) compared the converged results of the same experimental data obtained by the means of these methods including nonlinear least squares method. No significant differences were found for the systems investigated.

5-2.2 PRINCIPLE OF MAXIMUM LIKELIHOOD

The least squares method distinguishes between two types of measured variables the independent variables and dependent variables. A basic assumption of this method is that only dependent variables are subject to a random error. This assumption fails to account for the statistical properties of the independent variables, arbitrarily assigning to them a zero standard deviation. Therefore, it does not utilize all the available information in estimating the parameters.

Recently many authors have used the principle of maximum likelihood in data treatment. This principle was first proposed by Fisher (1922). The likelihood function L of a random sample of N independent observations of M variables to be measured is

$$L(X^*, X) = \prod_{i=1}^N f_i(X_i^*, X_i) \quad \text{..... (5-2.21)}$$

where,

X^* : $N \times M$ matrix containing the observations of M variables in N data points.

X : $N \times M$ matrix containing true values of M variables in N data points.

X_i^* : Vector containing the i th row of X^* .

X_i : Vector containing the i th row of X .

f_i Multivariable probability density function of M variables
measured in data point i .

If the fitting equation is able to represent the true value X_i with deviations of an order less than the experimental errors, then the calculated value, $X_i(c)$, from the model equation with the parameter C may be used in eq. (5-2.21) instead of the true values X_i :

$$L(X^*, C) = \prod_{i=1}^N f_i(X_i^*, C) \quad \text{..... (5-2.22)}$$

According to the principle of maximum likelihood, the optimal C is determined by maximizing L with respect to C .

$$L(X^*, C) = \text{Max} [L(X^*, C)] \quad \text{..... (5-2.23)}$$

If the experimental errors display a normal (Gaussian) distribution with zero mean from the true values, the likelihood function may be written as

$$L(X^*, C) = \text{Max} \left\{ (2\pi)^{-N/2M} \prod_{i=1}^N \frac{1}{|V_i|^{1/2}} \exp \left[\frac{-(X_i^* - X_i(c))^T V_i^{-1} (X_i^* - X_i(c))}{2} \right] \right\} \quad \text{..... (5-2.24)}$$

where V_i is variance-covariance matrix of measured variables for the i th observation. Eq. (5-2.24) is equivalent to

$$\sum_{i=1}^N (X_i^* - X_i(c))^T V_i^{-1} (X_i^* - X_i(c)) = \min \quad \text{..... (5-2.25)}$$

Let $r_i = X_i^* - X_i(c)$, which is defined as residuals of observed and calculated values of variables. Then eq. (5-2.25) becomes

$$S = \sum_{i=1}^N r_i^T V_i^{-1} r_i = \min \quad \text{..... (5-2.26)}$$

The minimum S may be found by a Gauss-Newton-Marquardt procedure. All $\partial s / \partial c_j$ are zero for $j=1, \dots, m$, with some constraints due to equilibrium equations. Lagrange's multipliers are used to take these constraints into account. A detailed discussion of the methods for determining the model parameters by maximum likelihood are given by Anderson et al. (1978) and Kemeny et al. (1982).

5-2.3 THE STATISTICAL TEST IN REDUCTION OF EXPERIMENTAL DATA

As it has been pointed in chapter 2, the accuracy of data from p - x data cannot be explored for internal consistency, or thermodynamic consistency, because the Gibbs-Duhem equation must be used to treat the experimental data. The accuracy of these experimental data and the adequacy of the model equation used in data reduction usually are judged by the degree of agreement between the calculated and the experimental total pressure values and various statistical tests.

CHI-SQUARE TEST

Let χ^2 be the sum of weighted squared deviations defined by

$$\chi^2 = \sum_{i=1}^N \frac{[Y_i^* - f(X_i, C_1, C_2, \dots, C_m)]^2}{\sigma_i^2} = \sum_{i=1}^N \frac{r_i^2}{\sigma_i^2} \quad \text{..... (5-2.27)}$$

It has been shown that χ^2 has χ -distribution with ν degree of freedom. Peneloux et al. (1975) have suggested the value of χ^2 obtained from a VLE data set as a test quantity to perform an effective consistency test. If the following is true

$$\chi^2 < \chi_{1-\alpha}^2(\nu) \quad \text{..... (5-2.28)}$$

the data are accepted as a thermodynamically consistent at α significance level.

DETECTION OF SYSTEMATIC ERRORS

If significant systematic errors exist in an experiment or are introduced from an inadequate model equation, the residual r_i will depart from their zero mean value. This can be detected efficiently by a t-test (Kemeny et al., 1982). The test quantity is

$$t = (\bar{r} N^{1/2})/R \quad \text{..... (5-2.29)}$$

$$\bar{r} = (\sum_{i=1}^N r_i)/N, \text{ and } R = [\sum_{i=1}^N (r_i - \bar{r})^2 / (N-1)]^{1/2} \quad \text{.....(5-2.30)}$$

The rejection region on a significance level α is $|t| > t_{1-\alpha/2}(N-1)$

The significant systematic errors also can be revealed by Abbe's test (Linnik, 1961), and a run test (Edgington, 1961).

F-TEST

The significance of a change in the value of an objective function when the model is changed from one to another may be judged by an F-test (Li, 1980; Green and Margerison, 1978)

The test quantity is the ratio of the squares of the standard deviations of the two models.

$$F = R_1^2 / R_2^2 \quad \text{..... (5-2.31).}$$

The criterion of rejection for the hypotheses: $r_1^2 = r_2^2$, where r_1 and r_2 are the variances of model 1 and model 2, respectively, is

$$R_1^2 / R_2^2 > F_{\alpha/2}(v_1, v_2) \text{ or } R_1^2 / R_2^2 < F_{1-\alpha/2}(v_1, v_2) \quad \text{..... (5-2.32)}$$

The criterion of rejection for the hypotheses: $r_1^2 \leq r_2^2$ is

$$R_1^2 / R_2^2 > F_{\alpha}(v_1, v_2) \quad \text{..... (5-2.33)}$$

$F_{\alpha/2}(v_1, v_2)$, $F_{1-\alpha/2}(v_1, v_2)$ and $F_{\alpha}(v_1, v_2)$ are the $\alpha/2$, $1-\alpha/2$, and α quantiles of the F-distribution, respectively, with the degrees of freedom v_1 and v_2 .

The significance of a change in the value of an objective function when the number of parameters is changed in a given model also can be judged by the F-test (Dohnal and Fenclova, 1985).

All the values of the quantiles of these distributions described above with significance levels can be found in statistical tables (Owen, 1962).

5-3. THE METHOD OF DATA REDUCTION USED IN THIS WORK

Barker's method with equal weight for each experimental point is used in the reduction of p-x data in this work. From equations (1-3.9) and (1-3.13) (V_{im}^l is replaced by V_i^l) the total vapour pressure of a multicomponent system may be given by:

$$p = \sum_i \frac{p_i^0 x_i \gamma_i}{\phi_i} \quad \text{.....} \quad (5-3.1)$$

where,

$$\phi_i = \exp \left[\frac{(B_{ii} - v_i^l)(p - p_i^0) + (1/2) p \sum_j \sum_k y_j y_k (2\delta_{ji} - \delta_{jk})}{RT} \right] \quad \text{.....} \quad (5-3.2)$$

Combining eq. (1-3.6A) and (1-3.6B), we have

$$RT \ln \gamma_i = \left[G^E - \sum_{k \neq i} x_k \left(\frac{\partial G^E}{\partial x_k} \right)_{x_1 \neq k, i} \right] \quad \text{.....} \quad (5-3.3)$$

The activity of the i th component in the liquid phase then can be derived from equation (5-3.3) with an expression of G^E on mole fraction. The notation used in the above equations are defined in sections 5-1 and 5-2.

5-3.1 BINARY SYSTEM

The Redlich-Kister equation (R-K equation) for a binary system can be written by

$$G^E / RT = x_1 (1 - x_1) \sum_{L=0}^m A_L (1 - 2x_1)^L \quad \text{.....} \quad (5-3.4)$$

The derivative of G^E with respect to x in eq. (5-3.4), and substitution into eq. (5-3.3), yield, after some rearrangements:

$$\ln \gamma_1 = x_2^2 \left\{ \sum_{L=0}^m [2L A_L x_1 (1-2x_2)^{L-1} + A_L (1-2x_2)^L] \right\} \dots\dots (5-3.5)$$

$$\ln \gamma_2 = x_1^2 \left\{ \sum_{L=0}^m [2L A_L x_2 (1-2x_1)^{L-1} + A_L (1-2x_1)^L] \right\} \dots\dots (5-3.6)$$

The total vapour pressure is given by:

$$P = P_1' \gamma_1 + P_2' \gamma_2 \quad \dots\dots\dots (5-3.7)$$

where,

$$p_1' = p_1^0 x_1 \exp\{[(v_1^L - B_{11})(p - p_1^0) - p\delta_{12} y_2^2] / RT\}$$

$$p_2' = p_2^0 x_2 \exp\{[(v_2^L - B_{22})(p - p_2^0) - p\delta_{12} y_1^2] / RT\} \quad \dots\dots\dots (5-3.8)$$

The partial derivatives of the total vapour pressure, p , with respect to the parameters, A_L , which are required by the calculation procedure in Barker's method, are given as

$$\begin{aligned} \partial p / \partial A_L = P_1' (\partial \gamma_1 / \partial A_L) + P_2' (\partial \gamma_2 / \partial A_L) = P_1' \gamma_1 x_2^2 [2L x_1 (1-2x_2)^{L-1} + (1-2x_2)^L] + \\ + P_2' \gamma_2 x_1^2 [2L x_2 (1-2x_1)^{L-1} + (1-2x_1)^L] \quad \dots\dots\dots (5-3.9) \end{aligned}$$

The mole fractions of the vapour phases may be expressed by the equation:

$$y_1 = \gamma_1 P_1' / p; \quad y_2 = \gamma_2 P_2' / p \quad \dots\dots\dots (5-3.10)$$

The mole fractions in the liquid phases are calculated by using the equations:

$$V_{\text{vapour}} = V_c + V_x - V_{\text{liquid}} \cong V_c + V_x - N_1^{\text{total}} v_1 - N_2^{\text{total}} v_2 \dots\dots\dots (5-3.11)$$

$$N_1^{\text{liquid}} = N_1^{\text{total}} - \gamma_1 p_1' V_{\text{vapour}} / RT$$

$$N_2^{\text{liquid}} = N_2^{\text{total}} - \gamma_2 p_2' V_{\text{vapour}} / RT \dots\dots\dots (5-3.12)$$

$$x_1 = N_1^{\text{liquid}} / (N_1^{\text{liquid}} + N_2^{\text{liquid}}); \quad x_2 = 1 - x_1 \dots\dots\dots (5-3.13)$$

where V_{vapour} , and V_{liquid} are the volumes of vapour phase, liquid phase; V_c and V_x are defined and determined in section 3-9. N_i^{liquid} , N_i^{total} , v_i are the number of moles of the i th component in the liquid phase, the total number of moles of the i th component in the cell and the molar volume of the i th liquid component, respectively.

5-3.2 TERNARY SYSTEM

A form of the Redlich-Kister (R-K) equation for a ternary system which is used for p - x data reduction by Goral et al. (1985) may be written as:

$$G^E / RT = Q^{12} + Q^{13} + Q^{23} + Q^{123} \dots\dots\dots (5-3.14)$$

where,

$$Q^{ij} = (x_i + x_j) x_i x_j \sum_{L=0}^m A_L (1 - 2x_i^*)^L \dots\dots\dots (5-3.15)$$

$$Q^{123} = x_1 x_2 x_3 [c_0 + c_1 (3x_1 - 1) + c_2 (3x_2 - 1)] \dots\dots\dots (5-3.16)$$

and the mole fraction x_i^* is normalized as $x_i^* = x_i / (x_i + x_j)$. Equation (5-3.15) is equivalent to the binary R-K equation (5-3.4), when $x_i + x_j = 1$. Q^{ij} is the binary term corresponding to each binary system, while Q^{123} is the ternary term corresponding to the ternary mixture. let:

$$\{L; i/ij\} = \sum_{L=0}^m A_L (1-2x_i^*)^L = \sum_{L=0}^m A_L [1-2x_i/(x_i+x_j)]^L \quad \text{..... (5-3.17A)}$$

$$\{L-1; i/ij\} = \sum_{L=1}^m A_L L (1-2x_i^*)^{L-1} = \sum_{L=0}^m A_L L [1-2x_i/(x_i+x_j)]^{L-1} \quad \text{..... (5-3.17B)}$$

Taking the derivative of G^E with respect to x in eq. (5-3.14) and substitution into equation (5-3.3) yields:

$$\ln \gamma_i = \ln \gamma_i^{12} + \ln \gamma_i^{13} + \ln \gamma_i^{23} + \ln \gamma_i^{123} \quad \text{..... (5-3.18)}$$

$$\ln \gamma_i^{12} = (x_2^2 + 2x_1x_2x_3)\{L; 1/12\} - 2x_1x_2^2/(x_1+x_2)\{L-1; 1/12\} \quad \text{..... (5-3.19)}$$

$$\ln \gamma_2^{12} = (x_1^2 + 2x_1x_2x_3)\{L; 1/12\} + 2x_1^2x_2/(x_1+x_2)\{L-1; 1/12\} \quad \text{..... (5-3.20)}$$

$$\ln \gamma_3^{12} = -2x_1x_2(x_1+x_2)\{L; 1/12\} \quad \text{..... (5-3.21)}$$

$$\ln \gamma_i^{13} = (x_3^2 + 2x_1x_2x_3)\{L; 1/13\} - 2x_1x_3^2/(x_1+x_3)\{L-1; 1/13\} \quad \text{..... (5-3.22)}$$

$$\ln \gamma_2^{13} = -2x_1x_3(x_1+x_3)\{L; 1/13\} \quad \text{..... (5-3.23)}$$

$$\ln \gamma_3^{13} = (x_1^2 + 2x_1x_2x_3)\{L; 1/13\} + 2x_1^2x_3/(x_1+x_3)\{L-1; 1/13\} \quad \text{..... (5-3.24)}$$

$$\ln \gamma_1^{23} = -2x_2x_3(x_2+x_3)\{L; 2/23\} \quad \text{..... (5-3.25)}$$

$$\ln \gamma_2^{23} = (x_3^2 + 2x_1x_2x_3)\{L; 2/23\} - 2x_2x_3^2/(x_2+x_3)\{L-1; 2/23\} \quad \text{..... (5-3.26)}$$

$$\ln \gamma_3^{23} = (x_2^2 + 2x_1x_2x_3)\{L; 2/23\} - 2x_2^2x_3/(x_2+x_3)\{L-1; 2/23\} \quad \text{..... (5-3.27)}$$

$$\begin{aligned} \ln \gamma_1^{123} = & c_0 (x_2x_3 - 2x_1x_2x_3) + c_1 [(x_2x_3 - 2x_1x_2x_3)(3x_1 - 1) + 3x_1x_2x_3(x_2 + x_3)] + \\ & + c_2 [(x_2x_3 - 2x_1x_2x_3)(3x_2 - 1) - 3x_1x_2^2x_3] \quad \text{..... (5-3.28)} \end{aligned}$$

$$\begin{aligned} \ln \gamma_2^{123} = & c_0 (x_1x_3 - 2x_1x_2x_3) + c_1 [(x_1x_3 - 2x_1x_2x_3)(3x_1 - 1) - 3x_1^2x_2x_3] + \\ & + c_2 [(x_1x_3 - 2x_1x_2x_3)(3x_2 - 1) + 3x_1x_2x_3(x_1 + x_3)] \quad \text{..... (5-3.29)} \end{aligned}$$

$$\ln \gamma_3^{123} = c_0 (x_1x_2 - 2x_1x_2x_3) + c_1 [(x_1x_2 - 2x_1x_2x_3)(3x_1 - 1) - 3x_1^2x_2x_3] +$$

$$+ c_2 [(x_1 x_2 - 2 x_1 x_2 x_3) (3x_2 - 1) + 3 x_1 x_2^2 x_3] \quad \dots\dots\dots (5-3.30)$$

where γ_i^{ij} is the part of total activity of the i th component in the liquid phase

which corresponds to each binary system. γ^{123} is the ternary term, contributed by ternary mixing.

The total vapour pressure, P , is

$$P = p'_1 \gamma_1 + p'_2 \gamma_2 + p'_3 \gamma_3 \quad \dots\dots\dots (5-3.31)$$

where

$$p'_i = p_i^0 x_i \phi_i^{-1} \quad \dots\dots\dots (5-3.32)$$

and

$$RT \phi_1 = \exp \left\{ (B_{11} - v_1^1)(p - p_1^0) + p [y_2^2 \delta_{12} + y_3^2 \delta_{13} + y_2 y_3 (\delta_{12} + \delta_{13} - \delta_{23})] \right\} \quad \dots\dots\dots (5-3.33)$$

$$RT \phi_2 = \exp \left\{ (B_{22} - v_2^1)(p - p_2^0) + p [y_1^2 \delta_{12} + y_3^2 \delta_{23} + y_1 y_3 (\delta_{12} + \delta_{23} - \delta_{13})] \right\} \quad \dots\dots\dots (5-3.34)$$

$$RT \phi_3 = \exp \left\{ (B_{33} - v_3^1)(p - p_3^0) + p [y_1^2 \delta_{13} + y_2^2 \delta_{23} + y_1 y_2 (\delta_{13} + \delta_{23} - \delta_{12})] \right\} \quad \dots\dots\dots (5-3.35)$$

A detailed derivation of equations (5-3.19) – (5-3.30) described above is given in appendix 2. The partial derivatives of the total vapour pressure with respect to the parameter K_L (binary parameter A_L^{ij} or ternary parameter C_L) are calculated by :

$$\partial p / \partial K_L = p'_1 x_1 \gamma_1 (\partial \ln \gamma_1 / \partial K_L) + p'_2 x_2 \gamma_2 (\partial \ln \gamma_2 / \partial K_L) + p'_3 x_3 \gamma_3 (\partial \ln \gamma_3 / \partial K_L) \quad \dots\dots\dots (5-3.36)$$

$$\partial \ln \gamma_i / \partial \ln A_L^{ij} = \partial \ln \gamma_i^{ij} / \partial A_L^{ij} \quad \dots\dots\dots (5-3.37)$$

$$\partial \ln \gamma_i / \partial \ln C_L = \partial \ln \gamma_i^{123} / \partial C_L \quad \dots\dots\dots (5-3.38)$$

$$\begin{aligned} \partial \ln \gamma_1^{12} / \partial A_L^{12} &= (x_2^2 + 2 x_1 x_2 x_3) [1 - 2 x_1 / (x_1 + x_2)]^L - \\ &\quad - 2 L [x_1 x_2^2 / (x_1 + x_2)] [1 - 2 x_1 / (x_1 + x_2)]^{L-1} \quad \dots\dots\dots (5-3.39) \end{aligned}$$

$$\begin{aligned} \partial \ln \gamma_2^{12} / \partial A_L^{12} &= (x_1^2 + 2 x_1 x_2 x_3) [1 - 2 x_1 / (x_1 + x_2)]^L + \\ &\quad + 2 L [x_1^2 x_2 / (x_1 + x_2)] [1 - 2 x_1 / (x_1 + x_2)]^{L-1} \quad \dots\dots\dots (5-3.40) \end{aligned}$$

$$\partial \ln \gamma_3^{12} / \partial A_L^{12} = - 2 x_1 x_2 (x_1 + x_2) [1 - 2 x_1 / (x_1 + x_2)]^L \quad \dots\dots\dots (5-3.41)$$

$$\begin{aligned} \partial \ln \gamma_1^{13} / \partial A_L^{13} = & (x_3^2 + 2 x_1 x_2 x_3) [1 - 2 x_1 / (x_1 + x_3)]^L - \\ & - 2 L [x_1 x_3^2 / (x_1 + x_3)] [1 - 2 x_1 / (x_1 + x_3)]^{L-1} \quad \text{.....} \quad (5-3.42) \end{aligned}$$

$$\partial \ln \gamma_2^{13} / \partial A_L^{13} = - 2 x_1 x_3 (x_1 + x_3) [1 - 2 x_1 / (x_1 + x_3)]^L \quad \text{.....} \quad (5-3.43)$$

$$\begin{aligned} \partial \ln \gamma_3^{13} / \partial A_L^{13} = & (x_1^2 + 2 x_1 x_2 x_3) [1 - 2 x_1 / (x_1 + x_3)]^L + \\ & + 2 L [x_1^2 x_3 / (x_1 + x_3)] [1 - 2 x_1 / (x_1 + x_3)]^{L-1} \quad \text{.....} \quad (5-3.44) \end{aligned}$$

$$\partial \ln \gamma_1^{23} / \partial A_L^{23} = - 2 x_2 x_3 (x_2 + x_3) [1 - 2 x_2 / (x_2 + x_3)]^L \quad \text{.....} \quad (5-3.45)$$

$$\begin{aligned} \partial \ln \gamma_2^{23} / \partial A_L^{23} = & (x_3^2 + 2 x_1 x_2 x_3) [1 - 2 x_2 / (x_2 + x_3)]^L - \\ & - 2 L [x_2 x_3^2 / (x_2 + x_3)] [1 - 2 x_2 / (x_2 + x_3)]^{L-1} \quad \text{.....} \quad (5-3.46) \end{aligned}$$

$$\begin{aligned} \partial \ln \gamma_3^{23} / \partial A_L^{23} = & (x_2^2 + 2 x_1 x_2 x_3) [1 - 2 x_2 / (x_2 + x_3)]^L - \\ & + 2 L [x_2^2 x_3 / (x_2 + x_3)] [1 - 2 x_2 / (x_2 + x_3)]^{L-1} \quad \text{.....} \quad (5-3.47) \end{aligned}$$

$$\partial \ln \gamma_1^{123} / \partial C_0 = (x_2 x_3 - 2 x_1 x_2 x_3) \quad \text{.....} \quad (5-3.48)$$

$$\partial \ln \gamma_2^{123} / \partial C_0 = (x_1 x_3 - 2 x_1 x_2 x_3) \quad \text{.....} \quad (5-3.49)$$

$$\partial \ln \gamma_3^{123} / \partial C_0 = (x_1 x_2 - 2 x_1 x_2 x_3) \quad \text{.....} \quad (5-3.50)$$

$$\partial \ln \gamma_1^{123} / \partial C_1 = (3 x_1 - 1)(x_2 x_3 - 2 x_1 x_2 x_3) + 3 x_1 x_2 x_3 (x_2 + x_3) \quad \text{.....} \quad (5-3.51)$$

$$\partial \ln \gamma_2^{123} / \partial C_1 = (3 x_1 - 1)(x_1 x_3 - 2 x_1 x_2 x_3) - 3 x_1^2 x_2 x_3 \quad \text{.....} \quad (5-3.52)$$

$$\partial \ln \gamma_3^{123} / \partial C_1 = (3 x_1 - 1)(x_1 x_2 - 2 x_1 x_2 x_3) - 3 x_1^2 x_2 x_3 \quad \text{.....} \quad (5-3.53)$$

$$\partial \ln \gamma_1^{123} / \partial C_2 = (3 x_2 - 1)(x_2 x_3 - 2 x_1 x_2 x_3) - 3 x_1 x_2^2 x_3 \quad \text{.....} \quad (5-3.54)$$

$$\partial \ln \gamma_2^{123} / \partial C_2 = (3 x_2 - 1)(x_1 x_3 - 2 x_1 x_2 x_3) + 3 x_1 x_2 x_3 (x_1 + x_3) \quad \text{.....} \quad (5-3.55)$$

$$\partial \ln \gamma_3^{123} / \partial C_2 = (3 x_2 - 1)(x_1 x_2 - 2 x_1 x_2 x_3) - 3 x_1 x_2^2 x_3 \quad \text{.....} \quad (5-3.56)$$

The mole fractions in the vapour phase are given by

$$y_1 = \gamma_1 P'_1 / P; \quad y_2 = \gamma_2 P'_2 / P; \quad y_3 = \gamma_3 P'_3 / P; \quad \text{.....} \quad (5-3.57)$$

The mole fractions in liquid phase are calculated by using the equations:

$$V_{\text{vapour}} = V_c + V_x - V_{\text{liquid}} \equiv V_c + V_x - N_1^{\text{total}} v_1 - N_2^{\text{total}} v_2 - N_3^{\text{total}} v_3 \quad \dots\dots\dots (5-3.58)$$

$$N_1^{\text{liquid}} = N_1^{\text{total}} - \gamma_1 p_1' V_{\text{vapour}} / RT$$

$$N_2^{\text{liquid}} = N_2^{\text{total}} - \gamma_2 p_2' V_{\text{vapour}} / RT$$

$$N_3^{\text{liquid}} = N_3^{\text{total}} - \gamma_3 p_3' V_{\text{vapour}} / RT \quad \dots\dots\dots (5-3.59)$$

$$x_1 = N_1^{\text{liquid}} / (N_1^{\text{liquid}} + N_2^{\text{liquid}} + N_3^{\text{liquid}})$$

$$x_2 = N_2^{\text{liquid}} / (N_1^{\text{liquid}} + N_2^{\text{liquid}} + N_3^{\text{liquid}})$$

$$x_3 = 1 - x_1 - x_2 \quad \dots\dots\dots (5-3.60)$$

The parameter C_L is determined from ternary data, and A_L^{ij} may be obtained from binary data or may, together with C_L , be obtained from binary and ternary data in terms of Barker's method.

5-3.3 THE PROCEDURE OF COMPUTATION

A generalized computation procedure optimizing the parameters and calculating γ_i , y_i , G^E is depicted in figure 5-1.

A set of total vapour pressure (p), vs the mole numbers of components (N_i) measured in experiments, the second virial coefficients (B_{ij}), the molar volumes of liquids (v_i), and the zeroth approximation of parameter vector ($K_L^{s=0}$) are input. The mole fraction is calculated by eq. (5-3.13) for the binary system or (5-3.60) for the ternary system with the approximation of $N^{\text{liquid}} = N^{\text{total}}$ at the start point. With eq. (5-3.5) and (5-3.6) or eq. (5-3.18) - (5-3.30), γ_i is calculated. The zeroth approximation of p_i' is obtained from eq. (5-3.8) or (5-3.32)-(5-3.35) with the assumption $\delta_{ij} = 0$, and is used to calculate y_i by eq. (5-3.10) or (5-3.57).

Substitution of y_i and δ_{ij} into eq. (5-3.8) or eq. (5-3.32) - (5-3.35) leads to more accurate p_i' which is, in turn, used to calculate more accurate y_i . This iteration continues until the difference between the values of two iterations is less than a

controlling quantity d_1 . The mole numbers of the i th components in the liquid phase are calculated from eq. (5-3.11) - (5-3.12) or (5-3.58) - (5-3.59). A higher order of approximation of liquid composition is then estimated and is used to calculate the higher order of approximation of γ_i , p' , y_i , etc. This second iteration is controlled by a quantity d_2 . When the x_i is accurate enough, the second iteration terminates and the total vapour pressure, p , then the residuals, $r = p(\text{calculation}) - p(\text{experiment})$, and the partial derivatives of p with respect to parameters K_L are calculated from (5-3.7) - (5-3.9) or (5-3.31) - (5-3.56). All the matrices described in section 5-2.1 are then computed and δ_L^{s+1} is obtained from eq. (5-2.17), which is compared with the third controlling quantity d_3 to determine whether the third iteration continues. When the change of δ_L^{s+1} is not significant after an iteration, the final γ_i , y_i , G^E , K_L , and the standard deviation, $R = [\sum r_i^2 / (N-m)]^{1/2}$ are computed and the error analysis is carried out. The computer programmes PLVR2 and PLVR3 have been written for carrying this calculation procedure and are given in appendix 3. These programmes and the derivations of the formulae used in the data reduction were checked by repeating the reduction of experimental data from Goral et al. (1985), and are compared in table 5-1, 5-2. Only part of the results of the reduction of p - x data are given in table 5-2, the listed values in table 5-2 being selected at random from the complete set.

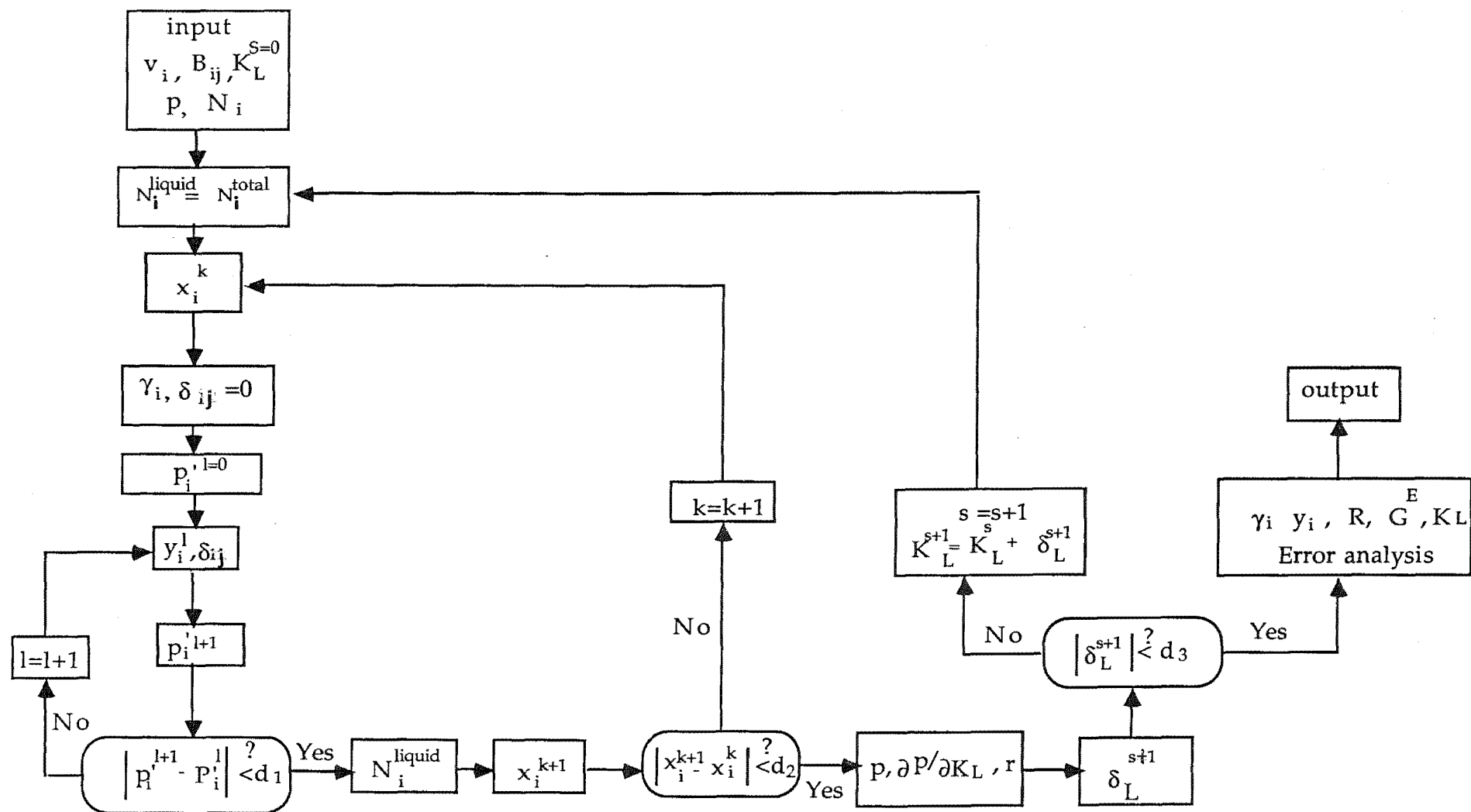


FIGURE 5-1. THE FLOWCHART OF COMPUTATION

Table 5-1 Comparison of Parameters A_L in eq.(5-3.4)
and C_L in eq.(5-3.16) from P-x Data Reductions

L	A_L (Goral et al.)	A_L (this Work)	$\sigma A_L^* (10^{-4})$
methanol + acetone (313.15k)			
0	0.6643	0.6648	6
1	0.01536	0.0147	12.2
2	0.01645	0.0173	27.1
methanol + chloroform (313.15k)			
0	1.2950	1.2972	4.1
1	-0.4911	-0.4921	11.3
2	0.06908	0.06873	29.7
3	-0.1505	-0.1490	31.0
4	0.1218	0.1226	57.3
chloroform + acetone (313.15k)			
0	-0.8981	-0.8979	11.9
1	-0.1753	-0.1754	37.1
2	0.09894	0.09894	44.8
3	0.05305	0.05225	86.4
L	C_L (Goral et al.)	C_L (this Work)	$\sigma C_L^* (10^{-4})$
methanol + chloroform + acetone (313.15k)			
0	0.1340	0.1381	168
1	-0.2229	-0.2268	420
2	-0.4580	-0.4637	330

* : the standard error of parameter A_L or C_L reported by Goral et al.

Table 5-2 Comparison of Mole Fractions of Vapour Phase and Deviations from R-K Equation Using Parameters from Table 5-1

X1	X2	Y1	Y2	r (kpa)	Y1	Y2	r (kpa)
Goral et al					This work		
methanol (1) + acetone (2)							
0.1050		0.1109			0.1110		
0.2056		0.1942			0.1943		
0.3984		0.3250			0.3250		
0.5955		0.4536			0.4535		
0.8968		0.7634			0.7634		
methanol (1) + chloroform (2)							
0.0346		0.1361			0.1361		
0.1683		0.2647			0.2648		
0.3812		0.3290			0.3289		
0.4313		0.3438			0.3436		
0.7692		0.5455			0.5454		
0.8867		0.7232			0.7232		
chloroform (1) + acetone (2)							
0.2082		0.1189			0.1189		
0.2878		0.1844			0.1844		
0.4270		0.3385			0.3385		
0.6381		0.6484			0.6484		
0.8602		0.9120			0.9120		
methanol(1) + chloroform(2) + acetone(3)							
0.0288	0.9232	0.1114	0.8672	0.08	0.1113	0.8673	0.07
0.0736	0.8684	0.1909	0.7858	-0.19	0.1908	0.7859	-0.20
0.1575	0.7785	0.2573	0.7187	-0.16	0.2571	0.7188	-0.17
0.1127	0.5568	0.2088	0.5236	-0.11	0.2089	0.5236	-0.10
0.5309	0.0397	0.4236	0.0336	-0.12	0.4239	0.0337	-0.13
0.0548	0.2709	0.0876	0.1741	0.20	0.0877	0.1741	0.20
0.8691	0.0649	0.7309	0.1367	0.06	0.7309	0.1367	0.05
0.3309	0.0247	0.2882	0.0152	-0.11	0.2881	0.0152	-0.12
0.3285	0.3084	0.3627	0.2823	-0.07	0.3629	0.2824	-0.06
0.2572	0.2414	0.2943	0.1815	-0.11	0.2944	0.1816	-0.12

5-4 ERROR ANALYSIS

5-4.1 UNCERTAINTY IN VAPOUR PRESSURE

(A) Uncertainty due to temperature fluctuation

The dependence of vapour pressure on temperature may be expressed by the Antoine equation:

$$\log p = A - B/(t+C) \quad \text{..... (5-4.1)}$$

where t is Celsius temperature, p is pressure and A , B , C are Antoine equation constants which may be found in the literature (Riddick and Bunger, 1977). The values used in this work are listed in table 7-4.

The uncertainty of pressure δp arising from uncertainty in temperature is

$$\delta p = (\partial p / \partial T) \delta T = (2.303BP / (t+C)^2) \delta T \quad \text{..... (5-4.2)}$$

As described in section 3-3, the temperature fluctuation in the air bath was ± 0.002 K. Therefore, at 298.15 K, the uncertainty in vapour pressure due to the temperature fluctuation calculated by eq. (5-4.4), is $8.6 \times 10^{-5} p$ for n-hexane and $1.1 \times 10^{-4} p$ for n-octane, where p is vapour pressure.

(B) Uncertainty in pressure measurement

As described in section 3-7, the maximum uncertainty in pressure measurement is ± 4 Pa and the probable uncertainty is ± 2.8 Pa.

(C) Uncertainty in mole fraction

The uncertainty in the mole fraction of a mixture in the liquid phase was mainly introduced from the uncertainties in determination of the mass of samples. These uncertainties were produced by weighing, buoyancy correction and determination of mass of air in the vapour pressure cell. As it is shown in figure 3-11, the uncertainty from the first two terms was about 0.2 mg for each weighing. The uncertainty introduced from the third source should be taken into account in the determination of the mass of involatile component, and it

was ± 0.1 mg on average (see section 3-6). As described in section 3-9, two weighings were taken in order to determine the mass of each component. Therefore, the total uncertainty in determination of mass is ± 0.4 mg for a volatile component and 0.5 mg for the involatile component; and the probable uncertainties are 0.28 mg and 0.3 mg, respectively. The mole fraction x_i for a multicomponent system is

$$x_i = (w_i/M_i) / \sum (w_i/M_i) \quad \text{..... (5-4.3)}$$

where w_i and M_i are the mass and mole mass of the i th component. According to the principle of propagation of errors, the probable error in mole fraction may be estimated by

$$(\sigma x_j)^2 = \sum_i \left(\frac{\partial x_j}{\partial w_i} \right)^2 (\delta w_i)^2 + 2 \sum_{i < h} \left(\frac{\partial x_j}{\partial w_i} \right) \left(\frac{\partial x_j}{\partial w_h} \right) [\text{cov}(w_i, w_h)]^2$$

..... (5-4.4)

Because each weighing may be considered as an independent measurement,

$$\text{cov}(w_i, w_h) = 0 \quad \text{and}$$

$$(\sigma x_j)^2 = \sum_i \left(\frac{\partial x_j}{\partial w_i} \right)^2 (\delta w_i)^2 \quad \text{..... (5-4.5)}$$

combining 5-4.3 and 5-4.5, we have

$$\begin{aligned} (\sigma x_j)^2 &= \frac{[(1/M_j) \sum_i w_i/M_i - w_j/M_j]^2 (\delta w_j)^2}{[\sum_i (w_i/M_i)]^4} + \sum_{i \neq j} \frac{[w_j/(M_j M_i)]^2 (\delta w_i)^2}{[\sum_i (w_i/M_i)]^4} \\ &= (x_j - x_j^2)^2 (\delta w_j/w_j)^2 + \sum_{i \neq j} (x_j x_i)^2 (\delta w_i/w_i)^2 \\ &= x_j^2 [(1-x_j)^2 (\delta w_j/w_j)^2 + \sum_{i \neq j} x_i^2 (\delta w_i/w_i)^2] \end{aligned}$$

The probable uncertainty is

$$\sigma x_j = x_j [(1-x_j)^2 (\delta w_j/w_j)^2 + \sum_{i \neq j} x_i^2 (\delta w_i/w_i)^2]^{1/2} \quad \text{..... (5-4.6)}$$

The maximum uncertainty is

$$|\delta x_j| = x_j [(1-x_j) |\delta w_j/w_j| + \sum_{i \neq j} x_i |\delta w_i/w_i|] \quad \text{..... (5-4.7)}$$

For a binary system,

$$\sigma_{x_1} = x_1 x_2 [(\delta w_1/w_1)^2 + (\delta w_2/w_2)^2]^{1/2}$$

and

$$|\delta x_1| = x_1 x_2 [|(\delta w_1/w_1)| + |(\delta w_2/w_2)|] \quad \text{..... (5-4.8)}$$

For a ternary system,

$$\sigma_{x_1} = x_1 [(x_2 + x_3)^2 (\delta w_1/w_1)^2 + x_2^2 (\delta w_2/w_2)^2 + x_3^2 (\delta w_3/w_3)^2]^{1/2}$$

$$|\delta x_1| = x_1 [(x_2 + x_3) |(\delta w_1/w_1)| + x_2 |(\delta w_2/w_2)| + x_3 |(\delta w_3/w_3)|]$$

$$\sigma_{x_2} = x_2 [(x_1 + x_3)^2 (\delta w_2/w_2)^2 + x_1^2 (\delta w_1/w_1)^2 + x_3^2 (\delta w_3/w_3)^2]^{1/2}$$

$$|\delta x_2| = x_2 [(x_1 + x_3) |(\delta w_2/w_2)| + x_1 |(\delta w_1/w_1)| + x_3 |(\delta w_3/w_3)|] \quad \text{..... (5-4.9)}$$

The uncertainty in vapour pressure caused by the uncertainty in mole fraction may be estimated approximately by

$$\delta p = \sum p_i^0 \delta x_i \quad \text{..... (5-4.10)}$$

for a binary system, because of $\delta x_1 = -\delta x_2$

$$\delta p = p_1^0 \delta x_1 - p_2^0 \delta x_2 \quad \text{..... (5-4.11)}$$

For a ternary system, an equation of the type of eq (5-4.4) was used to estimate the probable uncertainty, σp . If $p_3^0 = 0$, then

$$(\sigma p)^2 = (p_1^0)^2 (\delta x_1)^2 + (p_2^0)^2 (\delta x_2)^2 \quad \text{..... (5-4.12)}$$

It should be pointed out that (5-4.12) is not exact because x_1 and x_2 have some negative correlation.

The uncertainty in mole fraction due to the other sources such as the calibration of volume of vapour phase in the vapour pressure cell, and the loss of volatile components during pressure measurements was estimated and believed to be negligible. Table 5-3 and table 5-4 give the estimations of uncertainties in vapour pressure at 298.15 K and a particular composition. These estimations are in a good agreement with the uncertainties observed in the experiments.

Table 5-3 Estimation of Probable Uncertainty in vapour pressure

system	w_1 (g)	w_2 (g)	w_3 (g)	σx_1	σx_2	$\sigma p^{(x)}$ (pa)	$\sigma p^{(T)}$ (pa)	$\sigma p^{(p)}$ (pa)	σp (pa)
0.5 n-c ⁶ + 0.5 n-c ¹⁶	0.3	0.8		2.5×10^{-4}		5.0	0.9	2.8	5.6
0.5 n-c ⁸ + 0.5 n-c ¹⁶	0.5	0.9		1.6×10^{-4}		0.3	0.2	2.8	2.8
0.5 n-c ⁶ + 0.5 n-c ⁸	1.7	2.0		5×10^{-5}		1.0	1.1	2.8	3.2
0.5 n-c ⁶ + 0.25 n-c ⁸ +0.5 n-c ₁₆	0.5	0.3	0.6	1.9×10^{-4}	1.6×10^{-4}	3.8	1.0	2.8	4.8

Table 5-4 Estimation of Maximum Uncertainty in vapour pressure

system	w_1 (g)	w_2 (g)	w_3 (g)	δx_1	δx_2	$\delta p^{(x)}$ (pa)	$\delta p^{(T)}$ (pa)	$\delta p^{(p)}$ (pa)	δp (pa)
0.5 n-c ⁶ + 0.5 n-c ¹⁶	0.3	0.8		3.3×10^{-4}		6.6	0.9	4.0	11.5
0.5 n-c ⁸ + 0.5 n-c ¹⁶	0.5	0.9		2.2×10^{-4}		0.4	0.2	4.0	4.6
0.5 n-c ⁶ + 0.5 n-c ⁸	1.7	2.0		7.6×10^{-5}		1.4	1.1	4.0	6.5
0.5 n-c ⁶ + 0.25 n-c ⁸ +0.5 n-c ₁₆	0.5	0.3	0.6	3.2×10^{-4}	2.5×10^{-4}	6.9	1.0	4.0	11.9

5-4.2 THE UNCERTAINTY IN EXCESS GIBBS ENERGY

The difficulties in estimating the error in excess free energy obtained from reduction of p-x data are due to the application of a partial derivative equation in the data reduction and the dependences of the measured variables in this equation. Some discussions have been made by Goral et al. (1977,1985). For a binary mixture eq. (5-3.1) may be written as

$$p = \sum x_i p_i^0 \exp[(\mu_i^E - d_i) / RT] \quad \text{..... (5-4.13)}$$

where, $\mu_i^E = RT \ln \gamma_i$, and

$$d_i = (p - p_i^0) (B_{ii} - V_i^l) + P \delta_{12} y_i^2 \quad \text{..... (5-4.14)}$$

if $\delta_{12} = 0$, then

$$d_i = (p - p_i^0) (B_{ii} - V_i^l) \quad \text{..... (5-4.15)}$$

In order to examine the effect of the errors in total vapour pressure, pure component vapour pressure, mole fraction, and the second virial coefficient on the G^E , a derivative form of eq. (5-4.13) is written as

$$\begin{aligned} \delta p = & \sum x_i p_i^0 \exp[(\mu_i^E - d_i) / RT] \delta \mu_i^E / RT - \sum x_i p_i^0 \exp[(\mu_i^E - d_i) / RT] \delta d_i / RT \\ & + \sum p_i^0 \exp[(\mu_i^E - d_i) / RT] \delta x_i + \sum x_i \exp[(\mu_i^E - d_i) / RT] \delta p_i^0 \end{aligned} \quad \text{..... (5-4.16)}$$

dividing both sides of eq. (5-4.16) by p, and after some rearrangements, we obtain

$$\begin{aligned} \sum y_i \delta \mu_i^E / RT = & \delta p / p - \sum p_i^0 \exp[(\mu_i^E - d_i) / RT] \delta x_i / p + \sum y_i \delta d_i / RT - \\ & - \sum x_i \exp[(\mu_i^E - d_i) / RT] \delta p_i^0 / p \quad \text{..... (5-4.17)} \end{aligned}$$

The first two terms on the right side in eq. (5-4.17) have been estimated in a previous section and we use δQ_1 to represent them. The third and the fourth terms δQ_2 and δQ_3 may be estimated as follows:

$$\delta Q_2 = \sum y_i \delta d_i / RT \quad \text{..... (5-4.18)}$$

Taking the derivative of equation (5-4.15) and substituting into equation (5-4.18), yield

$$\delta Q_2 = \sum y_i (p - p_i^0) \delta B_{ii} / RT \quad \text{..... (5-4.19)}$$

and

$$\delta Q_3 = - \sum x_i \exp [(\mu_i^E - d_i) / RT] \delta p_i^0 / p \quad \text{..... (5-4.20)}$$

The quantity $\exp [(\mu_i^E - d_i) / RT]$ is close to 1 for the systems investigated in this work, therefore

$$\delta Q_3 \approx - \sum x_i \delta p_i^0 / p \quad \text{..... (5-4.21)}$$

The derivative of eq. (5-3.3) is

$$\delta \mu_i^E = RT \delta \ln \gamma_i = \delta G^E - \sum [x_i \delta (\partial G^E / \partial x_i) + (\partial G^E / \partial x_i) \delta x_i] \quad \text{..... (5-4.22)}$$

The term on the left side of eq. (5-4.17) is

$$\sum y_i \delta \mu_i^E / RT = \delta G^E / RT + \sum y_i \{ \sum [x_i \delta (\partial G^E / \partial x_i) + (\partial G^E / \partial x_i) \delta x_i] \} \quad \text{..... (5-4.23)}$$

At the maximum in G^E , $(\partial G^E / \partial x_i) = 0$, and $\delta (\partial G^E / \partial x_i) \approx 0$, so that

$$\delta G^E / RT \approx \sum y_i \delta \mu_i^E / RT \quad \text{..... (5-4.24)}$$

In an experiment, almost always the precision of measurement is better and easier to determine than is the accuracy of measurement. The error in excess Gibbs energy, G^E , due to inaccuracies of measurements of absolute pressure and temperature, is systematic. We use δQ_4 to represent this part of the contribution to the total error and neglect the effects of these inaccuracies on x and d in eq. (5-4.17) to get

$$\begin{aligned} \delta Q_4 &\approx \delta p / p - \sum x_i \exp [(\mu_i^E - d_i) / RT] \delta p^0 / p \\ &= \{ 1 - \sum x_i \exp [(\mu_i^E - d_i) / RT] \} \delta p^* / p \quad \text{..... (5-4.25)} \end{aligned}$$

where δp^* is the total error in the vapour pressure introduced from the inaccurate absolute pressure and temperature measurements. For the systems studied in this work, the value of $\{ 1 - \sum x_i \exp [(\mu_i^E - d_i) / RT] \}$ is usually less than 0.05. The probable error in G^E can then be calculated by

$$\sigma G^E = RT [(\delta Q_1)^2 + (\delta Q_2)^2 + (\delta Q_3)^2 + (\delta Q_4)^2]^{1/2} \quad \text{..... (5-4.26)}$$

and the maximum error in G^E can be calculated by

$$|\delta G^E| = RT (|\delta Q_1| + |\delta Q_2| + |\delta Q_3| + |\delta Q_4|) \quad \text{..... (5-4.27)}$$

Taking $\delta B_{ii} = 3 \times 10^{-5} \text{ m}^3 \text{ mol}^{-1}$, $\delta p^* = 20 \text{ pa}$ and δp_i^0 as the sum of the uncertainty in pressure measurement and the the uncertainty produced by variation of the temperature, the errors for the systems of n-hexane + n-hexadecane, n-hexane + n-octane and n-hexane + n-octane + n-hexadecane at 298.15 K and given composition were estimated and are listed in table 5-5. The estimated errors in G^E for the systems of n-octane + n-hexadecane was up to 10 J mol^{-1} due to the low total vapour pressure. As described in section 5-2, it can be expected that the statistical treatments should yield the smaller deviations of the total vapour pressures hence smaller estimated errors in G^E and this will be discussed in chapter 6.

5-4.3 THE ERROR OF OPTIMAL PARAMETERS

Taking the standard deviation, R , in fitting the experimental data with Barker's method as the total error, then R , instead of σ in eq. (5-2.20A), may be used to estimate the error of parameters. Neglecting the correlations between the parameters, the error in G^E can be calculated by

$$\sigma G^{E(i)} / RT = \{(x_i + x_j) \sum_{L=0}^m [x_i x_j (1-2x_i)^L \delta A_L]^2\}^{1/2} \quad \text{..... (5-4.28)}$$

$$\sigma G^{E(123)} / RT = x_1 x_2 x_3 [(\delta c_0)^2 + (3x_1-1)^2 (\delta c_1)^2 + (3x_2-1)^2 (\delta c_2)^2]^{1/2} \quad \text{..... (5-4.29)}$$

The procedure for estimation of σA_i and σc_i and corresponding σG^E was set in programme PVLR2 and PVLR3.

Table 5-5. Estimation of Error in G^E at 298.15 K

i	$ \delta Q_i (10^{-4})$	$ \delta G_i^E (J mol^{-1})$
0.5 n-hexane + 0.5 n-hexadecane		
1	5.6	1.4
2	1.2	0.3
3	1.5	0.4
4	1	0.2
maximum	9.3	2.3
probable	6.0	1.4
0.5 n-hexane + 0.5 n-octane		
1	3.2	0.8
2	1.2	0.3
3	1.4	0.3
4	1	0.2
maximum	6.8	1.6
probable	3.9	0.9
0.5 n-hexane + 0.25 n-octane + 0.25 n-hexadecane		
1	4.8	1.2
2	1.2	0.3
3	1.5	0.4
4	1	0.2
maximum	8.5	2.1
probable	5.3	1.3

CHAPTER 6 THE EXPERIMENTAL RESULTS OF VAPOUR LIQUID EQUILIBRIUM

6-1 GENERAL DESCRIPTION

Fourteen series of measurements were made on binary mixtures of n-hexane + n-hexadecane (system 1), n-hexane + n-octane (system 2), n-octane + n-hexadecane (system 3); and ternary mixtures of n-hexane + n-octane + n-hexadecane (system 4). As is described in section 3-9, in each series of a binary system, the amount of one component in the vapour pressure cell was constant, and the composition of the mixture was varied by distillation of quantities of the other component. The component remaining constant is n-hexadecane for systems 1 and 3; n-octane for series 3 of system 2, and n-hexane for series 4 of system 2. For the ternary system, a binary mixture of n-octane + n-hexadecane with a particular composition was prepared and remained constant in the cell while a series of distillations of n-hexane was made to form a series of mixtures. The total amounts of each component in the cell in each experiment are shown in table 6-1. In calculating the number of moles from the masses, the values $86.178 \text{ g mol}^{-1}$, $114.233 \text{ g mol}^{-1}$ and $226.449 \text{ g mol}^{-1}$ were used for the molar masses of n-hexane, n-octane, n-hexadecane, respectively.

The vapour pressures at 298.15 K for the mixtures of the four systems were measured. As a further test of our experimental techniques, the vapour pressures of system 1 at 303.15 K also were measured and compared with the literature values.

As in the measurement of vapour pressures of pure components, the pressure in the vapour pressure cell for a mixture became steady within 2 hours after the air bath had been closed. The first measurement was made after the stirrer had been switched off for 15 minutes. Several measurements then were made over a period of at least 3 hours, and an average was taken as the result. After each sequence of measurements of each mixture, the cell was cooled with liquid nitrogen and detached and weighed before the next loading. For the ternary system, the vapour pressure of each binary mixture of n-octane + n-hexadecane

Table 6-1 Amounts of Materials Used in Measurements

Series No	Run No	n_{C-6} (mole)	n_{C-8} (mole)	n_{C-16} (mole)
System 1				
1	1-2	2.7873×10^{-3}		0.022896
	3-4	6.0282×10^{-3}		0.022896
	5-6	0.010145		0.022896
	7-8	0.015002		0.022896
	9-10	0.022816		0.022896
System 2				
2	1-2	3.6448×10^{-3}		3.5464×10^{-3}
	3-4	5.9064×10^{-3}		3.5464×10^{-3}
	5-6	8.6407×10^{-3}		3.5464×10^{-3}
	7-8	0.014464		3.5464×10^{-3}
	9-10	0.030090		3.5464×10^{-3}
System 2				
3	1	2.5053×10^{-3}	0.017298	
	2	4.9792×10^{-3}	0.017298	
	3	8.5381×10^{-3}	0.017298	
	4	0.012965	0.017298	
	5	0.019391	0.017298	
System 3				
4	1	0.018589	2.1360×10^{-3}	
	2	0.018589	4.4506×10^{-3}	
	3	0.018589	7.9872×10^{-3}	
	4	0.018589	0.013019	
	5	0.018589	0.020081	
System 3				
5	1		2.0344×10^{-3}	0.017331
	2		4.3788×10^{-3}	0.017331
	3		8.0441×10^{-3}	0.017331
	4		0.011258	0.017331
	5		0.016623	0.017331
	6		0.025456	0.017331

Table 6-1 Continued

Series No	Run No	n_{C-6} (mole)	n_{C-8} (mole)	n_{C-16} (mole)
6	1		3.9446×10^{-3}	3.8963×10^{-3}
	2		9.0105×10^{-3}	3.8963×10^{-3}
	3		0.015245	3.8963×10^{-3}
	4		0.033969	3.8963×10^{-3}
System 4				
7	1		3.4698×10^{-3}	7.4162×10^{-3}
	2	1.6981×10^{-3}	3.4698×10^{-3}	7.4162×10^{-3}
	3	3.1377×10^{-3}	3.4698×10^{-3}	7.4162×10^{-3}
	4	4.8913×10^{-3}	3.4698×10^{-3}	7.4162×10^{-3}
	5	7.1236×10^{-3}	3.4698×10^{-3}	7.4162×10^{-3}
	6	0.010186	3.4698×10^{-3}	7.4162×10^{-3}
8	1		1.0277×10^{-3}	2.5405×10^{-3}
	2	3.7144×10^{-3}	1.0277×10^{-3}	2.5405×10^{-3}
	3	5.2914×10^{-3}	1.0277×10^{-3}	2.5405×10^{-3}
	4	8.1122×10^{-3}	1.0277×10^{-3}	2.5405×10^{-3}
	5	0.014508	1.0277×10^{-3}	2.5405×10^{-3}
	6	0.032512	1.0277×10^{-3}	2.5405×10^{-3}
9	1		0.011978	0.012065
	2	2.8963×10^{-3}	0.011978	0.012065
	3	5.9992×10^{-3}	0.011978	0.012065
	4	0.010779	0.011978	0.012065
	5	0.015948	0.011978	0.012065

Table 6-1 Continued.....

Series No	Run No	n _{C-6} (mole)	n _{C-8} (mole)	n _{C-16} (mole)
10	1		2.5676x10 ⁻³	2.7079x10 ⁻³
	2	5.8737x10 ⁻³	2.5676x10 ⁻³	2.7079x10 ⁻³
	3	8.5008x10 ⁻³	2.5676x10 ⁻³	2.7079x10 ⁻³
	4	0.012942	2.5676x10 ⁻³	2.7079x10 ⁻³
	5	0.021726	2.5676x10 ⁻³	2.7079x10 ⁻³
	6	0.044962	2.5676x10 ⁻³	2.7079x10 ⁻³
11	1		2.5536x10 ⁻³	1.1550x10 ⁻³
	2	3.5750x10 ⁻³	2.5536x10 ⁻³	1.1550x10 ⁻³
	3	5.6836x10 ⁻³	2.5536x10 ⁻³	1.1550x10 ⁻³
	4	8.5186x10 ⁻³	2.5536x10 ⁻³	1.1550x10 ⁻³
	5	0.015176	2.5536x10 ⁻³	1.1550x10 ⁻³
	6	0.032785	2.5536x10 ⁻³	1.1550x10 ⁻³
12	1		0.010724	4.7653x10 ⁻³
	2	2.1187x10 ⁻³	0.010724	4.7653x10 ⁻³
	3	4.0962x10 ⁻³	0.010724	4.7653x10 ⁻³
	4	7.1387x10 ⁻³	0.010724	4.7653x10 ⁻³
	5	0.010065	0.010724	4.7653x10 ⁻³
	6	0.015196	0.010724	4.7653x10 ⁻³

Table 6-1 Continued.....

Series No	Run No	n _{c-6} (mole)	n _{c-8} (mole)	n _{c-16} (mole)
13	1		1.7508x10 ⁻³	0.012990
	2	1.8384x10 ⁻³	1.7508x10 ⁻³	0.012990
	3	3.9709x10 ⁻³	1.7508x10 ⁻³	0.012990
	4	6.6363x10 ⁻³	1.7508x10 ⁻³	0.012990
	5	0.010473	1.7508x10 ⁻³	0.012990
	6	0.014751	1.7508x10 ⁻³	0.012990
	7	0.021807	1.7508x10 ⁻³	0.012990
	8	0.034454	1.7508x10 ⁻³	0.012990
	9	0.057112	1.7508x10 ⁻³	0.012990
14	1		8.0555x10 ⁻³	9.9839x10 ⁻⁴
	2	2.4665x10 ⁻³	8.0555x10 ⁻³	9.9839x10 ⁻⁴
	3	4.9247x10 ⁻³	8.0555x10 ⁻³	9.9839x10 ⁻⁴
	4	6.6084x10 ⁻³	8.0555x10 ⁻³	9.9839x10 ⁻⁴
	5	0.010043	8.0555x10 ⁻³	9.9839x10 ⁻⁴
	6	0.016895	8.0555x10 ⁻³	9.9839x10 ⁻⁴
	7	0.023696	8.0555x10 ⁻³	9.9839x10 ⁻⁴
	8	0.044401	8.0555x10 ⁻³	9.9839x10 ⁻⁴

was measured before the third component was distilled into the cell to make a check against the values which had been obtained in series 5 and 6. All these individual measurements along with the data of series 5 and 6 were fitted to the binary R-K equation.

6-2 n-HEXANE + n-HEXADECANE AT 303.15 K

The vapour pressures of mixtures of n-hexane + n-hexadecane at 303.15 K (the even run numbers in series 1 and 2) were measured and are listed in table 6-3. In order to compare the results in this work directly with that obtained by previous workers (Williamson 1957), the same procedure used in the previous work was followed to calculate the activity coefficients in the liquid phase:

$$p_1 = p - p_2^0 x_2 \quad \text{.....} \quad (6-2.1)$$

$$\ln \gamma_1 = \ln [p_1 / (p_1^0 x_1)] + (B_{11} - v_1^1)(p - p_1^0) / RT - (1/2)(B_{11} / RT)^2 (p^2 - p_1^0{}^2) \quad \text{.....} \quad (6-2.2)$$

where the subscripts 1, and 2 represent n-hexane and n-hexadecane, respectively. The other notations in eq. (6-2.1) and (6-2.2) are defined in Chapter 5. The values of B_{11} , v_1^1 used in this work are the same as those used in previous work, and are labelled by * in table 6-2.

Figure 6-1 and figure 6-2 compare $-\ln[p_1 / p_1^0 x_1]$ and $-\ln \gamma_1$ of this work with those from previous work. The curve in figure 6-2 is that calculated according to the equation:

$$-\ln \gamma_1 = 0.111969 x_2^2 + 0.0046601 x_2^2 (3-4x_2) \quad \text{.....} \quad (6-2.3)$$

The values of 0.111969 and 0.0046601 in eq. (6-2.3) were obtained from fitting this equation to the two sets of experimental results from this and previous work.

The solid curve in figure 6-1 is that calculated by the equation:

$$-\ln[p_1 / (p_1^0 x_1)] = -0.042777 x_2^3 + 0.15839 x_2^2 + 0.0085670 x_2 \quad \text{.....} \quad (6-2.4)$$

and the dotted curve is that calculated by the equation:

$$-\ln[p_1 / (p_1^0 x_1)] = -0.028453 x_2^3 + 0.13391 x_2^2 + 0.021466 x_2 \quad \text{.....} \quad (6-2.5)$$

in which the parameters were optimized by fitting this type of equation to the results of this work and previous work, respectively. The discrepancies in $\ln \gamma$

FIGURE 6-1 COMPARISON OF $\ln(P_1/P_1^0 X_1)$

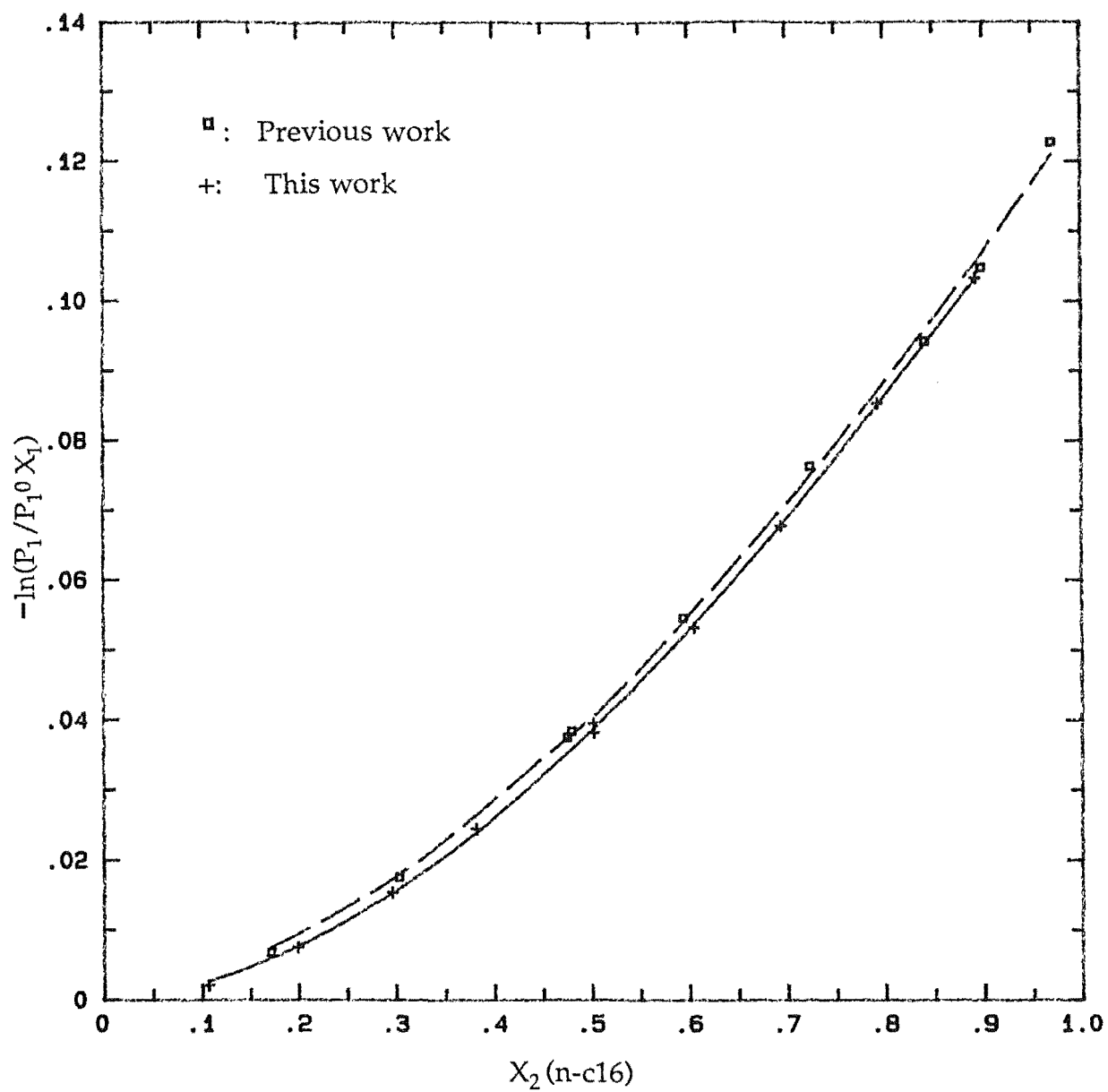


FIGURE 6-2 COMPARISON OF $\ln \gamma_1$

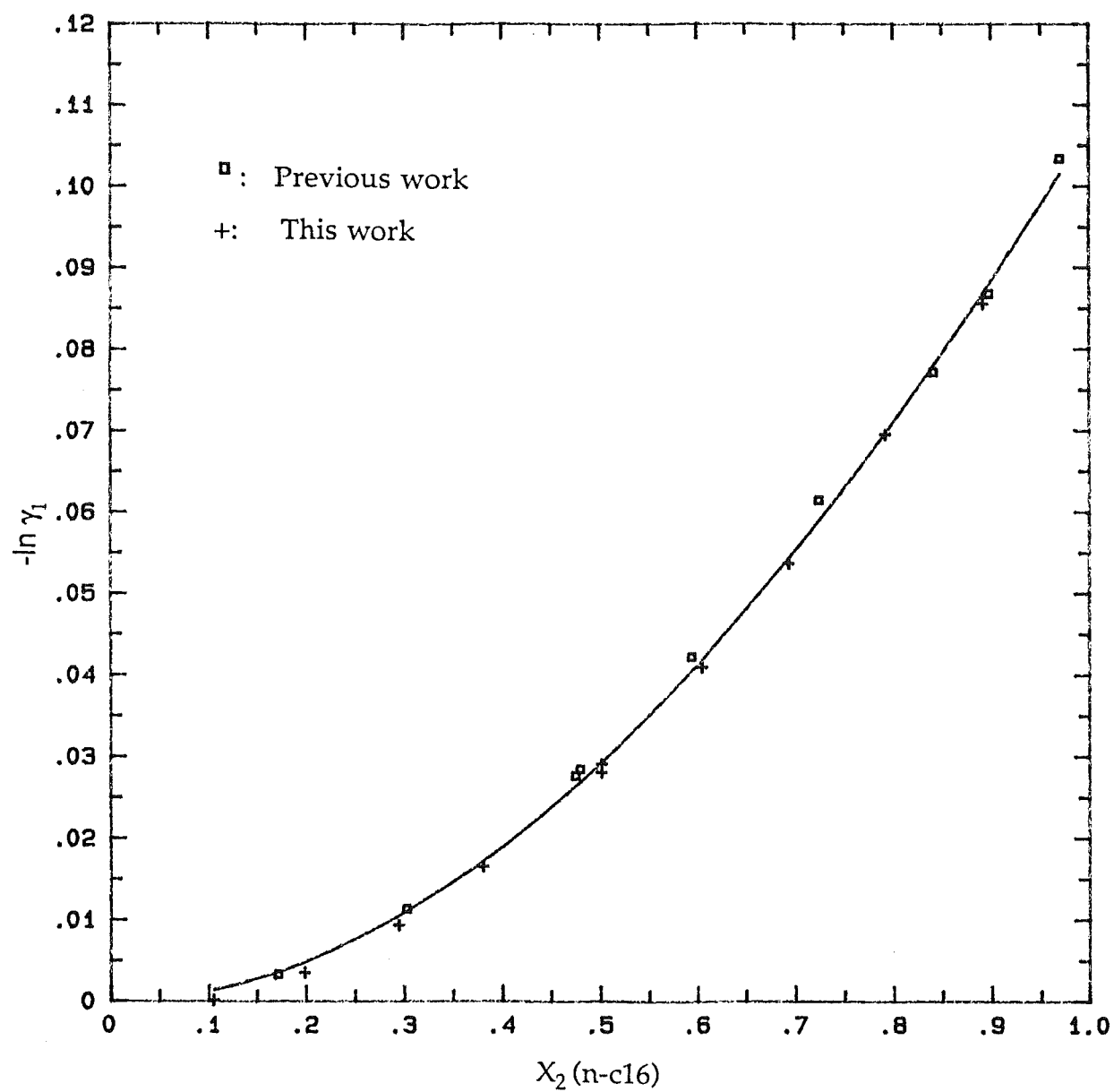


Table 6-2 Second Virial Coefficients, Molar Volumes,
And Critical Constants

component	temperature (K)	molar volume (cm ³ mol ⁻¹)	second virial coefficient (cm ³ mol ⁻¹)	V ^c (cm ³ mol ⁻¹)	T ^c (K)
n-hexane	298.15	131.602	-2057	368	507.9
	303.15	132.53 *	-1854 *		
	303.15		-1945		
n-octane	298.15	163.512	-4085	486	569.4
n-hexadecane	298.15	294.113			
	303.15	295.41 *			

The values with the label * are from the previous work (Williamson, 1957).

The molar volumes without label * are from TRC Thermodynamic Tables

(1985). The second virial coefficients without label * are from Dymond (1986).

V^c and T^c are from API tables (1953).

Table 6-3 Results For n-hexane (1) + hexadecane (2) At 303.15 K

$$p_1^0 = 24929 \text{ Pa}, \quad p_2^0 = 0 \text{ Pa}$$

Series No	Run No	x ₁	p(Pa)	p/p ₁ ⁰ x ₁	-ln(p/p ₁ ⁰ x ₁)	-lnγ ₁
1	2	0.1078	2424	0.9019	0.1033	0.0856
	4	0.2074	4748	0.9183	0.0853	0.0695
	6	0.3059	7126	0.9346	0.0678	0.0537
	8	0.3947	9330	0.9482	0.0532	0.0410
	10	0.4982	11954	0.9625	0.0382	0.0281
2	2	0.4980	11934	0.9613	0.0395	0.0291
	4	0.6184	15043	0.9758	0.0245	0.0166
	6	0.7046	17396	0.9847	0.0154	9.3x10 ⁻³
	8	0.8009	19818	0.9925	0.0075	3.5x10 ⁻³
	10	0.8939	22234	0.9978	0.0022	1.2x10 ⁻⁴

for two runs in the composition-overlap region is about 0.001. The values of $-\ln[p/(p_1^0 x_1)]$ and $-\ln\gamma_1$ in this work are slightly numerically less than those obtained in previous work. The differences between the two sets of measurements are as large as 2×10^{-3} in $-\ln[p/(p_1^0 x_1)]$ or in $-\ln\gamma_1$. Although these differences are in the range of the experimental error (Williamson, 1957), some systematic error appears to exist in the experimental techniques. The error in the both sets of measurements of absolute temperature and pressure could be one of the sources of this systematic discrepancies, but as described in chapter 5, these sources are not expected to cause such large differences. A more probable source of these discrepancies lies in the method of preparing mixtures. A numerically too large value of $-\ln[p/(p_1^0 x_1)]$ and $-\ln\gamma_1$ could be caused by loss of n-hexane due to solution in the stopcock grease during distillation in the previous work.

6-3 BINARY MIXTURES

The vapour pressure measurements made at 298.15 K for binary systems of n-hexane + n-hexadecane, n-hexane + n-octane, n-octane + n-hexadecane are summarized in table 6-4.

The third column in table 6-4 lists the mole fraction in the liquid phase calculated from moles of components in the vapour pressure cell corrected for the amount of volatile component in vapour phase. The molar volume of each liquid component which was used to calculate the volume of each liquid component in the cell and the vapour nonideality of each volatile component is listed in table 6-2.

The second virial coefficients for pure n-hexane and n-octane were calculated by the smoothing equations recommended by Dymond (1986). The mixed second virial coefficient for the system n-hexane + n-octane was calculated using the equation (McGlashan and Potter, 1962)

$$B/V^c = 0.430 - 0.886(T^c/T) - 0.694 (T^c/T)^2 - 0.0375(n-1) (T^c/T)^{4.5} \quad \text{..... (6-3.1)}$$

with the combining rules for pseudo critical constants:

$$V_{c12}^c = (1/8) (V_{c1}^{1/3} + V_{c2}^{1/3})^3 \quad \text{..... (6-3.2)}$$

Table 6-4 Vapour Pressures of Binary Mixtures At 298.15 K

Series No	Run No	X_1	p (Pa)	Δw (10^{-4} g)	r (Pa)
n-hexane (1) + n-hexadecane (2)					
$p_1^0 = 20157$ Pa; $p_2^0 = 0$ Pa					
1	1	0.1080	1972	-2	0.7
	3	0.2076	3858	1	-1.9
	5	0.3061	5788	-1	2.2
	7	0.3949	7574	3	-0.3
	9	0.4984	9693	-3	-7.0
2	1	0.4996	9707	1	5.3
	3	0.6196	12207	-2	2.1
	5	0.7055	14025	1	-1.4
	7	0.8013	16053	1	0.4
	9	0.8940	17989	0	-0.3
n-hexane (1) + n-octane (2)					
$p_1^0 = 20158$ Pa; $p_2^0 = 1872$ Pa					
3	1	0.1255	4140	-1	-4.0
	2	0.2221	5888	0	0.9
	3	0.3290	7830	0	4.1
	4	0.4270	9623	2	1.3
	5	0.5274	11462	-1	-0.9
4	5	0.4795	10587	0	-5.6
	4	0.5867	12550	1	2.0
	3	0.6979	14584	-1	3.0
	2	0.8055	16563	-2	-3.2
	1	0.8960	18240	0	-2.2

Table 6-4 Continued

Series No	Run No	x_1	P (Pa)	Δw (10^{-4} g)	r (Pa)
n-octane (1) + n- hexadecane (2)					
$p_1^0 = 1873$ Pa; $p_2^0 = 0$ Pa					
5	1	0.1050	185	2	1.4
	2	0.2016	364	1	-2.2
	3	0.3169	577	2	-2.8
	4	0.3937	719	-1	-0.5
	5	0.4895	900	0	-0.7
	6	0.5949	1100	-2	0.2
6	1	0.5024	923	-1	1.2
	2	0.6979	1297	1	0.3
	3	0.7963	1491	1	-4.4
	4	0.8971	1680	1	-1.3
13	1	0.1186	208	-2	3.2
8	1	0.2868	520	2	-1.4
7	1	0.3184	577	-1	0
10	1	0.4857	888	1	4.2
9	1	0.4980	915	-2	0.9
12	1	0.6921	1287	2	-0.2
11	1	0.6873	1277	1	-0.1

$$T_{12}^c = (T_1^c T_2^c)^{1/2} \quad \text{..... (6-3.3), and}$$

$$n_{12} = (n_1 + n_2)/2 \quad \text{..... (6-3.4)}$$

where V^c and T^c are the critical volume and temperature, respectively; which were taken from A P I tables (1953) and are listed in table 6-2 and n is the number of carbon atoms in a molecule. The calculated mixed second virial coefficient for the system n-hexane + n-octane is $-2809.6 \text{ cm}^3 \text{ mol}^{-1}$.

Column 5 in table 4, lists the differences Δw between the two weighings of the loaded cell made before and after the pressure measurements, which are less than $3 \times 10^{-4} \text{ g}$, within the range of errors in weighing. It is therefore believed that no change in composition due to the loss of materials during each measurement occurred.

The last column in table 6-4 lists r , the difference between the vapour pressure calculated according to the method described in chapter 5 and the experimental data, $r = p_{\text{cal}} - p_{\text{exp}}$. The values of r for the three binary systems at various compositions are shown in figures 6-3, 6-4, 6-5 and are less than the estimated maximum experimental error.

Table 6-5 lists the optimal parameters of the R-K equation (A_i), the errors in estimation of these parameters (σA_i), the standard deviations (R), and the number of experimental points (N) for the three binary systems. The deviations for each system are less than the probable uncertainties estimated in section 5-4. The number of parameters for each system was determined by minimizing the standard deviation.

Table 6-6 summarizes the calculated results including γ_i , the activity coefficient in the liquid phase; y_i , the mole fraction in the vapour phase; G^E , the excess molar Gibbs energy; and σG^E , the error in G^E calculated according to eq. (5-4.28). The calculated σG^E for the system of n-hexane + n-hexadecane and n-hexane + n-octane are in agreement with the values estimated in section 5-4.

The discrepancies in G^E for different runs in the composition-overlap regions were less than 1 J mol^{-1} .

Equation (5-2.20B) was used to calculate the standard errors of the estimated vapour pressures. This calculational procedure was included in the

FIGURE 6-3. DEVIATIONS OF VAPOUR PRESSURES FOR n-hexane + n-hexadecane

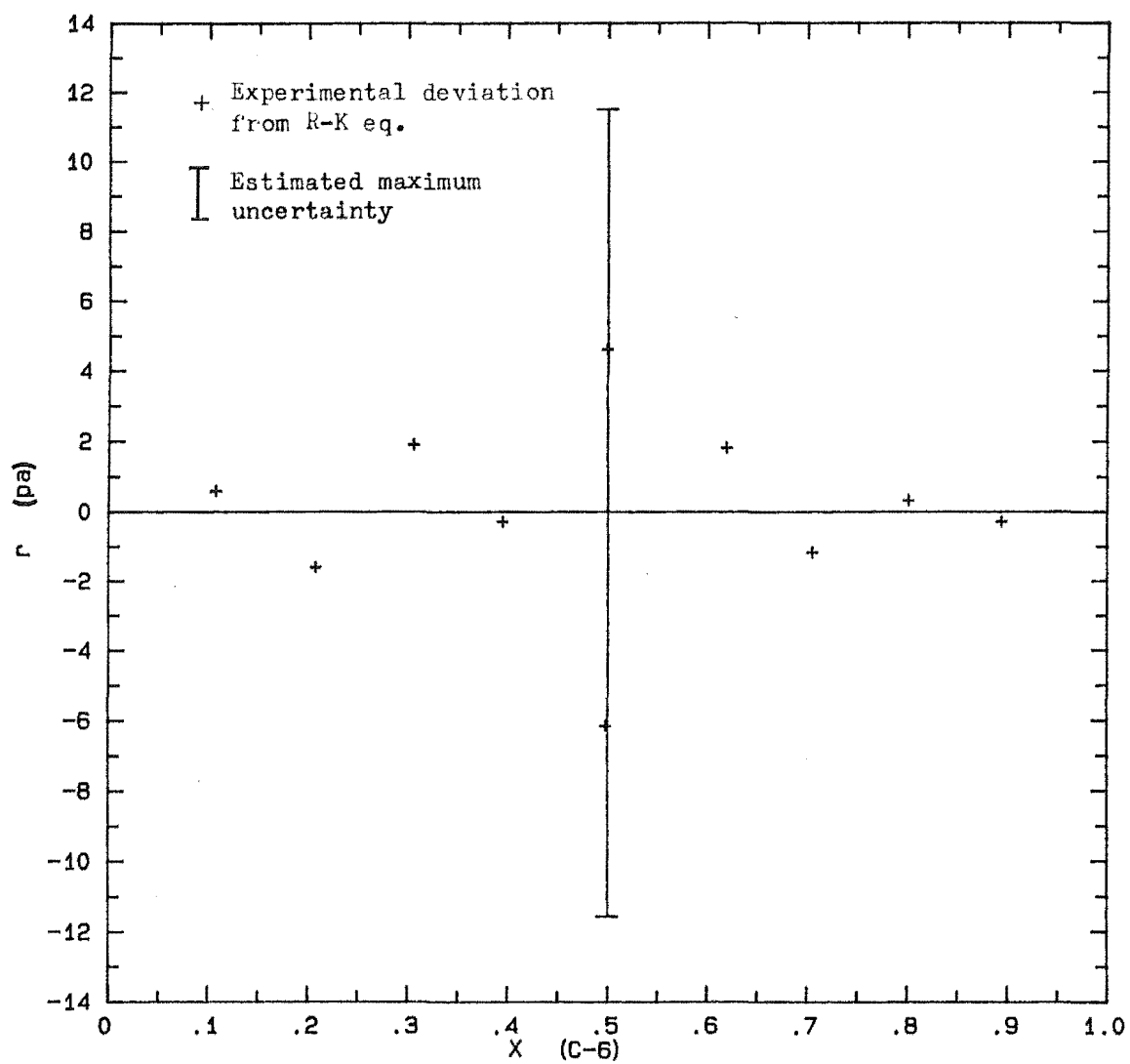


FIGURE 6-4. DEVIATIONS OF VAPOUR PRESSURES FOR n-hexane + n-octane

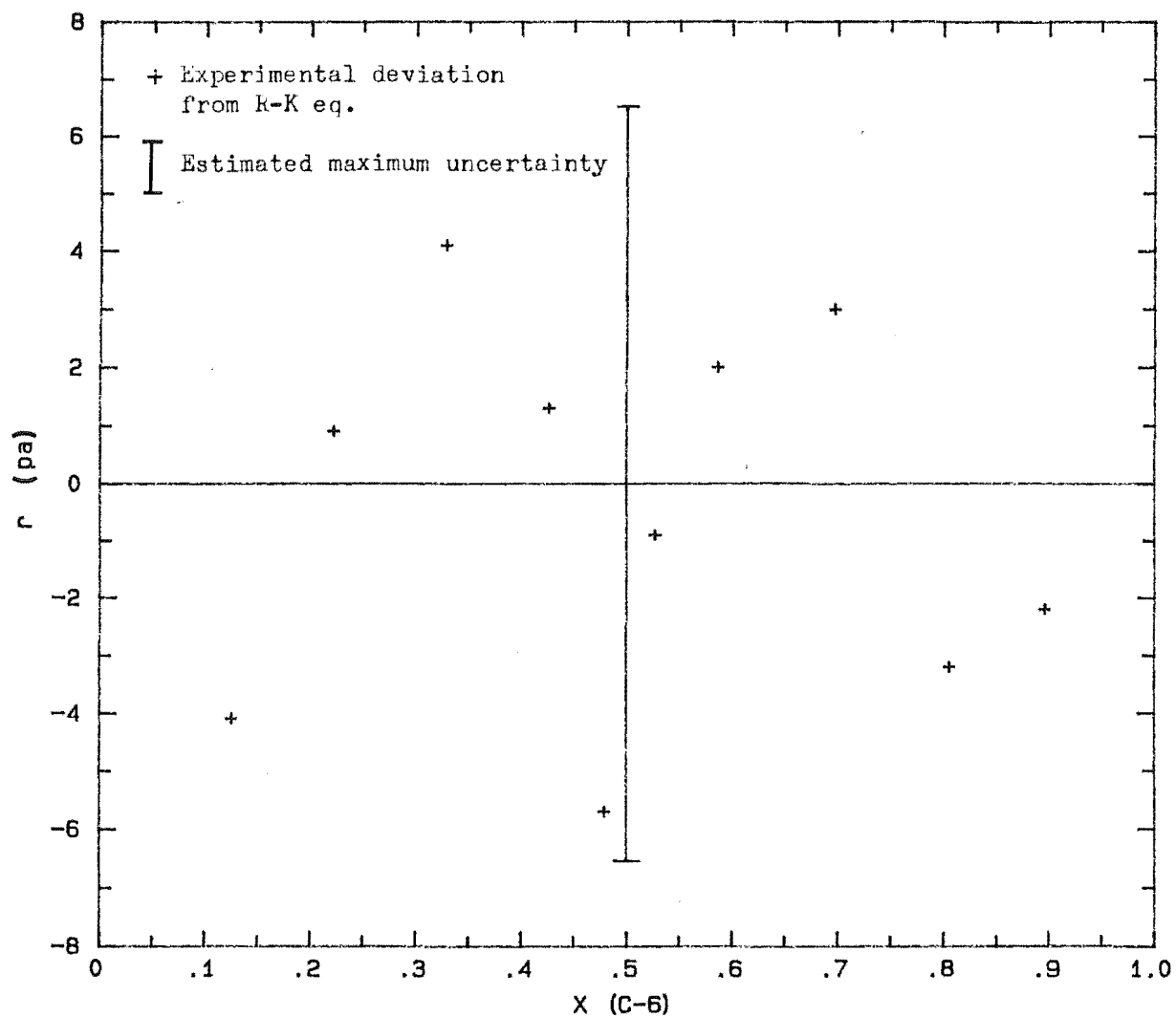


FIGURE 6-5. DEVIATIONS OF VAPOUR PRESSURES FOR n-octane + n-hexadecane

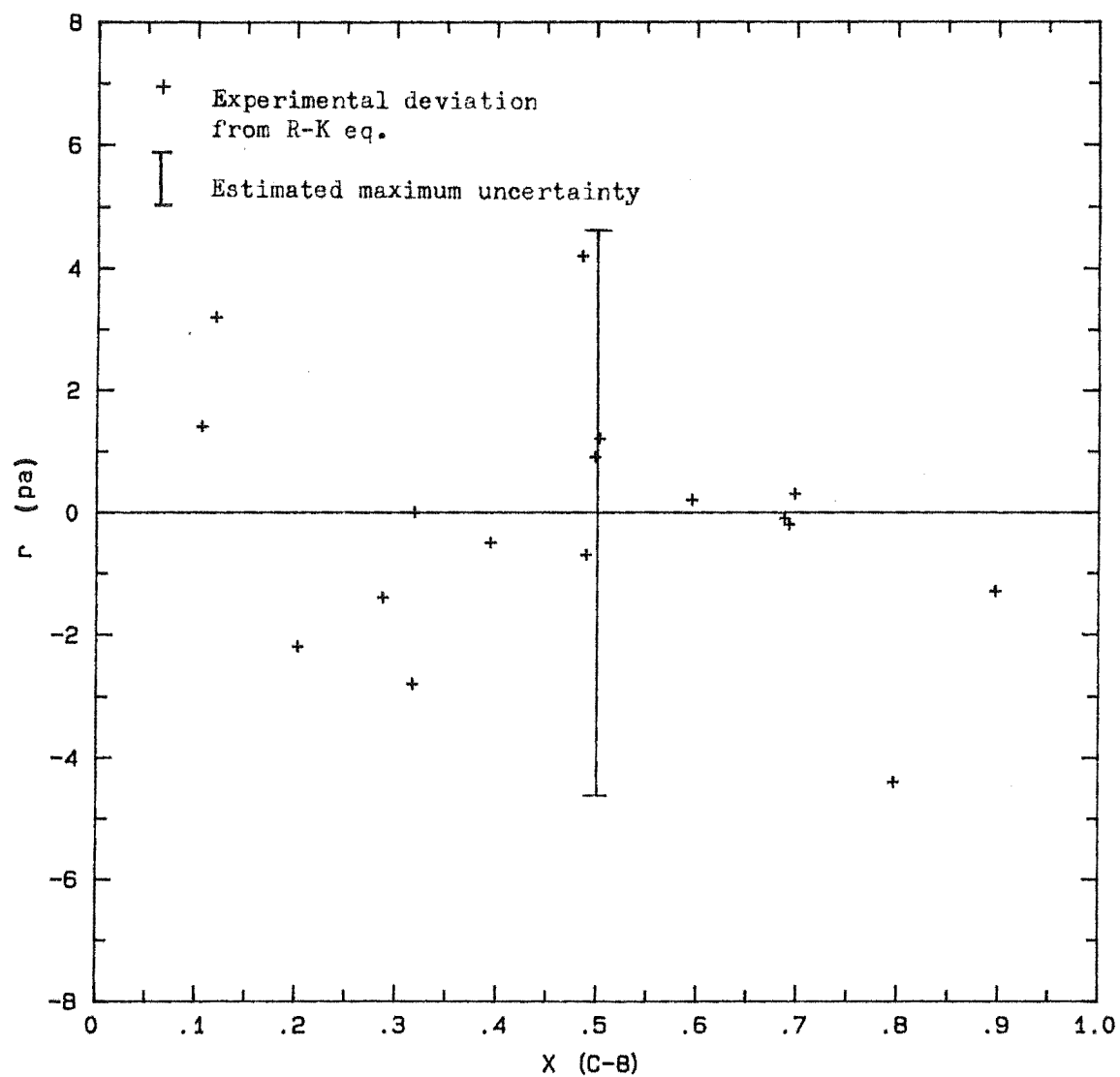


Table 6-5 Parameters of R-K Equation (5-3.4) for Binary Systems (298.15 K)

System	L	A_L	$\sigma A_L (10^{-4})$	R (Pa)	N
n-hexane+n-hexadecane	0	-0.10362	7.8	4.8	10
	1	0.00455	7.7		
	2	-0.00209	13.4		
	3	-0.00707	21.6		
	4	0.02715	32.9		
n-hexane+n-octane	0	0.00143	3.7	3.7	10
	1	-0.00399	5.0		
n-octane+n-hexadecane	0	-0.06400	24.9	2.2	17
	1	0.00435	29.8		

Table 6-6 Calculated Results of Binary Systems (298.15 K)

x_1	γ_1	γ_2	y_1	G^E (J mol ⁻¹)	σG^E (J mol ⁻¹)
n-hexane (1)+n-hexadecane (2)					
0.1080	0.9211	0.9997	1	-22.6	1.0
0.2076	0.9351	0.9968	1	-40.7	1.0
0.3061	0.9504	0.9913	1	-53.7	1.0
0.3949	0.9620	0.9848	1	-60.9	1.0
0.4984	0.9732	0.9757	1	-64.2	1.0
0.4996	0.9733	0.9756	1	-64.2	1.0
0.6196	0.9845	0.9614	1	-61.1	1.0
0.7055	0.9916	0.9479	1	-53.9	1.0
0.8013	0.9975	0.9308	1	-40.3	1.0
0.8940	1.0000	0.9181	1	-22.2	1.0
n-hexane (1) + n- octane (2)					
0.1255	0.9996	0.9999	0.6029	-0.4	0.3
0.2221	1.0006	0.9997	0.7513	-0.3	0.4
0.3290	1.0012	0.9994	0.8383	0.4	0.5
0.4270	1.0014	0.9993	0.8873	0.4	0.5
0.5274	1.0013	0.9994	0.9217	1.0	0.5
0.4795	1.0014	0.9993	0.9068	0.8	0.5
0.5867	1.0012	0.9996	0.9374	1.3	0.5
0.6979	1.0008	1.0003	0.9605	1.6	0.5
0.8055	1.0004	1.0015	0.9775	1.5	0.4
0.8960	1.0001	1.0030	0.9890	1.1	0.3

Table 6-6 Continued

x_1	γ_1	γ_2	y_1	G^E (J mol ⁻¹)	σG^E (mol ⁻¹)
n-octane (1) + n- hexadecane (2)					
0.1050	0.9519	0.9994	1	-14.1	0.9
0.2016	0.9605	0.9978	1	-24.5	1.2
0.3169	0.9701	0.9943	1	-33.5	1.3
0.3937	0.9758	0.9911	1	-37.3	1.3
0.4895	0.9824	0.9859	1	-39.6	1.2
0.5949	0.9886	0.9785	1	-38.7	1.3
0.5024	0.9832	0.9850	1	-39.7	1.2
0.6979	0.9935	0.9697	1	-34.3	1.3
0.7963	0.9970	0.9597	1	-26.8	1.2
0.8971	0.9992	0.9478	1	-15.4	0.9
0.1186	0.9532	0.9993	1	-15.7	1.0
0.2868	0.9677	0.9954	1	-31.5	1.3
0.3184	0.9702	0.9943	1	-33.6	1.3
0.4857	0.9821	0.9861	1	-39.6	1.3
0.4980	0.9829	0.9853	1	-39.6	1.2
0.6873	0.9930	0.9707	1	-35.0	1.3
0.6921	0.9932	0.9703	1	-34.7	1.3

computation programmes PVLR2 and PVLR3 . The standard errors in the estimated total vapour pressures for the system n-octane + n- hexadecane were greatly reduced as compared with the error in measurements. The value of the standard error at about 0.5 of mole fraction is ± 0.5 pa. With this value, δQ_1 , δQ_2 , δQ_3 were calculated in the manner as described in section 5-4 and were found to be 5.3×10^{-4} , 1.1×10^{-5} , 2.7×10^{-4} , respectively. The probable error in G^E was then calculated and was about 1.5 J mol^{-1} , which is in agreement with the value calculated by eq. (5-4.28).

All the results show that the R-K equation is capable of reducing the experimental data within experimental errors for the systems investigated in this work.

As shown in table 6-6, the maximum excess free Gibbs energies for the system n-hexane + n-octane is 1.6 J mol^{-1} , and the error in calculation of G^E is about 50 % of the value of G^E . Therefore the dependence of G^E on the mole fractions for this system described by the R-K equation with the optimal parameters is doubtful, but it is believed that the values of G^E are numerically less than 2 J mol^{-1} .

6-4 TERNARY MIXTURES

The measured vapour pressures vs mole fractions of of ternary mixtures of n-hexane + n-octane + n-hexadecane and all the calculated results are listed in tables 6-7, 6-8, and 6-9. Δw in table 6-7 is usually less than $3 \times 10^{-4} \text{ g}$. The deviations of the experimental results from the R-K equation are in the range of estimated experimental errors. An additional error in G^E for the ternary mixing is less than 0.4 J mol^{-1} . Thus the total error in G^E for the ternary system is from 1 to 2 J mol^{-1} . This is in agreement with the error analysis for the ternary system described in section 5-4.

Table 6-7 Vapour Pressures of Ternary System
n-hexane (1) + n-octane (2) + n-hexadecane (3) (298.15 K)

Series No	Run No	X_1	X_2	P (Pa)	$\Delta w(10^{-4} \text{ g})$	r(Pa)
7	2	0.1332	0.2760	3036	0	-1.6
	3	0.2214	0.2479	4706	-3	-3.1
	4	0.3075	0.2206	6367	2	-8.6
	5	0.3931	0.1933	8033	1	-6.7
	6	0.4810	0.1652	9773	-2	-11.9
8	2	0.5023	0.1430	10148	2	-2.9
	3	0.5911	0.1176	11930	-1	1.9
	4	0.6904	0.0891	13940	0	7.0
	5	0.8008	0.0573	16179	-4	5.8
	6	0.9006	0.0286	18193	-3	-10.1
9	2	0.1069	0.4448	2880	2	3.7
	3	0.1988	0.3990	4596	-3	4.4
	4	0.3086	0.3444	6678	-1	-0.2
	5	0.3979	0.2999	8393	2	-3.6
10	2	0.5220	0.2324	10786	1	1.5
	3	0.6133	0.1880	12580	-3	4.0
	4	0.7080	0.1420	14447	-1	4.2
	5	0.8034	0.0956	16328	2	-2.0
	6	0.8947	0.0513	18112	0	-6.3
11	2	0.4833	0.3554	12085	0	4.9
	3	0.5995	0.2755	12507	1	4.3
	4	0.6929	0.2113	14295	0	2.6
	5	0.8018	0.1364	16379	-2	-1.0
	6	0.8979	0.0703	18213	3	-5.1

Table 6-7 Continued.....

Series No	Run No	X_1	X_2	P (pa)	$\Delta w(10^{-4}g)$	r (Pa)
12	2	0.1192	0.6096	3468	0	6.1
	3	0.2076	0.5484	5109	1	0.2
	4	0.3138	0.4750	7094	0	-4.1
	5	0.3922	0.4207	8570	-2	-2.7
	6	0.4938	0.3504	10498	1	-1.5
13	2	0.1097	0.1056	2218		5.1
	3	0.2105	0.0937	4126		3.0
	4	0.3085	0.0821	6028		12.1
	5	0.4135	0.0696	8119		10.7
	6	0.4986	0.0595	9842	0	6.2
	7	0.5955	0.0480	11830		5.2
	8	0.6996	0.0357	13990	-2	9.0
	9	0.7945	0.0244	15963		9.2
14	2	0.2111	0.7018	5505	-3	4.1
	3	0.3489	0.5792	8042		4.1
	4	0.4187	0.5171	9327		9.8
	5	0.5233	0.4241	11266		9.0
	6	0.6494	0.3119	13615	0	3.7
	7	0.7224	0.2470	14979		-2.0
	8	0.8302	0.1511	16993	2	-8.9

Table 6-8 The Parameters of R-K equation (5-3.16) for ternary system (298.15 K)

L	C_L	$\sigma C_L(10^{-4})$	R (pa)	N
0	-0.1820	26.1	6.3	44
1	-0.0158	35.0		
2	0.0098	66.6		

Table 6-9 Calculated Results of Ternary System
n-hexane (1) + n-octane (2) + n-hexadecane (3) (298.15 K)

x_1	x_2	γ_1	γ_2	γ_3	y_1	y_2	G^E (J mol ⁻¹)	σG^E (J mol ⁻¹)
0.1332	0.2760	0.9554	0.9804	0.9887	0.8328	0.1672	-45.2	0.2
0.2214	0.2479	0.9637	0.9864	0.9832	0.9022	0.0978	-51.0	0.2
0.3075	0.2206	0.9711	0.9911	0.9771	0.9352	0.0648	-54.4	0.3
0.3931	0.1933	0.9775	0.9948	0.9703	0.9547	0.0453	-55.6	0.3
0.4810	0.1652	0.9836	0.9977	0.9622	0.9680	0.0320	-54.5	0.3
0.5023	0.1430	0.9840	0.9976	0.9617	0.9733	0.0267	-55.3	0.3
0.5911	0.1176	0.9898	0.9996	0.9512	0.9812	0.0188	-51.2	0.3
0.6904	0.0891	0.9955	1.0008	0.9374	0.9878	0.0122	-43.0	0.2
0.8008	0.0573	0.9994	1.0010	0.9226	0.9932	0.0068	-29.5	0.1
0.9006	0.0286	1.0003	1.0017	0.9161	0.9970	0.0030	-14.5	0
0.1069	0.4448	0.9701	0.9883	0.9797	0.7142	0.2858	-43.7	0.2
0.1988	0.3990	0.9752	0.9926	0.9737	0.8381	0.1619	-46.3	0.3
0.3086	0.3444	0.9810	0.9966	0.9659	0.9030	0.0970	-47.4	0.2
0.3979	0.2999	0.9855	0.9991	0.9587	0.9324	0.0676	-46.6	0.2
0.5220	0.2324	0.9914	1.0011	0.9474	0.9590	0.0410	-43.5	0.3
0.6133	0.1880	0.9955	1.0017	0.9369	0.9715	0.0285	-38.2	0.3
0.7080	0.1420	0.9986	1.0017	0.9260	0.9812	0.0188	-30.5	0.2
0.8034	0.0956	1.0001	1.0014	0.9177	0.9887	0.0113	-20.9	0.1
0.8947	0.0513	1.0003	1.0020	0.9158	0.9945	0.0055	-10.8	0.1
0.4833	0.3554	0.9955	1.0017	0.9369	0.9343	0.0657	-30.0	0.2
0.5995	0.2755	0.9985	1.0018	0.9263	0.9579	0.0421	-24.8	0.2
0.6929	0.2113	0.9999	1.0015	0.9193	0.9717	0.0283	-19.4	0.2
0.8018	0.1364	1.0004	1.0015	0.9150	0.9840	0.0160	-12.2	0.1
0.8979	0.0703	1.0003	1.0024	0.9167	0.9926	0.0075	-5.9	0

Table 6-9 Continued.....

x_1	x_2	γ_1	γ_2	γ_3	y_1	y_2	G^E (J mol ⁻¹)	σG^E (J mol ⁻¹)
0.1192	0.6096	0.9856	0.9961	0.9638	0.6720	0.3280	-35.1	0.3
0.2076	0.5484	0.9876	0.9980	0.9583	0.7984	0.2016	-34.9	0.4
0.3138	0.4750	0.9905	0.9999	0.9510	0.8735	0.1265	-33.9	0.3
0.3922	0.4207	0.9929	1.0010	0.9447	0.9069	0.0931	-32.3	0.2
0.4938	0.3504	0.9960	1.0017	0.9356	0.9365	0.0635	-29.2	0.2
0.1097	0.1056	0.9334	0.9645	0.9974	0.9142	0.0858	-33.4	0.1
0.2105	0.0937	0.9461	0.9743	0.9930	0.9585	0.0415	-47.0	0.2
0.3085	0.0821	0.9588	0.9821	0.9867	0.9748	0.0252	-56.1	0.2
0.4135	0.0696	0.9700	0.9885	0.9786	0.9840	0.0160	-61.0	0.2
0.4986	0.0595	0.9776	0.9930	0.9707	0.9886	0.0114	-61.6	0.2
0.5955	0.0480	0.9857	0.9965	0.9593	0.9923	0.0077	-58.4	0.2
0.6996	0.0357	0.9932	0.9991	0.9438	0.9951	0.0049	-49.8	0.1
0.7945	0.0244	0.9981	1.0002	0.9283	0.9971	0.0029	-37.0	0.1
0.2111	0.7018	0.9970	1.0000	0.9398	0.7601	0.2399	-15.0	0.3
0.3489	0.5792	0.9988	1.0004	0.9312	0.8638	0.1362	-13.3	0.2
0.4187	0.5171	0.9995	1.0004	0.9268	0.8950	0.1050	-12.1	0.2
0.5233	0.4241	1.0003	1.0004	0.9209	0.9284	0.0716	-9.9	0.1
0.6494	0.3119	1.0007	1.0005	0.9161	0.9562	0.0438	-6.9	0.1
0.7224	0.2470	1.0006	1.0008	0.9149	0.9684	0.0316	-5.1	0.1
0.8302	0.1511	1.0004	1.0017	0.9160	0.9829	0.0171	-2.7	0

CHAPTER 7 EXCESS VOLUMES OF MIXING

7-1. REVIEW OF EXPERIMENTAL METHODS FOR MEASUREMENT
OF EXCESS VOLUMES

The measurement of excess volumes (V^E) is an active-interest area because it is useful in testing theories of liquid mixtures and providing a guide for the formation of new theories, in the conversion of excess thermodynamic functions determined at constant pressure to the condition of mixing at constant volume, in determining composition from density measurements of mixtures and in industrial technology. Volume changes on mixing can arise from one or more of the following factors:

- (1) difference in size and shape of the component molecules
- (2) difference in the intermolecular interaction energy between like and unlike molecules
- (3) structural changes such as changes in the correlation of molecular orientation
- (4) formation of new chemical species or weak complexes such as charge-transfer complexes.

An enormous amount of experimental data and several review papers have been published. Battino (1971) compiled data and summarized experimental methods on the excess volumes for binary liquid mixtures published prior to 1969. Handa and Benson (1979) reviewed various experimental techniques and compiled V^E data for binary liquid mixtures reported from 1969 to 1978. Lacmann and Synowietz (1974) compiled density data for a large number of binary and multicomponent systems. Booth (1975) reviewed V^E for mixtures in which one of the components is a high-molecular weight homopolymer. The "Chemical Society "Specialist Periodical Report On Chemical Thermodynamics ", Vol 2 , (McGlashan 1978) give extensive bibliographies of measurements of V^E and a survey of experimental techniques. Stokes and Marsh (1972), Letcher (1975) and Swinton (1976) have also discussed the experimental aspects of measurement of V^E in their review articles.

Volume changes on mixing can be determined by two main methods:

- (1) directly by observing volume change in a dilatometer as two liquids are mixed,
- (2) indirectly by measuring the densities of pure liquids and their mixtures at known compositions.

7-1.1 DIRECT METHODS

Apparatus for the direct measurement of V^E has been designed in two basic styles namely: batch or single composition dilatometers and dilution dilatometers.

The operating principle of batch dilatometers can be explained as follows: A vessel is first filled with mercury. Known masses of each liquid are injected into the dilatometer and kept separated usually by mercury. An appropriate precision-bore capillary is fitted attached to the dilatometer. After thermal equilibrium has been achieved the mercury height in the capillary is adjusted and its height relative to a reference is measured with a cathetometer. Then the two liquids are mixed and after thermal equilibrium the mercury height is recorded.

Several variations of this basic design have been reviewed by Battino (1971). Some improvements have been reported by Brennan et al. (1978) and Ahmed et al. (1977). The disadvantages of the loss of volatile components due to evaporation during injection was overcome and a smaller dilatometer vessel, with detachable capillary, was designed so that it could be weighed directly on the balance pan.

Dilution dilatometers for measuring excess volumes offer the advantage that the whole composition range can usually be covered in two runs and partial molar excess volumes are readily obtained. Dilution dilatometers have undergone a number of modifications since the publication of the basic design by Geffcken et al. (1937).

Desmyter and Van der waals (1958) described an apparatus which requires the liquid to be distilled under vacuum before sealing by glass blowing. In Beath et al.'s version (1969) the second component was transferred into a mixing bulb containing the first component, sucking the mercury from the mixing bulb.

Stokes et al. (1970) modified the version of the apparatus designed by Geffcken

et al. and obtained a standard deviation of $0.0008 \text{ cm}^3 \text{ mol}^{-1}$ for the test system cyclohexane + benzene. Martin and Murray (1972) slightly modified Stokes's design to facilitate the cleaning, filling, and calibration. Pflug and Benson (1968) described an accurate dilatometer with which the volume of added components is determined from the mass of mercury displaced in a piston-type arrangement. The kind of dilution dilatometers described above involve greased stopcocks, which are regarded as a source of errors.

Bottomley and Scott (1974) constructed a tilting dilution dilatometer without greased stopcocks. Some improvements have been made to this design by Kumaran and McGlashan (1977) to facilitate operation, calibration, and loading. The apparatus can be used for measuring V^E of any magnitude.

A drawback in almost all of the dilution of dilatometers described so far is that they do not measure volume changes at a constant pressure. A correction for this effect should be applied. Consequently designs for dilution dilatometers which can be operated at constant pressure have been reported by Tanaka et al. (1975), and by Chareyron and Clechet (1971).

Dilution dilatometers are faster compared to batch dilatometers, and normally give low standard deviations, but they suffer from the facts that a dilution run is accompanied by an accumulation of errors and that it could suffer from systematic errors, the most important of which is in the accurate determination of the volumes of the mixing cell and the expansion bulbs.

7-1.2 INDIRECT METHODS

A PYCNOMETERS

Density measurements using pycnometers still remain one of the simplest and least expensive procedures. Bauer and Lewin (1971), and Battino et al. (1971) have reviewed the methodology, and shown diagrams of various kinds of pycnometers. The recommended size for pycnometers is 10 to 30 cm^3 and corrections for buoyancy and amount of liquid or liquid mixture in the vapour phase are necessary.

B MAGNETIC FLOAT DENSITOMETERS

These densitometers operate on the principle of balancing the opposing effects of gravity, buoyancy and magnetic field on a float containing a permanent magnet or soft iron core. This is done by passing current through a solenoid placed below the cell containing the liquid, Density is related to the current at which the float first lifts off from the bottom of the cell. Franks et al. (1967) described magnetic float techniques with sensitivities of 0.001% and 0.0001%, respectively and gave an analysis of errors in detail. Millero (1967) surveyed the literature on magnetic float measurement and described a highly versatile new apparatus with a precision of 0.0002%. Hales (1970) discussed the various precautions necessary in the design of such densimeters.

C MECHANICAL OSCILLATOR DENSIMETER

Recently a large number of studies have been reported where V^E has been determined from densities measured by a mechanical oscillator densimeter. Digital readout densimeters operate on the principle of measuring the resonant frequency of an electronically excited mechanical oscillator. Assuming that the mode of vibration of oscillators can be approximated by the undamped vibration of mass attached to a spring with a constant elasticity c , the resonant frequency (f) is given (Handa and Benson, 1979) by

$$2\pi f = [c/(M^o + V\rho)]^{0.5} \quad \text{..... (7-1.1)}$$

where M^o is the mass of the oscillator, ρ is the density, and V is the volume of sample in the vibration tube. Then

$$\rho = -M^o / V + (C / 4 \pi^2 V) (1/f^2) = A + B\tau^2 \quad \text{..... (7-1.2)}$$

where τ is the period ($= 1/f$) of oscillation and A and B are characteristic constants of the oscillator. These can be determined using reference materials such as distilled water and air.

The first densimeter based on this principle was designed by Kratky and co-workers (Stabinger et al., 1967; Kratky et al., 1969;) and has been developed into a commercial apparatus by Anton Paar, Graz, Austria (DMA). The other design (Picker, 1974) of the mechanical oscillator densimeter has been placed on

the market by Sodev Inc., Sherbrooke, Canada.

Under favourable circumstances, differences in density can be determined within $\pm 1.5 \times 10^{-6} \text{ g cm}^{-3}$ by the mechanical oscillator densimeter. It is therefore well suited to the study of dilute aqueous and organic solutions and to determining the partial molar volumes and excess volumes. For some organic mixtures in which the variations in density in the whole composition range are larger than the limitation for high accuracy of density measurement, it was recommended that the constant B in eq. (7-1.2) should be evaluated by measuring a number of liquids whose densities are known (Handa and Benson, 1979). The densities of these liquids should be evenly spaced and should cover the density range of interest. Kiyohara and Benson (1973) used two methods to calibrate an Anton Parr densimeter (i.e. by water and air only and by a number of references), and then measured the excess volume of cyclohexane + benzene mixtures and compared the results based on the two calibrations. Because, for the cyclohexane + benzene, the densities of the components differ only 0.1 g cm^{-3} , they believed, the values of excess volume were not altered significantly (i.e. less than $0.0002 \text{ cm}^3 \text{ mole}^{-1}$). Francois et al. (1971) found their Anton paar densimeter was sensitive to change in atmospheric pressure, but Kiyohara and Benson (1973) could not detect such an effect.

Goates et al. (1979) pointed out that the changes of composition because of evaporation during the sample preparation and measurements are a major source of error in vibrating tube densimeters. With a special mixing apparatus designed to minimize the evaporation error and carbon tetrachloride and nitrogen gas as reference substances, they estimated the total uncertainty in molar fraction as 5×10^{-5} for the system cyclohexane+ n-hexane, which results in an uncertainty of 0.002 to $0.003 \text{ cm}^3 \text{ mol}^{-1}$ in V^E . Garcia et al. (1984) determined V^E of the system of n-heptane + n-octane + cyclohexane with an Anton Paar densimeter. They prepared mixtures in a glass cell with a hermetically sealed capillary inlet allowing only the needle of a syringe to be introduced. They believed that the variation in mass was less than $1 \times 10^{-4} \text{ g}$. Radojkovic et al. (1976) designed a mixing cell with two limbs and a vertical mercury collector. These limbs are provided with specially designed closures to allow injection of pure components into the mixing cell and withdrawal of the resulting mixture. Other mixing cells have been designed by Rao and Naidu

(1981), Takenaka et al.(1980). The latter believed the uncertainty in mole fraction of mixtures prepared in their "Onion Cell" was less than 3×10^{-5} . Adams et al.(1974) have described an automated apparatus (using an Anton paar densimeter) for measuring the densities of pure liquids and liquid mixtures of varying composition.

7-1.3 TEST SYSTEM

Following the suggestion by Powell and Swinton (1968), cyclohexane + benzene at 298.15 K has been adopted as a test system for checking the technique used to determine V^E . Consequently a large number of studies of this system have been reported in the literature. Some of these are shown in table 7-1.

In table 7-1, D refers to density measurements but technique not reported, DF is density measurements with a magnetic float densimeter, DO is density measurement with a mechanical oscillator densimeter, DP is density measurements with a pycnometer, VB is direct measurements with a batch dilatometer VD is direct measurements with a dilution dilatometer, N is the number of experimental points, R is standard deviation, A_1, A_2, \dots are the parameters in eq. (7-1.3) :

$$V^E = x_1 (1 - x_1) [A_1 + A_2 (1 - 2x_1) + A_3 (1 - 2x_1) + \dots] \quad \dots (7-1.3)$$

where x_1 is mole fraction of cyclohexane.

From table 7-1 we can see the differences between the different measurements for different dilution dilatometers are as large as 2 % . Two sets of measurements in close agreement with each other are those of Stokes et al. (1970) (72 data points) and, Kumaran and McGlashan (1977) (42 points). The agreement is better than 0.1 % over most of the mole fraction range. The data due to Tanaka et al. (1975) (50 points) is 0.5 % higher over the entire mole fraction. Fitting the three sets of data jointly (164 points all together), with all points weighted equally, Handa and Benson (1978) arrived at equation:

$$V^E (\text{cm}^3 \text{mole}^{-1}) = x_1 (1 - x_1) [2.60360 - 0.9339 (1 - 2x_1) + 0.04179 (1 - 2x_1)] \quad \dots (7-1.4)$$

with a standard deviation of $0.00157 \text{ cm}^3 \text{mole}^{-1}$. If all the points in individual set

Table 7-1 Values of Parameters in Equation 7-1.3 for
cyclohexane + benzene

EXP. TECH.	TEMP. (C)	N	A1	A2	A3	A4	A5	R	Re ferences
DP	20.0	9	2.618	-0.0483	0.2388			0.0078	Nissema, 1970
DF	25.0	31	2.6141	-0.0744	0.0337			0.0015	Weeks, 1973
DO	25.0	29	2.61313	-0.10497				0.0017	Kiyohara, 1973
DO	25.0	10	2.588	-0.068	0.135			0.0040	Grolier, 1974
DO	25.0	16	2.565	-0.095	0.063			0.0019	Redojkovic, 1 976
DO	25.0	10	2.620	-0.1117	0.0443			0.0015	Goates, 1977
VD	25.0	72	2.5988	-0.0901	0.03445			0.0008	Stokes, 1970
VD	25.0		2.5246	-0.1107	0.1905			0.00003 *	Jansserns, 1972
VD	25.0	39	2.574	-0.092	0.064			0.0020	Dickinson, 1975
VD	25.0	50	2.6129	-0.10103	0.06444	0.02751	-0.03163	0.00043	Tanaka, 1975
VD	25.0	42	2.5983	-0.0990	0.0518			0.0007	Kumaran, 1977
DP	30.0	9	2.58	-0.351	-0.762			0.047	Suri, 1969
DP	30.0	9	2.6 48	-0.0933				0.0075	Nissema, 1970
VB	35.0	12	2.510	-0.0540	0.269	0.875		0.012	Varma, 1976
D	40.0	8	3.47	-1.04				0.031	Sanni, 1971
DP	40.0	9	2.653	- 0.1026				0.0059	Nissema, 1970
D	60.0	8	3.68	-1.08				0.036	Sanni, 1971

Table 7-1. Continued ...

EXP. TECH.	TEMP. (C)	N	A1	A2	A3	A4	A5	R	REF.
VD	20.0	33	2.58960	-0.08494	0.01328			0.0007	Wieczorek, 1983
VD	25.0	35	2.60429	-0.09246	0.0251			0.0008	Wieczorek, 1983
VD	30.0	33	2.61271	-0.08615	0.00755			0.0006	Wieczorek, 1983
VD	35.0	35	2.62285	-0.09646	0.02170			0.0006	Wieczorek, 1983
VD	50.0	20	2.67225	0.12370	0.04859			0.0008	Kumaran, 1984
VD	25.0	30	2.5742	0.1069				0.0055	Beath, 1969
DO	25.0	13	2.6027	-0.12142				0.004	Stookey, 1973
DO	20.0	20	2.60485	-0.09715	0.03240	0.03488	0.01341	0.00018	Takenaka, 1980
DO	25.0	20	2.61556	-0.10421	0.04747	0.02915	-0.00922	0.00019	Takenaka, 1980
DO	30.0	20	2.62739	-0.10705	0.05062	0.02190	-0.01405	0.00024	Takenaka, 1980
DO	25.0	10	2.6202	-0.0980	0.0439	-0.0449			Goates, 1977
DO	25.0	10	2.6099	-0.0958	0.0444	-0.0136		0.0004 *	Goates, 1979
DO	25.0	10	2.6059	-0.1236	0.0367			0.0013	**
DO	25.0	10	2.6156	-0.0891	0.0315	-0.0484		0.0014	***

*: average deviation.

**: this work, mixing cell.

***: this work, "pressure-lok" syringe.

were assigned a weight equal to the reciprocal of the squared deviation of fit of that set to eq. (7-1.3), the total of 164 points, thus weighted, yielded the equation:

$$V^E (\text{cm}^3 \text{mole}^{-1}) = x_1 (1 - x_1)[2.60725 - 0.09271 (1 - 2x_1) + 0.04476 (1 - 2x_1)] \dots\dots (7-1.5)$$

with a standard deviation of $0.00161 \text{ cm}^3 \text{mole}^{-1}$. Equation (7-1.4) and (7-1.5) represent the excess volumes of the test system as measured by three dilution dilatometers with different characteristics: dilatometer with greased stopcocks, without greased stopcock, and with a greased stopcock but operated at constant pressure. The comparison between the results from dilution dilatometers and oscillator densimeters in whole mole fraction is shown in table 7-2.

Recently, Frabnluka and Holub (1983) analysed the results of measurements for V^E of benzene + cyclohexane at 298.15 K in the literature. Smith et al. (1982) carried out a more detailed critical evaluation, and formulated an equation based on the smoothed values of V^E at $x_1=0.25, 0.5, 0.75$ obtained from a consideration of all published results including those at temperature other than 298.15 K. Those two authors recommended the results of Kumaran and McGlashan (1978) as most closely representing the true behaviour at 298.15 K.

7-2. EXPERIMENTAL APPARATUS AND PROCEDURE

7-2.1 OSCILLATOR DENSIMETER

A Mettler DMA 60/ DMA 602H digital vibrating tube densimeter was used to measure the densities of pure components and mixtures in this work. According to the manual the accuracy in measurement of density is $1.5 \times 10^{-6} \text{ g cm}^{-3}$ in the range of $\pm 0.5 \text{ g cm}^{-3}$ around the density value of the calibration substances. With period selection switch at 5 k, the vibration period (τ) can be read to 1 part in 10^6 .

7-2.2 PREPARATION OF MIXTURES

Two methods of preparation of the mixtures were used in this work.

Table 7-2 Comparison of Values of Molar Excess Volumes
of cyclohexane + benzene Calculated by
Equation 7-1.3 at 298.15 K

X_1	a	b	c	d	e
0.1	0.2286	0.2277	0.2297	0.2276	0.2299
0.2	0.4101	0.4072	0.4092	0.4080	0.4105
0.3	0.5422	0.5391	0.5390	0.5399	0.5413
0.4	0.6237	0.6198	0.6193	0.6221	0.6222
0.5	0.6539	0.6515	0.6496	0.6533	0.6525
0.6	0.6324	0.6317	0.6289	0.6322	0.6314
0.7	0.5585	0.5589	0.5558	0.5576	0.5578
0.8	0.4305	0.4309	0.4283	0.4282	0.4298
0.9	0.2459	0.2455	0.2440	0.2427	0.2450

a: this work (syringe), $A_0=2.6156$, $A_1=-0.0891$, $A_2=0.0315$, $A_3=-0.0484$.

b: this work (mixing cell), $A_0=2.6059$, $A_1=-0.1236$, $A_2=0.0367$.

c: Kumaran and McGlashan, (1977); dilution dilatometric method,
 $A_0=2.5983$, $A_1=-0.0990$, $A_2=0.0518$.

d: Kiyohara and Benson, (1973); DMA, $A_0=2.61313$, $A_1=-0.10497$.

e: Goates et. al, 1979, Sodev Model OI, $A_0=2.6099$, $A_1=-0.0958$, $A_2=0.0444$,
 $A_3=-0.0136$

(1) Mixing Cell

The mixing cell is shown in figure 7-1. A hypodermic needle was inserted into the cell through the silicone rubber in septum 1 and the air in the cell was drawn out by a vacuum pump. The cell then was weighed on a Mettler B5 balance before component 1 was injected into the cell with a precision safety corporation "pressure-lok" syringe by inserting the needle through the silicone rubber. The cell loaded with component 1 was weighed again to determine the amount of component 1 in the cell. Then the second component was injected into the cell in the same way, and the cell was almost completely filled with liquids. The cell was weighed once more. With buoyancy correction, the accuracy of each weighing was believed to be ± 0.0001 g. The liquids in the cell were mixed by shaking the cell. A needle of a empty "pressure-lok" syringe A was inserted through septum 1, while a needle of another syringe B filled mercury was inserted through septum 2. The mixture was withdrawn from cell to the syringe A as the mercury in syringe B was drawn into the cell, so that the volume of the space above the liquids in the cell remained nearly constant. The needles of the syringes then were pulled out after the valve on the pressure-lok syringe A was closed. The mixture was then injected into the vibrating tube of the densimeter.

(2) "Pressure-Lok" Syringe

The "pressure-lok syringe" is shown in figure 7-2. After it was cleaned and dried, the "pressure-lok" syringe was weighed and component 1 was drawn into the syringe with a hypodermic needle. The valve on the syringe was closed and the needle was detached from the syringe. The syringe was weighed again. The second component was drawn into the syringe with another clean needle until the total volume of two components was about 5 cm^3 . The needle then was detached and about 0.5 cm^3 air was sucked^{ed} into the syringe. The valve on the syringe was closed and the volume of vapour space in the syringe was recorded. The syringe was shaken to mix the liquids and then weighed once more. The mixture was then injected into the densimeter.

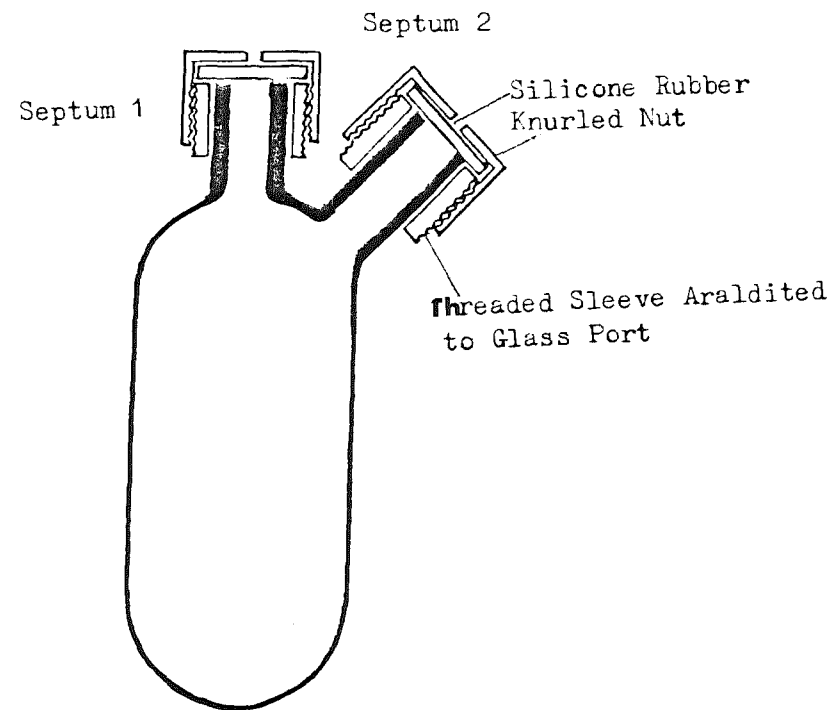


Figure 7-1 Mixing Cell

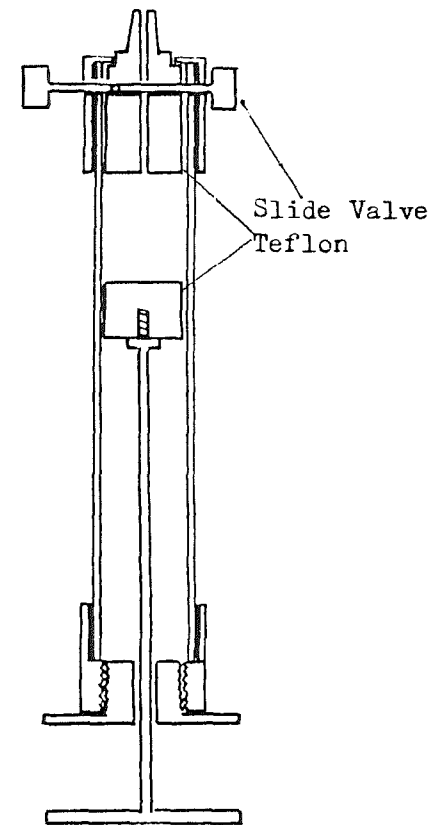


Figure 7-2 "Pressure-Lok" Syringe

7-2.3 CALIBRATION OF DENSIMETER

Doubly distilled water and air were used to calibrate the densimeter. Prior to use, the water was boiled to remove dissolved air. The density of water was taken from the "Hand Book of Chemistry and Physics" (Weast, 1975). The density of moist air was calculated by the equation given in the same source:

$$\rho_a \text{ (g m}^3\text{)} = 1.2929 (273.13/T) (B-0.3783e)/760 \quad \text{..... (7-2.1)}$$

where, B is barometric pressure (mmHg), T is absolute temperature, e is the vapour pressure of the moisture in the air (mmHg). The value of e was estimated from dew point measurement using table given by Weast (1975).

7-2.4 MEASUREMENT OF ATMOSPHERIC PRESSURE AND DEW POINT

Atmospheric pressure was measured by a mercury barometer [Casella, model 4898] and was corrected for temperature and gravity acceleration, but the correction of height was neglected. Dew point was measured with EG & G Digital Humidity Analyzer, model 911, with an accuracy of $\pm 0.5^\circ\text{C}$.

7-2.5 TEMPERATURE CONTROL AND MEASUREMENT

The densimeter was set in an air conditioned room, in which the temperature was maintained within ± 1 K. The temperature of the vibrating tube was regulated at 298.15 K by circulating thermostated water and monitored by a miniature bead thermistor which was close to the sample chamber. The temperature stability in the sample chamber was better than ± 0.003 K. The temperature of the water bath was controlled by the control system described in section 3-3.

The difference in temperatures between the water bath and the sample chamber was less than ± 0.01 K. The water temperature was measured by a platinum resistance thermometer [Rosemount, model WS104, serial No. 240], and a precision comparison bridge [Rosemount, model VLF51A-150]. The calibration of this thermometer is described in section 3-4. The accuracy of the

absolute temperature measurement was believed to be better than ± 0.02 K.

7-2.6 CHEMICALS

Benzene was analytical reagent from M & B, and the quoted purity was better than 99.8 %. Cyclohexane was analytical reagent from BDH with quoted purity better than 99.5 %. The purities of both chemicals were confirmed by gas-liquid chromatography using 2 m column of porapak Q.

Branched hexanes were from Aldrich with quoted purities better than 98 % for 2,2-dimethylbutane, 97 % for 2,3-dimethylbutane, 99 % for 2-methylpentane and 3-methylpentane and n-alkanes were "puriss" grade from Koch-light, with quoted purities of 99 % minimum.

All the branched hexanes and n-alkanes were taken from freshly opened bottles and were used without further purification. As a check of the purities, the densities of all these chemicals were measured and compared with literature values and are listed in table 7-3. The molar mass are listed in table 7-4.

7-2.7 PREPARATION OF PSEUDO ALKANES

Pseudo dodecane was prepared in a stoppered flask by weighing the empty flask, the filled flask with n-tetradecane and filled flask with n-decane + n-tetradecane. The mole fractions of mixtures were accurate to ± 0.001 . The change of density of this pseudo liquid during a series of measurements of densities in the whole composition range for each system was less than 4×10^{-5} g cm⁻³.

7-2.8 DETERMINATION OF DENSITY OF MIXTURES

After the densimeter was calibrated by doubly distilled degassed water and air, the densities of the two "pure" components, then the densities of mixtures were measured. After each two or three measurements of the densities of mixtures, the densimeter was recalibrated and the densities of two "pure" components were measured again and taken for determination of excess volumes to reduce

Table 7-3 Densities (g cm⁻³) of Chemicals Used in This Work at 298.15 K

Compound	Source					
	This Work	Hutchings 1985	Goates 1981	Awwad 1985	Riddick 1970	TRC. Table 1985
benzene	0.873369				0.87370	
cyclohexane	0.773645				0.77389	
octane	0.698540	0.69876	0.69866		0.69849	0.69862
decane	0.726004	0.72622	0.72609	0.72588	0.72625	0.72635
undecane	0.736288	0.73652				0.7365
dodecane	0.745097			0.74519	0.74516	0.74518
tridecane	0.753411	0.75315				0.75271
tetradecane	0.759052			0.75906		0.75920
hexadecane	0.770686			0.77006		0.76994
2-MP	* 0.648526				0.64852	
3-MP	0.659602				0.65976	
2,3-DMB	0.656768				0.65702	
2,2-DMB	0.644314				0.64446	

2-MP = 2-methylpentane; 3-MP = 3-methylpentane; 2,3-DMB = 2,3-dimethylbutane;
2,2-DMB = 2,2-dimethylbutane.

*: The density of 2-MP used in measurement of V^E of n-dodecane + 2-MP is 0.648613, although it came from the same company as other 2-MP.

Table 7-4 Values of Constants in Antoine Equation
And Molar Weights

Compound	A	B	C	molar weight (g)
benzene	6.90565	1211.033	220.790	78.115
cyclohexane	6.84498	1203.526	222.863	84.162
octane	6.92377	1355.126	209.517	114.233
decane	6.95367	1501.268	194.480	142.287
dodecane	6.98059	1625.928	180.311	170.341
tridecane				184.368*
tetradecane				198.395*
hexadecane				226.449*
n-hexane	6.87776	1171.530	224.366	86.178
2-methylpentane	6.83910	1135.410	226.572	86.178
3-methylpentane	6.84887	1152.368	227.129	86.178
2,2-dimethylbutane	6.75483	1081.176	229.343	86.178
2,3-dimethylbutane	6.80983	1127.187	228.900	86.178

*, from TRC. Thermodynamic Table (1985); the others, from Techniques of Chemistry, Vol 2, Organic Solvent (Riddick and Bunger, 1970).

the error caused by any drift of the instrument and the change of the density of pseudo liquid.

7-3 CALCULATION PROCEDURE

V^E can be calculated from the densities of two pure components and their mixtures by the equation:

$$V^E = x_1 M_1 (1/\rho - 1/\rho_1) + x_2 M_2 (1/\rho - 1/\rho_2) \quad \text{..... (7-3.1)}$$

where ρ, ρ_1, ρ_2 are the densities of mixture, component 1, and component 2, respectively and x_i is the mole fraction of component i. The density of a sample obtain from the observations on the densimeter as

$$\rho_s = \rho_w + (\rho_w - \rho_a)(\tau_s^2 - \tau_w^2) / (\tau_w^2 - \tau_a^2) \quad \text{..... (7-3.2)}$$

where, τ is the period of oscillation, and the subscripts s, w, a represent the pure component or mixture, doubly distilled degassed water, and air, respectively.

7-3.1 MIXING CELL

As described in section 7-2.2, the mixtures were prepared in the evacuated mixing cell. Assuming no change in air density between the two weighings of the empty cell and the cell including the component, only the buoyancy correction to the weights is required. Then the mass of liquid w_s is

$$w_s = (1 - \rho_a / \rho_w) (w^f - w^e) \quad \text{..... (7-3.3)}$$

where w^f and w^e are the weight of the cell including the component concerned and the weight of the cell before the component is filled, respectively, and ρ_a and ρ_w are the densities of the air and weights. The composition is then given by

$$x_i = (w_{si} / M_i) / \sum (w_{si} / M_i) \quad \text{..... (7-3.4)}$$

where M is molar mass. A correction is necessary for the change of mole fraction in the liquid phase due to the evaporation of liquid into the space above the liquid. Assuming the mixture is an ideal solution and the vapour is an ideal

gas, then

$$\Delta n_1 = p_1^0 v_{spa} x_1 / RT, \quad \Delta n_2 = p_2^0 v_{spa} x_2 / RT \quad \text{..... (7-3.5)}$$

where Δn is the quantity evaporated into the space above the liquid in the mixing cell. p_i^0 is the saturated vapour pressure at given temperature and V_{spa} is the volume of space above the liquid in the mixing cell. The saturated vapour pressure can be calculated by the Antoine equation with known parameters A, B, C which are listed in table 7-4 (Riddick and Bunger, 1977).

$$p^0 \text{ (mmHg)} = \exp \{ [2.30259 [A-B/(t+c)]] \} \quad \text{..... (7-3.6)}$$

where t is the Celsius temperature. The corrected mole fraction x is

$$x_i' = (w_{si} / M_i - \Delta n_i) / \Sigma (w_{si} / M_i - \Delta n_i) \quad \text{..... (7-3.7)}$$

The zeroth approximation of x_i , which is calculated by eq. (7-3.4), is substituted into eq. (7-3.5) to obtain Δn_1 and Δn_2 . The first approximation of x_i' is then calculated by eq. (7-3.7) and is substituted into eq. (7-3.5) again. This cycle is continued until sufficient accuracy of x_i' is achieved. A programme DVEC for carrying this calculation is listed in appendix 3.

7-3.2 "PRESSURE-LOK" SYRINGE

With buoyancy correction, the weight of liquid is

$$w_{s1} = (1 - \rho_a / \rho_w + \rho_a / \rho_1) (w_{f1} - w_{e1}) + (p_1^0 \rho_a v_{spa1} / p_a) \quad \text{..... (7-3.8)}$$

$$w_{s2} = (1 - \rho_a / \rho_w + \rho_a / \rho_2) (w_{f2} - w_{e2}) + [(p_1^0 x_1 + p_2^0 x_2) \rho_a v_{spa2} / p_a] \quad \text{..... (7-3.9)}$$

where v_{spa} is the volume of space above liquid in the syringe and p_a is the atmospheric pressure; $\rho_a, \rho_w, \rho_1, \rho_2$ are the densities of air, weights, component 1, and component 2; w_f and w_e are the weights of the cell including the component and the cell before the component is filled; subscripts 1 and 2 refer to component 1 and component 2. The last terms in eq. (7-3.8) and (7-3.9) are the corrections for evaporation of liquid when some air is drawn into the syringe. As the piston is moved, the volume of space above liquid in syringe increases and some air is drawn into the space and some liquid in the syringe evaporates

into the space. If the pressure in the syringe is constant, more air is exhausted from the opened end of the syringe than it is drawn into the syringe. The difference is

$$p_1^0 \rho_a v_{spa1} / p_a \text{ for eq. (7-3.8), and } (p_1^0 x_1 + p_2^0) x_2 \rho_a v_{spa2} / p_a \text{ for eq. (7-3.9).}$$

Usually, the air drawn into the syringe was less than 0.5 cm^3 , therefore these corrections were less than $2.5 \times 10^{-4} \text{ g}$. At first, let the last terms in eq. (7-3.8) and (7-3.9) be zero, and the zeroth approximation of w_{si} is obtained. Substitute w_{s1} and w_{s2} into (7-3.4), the zeroth approximation of x_i is obtained, then the first, second, approximations of x_i' are calculated from eq. (7-3.4) to (7-3.9). This cycle is continued until sufficient accuracy is achieved. A computation programme DVES for the calculation described above is listed in appendix 3.

7-4 TEST OF EXPERIMENTAL METHOD

7-4.1 REPEATABILITY OF MEASUREMENT OF PERIOD OF OSCILLATION

The measurements of period of oscillation (τ) for cyclohexane, benzene, doubly distilled water, 3-methylpentane, and 2,3-dimethylbutane were repeated several times. The repeatability in τ for short time intervals (two hr) was about one part in 10^6 .

7-4.2 PREPARATION OF MIXTURES BY MIXING CELL

The seal of silicone rubber in the septum of the mixing cell was tested by reproducing the procedure for the preparation of mixtures. Some n-hexane was injected into the mixing cell and the two gland nuts were tightened. A needle attached to a "pressure-lok" syringe was then passed through the silicone rubber septum several times. Before and after each time, the cell was weighed again. No significant change in weight were detected after each operation. A dry clean evacuated cell was weighed and then a needle attached to a pressure-lok syringe was passed through the silicone rubber septum several times. The cell was weighed before and after each operation. No significant change in weight was

detectable. The silicone rubber seal thus appeared good enough for accurate preparation of mixtures.

The mixing operation could cause a number of problems, which are summarized in the following questions:

(a) Does the mercury contaminate the samples so that it causes a change of the density of mixture?

(b) Does the silicone rubber contaminate the samples so that it causes a change of the density of the samples?

(c) Does the mixing operation change the quantity of air dissolved in the liquid samples so that it causes a change in the density of mixture?

(d) Is there a difference between the volume of the mixture drawn into the syringe and the volume of mercury drawn into the mixing cell?

A test was designed to examine these problems. A pure liquid instead of two liquids was injected into and afterwards sucked out of the mixing cell, following the procedure described in 7-2. The period of vibration of the densimeter for this liquid was obtained before and after this operation. The differences between the two periods of vibration of liquids with and without the operations are within the error of the measurement of the instrument and the difference of volume of mixture drawn out the mixing cell and of mercury drawn into the mixing cell was less than 0.1 cm^3 .

7-4.3 PREPARATION OF MIXTURES IN "PRESSURE-LOK" SYRINGE

The "pressure-lok syringe" was filled with n-hexane and weighed intermittently. This test showed that change rate of weight due to leakage was $2 \times 10^{-5} \text{ g min}^{-1}$. Usually, the operation time after the volatile component was sucked into the syringe was less than 5 minutes so that the error in mass from the leakage was less than 10^{-4} g .

As described in section 7-3, the correction of weight due to the difference between the amounts drawn into the syringe and withdraw from the open end of the syringe is equal to the third terms of eq. (7-3.8) and (7-3.9). This prediction was tested by a following experiment:

Some n-hexane was sucked into the syringe and the syringe was weighed after the valve on the syringe was closed. Some air was sucked into the syringe and

the syringe was weighed again. The difference between two weighings agreed with the prediction by eq. (7-3.8) within the accuracy of weighing.

7-5 ERROR ANALYSIS

The maximum total error in measurement of V^E is

$$|\delta V^E| = |\delta V^E(x)| + |\delta V^E(t)| + |\delta V^E(o)| \quad \text{..... (7-5.1)}$$

and probable error is

$$\sigma V^E = \{[\delta V^E(x)]^2 + [\delta V^E(t)]^2 + [\delta V^E(o)]^2\}^{0.5} \quad \text{..... (7-5.2)}$$

where, $\delta V^E(x)$ = the error from the uncertainty of mole fraction;

$\delta V^E(t)$ = the error from the temperature fluctuation.

$\delta V^E(o)$ = the error from the uncertainty in measurements with the oscillator densimeter.

7-5.1 ERROR OF MOLE FRACTION

(A) Due To The Error in Weighing ($|\delta x^{(A)}|$, or $\sigma x^{(A)}$)

From eq. (7-3.3), the error in weight for the mixing cell may be estimated by

$$|\delta w_s| = 2(1-\rho_a/\rho_w) |\delta w| + [(w^f - w^e)/\rho_w] |\delta \rho_a| + [\rho_a (w^f - w^e)/\rho_w^2] |\delta \rho_w| \quad \text{..... (7-5.3)}$$

The first term in eq. (7-5.3) is much larger than the other terms. Therefore,

$$|\delta w_s| = 2(1-\rho_a/\rho_w) |\delta w| = 2 |\delta w| \quad \text{..... (7-5.4)}$$

and the probable error is

$$\sigma w_s = 2^{0.5} |\delta w| \quad \text{..... (7-5.5)}$$

The same results may be obtained for the "pressure-lok" syringe from eq. (7-3.8) and (7-3.9). From eq. (5-4.8), the error in mole fraction caused by the error in weighing can be calculated by

$$|\delta x^{(A)}| = x_1 x_2 (1/w_{s1} + 1/w_{s2}) |\delta w_s| \quad \text{..... (7-5.6)}$$

and

$$\sigma x^{(A)} = x_1 x_2 [(\delta w_s / w_{s1})^2 + (\delta w_s / w_{s2})^2]^{0.5} \quad \text{..... (7-5.7)}$$

For "the pressure-lok" syringe, an error caused by loss of an amount of volatile material (δw_{evp}) due to evaporation during preparation of the mixture is introduced. Thus

$$|\delta x^{(A)}| = x_1 x_2 (1/w_{s1} + 1/w_{s2}) |\delta w_s| + x_1 x_2 (\delta w_{\text{evp}}/w_{s1}) \quad \text{..... (7-5.8)}$$

$$\sigma x^{(A)} = x_1 x_2 [(\delta w_s / w_{s1})^2 + (\delta w_s / w_{s2})^2 + (\delta w_{\text{evp}}/w_{s1})^2]^{0.5} \quad \text{..... (7-5.9)}$$

(B) Due To The Error in Estimation of the Amount of Volatile Material

Evaporated into the Vapour Phase ($|\delta x^{(B)}|$, or $\sigma x^{(B)}$):

From eq. (7-3.7), we have

$$\delta x_i^{(B)} = -[n_i/(n_i+n_j)^2] \delta(\Delta n_i) + [n_i/(n_i+n_j)^2] \delta(\Delta n_j) \quad \text{..... (7-5.10)}$$

where n is the mole number and Δn is defined by (7-3.5). If $p_j^0 \gg p_1^0$, we neglect the subscript i of $\delta x_i^{(B)}$, then

$$\text{Max } \delta x^{(B)} = -[n_2/(n_1+n_2)^2] \delta(\Delta n_1) \quad \text{..... (7-5.11)}$$

According eq. (7.35), we have

$$\delta(\Delta n_1) = \Delta n_1 (\delta p_1^0/p_1^0) + \Delta n_1 (\delta v_{\text{spa}}/v_{\text{spa}}) \quad \text{..... (7-5.12)}$$

Substitute (7-5.12) into (7-5.11) we have

$$\text{Max } |\delta x^{(B)}| = \Delta n_1 n_2/(n_1+n_2)^2 [(\delta p_1^0/p_1^0) + (\delta v_{\text{spa}}/v_{\text{spa}})] \quad \text{..... (7-5.13)}$$

and

$$\sigma x^{(B)} = \Delta n_1 n_2/(n_1+n_2)^2 [(\delta p_1^0/p_1^0)^2 + (\delta v_{\text{spa}}/v_{\text{spa}})^2]^{0.5} \quad \text{..... (7-5.14)}$$

From eq. (7-3.6),

$$\delta p_1^0 = [2.303 B p_1^0 / (t+c)^2] \delta t' \quad \text{..... (7-5.15)}$$

where t is the room temperature and $\delta t'$ is the error in measurement of room temperature. The total error in mole fraction is then

$$|\delta x| = |\delta x^{(A)}| + \text{Max } |\delta x^{(B)}| \quad \text{..... (7-5.16)}$$

and

$$\sigma_x = [(\sigma_{x^{(A)}})^2 + (\sigma_{x^{(B)}})^2]^{0.5} \quad \text{..... (7-5.17)}$$

According to eq. (7-3.1), the error in V^E due to the error in mole fraction is

$$|\delta V^E(x)| = M_1 |(1/\rho - 1/\rho_1) \delta x| + M_2 |(1/\rho - 1/\rho_2) \delta x| \quad \text{..... (7-5.18)}$$

7-5.2 TEMPERATURE FLUCTUATION

Temperature fluctuation causes fluctuations of densities of pure components and the mixtures and hence introduces an error in V^E . This error may be estimated as

$$\begin{aligned} |\delta V^E(t)| = & [(M_1 x_1 + M_2 x_2)/\rho^2] |(\partial \rho / \partial t) \delta t| + (M_1 x_1 / \rho_1^2) |(\partial \rho_1 / \partial t) \delta t| + \\ & + (M_2 x_2 / \rho_2^2) |(\partial \rho_2 / \partial t) \delta t| \quad \text{..... (7-5.19)} \end{aligned}$$

$$\begin{aligned} \sigma V^E(t) = & [\{ [(M_1 x_1 + M_2 x_2)/\rho^2] (\partial \rho / \partial t) \delta t \}^2 + \{ (M_1 x_1 / \rho_1^2) |(\partial \rho_1 / \partial t) \delta t| \}^2 + \\ & + \{ (M_2 x_2 / \rho_2^2) |(\partial \rho_2 / \partial t) \delta t| \}^2]^{0.5} \quad \text{..... (7-5.20)} \end{aligned}$$

7-5.3 UNCERTAINTY IN MEASUREMENT WITH OSCILLATOR DENSIMETER

As described in section 7-4.1, the uncertainty in measurement of the period of oscillation was about 10^{-6} which is the sum of random error and a systematic drift of the instrument. According to eq. (7-1.2), we have

$$\delta \rho = 2B\tau \delta \tau \quad \text{..... (7-5.21)}$$

With distilled water and air as references, B is approximately equal to 0.56. For the systems investigated in this work, an error of 10^{-6} in τ cause an error of about 2×10^{-6} g cm⁻³ in density. The error in V^E can be calculated by

$$\begin{aligned} |\delta V^E(o)| = & [(M_1 x_1 + M_2 x_2)/\rho^2] |\delta \rho| + (M_1 x_1 / \rho_1^2) |\delta \rho_1| + (M_2 x_2 / \rho_2^2) |\delta \rho_2| \\ & \text{..... (7-5.22)} \end{aligned}$$

$$\sigma V^E(o) = \left[\left\{ \frac{(M_1 x_1 + M_2 x_2)}{\rho^2} \delta \rho \right\}^2 + \left\{ \frac{(M_1 x_1)}{\rho_1^2} \delta \rho_1 \right\}^2 + \left\{ \frac{(M_2 x_2)}{\rho_2^2} \delta \rho_2 \right\}^2 \right]^{0.5}$$

..... (7-5.23)

The maximum errors and probable errors were estimated for the system cyclohexane + benzene and 2,2-dimethylpentane + dodecane at equimolar composition and are listed in table 7-5 and 7-6. The data used in estimation are given as follows:

$$v_{spa} = 0.5 \text{ cm}^3, \delta t = 0.003 \text{ K}, \delta t' = 1 \text{ K}, \delta \rho = 2 \times 10^{-6} \text{ g cm}^{-3}, \delta v_{spa} = 0.1 \text{ cm}^3$$

cyclohexane (1) + benzene (2) :

$$w_{s1} = 2.9 \text{ g}, w_{s2} = 2.8 \text{ g}, M_1 = 84.2 \text{ g mol}^{-1}, M_2 = 78.1 \text{ g mol}^{-1}, \rho_1 = 0.77 \text{ g cm}^{-3},$$

$$\rho_2 = 0.87 \text{ g cm}^{-3}, \partial \rho / \partial t = 10^{-3} \text{ g cm}^{-3} \text{ K}^{-1}, p_1^o = 1.31 \times 10^4 \text{ pa}, p_2^o = 1.26 \times 10^4 \text{ pa}.$$

2,2-dimethylpentane (1) + dodecane (2):

$$w_{s1} = 2.5 \text{ g}, w_{s2} = 1.4 \text{ g}, M_1 = 86.2 \text{ g mol}^{-1}, M_2 = 170 \text{ g mol}^{-1}, \rho_1 = 0.64 \text{ g cm}^{-3},$$

$$\rho_2 = 0.75 \text{ g cm}^{-3}, \partial \rho / \partial t = 10^{-3} \text{ g cm}^{-3} \text{ K}^{-1}, p_1^o = 4.27 \times 10^4 \text{ pa}, p_2^o = 16 \text{ pa}.$$

7-6 EXPERIMENTAL RESULTS

The densities of mixtures of cyclohexane + benzene prepared by the mixing cell and "pressure-lok" syringe were measured separately and the excess volumes were derived from the measured densities of pure components and their mixtures by eq. (7-3.1). The results are listed in table 7-7. The experimental data were fitted to eq. (7-1.3) to optimize the parameters by using the linear least squares method described in section 5-2.1. The optimum values of these parameters and the standard deviations (R) are listed and compared with those from the other authors in table 7-1. The excess volumes for varying mole fractions of cyclohexane and benzene calculated by eq. (7-1.3) using the optimum parameters are listed and compared in table 7-2. The differences between the results from our work and from the reference values and between our two methods of preparation of mixtures were less than $4 \times 10^{-3} \text{ cm}^3 \text{ mol}^{-1}$. The deviations of fitting eq. (7-1.3) ($r = V_{cal}^E - V_{exp}^E$) are compared in figure 7-3. The

Table 7-5 Maximum Estimated Errors at $x=0.5$

System and method	$ \delta x $	$ \delta V^E(x) $ ($\text{cm}^3\text{mol}^{-1}$)	$ \delta V^E(t) $ ($\text{cm}^3\text{mol}^{-1}$)	$ \delta V^E(o) $ ($\text{cm}^3\text{mol}^{-1}$)	$ \delta V^E $ ($\text{cm}^3\text{mol}^{-1}$)
mixing Cell:					
cyclohexane + benzene	3.5×10^{-5}	4.3×10^{-4}	7.2×10^{-4}	4.8×10^{-4}	1.6×10^{-3}
syringe:					
cyclohexane + benzene	4.4×10^{-5}	5.4×10^{-4}	7.2×10^{-4}	4.8×10^{-4}	1.7×10^{-3}
2,2-dimethylbutane + n-hexadecane	8.7×10^{-5}	2.4×10^{-3}	1.6×10^{-3}	1.1×10^{-3}	5.1×10^{-3}

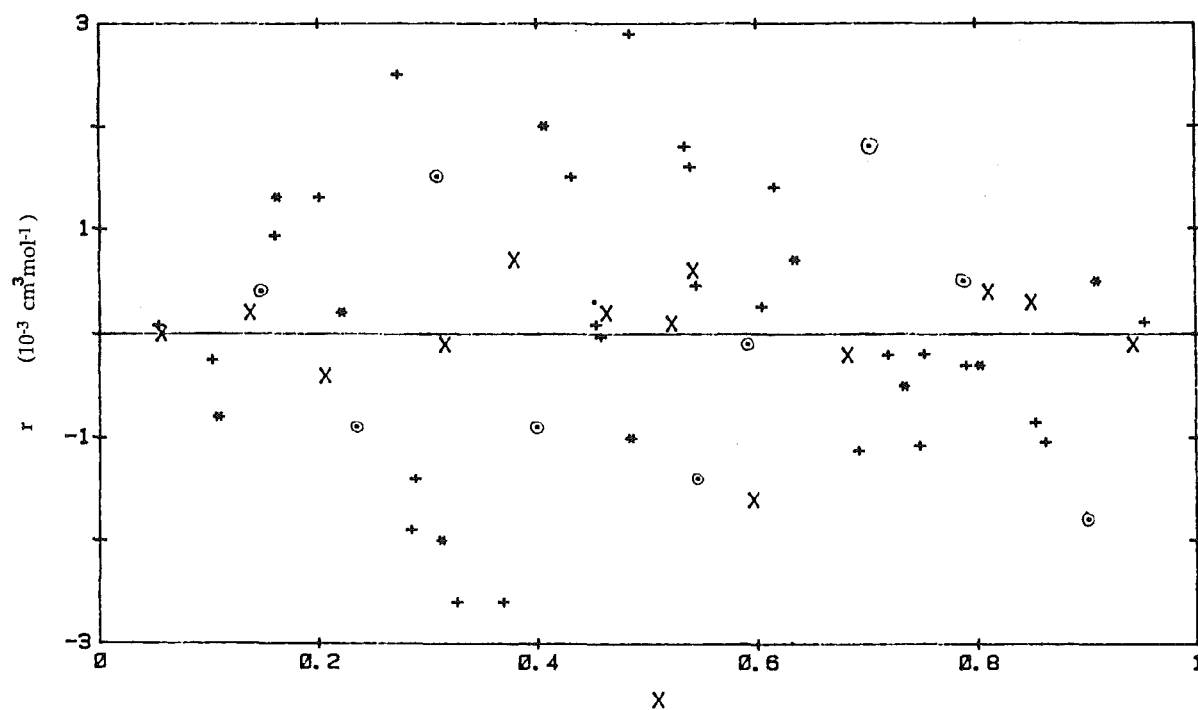
Table 7-6 Probable Estimated Errors at $x=0.5$

System and method	σx	$\sigma V^E(x)$ ($\text{cm}^3\text{mol}^{-1}$)	$\sigma V^E(t)$ ($\text{cm}^3\text{mol}^{-1}$)	$\sigma V^E(o)$ ($\text{cm}^3\text{mol}^{-1}$)	σV^E ($\text{cm}^3\text{mol}^{-1}$)
mixing Cell:					
cyclohexane + benzene	2.5×10^{-5}	3.1×10^{-4}	4.4×10^{-4}	2.9×10^{-4}	6×10^{-4}
syringe:					
cyclohexane + benzene	3.1×10^{-5}	3.8×10^{-4}	4.4×10^{-4}	2.9×10^{-4}	7×10^{-4}
2,2-dimethylbutane + n-hexadecane	4.6×10^{-5}	1.3×10^{-3}	9.6×10^{-4}	6.4×10^{-4}	1.7×10^{-3}

Table 7-7 Experimental Densities and Excess Volumes for
cyclohexane₍₁₎ + benzene₍₂₎ at 298.15 K

$X_{(1)}$	ρ g/cm ³	V^E cm ³ /mol	V^r cm ³ /mol	$X_{(1)}$	ρ g/cm ³	V cm ³ /mol	V^r cm ³ /mol
Mixing Cell							
0	0.873367			0.54438	0.809031	0.6505	-0.0014
0.14758	0.853101	0.3188	0.0004	0.59061	0.804792	0.6359	-0.0001
0.23363	0.842319	0.4575	-0.0009	0.70218	0.795160	0.5549	0.0018
0.30795	0.833698	0.5449	0.0015	0.78747	0.788438	0.4495	0.0005
0.39868	0.823620	0.6200	-0.0009	0.90021	0.780178	0.2469	-0.0018
0.45077	0.818224	0.6419	0.0003	1	0.773645		
" Pressure-Lok" Syringe							
0	0.873368			0.48489	0.814760	0.6536	-0.0010
0.10945	0.858089	0.2486	-0.0008	0.63489	0.800849	0.6119	0.0007
0.16324	0.851055	0.3477	0.0013	0.73431	0.792500	0.5213	-0.0005
0.22158	0.843759	0.4426	0.0002	0.80318	0.787175	0.4259	-0.0003
0.31269	0.830991	0.5574	-0.0020	0.90936	0.779557	0.2250	0.0005
0.40719	0.822701	0.6256	0.0020	1	0.773645		

Figure 7-3 Deviations From Eq. (7-1.3) For cyclohexane + Benzene



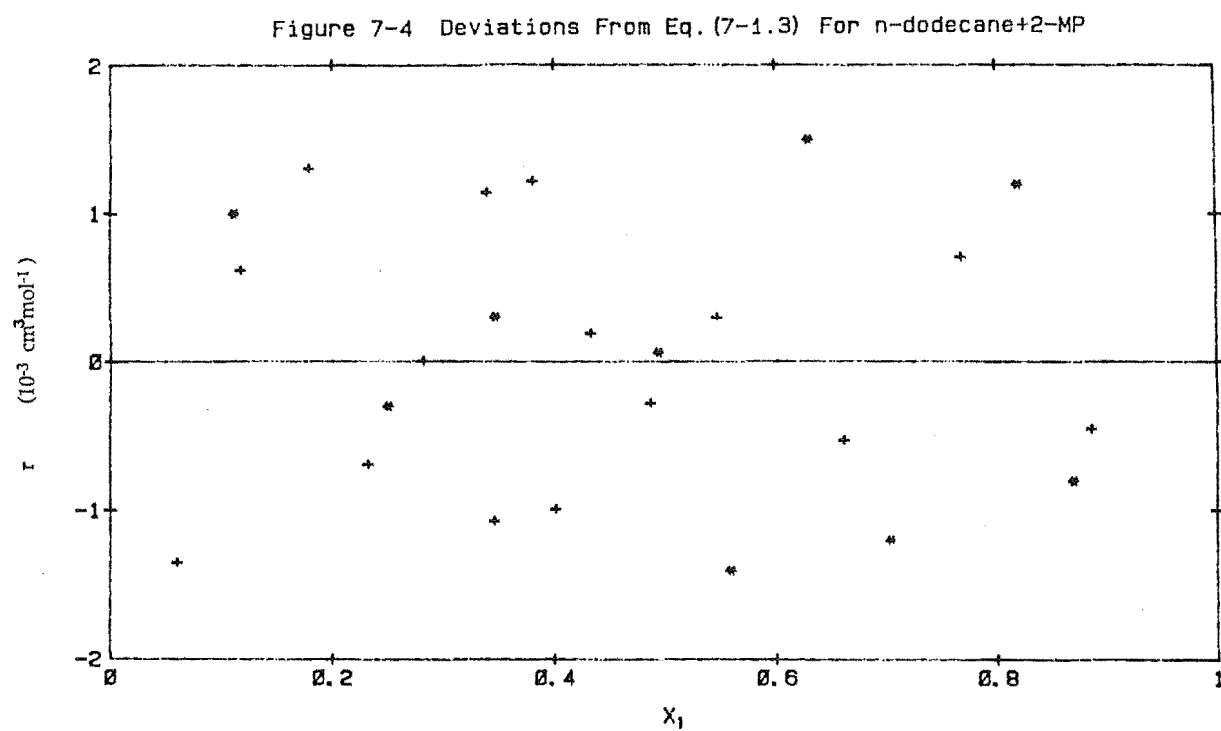
⊙ : From this work (mixing cell)

* : From this work ("pressure-lok" syringe)

x : From Goates et al. (1979)

+ : From Kiyohara et al. (1973)

X_i: Mole fraction of cyclohexane



* : From this work

+ : From Hamam et al. (1984a)

X_1 : Mole fraction of n-dodecane

standard deviation R were slightly higher than the probable error but less than maximum error estimated in section 7-5. The standard deviation for the results from the mixing cell was a little less than that for the results obtained using the "pressure-lok" syringe. This agrees with the error estimations.

The densities and excess volumes of n-dodecane + 2-methylpentane (2-MP) determined by using the syringe method are listed in table 7-8. The optimum parameters in eq.(7-1.3) and standard deviation are listed and compared with those obtained by Hamam et al. (1984a) in rows 1 and 2 of table 7-9. The calculated excess volumes with our and Hamam et al.'s parameters using eq. (7-1.3) are listed and compared in columns 1 and 2 of table 7-10. Two sets measurements agreed within $0.005 \text{ cm}^3 \text{ mol}^{-1}$. The deviations from eq. (7-1.3) are compared with Hamam et al's in figure 7-4.

The densities and excess volumes of pseudo n-dodecane +2-MP, 3-methylpentane (3-MP), 2,3-dimethylbutane (2,3-DMB), 2,2-dimethylbutane (2,2-DMB) using the syringe method were measured and listed in table 7-8, and the parameters with the standard deviations are listed in table 7-9.

The magnitude of excess volume of pseudo n-dodecane + isomers of hexane decrease in the order: 2,2-DMB > 2-MP > 2,3-DMB > 3-MP, just as Hamam et al. observed from their measurements for n-dodecane + isomers.

Table 7-8 Experimental Densities and Excess Volumes for
n-dodecane + hexane Isomers at 298.15 K.

$X_{(1)}$	ρ g/cm ³	V^E cm ³ /mol	r cm ³ /mol	$X_{(1)}$	ρ g/cm ³	V^E cm ³ /mol	r cm ³ /mol
n-dodecane ₍₁₎ + 2-MP ₍₂₎							
0	0648613			0.63046	0.722080	-0.3934	0.0015
0.11102	0.666910	-0.2601	0.0001	0.70458	0.727378	-0.3306	-0.0012
0.25050	0.685786	-0.4409	-0.0003	0.82028	0.734964	-0.2193	0.0012
0.34763	0.696826	-0.4882	0.0003	0.86913	0.737880	-0.1626	-0.0008
0.49401	0.710964	-0.4712	0.0006	1	0.745097		
0.55943	0.716462	-0.4373	-0.0014				
(0.500 n-decane+0.500 n-tetradecane) ₍₁₎ + 2-MP ₍₂₎							
0	0648526			0.55575	0.716149	-0.4425	0.0020
0.10447	0.665845	-0.2534	-0.0003	0.62089	0.721277	-0.3983	-0.0015
0.19053	0.678074	-0.3834	-0.0012	0.71076	0.727788	-0.3267	-0.0009
0.29181	0.690559	-0.4615	-0.0018	0.75091	0.730507	-0.2914	0.0013
0.40122	0.702228	-0.4884	0.0013	0.89030	0.739088	-0.1381	-0.0002
0.51252	0.712502	-0.4601	-0.0011	1	0.745072		

Table 7-8 Continued ...

$X_{(1)}$	ρ g/cm ³	V^E cm ³ /mol	r cm ³ /mol	$X_{(1)}$	ρ g/cm ³	V^E cm ³ /mol	r cm ³ /mol
(0.500 n-decane + 0.500 n-tetradecane) ₍₁₎ + 3-MP ₍₂₎							
0	0.659602			0.59701	0.722436	-0.3002	0.0003
0.09883	0.674212	-0.1763	-0.0013	0.69308	0.728733	-0.2486	0.0012
0.20678	0.687704	-0.2914	0.0018	0.80843	0.735465	-0.1642	-0.0015
0.29558	0.697254	-0.3351	-0.0003	0.91040	0.748070	-0.0813	0.0007
0.42063	0.708869	-0.3489	-0.0007	1	0.745085		
0.49307	0.714790	-0.3371	-0.0004				
(0.500 n-decane + 0.500 n-tetradecane) ₍₁₎ + 2,3-DMB ₍₂₎							
0	0.656768			0.57750	0.720397	-0.3733	-0.0043
0.09996	0.672129	-0.2171	0.0010	0.68273	0.727622	-0.3096	0.0005
0.1963	0.684679	-0.3388	-0.0013	0.70236	0.728872	-0.2938	0.0002
0.29587	0.695866	-0.4067	0.0002	0.78190	0.733681	-0.2242	0.0009
0.41934	0.707727	-0.4260	-0.0002	0.89197	0.739712	-0.1114	-0.0006
0.49767	0.714327	-0.4129	0.0018	1	0.745073		
0.52294	0.716320	-0.4043	0.0019				

Table 7-8 Continued ...

$X_{(1)}$	ρ g/mol	V^E cm ³ /mol	r cm ³ /mol	$X_{(1)}$	ρ g/cm ³	V^E cm ³ /mol	r cm ³ /mol
(0.500 n-decane + 0.500 n-tetradecane) ₍₁₎ + 2,2-DMB ₍₂₎							
0	0.644314			0.56867	0.716279	-0.5689	0.0012
0.10041	0.661931	-0.3189	0.0004	0.69146	0.725845	-0.4478	-0.0011
0.19842	0.676518	-0.5071	-0.0016	0.74679	0.729766	-0.3828	0.0015
0.28459	0.687670	-0.6020	0.0018	0.84940	0.736427	-0.2382	0.0001
0.42029	0.702654	-0.6372	0.0005	0.91892	0.740578	-0.1302	0.0008
0.50004	0.710276	-0.6091	-0.0022	1	0.745071		

Table 7-9 Values of Parameters in Equation (7-1.3) for
n-dodecane + hexane Isomers at 298.15 K

SYSTEMS	A1	A2	A3	A4	A5	R
1 *	-1.8745	-0.7534	-0.2752	-0.0666		0.0010
2	-1.8728	-0.8217	-0.3391	0.0672	0.1410	0.0014
3	-1.8647	-0.7574	-0.3144	-0.1031		0.0017
4 *	-1.3476	-0.5567	-0.2407	-0.0964		0.0008
5	-1.3428	-0.5375	-0.2363	-0.1321		0.0014
6 *	-1.6282	-0.6940	-0.2891	-0.0776		0.0012
7	-1.6417	-0.6338	-0.2099	-0.2314		0.0021
8 *	-2.4410	-0.9983	-0.4252	-0.1646		0.0007
9	-2.4454	-0.9972	-0.3310	-0.1427		0.0017

1,2 : n-dodecane + 2-MP;

3: pseudo n-dodecane + 2-MP;

4: n-dodecane + 3-MP

5: pseudo n-dodecane + 3-MP;

6: n-dodecane + 2,3-DMB;

7: pseudo n-dodecane + 2,3-DMB;

8: n-dodecane + 2,2-DMB;

9: pseudo n-dodecane + 2,2-DMB;

*: from Hamam et al. (1984a).

Table 7-10 Comparison of V^E for n-dodecane and pseudo
n-dodecane + hexane Isomers Calculated by Eq. (7-1.3) at 298.15 K
(x: mole fraction of c_{12})

X	1*	2	3	4*	5	6*	7	8*	9
0.1	-0.2419	-0.2390	-0.2452	-0.1797	-0.1793	-0.2167	-0.2163	-0.3236	-0.3175
0.2	-0.3904	-0.3928	-0.3927	-0.2863	-0.2846	-0.3465	-0.3437	-0.5166	-0.5110
0.3	-0.4671	-0.4720	-0.4672	-0.3391	-0.3369	-0.4110	-0.4082	-0.6130	-0.6103
0.4	-0.4888	-0.4920	-0.4871	-0.3526	-0.3506	-0.4270	-0.4269	-0.6382	-0.6383
0.5	-0.4686	-0.4682	-0.4662	-0.3369	-0.3357	-0.4071	-0.4104	-0.6103	-0.6114
0.6	-0.4162	-0.4134	-0.4140	-0.2988	-0.2985	-0.3609	-0.3652	-0.5417	-0.5419
0.7	-0.3387	-0.3358	-0.3371	-0.2430	-0.2430	-0.2923	-0.2954	-0.4408	-0.4390
0.8	-0.2411	-0.2397	-0.2402	-0.1727	-0.1723	-0.2079	-0.2058	-0.3135	-0.3097
0.9	-0.1272	-0.1268	-0.1266	-0.0906	-0.0897	-0.1096	-0.1034	-0.1647	-0.1608

1,2 : n-dodecane + 2-MP;
 3: pseudo n-dodecane + 2-MP;
 4: n-dodecane + 3-MP
 5: pseudo n-dodecane + 3-MP;
 6: n-dodecane + 2,3-DMB;
 7: pseudo n-dodecane + 2,3-DMB;
 8: n-dodecane + 2,2-DMB;
 9: pseudo n-dodecane + 2,2-DMB;
 *: from Hamam et al. (1984a).

CHAPTER 8 EXCESS ENTHALPIES OF MIXING

8-1 GENERAL DESCRIPTION OF THE EXPERIMENTAL APPARATUS AND METHODS

The isothermal displacement calorimeter used in this work is similar in construction to that reported by Marsh et al. (Stokes, 1969; Ewing, 1970). Some modifications were made to ensure that the chemicals in the calorimeter do not directly contact materials such as "araldite". The glass ports through which the stainless steel tubes and the shaft of the stirrer were introduced were ground internally to a 12 degree angle. Teflon tapers were made with holes to fit the shaft and tubes. Threaded sleeves made from stainless steel were araldited to the glass ports. Knurled nuts then were used to tighten the teflon tapers to make the seals at the bottoms of the tapered holes in the glass ports. The calorimeter contents are thus exposed only to glass teflon and stainless steel.

The details of the calorimeter and the injection system are shown in figure 8-1 and figure 8-2. The volume of the calorimeter vessel (A) was 59.41 cm^3 , calibrated with xylene, and accurate to $\pm 0.06 \text{ cm}^3$. The density of xylene was measured by a Mettler DMA 60/ DMA 602H vibrating tube densitometer described in section 7-2. The volume of the pipette (X) was approximately 35 cm^3 , filled with mercury. The volume of mercury in the calorimeter was 32.59 cm^3 at $298.15 \text{ K} (\pm 0.01 \text{ cm}^3)$. Thus the volume of component 1 in the calorimeter was $26.82 \text{ cm}^3 (\pm 0.06 \text{ cm}^3)$. The pipette level was adjusted so that there was always a positive pressure on the calorimeter vessel of 2-3 kpa above atmospheric pressure. The second liquid (component 2) to be injected into the calorimeter was drawn into a bulb (M) with an approximate volume of 50 cm^3 . The injection was driven by a motorized burette (N) with a volume of 10 cm^3 . The estimated uncertainty for each injection was $\pm 0.01 \text{ cm}^3$. The total error in mole fraction for the binary mixtures was about 0.001. The mercury reservoir (O), with an approximate volume of 50 cm^3 , was used to feed the burette, and load and unload the bulb by adjusting its level.

The experiment was carried out in an air conditioned room, in which the temperature was stabilized within $\pm 1 \text{ K}$. The water bath was consisted of a

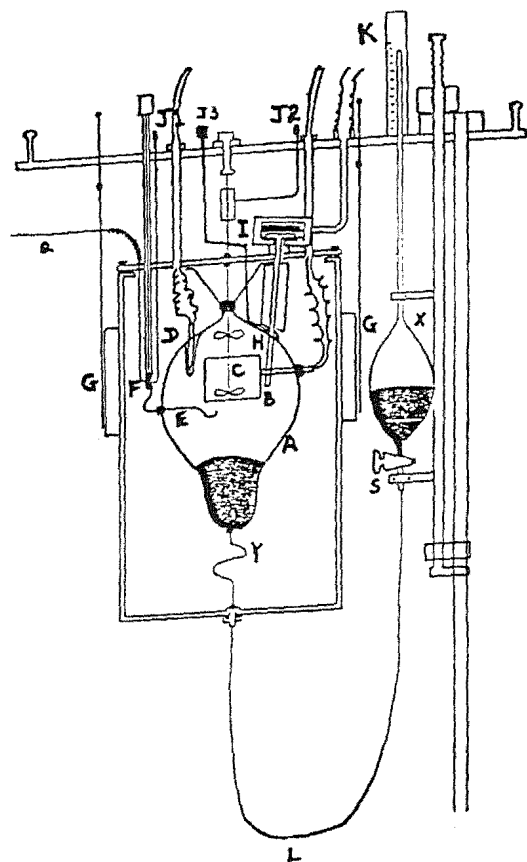


Figure 8-1 The Calorimeter Vessel

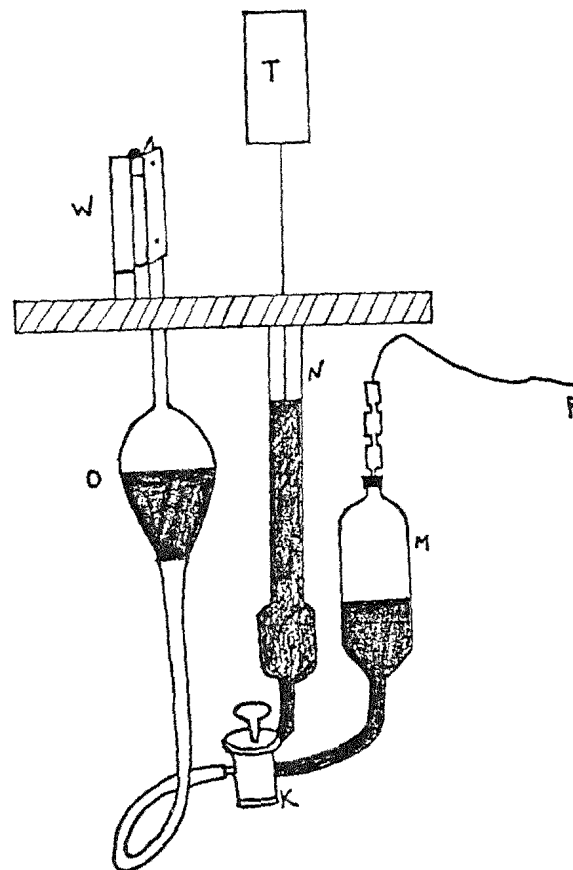


Figure 8-2 The Injection System

Key to Figure 8-1 and 8-2

A : Calorimeter glass vessel.
B : Calorimeter heating element.
C : Stirrer.
D : Thermistor for measurement of temperature in the calorimeter.
E : Exit of the injection line.
F : Calorimeter inlet valve.
G : Glass window.
H : Peltier.
I : Stirrer shaft.
J1, J2, J3: Valves of vents of F, I, and H.
K : Mark for the level of pipette.
L : Pipette connecting line.
Q : Injection inlet line.
S : Pipette valve.
X : Pipette.
Y : Calorimeter bottom inlet tub.

K : Three way valve
M : Bulb.
N : Burette.
O : Mercury reservoir.
P : Injection inlet line.
T : Burette motor and gearbox
W : Clip.

48X48X60 cm tank insulated with a 2.5 cm thick layer of polystyrene. The temperature in the water bath was maintained to ± 0.0004 K by base and on/off temperature controllers described in section 3-3. The temperature was measured by a platinum resistance thermometer [Rosemount, model WS104, serial No. 240], and a precision comparison bridge [Rosemount model VLF51A-150]. The calibration of this thermometer was described in section 3-4.

The 108.03Ω calorimeter heater was operated manually in on/off mode to compensate the positive enthalpies of mixing. The temperature change during the mixing and heating was recorded by a chart recorder. [Technicorder F type 3052] through a thermistor, a Wheatstone bridge and a null detector [Leeds and Northrup CAT. 9834]. The energy dissipated by the heater was calculated from the voltage (E) across the heater, the current (I) through the heater and accumulated time (t) during which the heater was on. The power dissipated by the stirrer inside the calorimeter vessel caused the steady state temperature of the vessel to be higher than that of the thermostat by an amount $T(\text{corr})$. When a liquid was injected from the burette to "mix" with the same liquid in the calorimeter vessel, a small blank effect could be observed due to the temperature difference $T(\text{corr})$. This small amount of heat may be calculated by

$$Q(\text{corr}) = AN_2 C_{p2} T(\text{corr}) \quad \text{..... (8-1.1)}$$

where N_2 is the number of moles of component 2, which was injected into the calorimeter; C_{p2} is the heat capacity of component 2; $T(\text{corr})$ may be determined as the difference of temperature between two modes (stirrer on and stirrer off). The factor A was less than 1 and determined from the blank experiment of "mixing" the same liquids and was equal to 0.7 (Stokes et al., 1969). The stirring speed was 83 turns per minute. H^E was calculated by

$$H^E = [E I t - Q(\text{corr})]/N \quad \text{..... (8-1.2)}$$

where N is the total number of moles in the calorimeter. The mole fraction in calorimeter after each injection was calculated by:

$$N_2 = \rho_2 V_2 / M_2 \quad \text{..... (8-1.3)}$$

$$N_1 = \rho_1 V_1 / M_1 \quad \text{..... (8-1.4)}$$

$$X_1 = N_1 / (N_1 + N_2); \quad X_2 = N_2 / (N_1 + N_2) \quad \text{..... (8-1.5)}$$

where N_i , ρ_i , V_i , M_i are the number of moles in the calorimeter, density at the temperature in the water bath, volume in calorimeter and molar mass of liquid respectively. 1, 2 refer to component 1, and 2.

8-2 EXPERIMENTAL OPERATIONS

8-2.1 EMPTYING AND CLEANING CALORIMETER

The stirrer shaft was disconnected and then the stirrer motor was removed from its holder. The injection inlet lines (Q, P) were disconnected at the coupling. The null detector was turned to "NON-LIN" mode. The calorimeter light cord, calorimeter thermometer cord and calorimeter heater cord were disconnected. The calorimeter system was lifted from the water bath and placed on lab bench holder.

The stirrer shaft vent (J2) was opened and vacuum was used to draw mercury up in the pipette until the level of mercury was visible below the calorimeter bottom inlet tube (Y). The pipette valve (S) was closed and the vacuum was removed from the pipette. The connecting line (L) was disconnected from Y and all the vents (J) and calorimeter inlet valve (F) were opened to allow the calorimeter contents to drain into a beaker. The calorimeter vessel was filled with a solvent (e.g. cyclohexane) from a syringe through Q after Y is blocked, and the solvent was held in the calorimeter, the inlet line and vent line for half an hour. Y was opened and the solvent was drain into a beaker. This cleaning procedure was repeated once more, then the system was dried for half an hour

with a vacuum hose attached to Y.

8-2.2 EMPTYING AND CLEANING BULB

The injection system was lifted from the water bath and placed on the holder. The mercury reservoir was lifted and the three way valve (K) was set at the position of reservoir-to-bulb to eject the content of the bulb through the injection inlet line (P) into a beaker until mercury was near the end of tube P in the bulb. About 10 cm³ of solvent was drawn into the bulb, and then the mercury in the bulb was lowered slowly. The solvent was ejected and this procedure was repeated once more with another 10 cm³ solvent. The mercury level in the bulb was lowered and the bulb was evacuated for half an hour.

8-2.3 LOADING THE CALORIMETER

With the pipette at maximum elevation, S was opened and mercury was transferred from the pipette into the calorimeter. S was closed when the mercury level dropped to about 2 cm above the bottom mark on the pipette. The liquid to be placed in the calorimeter was loaded into a syringe and attached to the calorimeter inlet line Q with a piece of flexible tubing. J1 was closed, and the liquid in the syringe was then pushed into the calorimeter. It could be necessary to refill the syringe and F should be closed during refilling. The Peltier shaft vent (J3) was closed when the liquid came out it. loading was continued until liquid came out the stirrer shaft vent J2. If there was an air bubble at the stirrer shaft exit, it must be removed by squirting liquid into the calorimeter. F was closed and the calorimeter was put back into the water bath and J2 was closed and valve S was opened. All the cables and the stirrer were then reconnected.

8-2.4 LOADING THE BULB

The mercury was transferred from mercury reservoir to the bulb until the bulb was filled. A syringe containing the liquid to be loaded was attached to P

through a clean flexible tubing. With the valve K in the "injection" position, the level of mercury in the reservoir was adjusted so that the mercury level in the reservoir was lower than that in the bulb. The valve K was turned to the "reservoir-to-bulb" position and the liquid was pushed from the syringe into the bulb until about 35 cm^3 liquid was in the bulb. The valve K was turned to the "injection" position and the flexible tubing was removed. The valve K was turned to the "reservoir-to-bulb" position and all of the air was removed from the bulb after the reservoir was lifted. K was turned to the "injection" position and the level of the reservoir was adjusted so that the levels of mercury in the reservoir and the bulb were nearly the same. The injection system then was put into the water bath. The injection inlet lines P and Q were connected with a coupling and sealed viz the tapered teflon insert. Vent J1 was opened.

8-2.5 OPERATION OF THE CALORIMETER

At least 10 hours prior to a run, the calorimeter and bulb should be loaded, and the stirrer turned on at the run speed.

The chart recorder was turned on and the stirrer was switched off after a steady calorimeter temperature was achieved. The calorimeter temperature reached a new steady state value after about one hour. The difference of temperatures between the two states with the stirrer on and off is then recorded and this is the temperature correction T_{corr} . The stirrer was turned on and the calorimeter temperature went back to the starting state.

The burette motor was switched on after checking that the inlet valve F was closed and the vent J1 was open, and valve K was set to the "injection" position. In order to ensure that only component 2 was in the inlet line before a run the motor was run until about 0.5 cm^3 of liquid had been injected to flush the inlet line. J1 was then closed, and J3, and J2 were opened to allow liquid in the calorimeter to flow out the vents until the mercury in the pipette was at the bottom mark. J3 and J2 were closed. The pipette was lowered so that the top was at the "0" mark. With the light which was fixed on the calorimeter jacket on for only an instant, a check was made to ensure that there were no bubbles in the

calorimeter just before the run started. It took about 10 minutes for the temperature in the calorimeter to reach the steady state after the disturbance due to switching on the light.

An injection was made by opening the valve F, running the burette motor with K in the "injection" position, and balancing with the addition of heat. When the required volume had been injected, the burette was turned off, the valve F was closed, and the pipette top was adjusted to the level corresponding to the total volume that had been injected into the calorimeter in all injections up to the current one. When a total of 10 cm^3 had been delivered from the burette, the burette was refilled by changing valve K to "burette-to-reservoir", turning the burette motor to "suck" until the reading on gearbox was -0.4. The operation of motor was changed to "injection" and was run until the reading was 0.00. The valve K then was changed back to "injection". All of these operations were done with the calorimeter inlet valve F firmly closed. After about 32 cm^3 liquid 2 had been injected into the calorimeter, the run was discontinued. The valve F was opened and liquid was injected from the bulb until the mercury in the pipette was at the top mark. The burette reading was recorded for the balance of materials. Volume change on mixing should be taken into account in the volumetric material balance.

8-3 MATERIALS AND PREPARATION OF PSEUDO n-DODECANE

Branched hexanes were Aldrich "puriss" materials with quoted purities better than 98% for 2,2-dimethylbutane (2,2-DMB), 97% for 2,3-dimethylbutane (2,3-DMB), 99% for 2-methylpentane (2-MP), and 3-methylpentane (3-MP). n-Alkanes were Koch-light "puriss" grade (99 % minimum purity). All chemicals were taken from freshly opened bottles and were used without further purification. As a check on the purities of the materials, the densities of all these chemicals were measured with a Mettler DMA 60/ DMA 602H vibrating tube densitometer and are compared with literature values in table 7-3.

Pseudo n-dodecanes were prepared in flasks with stoppers by weighing the n-alkanes into the flasks. The density of each batch of newly prepared pseudo n-dodecane was measured and is listed in table 8-1. The differences in the densities of four preparations of $[0.500\text{ n-decane} + 0.500\text{ n-tetradecane}]$ (see No.

Table 8-1 Densities of pseudo n-alkanes at 298.15 K.

n-Alkanes	Batch	Density (g/cm ⁻³)
N-C ₁₀ + N-C ₁₄	1	0.74508
	2	0.74505
	3	0.74508
	4	0.74508
N-C ₁₁ + N-C ₁₃	5	0.74532
N-C ₈ + N-C ₁₆	6	0.74631
	7	0.74633

1 to 4) were less than $3 \times 10^{-5} \text{ g cm}^{-3}$, which corresponds to an error of 10^{-3} in mole fraction. The density of [0.500 n-octane + 0.500 n-hexadecane] was measured before it was loaded into the calorimeter or the bulb for each run which (see N0 6 and N0 7) indicated no significant change in composition between the two runs.

8-4 EXPERIMENTAL RESULTS

The excess molar enthalpies of n-dodecane +2-MP and of six ternary systems: [0.500-decane + 0.500 n-tetradecane] + 2-MP, 3-MP, 2,3-DMB, 2,2-DMB; and [0.500 n-undecane + 0.500 n-tridecane], [0.500 n-octane + 0.500 n-hexadecane] + 2-MP, were measured and are listed in table 8-2. For each system, two runs were carried out to constitute a whole H^E vs x curve. The discrepancies of two runs for all systems in the composition-overlap region were less than 1 J mol^{-1} . The temperature corrections (T_{corr}) obtained by stirrer on/off measurements depended on the materials in the calorimeter and varied from 0.011 K to 0.016 K. The discrepancies in materials balances were less than 0.15 cm^3 which agreed well with the total accumulated error in volume of component 2 injected into calorimeter. The molar weights and heat capacities of pseudo n-dodecanes (which were required for calculation of Q (corr) by eq. (8-1.1)) were taken from the average of the two corresponding liquids.

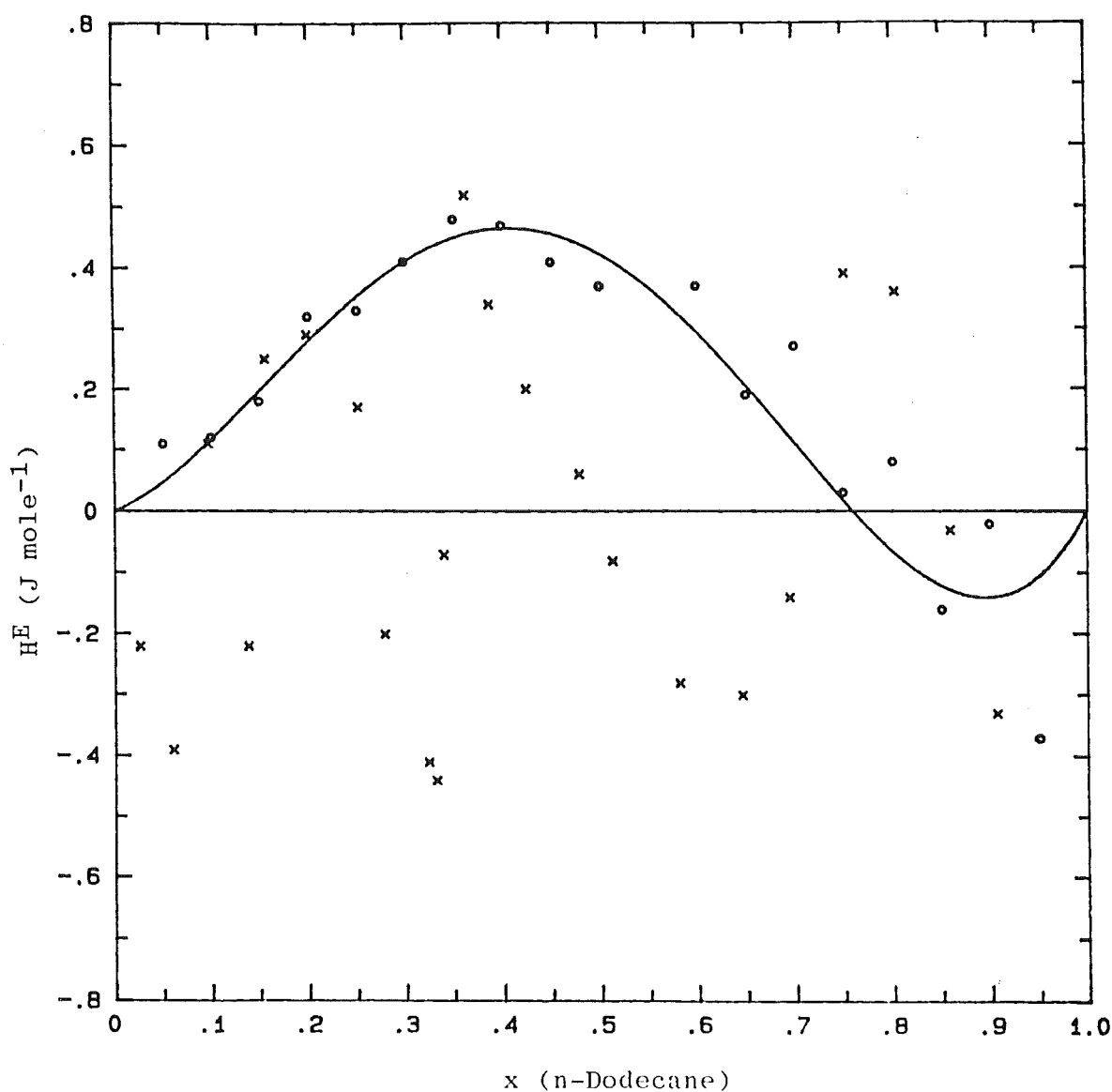
The results of [n-dodecane + 2-MP] agree with those of Hamam et al. (et al., 1984a) within 0.5 J mol^{-1} at $x=0.5$. The comparison is shown in figure 8-3.

An equation of the type:

$$H^E(\text{J mole}^{-1}) = x (1-x) \sum_L A_L (1-2x)^{L-1} \dots \dots \dots (8-4.1)$$

where x is the mole fraction of n-dodecane or pseudo n-dodecane, was fitted to each set of results by the method of linear least-squares described in section 5-2 with all points weighted equally. Almost all deviations, $r = H^E_{\text{eq. (8-4.1)}} - H^E_{\text{exp.}}$, listed in table 8-2 are less than 0.5 J mol^{-1} . The parameters for this presentation

FIGURE 8-3 DEVIATIONS OF ENTHALPIES FOR n-DODECANE AND 2-MP



Curve : H^E Calculated with Eq. (8-4.1) (Hamam) - H^E Calculated with Eq. (8-4.1) (This Work).

x: H^E Exp. (This Work) - H^E Calculated with Eq. (8-4.1) (This Work).

o: H^E Exp. (Hamam) - H^E Calculated with Eq. (8-4.1) (This Work).

Table 8-2 Excess molar enthalpies H^E of $(x\text{n-C}_{12} + (1-x) \text{C}_6)$
at 298.15 K.

n-Dodecane + 2-MP					
x	H^E (J mole ⁻¹)	r (J mole ⁻¹)	x	H^E (J mole ⁻¹)	r (J mole ⁻¹)
0.026	7.55	0.22	0.387	74.42	-0.34
0.060	16.78	0.39	0.424	76.60	-0.20
0.097	26.94	-0.11	0.478	78.20	-0.06
0.138	36.28	0.22	0.512	78.22	0.08
0.156	40.75	-0.25	0.581	76.03	0.28
0.199	49.45	-0.29	0.645	71.44	0.30
0.251	58.50	-0.17	0.694	66.29	0.14
0.278	62.06	0.20	0.752	58.68	-0.39
0.331	68.59	0.44	0.804	49.48	-0.36
0.363	72.67	-0.52	0.859	37.53	0.03
0.323	67.66	0.41	0.906	25.90	0.33
0.339	69.72	0.07			

Table 8-2 Continued...

[0.500 n-Decane + 0.500 n-Tetradecane] + 2-MP					
x	H^E (J mole ⁻¹)	r (J mole ⁻¹)	x	H^E (J mole ⁻¹)	r (J mole ⁻¹)
0.027	7.83	0.09	0.417	74.69	-0.26
0.063	17.57	0.02	0.472	76.43	0.07
0.107	28.72	-0.16	0.508	77.22	-0.37
0.156	39.78	-0.27	0.573	75.36	0.05
0.200	48.74	-0.41	0.644	70.90	-0.08
0.245	56.19	-0.10	0.724	61.87	-0.09
0.278	60.55	0.34	0.779	53.58	-0.31
0.337	67.39	0.67	0.827	44.04	0.17
0.361	69.61	0.83	0.908	25.73	0.20
0.329	67.38	-0.14	0.954	12.96	0.50
0.379	72.32	-0.39			

Table 8-2 Continued...

[0.500 n-Decane + 0.500 n-Tetradecane] + 3-MP					
x	H ^E (J mole ⁻¹)	r (J mole ⁻¹)	x	H ^E (J mole ⁻¹)	r (J mole ⁻¹)
0.042	12.10	-0.16	0.446	74.02	-0.23
0.091	24.60	-0.05	0.533	74.17	0.06
0.148	37.77	-0.18	0.597	71.79	-0.18
0.199	47.84	-0.35	0.650	67.97	-0.42
0.253	56.55	-0.12	0.669	65.95	-0.22
0.312	63.93	0.21	0.736	57.55	-0.10
0.355	68.04	0.35	0.784	49.94	0.08
0.405	71.59	0.39	0.828	41.81	0.07
0.352	68.04	0.10	0.898	26.65	0.26
0.401	71.58	0.18	0.949	13.55	0.57

Table 8-2 Continued...

[0.500 n-decane + 0.500 n-Tetradecane] + 2,3-DMB					
x	HE (J mole ⁻¹)	r (J mole ⁻¹)	x	HE (J mole ⁻¹)	r (J mole ⁻¹)
0.030	9.68	0.34	0.475	83.84	0.07
0.053	16.82	0.40	0.514	84.07	-0.24
0.084	26.12	0.17	0.563	82.40	-0.11
0.138	41.07	-0.33	0.611	79.26	-0.08
0.194	53.86	-0.38	0.652	75.50	-0.16
0.249	64.12	-0.47	0.697	70.14	-0.23
0.309	72.32	0.22	0.748	62.53	-0.39
0.351	77.18	-0.01	0.796	52.83	0.50
0.403	80.86	0.43	0.846	42.35	0.12
0.356	77.65	0.04	0.891	31.50	0.16
0.386	79.92	0.27	0.950	15.25	-0.02
0.420	81.98	0.25			

Table 8-2 Continued...

[0.500 n-Decane + 0.500 n-Tetradecane] + 2,2-DMB					
x	H^E (J mole ⁻¹)	r (J mole ⁻¹)	x	H^E (J mole ⁻¹)	r (J mole ⁻¹)
0.015	7.70	0.52	0.393	114.52	0.40
0.051	25.99	0.27	0.441	117.32	0.20
0.077	37.77	0.23	0.493	118.15	-0.17
0.111	52.28	-0.11	0.553	116.01	-0.47
0.147	65.17	0.02	0.600	111.70	-0.35
0.184	77.33	-0.32	0.652	104.61	-0.16
0.245	93.56	-0.50	0.694	96.97	0.05
0.270	98.51	-0.32	0.746	85.31	0.35
0.343	110.18	-0.26	0.793	72.64	0.45
0.368	112.44	0.26	0.847	56.29	0.18
0.323	106.88	0.40	0.893	41.50	-0.59
0.353	110.68	0.47	0.951	19.12	-0.07

Table 8-2 Continued...

[0.500 n-Undecane + 0.500 n-Tridecane] + 2-MP					
x	H^E (J mole ⁻¹)	r (J mole ⁻¹)	x	H^E (J mole ⁻¹)	r (J mole ⁻¹)
0.054	15.24	0.43	0.391	73.29	-0.61
0.101	27.43	0.13	0.428	75.22	-0.29
0.145	37.67	-0.02	0.490	77.55	-0.74
0.154	39.86	-0.45	0.537	77.18	-0.58
0.204	49.28	-0.27	0.586	75.18	-0.36
0.247	56.33	-0.00	0.645	70.37	0.23
0.280	61.16	-0.14	0.685	65.89	0.43
0.345	68.01	0.69	0.736	58.92	0.43
0.358	69.38	0.62	0.788	50.58	-0.03
0.394	72.72	0.20	0.825	43.22	0.12
0.416	73.53	0.75	0.894	28.29	-0.50
0.322	65.92	0.34	0.941	15.93	-0.09
0.351	69.53	-0.19			

Table 8-2 Continued...

[0.500 n-Octane + 0.500 n-Hexadecane] + 2-MP					
x	H ^E (J mole ⁻¹)	r (J mole ⁻¹)	x	H ^E (J mole ⁻¹)	r (J mole ⁻¹)
0.025	7.18	0.10	0.358	71.04	-0.02
0.058	16.12	0.16	0.384	73.09	0.14
0.104	28.37	-0.24	0.417	75.31	0.00
0.145	37.79	-0.25	0.490	77.58	-0.02
0.168	42.90	-0.38	0.551	77.02	-0.25
0.209	50.76	-0.32	0.601	74.63	-0.28
0.253	58.09	-0.17	0.653	70.55	-0.49
0.284	62.70	-0.14	0.695	65.88	-0.49
0.330	67.95	0.23	0.747	57.99	0.08
0.364	71.05	0.47	0.799	49.15	-0.02
0.395	73.48	0.54	0.839	40.75	0.30
0.322	66.75	0.54	0.899	29.43	0.41
			0.891	16.14	0.54

and their standard deviations (R) are listed in table 8-3.

The magnitude of the excess molar enthalpies for pseudo n-dodecane + hexane isomers decreases in the order: 2,2-DMB > 2,3-DMB > 2-MP > 3-MP, just as Hamam et al. observed from their measurements for n-dodecane + hexane isomers.

Table 8-3 Parameters and Standard Deviations (J mole^{-1}) for Representation of H^E for ($n\text{-C}_{12} + \text{C}_6$ Isomers) with Eq. (8-4.1) at 298.15 K.

SYSTEM	A1	A2	A3	A4	A5	R
1	315.03	-0.43	-11.88			0.10
2	313.33	-2.19	-8.98			0.31
3	307.38	-6.45	-4.69			0.36
4	307.54	-8.51	-14.84	24.53		0.45
5	310.41	-0.82	-14.27			0.34
6	298.54	5.92	-9.38			0.10
7	298.39	2.74	-5.81			0.28
8	340.56	19.57	-2.85			0.11
9	335.91	11.45	-3.75			0.30
10	480.10	52.54	8.90	12.13		0.11
11	471.47	40.63	28.55	38.79	-31.54	0.38

1. n -Dodecane + 2-MP (From Hamam et al.);
2. n -Dodecane + 2-MP (this work);
3. [0.500 n -Decane + 0.500 n -Tetradecane] + 2-MP;
4. [0.500 n -Undecane + 0.500 n -Tridecane] + 2-MP;
5. [0.500 n -Octane + 0.500 n -Hexadecane] + 2-MP;
6. n -Dodecane + 3-MP (From Hamam et al.);
7. [0.500 n -Decane + 0.500 n -Tetradecane] + 3-MP;
8. n -Dodecane + 2,3-DMB (From Hamam et al.);
9. [0.500 n -Decane + 0.500 n -Tetradecane] + 2,3-DMB;
10. n -Dodecane + 2,2-DMB (From Hamam et al.);
11. [0.500 n -Decane + 0.500 n -Tetradecane] + 2,2-DMB.

CHAPTER 9 THEORIES OF MIXTURES OF ALKANES

9-1 INTRODUCTION

According to the principles of statistical thermodynamics (Munster, 1969), the macroscopic equilibrium properties of a system at prescribed temperature, volume, and composition are the average over all accessible quantum states of system, attaching a statistical weight, $\exp(-E_r/kT)$ to each quantum state, where E_r is the energy of the quantum state r . If the energy level is characterized by a degeneracy g_r , the statistical weight corresponding to E_r is $g_r \exp(-E_r/kT)$. Thus the probability of finding the system at given temperature, volume and composition in the state r is

$$g_r \exp(-E_r/kT) / \sum g_r \exp(-E_r/kT) \quad \text{.....} \quad (9-1.1)$$

In eq. (9-1.1) Σ is the summation over the energy levels and k is Boltzmann's constant, T is absolute temperature. The macroscopic equilibrium value p of a property p^* whose value is p_r when the system is in the state r is given by

$$p = p_r g_r \exp(-E_r/kT) / \sum g_r \exp(-E_r/kT) \quad \text{.....} \quad (9-1.2)$$

If we write $Q = \sum g_r \exp(-E_r/kT) \quad \text{.....} \quad (9-1.3)$

the quantity Q , called the canonical partition function, is related to the Helmholtz function F by the expression

$$F = -kT \ln Q \quad \text{.....} \quad (9-1.4)$$

The other properties of the system can be derived from eq. (9-1.2) and some of them are given as follows:

$$U = kT^2 (\partial \ln Q / \partial T) \quad \text{.....} \quad (9-1.5)$$

$$S = k \ln Q + kT (\partial \ln Q / \partial T) \quad \text{.....} \quad (9-1.6)$$

$$p = kT (\partial \ln Q / \partial v)_T \quad \text{.....} \quad (9-1.7)$$

In order to simplify the application of the partition function to dealing with the liquids and liquid mixtures one may separate the degrees of freedom of a system into some independent parts. The energy of the system can be expressed

as the sum of the energies of these degrees of freedom and the partition function of the system can be written as the product of the corresponding partition functions. The separation of the translational contribution due to the position and motions of the centres of mass of molecules from the all other degrees of freedom is a good approximation for mixtures of molecules with nearly spherical symmetry. In this case, we may write

$$Q = Q_{\text{int}} Q_{\text{tra}} \quad \text{.....} \quad (9-1.8)$$

where Q_{int} , the internal partition function, refers to the internal degree of freedom, including all degrees of freedom other than the translational degree of freedom and Q_{tra} is the translational partition function. This separation leads to a simple expression for the properties of mixing due to the cancellation of Q_{int} . The translational degree may be further separated again into two terms: one related to the kinetic energy (Q_{kin}), the other to potential energy (Q_{con}). The partition function then is written as

$$Q_{\text{tra}} = Q_{\text{kin}} Q_{\text{con}} \quad \text{.....} \quad (9-1.9)$$

The latter, Q_{con} , is called the configurational partition function. The partition function due to the kinetic energy also cancels when the expressions for the properties of mixing are derived, and therefore it makes no contribution to thermodynamic properties of mixing. The problem of obtaining the properties of mixing is now reduced to that of obtaining a configurational partition function from eq. (9-1.3) with the knowledge of intermolecular potentials.

9-2 THE PRINCIPLE OF CORRESPONDING STATES

The principle of corresponding states can be derived for a system of spherical molecules satisfying the following conditions (Prigogine, 1957):

- (1) Eq. (9-1.8) and (9-1.9) are valid.
- (2) Quantum effects may be neglected.
- (3) The total energy of the system is the sum of contributions of pairs of molecules.
- (4) The energy of a pair of molecules can be represented by some universal function ϕ together with two scale factors r^* and ϵ^* characteristic of the

molecular species:

$$\epsilon(r) = \epsilon^* \phi(r/r^*) \quad \text{.....} \quad (9-2.1)$$

where r is the separation of a pair of molecules. The configurational partition function for such a system of N molecules may be expressed in reduced form (Prigogine, 1957) as

$$Q_N = g_r r^{*3N} Q^*_N(kT/\epsilon^*, r/r^*) \quad \text{.....} \quad (9-2.2)$$

where Q^* is a universal function.

The application of the principle of corresponding state to dealing with mixtures consists of three steps as stated by Scott and Fenby (1969); and Patterson (1976).

(1) The establishment of the equation of state of the pure liquids in a reduced form giving the dependence of the thermodynamic quantities on V and T . This may be done by using experimental data for the pure liquids or results of computer calculation with an assumed intermolecular potential, or through a theoretical model.

(2) A prescription for the extension of the equation of state and the thermodynamic properties from the pure component to the mixture. The simplest prescription is the one-liquid model where the mixture is taken to be equivalent to a single fluid with molecular parameters r^*_m and ϵ^*_m , where subscript m refer to the "mixture". These may be obtained by various averaging rules for r^*_{ij} and ϵ^*_{ij} with respect to the mole fraction of the mixture. More complex prescriptions are made by using two and three fluid models and have been reviewed in detail by Scott and Fenby (1969).

(3) A prescription for the assignment of values to ϵ_{12} and r_{12} , the molecular parameters related to the pair of unlike molecules. This is usually done by combining rules such as

$$r_{12} = (1/2)(r_{11} + r_{22}) \quad \text{.....} \quad (9-2.3)$$

and

$$\epsilon_{12} = (\epsilon_{11} + \epsilon_{22})^{1/2} \quad \text{.....} \quad (9-2.4)$$

$$\text{or } \epsilon_{12} = (\epsilon_{11} \epsilon_{22})^{1/2} \dots\dots\dots (9-2.5)$$

$$\text{or } \epsilon_{12} = (1-\lambda)(\epsilon_{11} \epsilon_{22})^{1/2} \dots\dots\dots (9-2.6)$$

where $(1-\lambda)$ is a correction factor expressing the deviation of the real combining rule from eq. (9-2.5).

9-3 LATTICE MODEL

The lattice model was introduced by various authors but its most complete and rigorous development is due to Guggenheim (1952) and Barker (1963). The basic assumptions of the model are:

- (1) The liquid may be treated as if the molecules were arranged on regular lattices and the motion of the molecules reduces to oscillations about some equilibrium position.
- (2) Eq. (9-1.8) and (9-1.9) are valid.
- (3) Only the interaction between the nearest neighbour molecules need to be taken into account. The total configurational energy is the sum of the contributions of all the pairs of the nearest neighbours on the lattices.
- (4) The lattice is treated as rigid: $V^E = 0$
- (5) Each molecule occupies a single lattice point.

The earlier treatments of mixtures were confined to molecules of roughly the same size, each molecule being assumed to occupy one lattice site. Later the lattice model was extended to treat mixtures in which the sizes of the molecules of two components are considerable different. In this case, the molecules of large size are imagined to be divided into r segments and each segment occupies a site on the lattice. The configurational energy is then the sum of contributions from all pairs of neighbouring sites not occupied by segments of the same molecule. In simple models the r -mer chain of n -alkanes is divided into two kind of segments: interior segments (A) and end segments (B). Assuming the contacts between A and B, B and B, A and A are random, the zeroth approximation to the configurational partition function may be determined and hence the Helmholtz function of mixing is given by (Guggenheim, 1952)

$$F^M / RT = x_1 \ln [r_1 x_1 / (x_1 r_1 + x_2 r_2)] + (1/2) z q_1 x_1 \ln [q_1 (x_1 r_1 + r_2 r_2)] /$$

$$r_1(x_1q_1 + x_2q_2)] + x_2 \ln [r_2x_2/(x_1r_1 + x_2r_2)] + (1/2)zq_2x_2 \ln [q_2(x_1r_1 + x_2r_2)/r_2(x_1q_1 + x_2q_2)] + [x_1x_2q_1q_2/(x_1q_1 + x_2q_2)] \\ (u_1v_2 + u_2v_1 - u_1v_1 - u_2v_2)w/kT \quad \dots\dots\dots (9-3.1)$$

where, r_1, r_2 = the number of segments per molecules of 1 and 2.

x_1, x_2 = the mole fraction of 1 and 2.

z = the coordination number of the lattice

k = Boltzmann's constant

q_i may be defined as follows. Consider a particular r -mer of i th component occupying a group of r sites. Each of these sites has z neighbouring sites and some occupied by other elements of the same r -mer. We denote by zq_i the number of pairs of neighbouring sites of which one is a number of the group occupied by the given r -mer and the other is not. q_i is related to r_i by the relation

$$(1/2) z (r - q_i) = r_i - 1 \quad \dots\dots\dots (9-3.2)$$

u_1, u_2, v_1, v_2 are defined as follows. In the zq_1 contacts of each molecule 1, zq_1u_1 come from A segments and zq_1v_1 from B segments. Similarly, in the zq_2 contacts of each molecule 2, zq_2u_2 come from segment A and zq_2v_2 come from B segments.

w_{ij} = the contributions of $(z/2)$ contacts of A-A, or B-B, or A-B to the total configurational potential energy of system.

$$W = 2W_{AB} - W_{AA} - W_{BB}$$

The assumption of random distribution of the contacts is obviously incorrect because of the different potential energies of A-A, B-B, and A-B contacts. Therefore a more complete treatment by using a quasi-chemical approximation was introduced. This treatment and the corresponding first approximation to the partition function and the properties of mixing are described in detail in the textbook on "Mixtures" (Guggenheim, 1952). The comparison of this theory with experiments of measurements of Helmholtz function for n -alkanes were given by Williamson (1953). An extension of this model to ternary systems described by Guggenheim's book (1952).

The lattice theory is capable of dealing with mixtures of non-polar liquids over

the range from spherical molecules to macromolecules. However, this model is not sufficient for a complete understanding of the thermodynamic functions of solution. This model cannot predict the volume behaviours of mixing and the relation of the excess functions and temperature. This has been improved by allowing for vacant lattice sites (Lacombe, 1976) and by allowing w to vary with temperature (Guggenheim, 1948).

9-4 CELL MODEL AND THE NUMBER OF EXTERNAL DEGREES OF FREEDOM

A detailed description of the cell model (or so called free volume theory) is given in the book of "the Molecular Theory of Solution " by Prigogine (1957). In a liquid consisting of spherical molecules, the movement of a given molecule is confined to a cell formed by its nearest neighbours. The field acting on each molecule in its cell by nearest molecules, which is pictured as being moving on the wall of the cell, is rapidly fluctuating and may be replaced by an average field of spherical symmetry. It is assumed that the mean energy of interaction with the neighbouring molecules depends only on the distance r of the molecule from the centre of the cell. The cell partition function then is given by

$$V_f = 4\pi \int \exp [-w(r)/kT - w(0)/kT] r^2 dr \quad \dots\dots (9-4.1)$$

where V_f is called the free volume, $w(0)$ is the value of $w(r)$ at the centre of the cell and the integral is taken over the whole space of the cell. The configurational partition function of the system of N particles may now be written in the form

$$Q = V_f^N \exp (- Nw(0)/2kT) \quad \dots\dots\dots (9-4.2)$$

The problem is now to find a proper expression for $w(0)$ and $w(r)$, and a suitable technique of integration of eq. (9-4.1). The applications of the cell model to mixtures were made by using appropriate combining rules and prescriptions for the extension of the reduced equation of state from pure components to mixtures. The various expressions of the potential energy for both pure

components and solution are discussed by Prigogine (1957) in his book.

The extension of this theory to polymer solution was made by assuming that the r -mer molecules could be regarded as $c r$ point-centres each of which is subjected to a cell with the central potential exerted by the neighbour molecules. c was firstly introduced by Prigogine (1957) and defined as follows. The number of external degrees of freedom for a independent particle is 3, but the average number of external degrees of freedom for per segment of an r -mer chain molecule is less than that of r independent particles because of the chemical bonds within the molecule and is denoted by $3c$, ($c < 1$). The smaller the value of c , the more rigid and inflexible is a chain molecule. The application of the concept of external degrees of freedom and the introduction of the c factor into the theory of polymer solutions has been considered as the key to successful treatment of n -alkanes mixtures (Bhattacharyya et al, 1985),

Similarly, the corresponding states theory has been extended to pure polymer liquids and their mixtures. The partition function may expressed in reduced quantities by

$$Q^{1/N} = g_r^{1/N} r^{*3cr} [Q^{\wedge} (V^{\wedge}, T^{\wedge})]^{cr} \quad \text{..... (9-4.3)}$$

where V^{\wedge} and T^{\wedge} are reduced values of volume and temperature.

More phenomenological postulates are made to extend the principle of corresponding states to polymer solution by Hijmans and Holleman (1961,1962). They chose independent spherical segments as a hypothetical reference substance, and defined 3 parameters $q^*(r)$, $r^*(r)$, $c(r)$ to describe the different behaviours between a segment of r -mer molecule and an independent particle:

- (1) $q^*(r) r$ is the number of independent reference segments which together have the same total excluded volume as one r -mer.
- (2) $r^*(r) r$ is the number of independent reference segments which have the same total potential energy as one r -mer.
- (3) $c(r) r$ is the number of independent reference segments have the same total number of external degrees of freedom as one r -mer.

With these postulates, Holleman and Hijmans (1962, 1963) presented a formulation of the principle of corresponding state for the excess functions of

mixing of chain molecules. This treatment is independent of any solution model but involves an application of the principle of congruence.

The cell model has been modified by allowing for the vacant sites or holes (Barker, 1963). This modification has been extended to the mixtures by Chai (1987).

9-5 FLORY THEORY

The theory bearing this name was introduced by Flory and co-workers firstly to treat n-alkane mixtures (Flory et al., 1964, Flory, 1965, Eichinger et al., 1968). The assumptions of this theory may be summarized as follows:

(1) The polymer molecules may be subdivided into r segments and r is not necessarily to be equal to the number of carbons for n-alkanes. Each segment of polymer molecule has a hard-core volume v^* and the hard-core volume of a molecule, V^* is rv^* . The hard-core of the segments of different molecules i and j interact with one another with an attractive potential $-\eta_{ij}/v$, where v is the volume of per segment. In the binary mixture, the interactions also include those between the segments of unlike molecules.

(2) The segments of chain molecules are randomly distributed. Therefore the probability of interaction between the two molecules of component 1 or the interaction between the two molecules of component 2 is proportional to the probability of finding two segments of component 1 or 2 neighbouring each other, i.e. proportional to ϕ_1^2 and ϕ_2^2 where ϕ is defined by

$$\phi_1 = x_1 r_1 v^* / (x_1 r_1 v^* + x_2 r_2 v^*) = 1 - \phi_2 \quad \dots\dots\dots (9-5.1)$$

(3) Following Prigogine and co-workers, the number of external degrees of freedom was introduced as a parameter in the Flory theory . The free volume for each cell is given by

$$V_f = \text{constant} (v^{1/3} - v^{*1/3})^3 \quad \dots\dots\dots (9-5.2)$$

The molar properties of mixing derived from this theory are given (Eichinger and Flory, 1968) by

$$\Delta U = (V_1^* x_1 + V_2^* x_2) \{ (1/v_1^* - 1/v_m^*) \phi_1 p_1^* + (1/v_2^* - 1/v_m^*) \phi_2 p_2^* +$$

$$+ \phi_1 \phi_2 [s_2 / (\phi_1 s_1 + \phi_2 s_2)] (X_{12} / v_m^{\wedge}) \quad \text{.....} \quad (9-5.3)$$

$$\Delta S = -k[N_1 \ln \phi_1 + N_2 \ln \phi_2] - (3N_1 P^*_1 V^*_1 / T^*_1) \ln[(v_1^{\wedge 1/3} - 1) / (v_m^{\wedge 1/3} - 1)] - \\ (3N_2 P^*_2 V^*_2 / T^*_2) \ln[(v_2^{\wedge 1/3} - 1) / (v_m^{\wedge 1/3} - 1)] \quad \text{.....} \quad (9-5.4)$$

$$\Delta V = (V^*_1 x_1 + V^*_2 x_2) (v_m^{\wedge} - \phi_1 v_1^{\wedge} - \phi_2 v_2^{\wedge}) \quad \text{.....} \quad (9-5.5)$$

$$\Delta H = \Delta U_m - p \Delta V_m \quad \text{.....} \quad (9-5.6)$$

$$\Delta F = \Delta U_m - T \Delta S_m \quad \text{.....} \quad (9-5.7)$$

and

$$\Delta G = \Delta H_m - T \Delta S_m \quad \text{.....} \quad (9-5.8)$$

where, $v_i^{\wedge} = v_i / v_i^*$. The parameters p_i^* , T_i^* have the dimensions of pressure and temperature respectively. p_i^* is proportional to η_{ij} , and T_i^* is defined as

$$T_i^* = p_i^* v_i^* / k c_i \quad \text{.....} \quad (9-5.9)$$

where k is Boltzmann's constant. The quantities p_i^* , v_i^* , T_i^* may be obtained by a reduced equation of state, the molar volumes and the coefficients of thermal expansion of pure liquids. The parameter X_{12} in eq. (9-5.3) is chosen to express the difference between interactions of neighbouring pairs of like and unlike species as

$$X_{12} = (s_1 / 2v^*{}^2) (\eta_{11} + \eta_{22} - 2\eta_{12}) \quad \text{.....} \quad (9-5.10)$$

The parameter s_1 is given as the ratio, surface/volume of the hard core. The parameters c , r , s are divided into two parts for a r -mer molecule: one is due to the contributions of r internal segments and the other is an added quantity for the chain end. η is regarded as the sum of the contributions of the interaction of internal-end, internal-internal, end-end segments (Flory et al., 1964). The quantity X_{12} may be calculated from the parameters which are determined by the behaviour of pure liquid through a reduced corresponding state equation. However it is more usually obtained from experimental values of excess enthalpies of given mixtures. Then X_{12} is used to predict the excess volume,

excess Gibbs function etc. and the predicted values are compared with experimental results for the same mixtures. Flory theory has been made successful in explaining the properties of mixing for many binary mixtures.

9-6 THE CORRELATION OF MOLECULAR ORIENTATION AND THERMODYNAMICS OF ALKANE MIXTURES

The heats of mixing of alkanes with unequal chain lengths were attributed to the energy difference between methyl chain end and methylene middle segments in both the lattice model and the early version of Flory theory. A number of difficulties associated with this concept have been pointed out by Patterson et al (Lam,1974; Bhattacharyya,1985) and are summarized as follows:

- (1) In terms of the Flory theory, the X_{12} parameter derived from heat of mixing is about 5 J cm^{-3} for n-hexane + n-hexadecane. This is a moderate value for the interaction between whole n-alkane molecules, but unreasonably large to be attributed to the difference of the interaction between methyl and methylene.
- (2) The experimental heat of mixing of normal and branched alkanes with a common liquid as the second component showed an unexpected isomer effect.
- (3) This concept could not explain the dependence of the excess thermodynamic functions of mixing on the temperature and pressure.

A theory of correlation of molecular orientation (CMO) has been used to explain the experimental results of alkane solutions (Lam et al., 1974). For each structural unit of a single alkane molecule, in principle, three different angles of rotation along the c-c axis are possible: one trans-(t), and two gauche- (g^+ , g^-) conformations. Figure 9-2 shows schematically the conformations of n-butane. The greater the number of carbon atoms, the more conformations there are. Because of the strongly repulsive forces between two methyl groups, the t-conformation is energetically more stable than the two g-conformations. A distribution of different rotational isomers exists according to the statistical principles. Although the small angle neutron-scattering experiment showed that this distribution does not change within each molecule on going from the dilute alkane in cyclohexane to pure liquids, a small range of correlations possibly favouring a parallel orientation of t-sequence of different molecules with one

another were observed by the Rayleigh scattering of polarized light. Rayleigh scattering of polarized light provides evidence of CMO effect because the order of CMO corresponds to the molecular optical anisotropy and hence corresponds to the scattered intensity. This favoured packing phenomena of n-alkane chains also increases the attractive interaction. CMO occurs particularly with n-alkanes ($n > 6$), but is not observed for corresponding isomeric alkanes which are highly branched.

A net disruption in order of CMO is caused when an alkane is mixed with a liquid of spherical molecules or a shorter chain alkane. The contribution of the change of CMO may be revealed by the difference of the parameter X_{12} in Flory theory

$$X_{12}(\text{CMO}) = X_{12} - X_{12}^{\infty} \quad \text{.....} \quad (9-6.1)$$

where X_{12}^{∞} is independent of orientation and denotes the contribution from the different interaction between segments. For alkane mixtures, X_{12}^{∞} is small and constant (Lam et al., 1974; Heintz and Lichtenthaler et al., 1982), therefore the relation of properties of mixing and the number of carbon atoms at the described temperature and pressure depends only on the effect of CMO.

A series of measurements of heat of mixing have been made for mixtures of cyclohexane and various alkanes of different chain length and different degree of branching and the corresponding X_{12} were calculated through the Flory equations. For mixtures containing n-alkanes X_{12} increases significantly with n , because the CMO increase with the number of carbon atoms therefore more order is destroyed upon mixing. However for these mixtures containing branched alkanes X_{12} remains practically constant due to the absence of CMO in more branched molecular liquid.

The CMO also is successful in explaining the dependence of excess functions of mixing on temperature and pressure (Bhattacharyya and Patterson, 1980; Heintz and Lichtenthaler, 1980). For mixtures of n-alkanes a significant decrease of H^E with increase of temperature is expected by theory of CMO. The CMO for pure n-alkanes is not large at higher temperature because of thermal motion, and therefore less order is destroyed upon mixing. Since the higher the pressure, the

closer the molecules are packed together, the stronger is the CMO, the increase of X_{12} with pressure observed by experiments is expected.

So far the CMO theory has been applied exclusively to H^E . The temperature dependence of X_{12} also significantly improve the description of V^E of n-alkane + cyclohexane mixtures at various temperatures (Heintz, 1979). The prediction of ΔS for n-alkane mixtures is also much better with CMO theory as compared with the original Flory theory (Meixner and Lichtenthaler, 1979).

A detailed review of the liquid structure and thermodynamics of alkane mixtures was given by Heintz and Lichtenthaler (1982).

9-7 THE PRINCIPLE OF CONGRUENCE

The principle of congruence was first proposed by Bronsted and Koefoed (1946). In an extended form, this principle may be described as follows (Van Hook, 1985): "Mixtures with the same average number of segments (the so called congruent mixtures) should agree in the excess Gibbs function and its derivative properties". This principle is often expressed in the form "there exists a function universal across the homologous series, which relates the given property for the mixture and the pure liquids to the chain length or segment number."

A general review of the principle of congruence has been given by Koh and Williamson (1979). The tests of the principle were divided into two categories, analytical and graphical methods .

The analytical method suggests that the properties of pure liquid and mixtures may be expressed as universal function of the number of carbon or the average number of carbons (for the mixtures) at given temperature and pressure.

$$X = F(T, P, n) \quad \text{.....} \quad (9-7.1)$$

Then the properties of mixing may be written as

$$\Delta X = F(T, P, n) - X_1 F(T, P, n_1) - X_2 F(T, P, n_2) \quad \text{.....} \quad (9-7.2)$$

eq. (9-7.2) may also be written in a simple form with some universal parameters A, B for a whole series homologous.

$$\Delta X = f(T, P, n, n_1, n_2, A, B, \dots) \quad \dots\dots\dots (9-7.3)$$

The experimental data of ΔX are then fitted to eq (9-7.3) to obtain A, B, , and a successful fitting usually denotes a good agreement between the principle of congruence and the experimental results.

A number of forms of function $f(T, P, n, n_1, n_2, A, B, \dots)$ have been used to test the principle of congruence. A set of thermodynamically consistent forms was given by Pena and Fernandez-Martin (1964); and Bellemans and Mat (1963). The excess Gibbs function is given by

$$G^E/RT = -Q_0 + g_{-1}Q_1 + g_{-2}Q_2 \quad \dots\dots\dots (9-7.4)$$

where g_{-i} are the parameters to be optimized.

$$Q_0 = \ln n - x_1 \ln n_1 - x_2 \ln n_2 \quad \dots\dots\dots (9-7.5)$$

$$Q_1 = n^{-1} - x_1 n_1^{-1} - x_2 n_2^{-1} \quad \dots\dots\dots (9-7.6)$$

where, $l = 1, 2, \dots\dots\dots$

The plot of $(G^E/RT + Q_0)/Q_1$ versus Q_2/Q_1 for the measurements of G^E , yields a straight line if the principle of congruence is obeyed. The excess enthalpy and excess volume may be written as

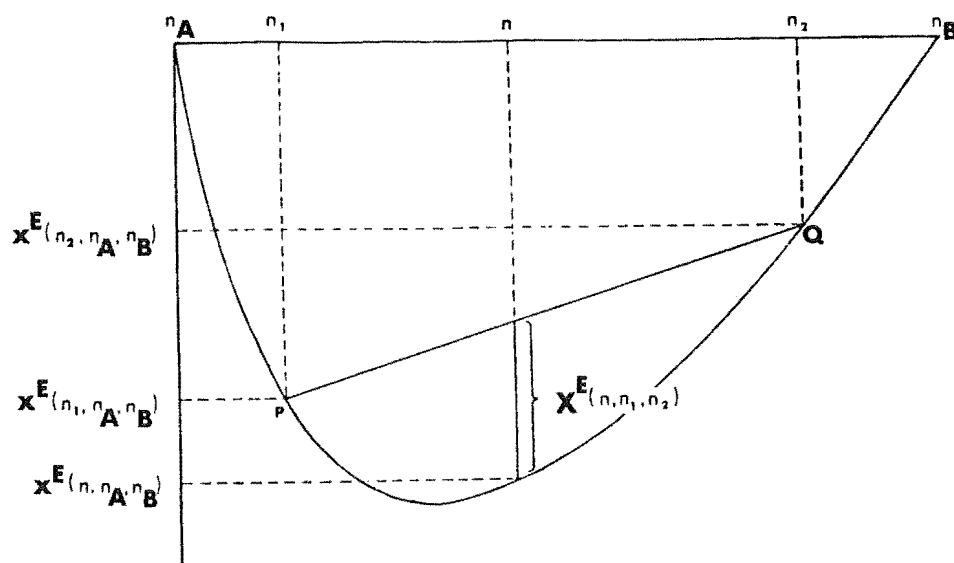
$$X^E = C_{-1} Q_1 + C_{-2} Q_2 \quad \dots\dots\dots (9-7.7)$$

where C_{-i} is the parameters to be optimized.

This set of equations has been tested against excess enthalpies, volumes, and Gibbs function (Pope et al., 1967; Pflug and Benson, 1968; Bellemans and Mat, 1963).

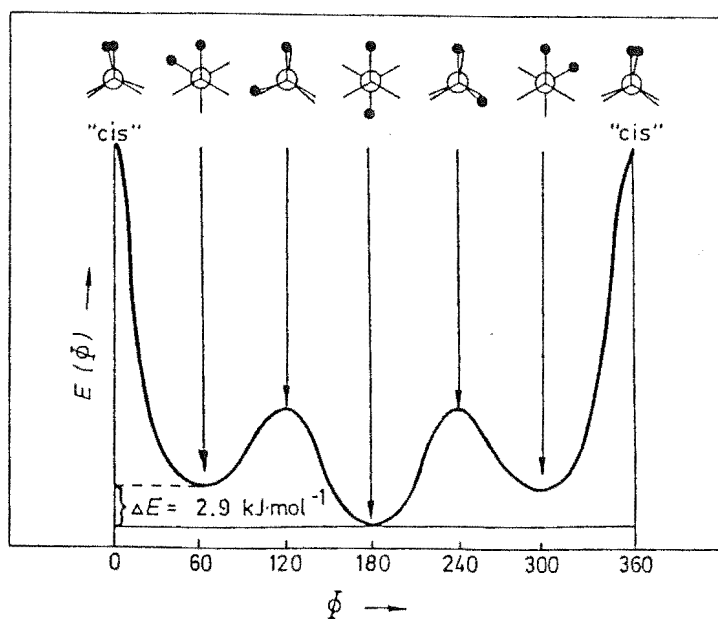
The graphical method is illustrated in figure 9-1, which was devised by Hijmans (1958). A curve for a excess property X^E formed from mixture A+B, where A has the lowest n_A and B, the highest n_B , of the set under investigation, is established as a reference curve. The chord PQ is next drawn as a base line for mixtures formed from (1+2). $n_A \leq n_1 < n_2 \leq n_B$. The X^E of mixtures of component 1 and component 2 with average n is plotted as the vertical distance from the base line at n . If the principle of congruence is obeyed, this point should

Fig. 9-1



Construction from Hijmans' method of comparison of excess properties of different mixtures.

Fig. 9-2



Potential energy E as a function of the angle of rotation ϕ of the hindered rotation around the central C—C bond of n -butane. 180° : t , $60^\circ, 300^\circ$: g^+ or g^- ; maxima: "cis"-conformation.

fall on the reference curve. The graphical method was used to test V^E , H^E (Holleman, 1963; Holleman and Hijmans, 1962; 1965), for binary n-alkane mixtures and G^E for binary mixtures of cyclohexane + n-alkanes (Gomez-Ibanez, 1971). Excellent agreement was observed. This test also has been extended to multiple n-alkane mixtures (Looi et al., 1974; Lim et al., 1980). A pseudo n-alkane (a mixture of alkanes with given average number of carbon atoms) is prepared as component 1, and mixed with component 2, which may be a pure liquid or another pseudo n-alkane and the excess functions are measured. The measured values then are compared with those of mixing other two pairs of liquids which are congruent with the component 1 and component 2 of the first mixture respectively. The excess functions on the two mixing should be the same if the principle of congruence is valid.

Larger deviations from the principle of congruence were noticed and discussed by Holleman (1965) when the properties of pure liquid (e.g. molar volumes and molar enthalpies) with the number of carbon, n , are compared with the value of a mixture which has the same average number of carbon n . Recently Van Hook (1985) discussed the deviation of the principle of congruence in prediction of excess volumes from molar volumes of pure liquid and described these deviations as

$$V^E - V^\# = \Phi_1 \Phi_2 \sum_j A_j (1 - 2\Phi_1)^j \quad \text{..... (9-7.8)}$$

$$\text{where, } V^\# = V(n) - x_1 V(n_1) - x_2 V(n_2) \quad \text{..... (9-7.9)}$$

and $V(n)$ is calculated by the formula with the parameters obtained by fitting the molar volumes of pure liquid to an empirical equation, Φ is the volume fraction, and Σ is the summation from $j=0$. Van Hook pointed out that a very good approximation was obtained when the eq. (9-7.8) was truncated after the first term.

CHAPTER 10 DISCUSSION OF THE EXPERIMENTAL RESULTS

As described in section 9-7, the principle of congruence has been successively applied in explanation of the properties of mixing of many systems. A number of theoretical discussions of mixtures of chain molecules started with the introduction of the principle or gave an interpretation of the principle. It may be properly said that a good theoretical model of solutions of chain molecules should explain the principle and deviation of the principle from the real properties of mixtures over an extensive temperature and pressure range. Tests of the principle of congruence form an interesting area for both theoretical study and prediction of the properties of mixing. In this chapter, we will discuss our experimental results in term of the principle of congruence.

10-1 GRAPHICAL TEST OF THE PRINCIPLE OF CONGRUENCE FOR G^E OF BINARY MIXTURES

For pure normal alkanes, A property X of the system at given temperature and pressure is reasonably and simply expressed as a function of the number of carbon atoms:

$$X = f(n) \quad \text{..... (10-1.1)}$$

Considering a mixture of n-alkanes which has the same average number of carbon (n) as a pure reference n-alkane, if the principle of congruence is valid then we have

$$X(n, n_A, n_B) = f(n) + s \sum x \ln x \quad \text{..... (10-1.2)}$$

where n_A, n_B are the carbon number of component 1 and component 2 of the mixture, s =constant for those cases such as entropy in which the properties on mixing are not equal to the corresponding excess properties, otherwise, for example, in the case of the volumes $s=0$; and

$$n = x_A n_A + x_B n_B \quad \text{..... (10-1.3)}$$

As it has been discussed by Holleman and Hijmans (1965) and Van Hook (1985), the deviations from the principle of congruence were found to be quite large when the properties of a pure n-alkane and its congruent mixture were compared with each other. Let $\delta f(n_A, n_B, n)$ denote the departure of the property X of a mixture from the principle of congruence, the property of the mixture

may then be expressed as

$$X(n, n_A, n_B) = f(n) + s \sum x \ln x + \delta f(n_A, n_B, n) \dots\dots (10-1.4)$$

The property on mixing component A and B to form a mixture with an average carbon number n is given by

$$\begin{aligned} \Delta f(n, n_A, n_B) &= f(n) - x_A f(n_A) - x_B f(n_B) + s(x_A \ln x_A + x_B \ln x_B) \\ &\quad + \delta f(n_A, n_B, n) \dots\dots\dots (10-1.5) \end{aligned}$$

Similarly, the property on mixing x_{iA} of component A and x_{iB} of component B to form a mixture with an average carbon number n_i are given as

$$\begin{aligned} \Delta f(n_i, n_A, n_B) &= f(n_i) - x_{iA} f(n_A) - x_{iB} f(n_B) + s(x_{iA} \ln x_{iA} + x_{iB} \ln x_{iB}) \\ &\quad + \delta f(n_A, n_B, n_i) \dots\dots\dots (10-1.6) \end{aligned}$$

for $i=1$; and

$$\begin{aligned} \Delta f(n_2, n_A, n_B) &= f(n_2) - x_{2A} f(n_A) - x_{2B} f(n_B) + s(x_{2A} \ln x_{2A} + x_{2B} \ln x_{2B}) \\ &\quad + \delta f(n_A, n_B, n_2) \dots\dots\dots (10-1.7) \end{aligned}$$

for $i=2$; where, $n_A \leq n_1 \leq n_2 \leq n_B$. The property on mixing component 1 with n_1 and component 2 with n_2 to form a mixture with an average number of carbon n is given by

$$\begin{aligned} \Delta f(n, n_1, n_2) &= f(n) - x_1 f(n_1) - x_2 f(n_2) + s(x_1 \ln x_1 + x_2 \ln x_2) \\ &\quad + \delta f(n_1, n_2, n) \dots\dots\dots (10-1.8) \end{aligned}$$

From eq. (10-1.5) to (10-1.7), we have

$$\begin{aligned} X^E(n, n_A, n_B) &- x_1 X^E(n_1, n_A, n_B) - x_2 X^E(n_2, n_A, n_B) \\ &= f(n) - x_A f(n_A) - x_B f(n_B) + \delta f(n_A, n_B, n) - x_1 f(n_1) + x_1 x_{1A} f(n_A) \\ &\quad + x_1 x_{1B} f(n_B) - x_1 \delta f(n_A, n_B, n_1) - x_2 f(n_2) + x_2 x_{2A} f(n_A) \\ &\quad + x_2 x_{2B} f(n_B) - x_2 \delta f(n_A, n_B, n_2) \dots\dots\dots (10-1.9) \end{aligned}$$

where X^E is the excess function on mixing. Considering

$$n = x_A n_A + x_B n_B, \text{ and}$$

$$\begin{aligned}
 n &= x_1 n_1 + x_2 n_2 = x_1 (x_{1A} n_A + x_{1B} n_B) + x_2 (x_{2A} n_A + x_{2B} n_B) \\
 &= (x_1 x_{1A} + x_2 x_{2A}) n_A + (x_1 x_{1B} + x_2 x_{2B}) n_B
 \end{aligned}$$

we have

$$x_A n_A + x_B n_B \equiv (x_1 x_{1A} + x_2 x_{2A}) n_A + (x_1 x_{1B} + x_2 x_{2B}) n_B$$

then

$$x_A = x_1 x_{1A} + x_2 x_{2A} \quad \text{..... (10-1.10)}$$

$$x_B = x_1 x_{1B} + x_2 x_{2B} \quad \text{..... (10-1.11)}$$

Substituting (10-1.10) and (10-1.11) into (10-1.9), we have

$$\begin{aligned}
 X^E(n, n_A, n_B) - x_1 X^E(n_1, n_A, n_B) - x_2 X^E(n_2, n_A, n_B) &= \\
 = f(n) - x_1 f(n_1) - x_2 f(n_2) + \delta f(n_A, n_B, n) - x_1 \delta f(n_A, n_B, n_1) \\
 - x_2 \delta f(n_A, n_B, n_2) &\quad \text{..... (10-1.12)}
 \end{aligned}$$

From equation (10-1.8), $X^E(n, n_1, n_2)$ may be expressed as

$$X^E(n, n_1, n_2) = f(n) - x_1 f(n_1) - x_2 f(n_2) + \delta f(n_1, n_2, n) \quad \text{..... (10-1.13)}$$

Combining (10-1.12) and (10-1.13),

$$\begin{aligned}
 X^E(n, n_1, n_2) &= [X^E(n, n_A, n_B) - x_1 X^E(n_1, n_A, n_B) - x_2 X^E(n_2, n_A, n_B)] \\
 &\quad - \delta f(n_A, n_B, n) + x_1 \delta f(n_A, n_B, n_1) + x_2 \delta f(n_A, n_B, n_2) \\
 &\quad + \delta f(n_1, n_2, n) \quad \text{..... (10-1.14)}
 \end{aligned}$$

$$\text{Let } \Delta = -\delta f(n_A, n_B, n) + x_1 \delta f(n_A, n_B, n_1) + x_2 \delta f(n_A, n_B, n_2) + \delta f(n_1, n_2, n)$$

Then (10-1.14) becomes

$$\begin{aligned}
 X^E(n, n_1, n_2) &= [X^E(n, n_A, n_B) - x_1 X^E(n_1, n_A, n_B) \\
 &\quad - x_2 X^E(n_2, n_A, n_B)] + \Delta \quad \text{..... (10-1.15)}
 \end{aligned}$$

Let $X=G$, the Gibbs function, then

$$\begin{aligned}
 G^E(n, n_1, n_2) &= [G^E(n, n_A, n_B) - x_1 G^E(n_1, n_A, n_B) - x_2 G^E(n_2, n_A, n_B)] \\
 &\quad + \Delta \quad \text{..... (10-1.16)}
 \end{aligned}$$

From $n = x_1 n_1 + x_2 n_2$, we have

$$n - n_1 = (n_2 - n_1) x_2, \quad x_2 = (n - n_1) / (n_2 - n_1)$$

Similarly, $x_1 = (n_2 - n) / (n_2 - n_1)$

Equation (10-1.16) then may be written as

$$G^E(n, n_1, n_2) = G^E(n, n_A, n_B) - [(n_2 - n) / (n_2 - n_1)] G^E(n_1, n_A, n_B) \\ - [(n - n_1) / (n_2 - n_1)] G^E(n_2, n_A, n_B) + \Delta \quad \text{..... (10-1.17)}$$

It is easy to show geometrically that the first three terms in the above equation are equal to the distance denoted by $X^E(n, n_1, n_2)$ in figure 9-1. Therefore, it may be said that the graphical test of the principle of congruence for a series of homogeneous mixtures is to judge the order of Δ . Usually, Δ is much smaller than the terms of " δf " in eq. (10-1.5) to (10-1.8) due to cancellations of these terms, hence smaller departures are found when the principle of congruence is applied to a series of homogeneous mixtures than it is applied to a pure n-alkane and its congruent mixture.

Figure 10-1 illustrates the graphical test in which experimental G^E of the system n-hexane + n-hexadecane determined in this work at 298.15 K is plotted against the average carbon number n to obtain a smooth curve. The G^E of n-hexane + n-decane, n-undecane, n-dodecane at 298.15 K determined by Marsh and Ott (Marsh et al., 1980a; b; Ott et al., 1981); and of n-octane + n-hexadecane at 298.15 K determined in this work then are plotted as described in section 9-7. For all the points in figure 10-1 the values of Δ are less than the experimental errors. The G^E of the system of n-hexane + n-octane predicted by Hijmans' plot are small (about 1–2 J mol⁻¹). This also agrees with the experimental data which vary within ± 2 J mol⁻¹ (close to the order of experimental errors) over the whole range of mole fraction.

10-2 GRAPHICAL TEST OF THE PRINCIPLE OF CONGRUENCE FOR G^E OF TERNARY MIXTURES

The excess Gibbs function of mixing x_1 of mole of component 1, x_2 of

Fig. 10-1

TEST OF THE PRINCIPLE OF CONGRUENCE BY GE OF BINARY SYSTEMS

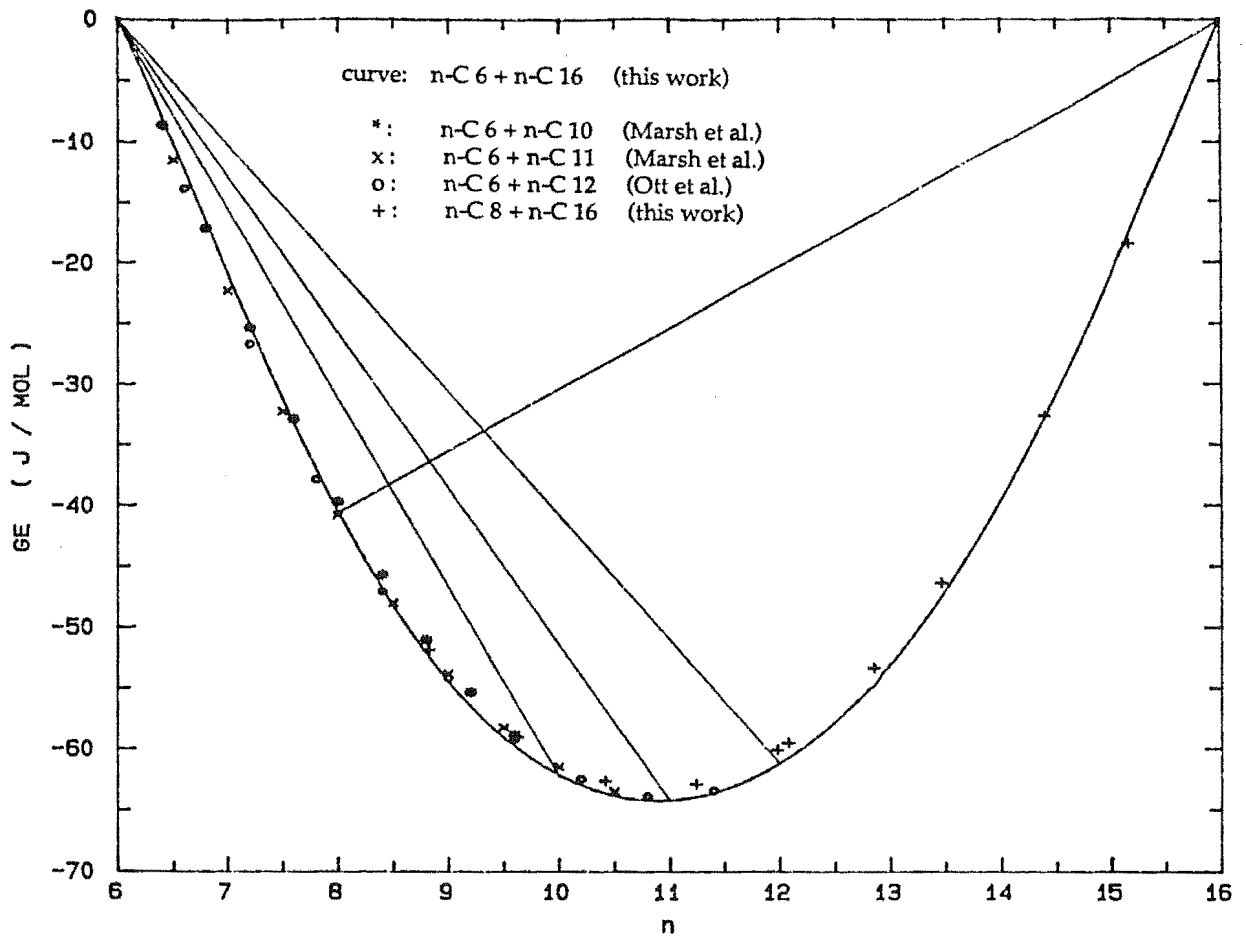
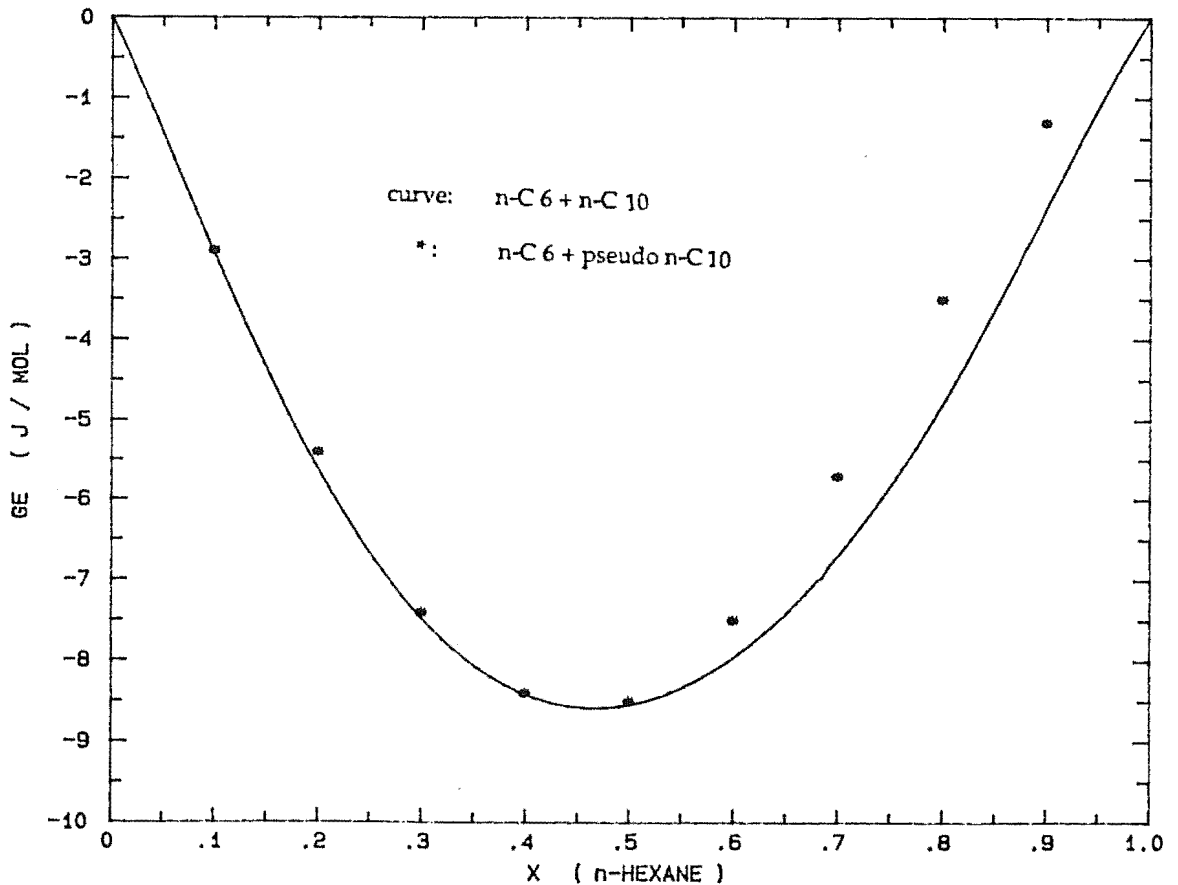


Fig. 10-2

COMPARISON OF GE BETWEEN n-decane AND PSEUDO n-DECANE + n-HEXANE



component 2, and x_3 of component 3 is

$$G_{\text{ternary}}^E = G_{\text{ternary mixture}} - x_1 G_1 - x_2 G_2 - x_3 G_3 \quad \text{.....} \quad (10-2.1)$$

One may chose another process of mixing to derive G^E .

If x_2 of mole component 2 and x_3 of component 3 are mixed at first to form a pseudo liquid denoted (2/3), then (x_2+x_3) mole of pseudo (2/3) and x_1 mole of component 1 are mixed to form a ternary mixture. The total excess Gibbs function is

$$\begin{aligned} G_{\text{ternary}}^E &= [G_{\text{ternary mixture}} - (x_2+x_3) G_{(2/3)} - x_1 G_1] + [(x_2+x_3) G_{(2/3)} - x_2 G_2 - x_3 G_3] \\ &= G^E (\text{pseudo (2/3) + component 1}) \\ &\quad + (x_2+x_3) G_{\text{binary}}^E (\text{component 2 + component 3}) \quad \text{.....} \quad (10-2.2) \end{aligned}$$

because G^E is a state function independent of the mixing process, G_{ternary}^E in eq. (10-2.1) and (10-2.2) are the same.

$$G^E (\text{pseudo (2/3) + component 1}) = G_{\text{ternary}}^E - (x_2+x_3) G_{\text{binary}}^E (\text{component 2 + component 3}) \quad \text{.....} \quad (10-2.3)$$

According to eq. (10-2.3), the excess Gibbs function of a pseudo n-alkanes (made by mixing component 2 and and component 3 in certain proportion) + component 1 may be calculated from the excess Gibbs functions of the corresponding ternary mixture and corresponding binary mixture.

The average number of carbon for the pseudo n-alkane is

$$n(2/3) = [x_2 / (x_2+x_3)] n_2 + [x_3 / (x_2+x_3)] n_3 = [x_2 / (x_2+x_3)] (n_2 - n_3) + n_3$$

the mole fraction of component 2 for the given n_2 , and n_3 , and required $n(2/3)$

may then be calculated by

$$x_2 = (n(2/3) - n_3)(1-x_1) / (n_2 - n_3) \quad \text{.....} \quad (10-2.4)$$

G^E of the ternary mixtures of n-hexane (component 1) + n-octane (component 2) + n-hexadecane (component 3) at 298.15 k have been determined in this work and expressed as a functions of mole fraction by the equations described in section 5-3.2 with the optimized parameters listed in section 6-4. G_{binary}^E (component 2 + component 3) have also been determined in this work and may be calculated by the equations described in section 5-3.1 with the optimized parameters listed in section 6-3. The computation programme PVL4 for calculation of G^E of binary and ternary mixtures from these equations is listed in

appendix 3. The literature values of G^E for binary systems of n-hexane + n-decane, + n-undecane, + n-dodecane at 298.15 K are available (Marsh et al, 1980 a; b; Ott et al., 1981) The pseudo liquids are supposed to be "made" by "mixing" n-octane and n-hexadecane. According to eq. (10-2.4) The mole fraction of n-octane in the ternary mixture for a required constant $n(2/3)$ at various mole fraction of n-hexane is given by

$$x_2 = (2 - n(2/3) / 8)(1 - x_1) \quad \text{..... (10-2.5)}$$

Table 10-1 lists the mole fractions for required values of $n(2/3)$, calculated G^E_{binary} and G^E_{ternary} at 298.15 K. G^E (pseudo (2/3) + component 1) are calculated by eq. (10-2.3) and also listed in table 10-1. The comparison of G^E of n-hexane + pure n-alkanes determined by Marsh and Ott with that of n-hexane + pseudo n-alkanes which are congruent with the pure n-alkanes for $n=10, 11, 12$ at 298.15 K are shown in figures 10-2 to 10-4. Although the values of G^E for pseudo n-alkane + n-hexane are slightly numerically lower than their congruent pure n-alkanes + n-hexane, these deviations are of the order of experimental errors.

Hijmans' graphical method may be extended to ternary mixtures. We chose the excess function of a binary system of component A with n_A and component B with n_B as a reference. Assuming that a ternary mixture is made by mixing component 1 with n_1 , component 2 with n_2 , component 3 with n_3 , the average number of carbon of the ternary mixture is

$$n = n_1 x_1 + n_2 x_2 + n_3 x_3 \quad \text{..... (10-2.6)}$$

where, $n_A \leq n_1 \leq n_2 \leq n_3 \leq n_B$.

The average carbon number for a binary mixture which is congruent with the ternary mixture is the same as the ternary mixture:

$$n = n_A x_A + n_B x_B \quad \text{..... (10-2.7)}$$

The carbon number of component 1, 2, and 3 also may be represented by the average number of carbon of their congruent binary mixtures:

$$n_1 = n_A x_{A1} + n_B x_{B1} \quad \text{..... (10-2.8)}$$

$$n_2 = n_A x_{A2} + n_B x_{B2} \quad \text{..... (10-2.9)}$$

$$n_3 = n_A x_{A3} + n_B x_{B3} \quad \text{..... (10-2.10)}$$

Combining equations of (10-2.6) to (10-2.10), we have

$$x_A = x_1 x_{1A} + x_2 x_{2A} + x_3 x_{3A} \quad \text{..... (10-2.11)}$$

Fig. 10-3
COMPARISON OF GE BETWEEN n-UNDECANE AND PSEUDO n-UNDECANE + n-HEXANE

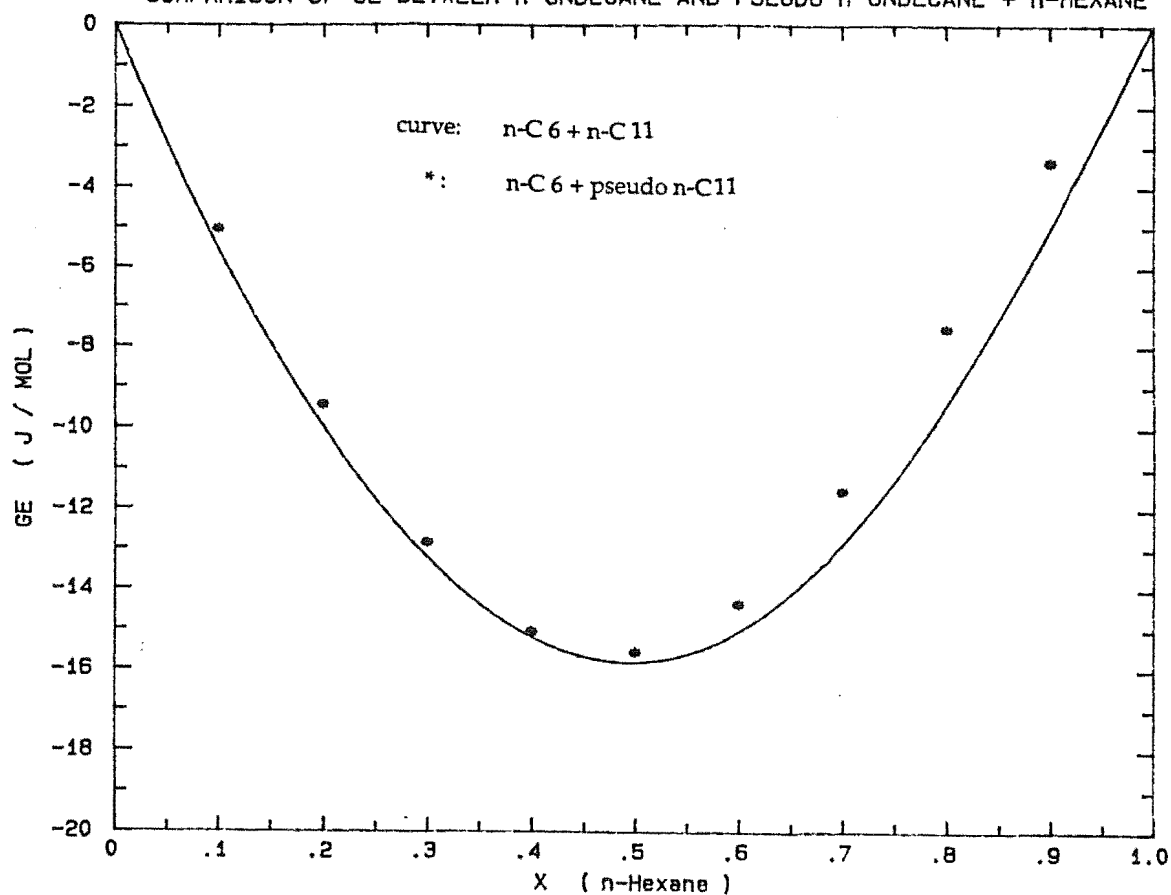


Fig. 10-4
COMPARISON OF GE BETWEEN n-DODECANE AND PSEUDO n-DODECANE+n-HEXANE

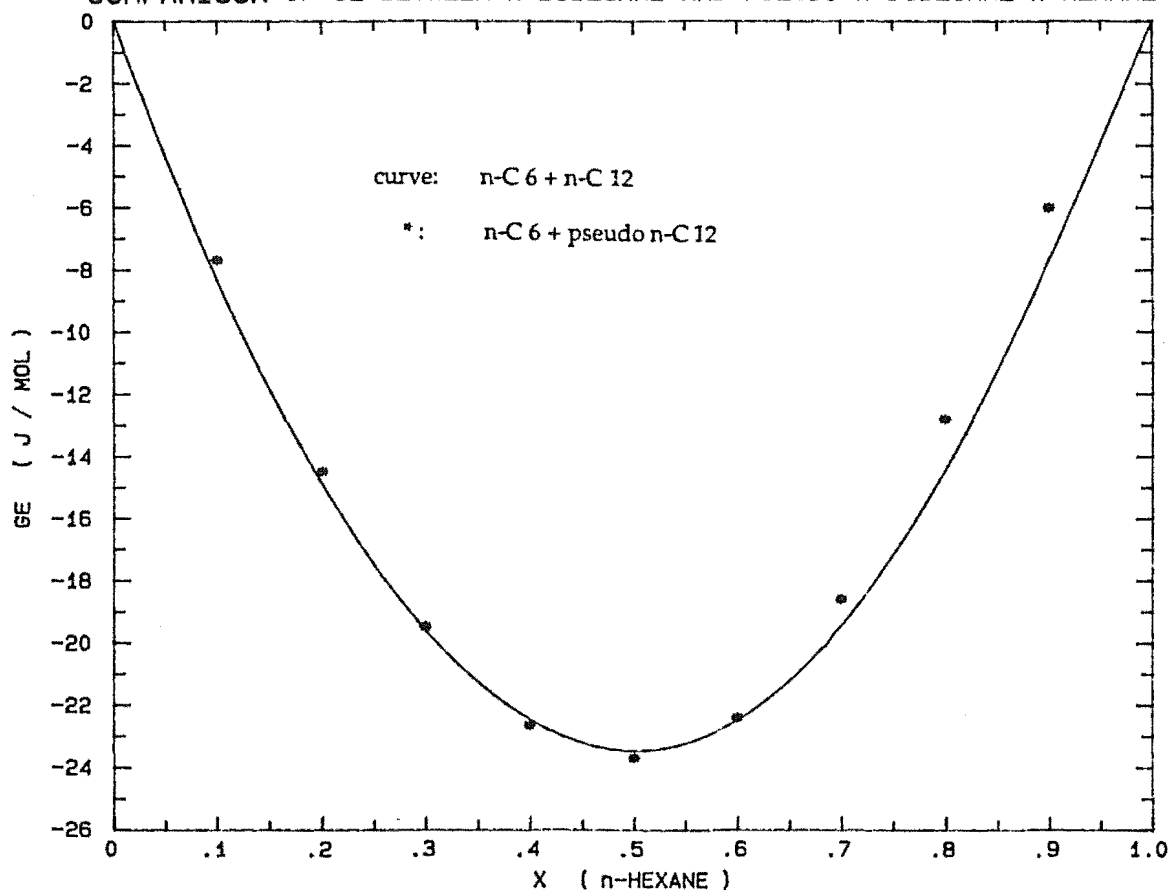


Table 10-1 Calculated G^E for n-hexane + Pseudo n-alkanes

x_1	x_2	x_3	G^E (ternary) (x_2+x_3) (J mol ⁻¹)	G^E (c-8 + c-16) (J mol ⁻¹)	G^E (c-6+pseudo) (J mol ⁻¹)
n(2/3)=12					
0.1	0.45	0.45	-43.36	-35.69	-7.7
0.2	0.4	0.40	-46.25	-31.73	-14.5
0.3	0.35	0.35	-47.28	-27.76	-19.5
0.4	0.30	0.30	-46.48	-23.80	-22.7
0.5	0.25	0.25	-43.57	-19.83	-23.7
0.6	0.20	0.20	-38.25	-15.86	-22.4
0.7	0.15	0.15	-30.47	-11.90	-18.6
0.8	0.10	0.10	-20.68	-7.93	-12.8
0.9	0.05	0.05	-9.93	-3.97	-6.0
n(2/3)=11					
0.1	0.5625	0.3375	-39.10	-34.03	-5.1
0.2	0.5000	0.3000	-39.76	-30.24	-9.5
0.3	0.4375	0.3625	-39.37	-26.47	-12.9
0.4	0.3750	0.2250	-37.72	-22.61	-15.1
0.5	0.3125	0.1875	-34.49	-18.91	-15.6
0.6	0.2500	0.1500	-29.52	-15.12	-14.4
0.7	0.1875	0.1125	-22.93	-11.34	-11.6
0.8	0.1250	0.0750	-15.19	-7.56	-7.6
0.9	0.0625	0.0375	-7.15	-3.78	-3.4
n(2/3)=10					
0.1	0.675	0.225	-30.53	-27.68	-2.9
0.2	0.600	0.200	-29.98	-24.61	-5.4
0.3	0.525	0.175	-28.89	-21.53	-7.4
0.4	0.450	0.150	-26.89	-18.46	-8.4
0.5	0.375	0.125	-23.88	-15.38	-8.5
0.6	0.300	0.100	-19.82	-12.30	-7.5
0.7	0.225	0.075	-14.93	-9.23	-5.7
0.8	0.150	0.050	-9.6	-6.15	-3.5
0.9	0.075	0.025	-4.39	-3.08	-1.3

$$x_B = x_1 x_{1B} + x_2 x_{2B} + x_3 x_{3B} \dots\dots\dots (10-2.12)$$

Following the procedure described in section 10-1 , we have

$$X^E(n, n_1, n_2, n_3) = [X^E(n, n_A, n_B) - x_1 X^E(n_1, n_A, n_B) - x_2 X^E(n_2, n_A, n_B) - x_3 X^E(n_3, n_A, n_B)] + \Delta' \dots\dots\dots (10-2.13)$$

where Δ' is the deviation from the principle of congruence when the graphical method is applied to the ternary mixture.

Let $X=G$, $A=1$, $B=3$, the above equation becomes

$$G^E(n, n_1, n_2, n_3) = G^E(n, n_1, n_3) - x_2 G^E(n_2, n_1, n_3) + \Delta' \dots\dots\dots (10-2.14)$$

$$\text{Let } n' = x_1 n_1 / (x_1 + x_3) + x_3 n_3 / (x_1 + x_3) \dots\dots\dots (10-2.15)$$

obviously, n' is the average number of the pseudo n -alkanes made by mixing x_1 mole of component 1 and x_3 mole of component 3. From eq. (10-2.15), we have

$$\begin{aligned} n_2 - n' &= n_2 - x_1 n_1 / (x_1 + x_3) - x_3 n_3 / (x_1 + x_3) \\ &= x_1 (n_2 - n_1) / (x_1 + x_3) + x_3 (n_2 - n_3) / (x_1 + x_3) \dots\dots\dots (10-2.16) \end{aligned}$$

$$\begin{aligned} n - n' &= -n_1 x_1 x_2 / (x_1 + x_3) - n_3 x_2 x_3 / (x_1 + x_3) + (n_2 x_1 x_2 + n_2 x_2 x_3) / (x_1 + x_3) \\ &= x_2 [(n_2 - n_1) x_1 / (x_1 + x_3) + (n_2 - n_3) x_3 / (x_1 + x_3)] \dots\dots\dots (10-2.17) \end{aligned}$$

comparing eq. (10-2.16) and (10-2.17) we have

$$x_2 = (n - n') / (n_2 - n') \dots\dots\dots (10-2.18)$$

Substitute eq. (10-2.18) into eq. (10-2.14), then

$$G^E(n, n_1, n_2, n_3) = G^E(n, n_1, n_3) - [(n - n') / (n_2 - n')] G^E(n_2, n_1, n_3) + \Delta' \dots\dots\dots (10-2.19)$$

Referring to figure 10-5, the line segment, $n_2 A = G^E(n_2, n_1, n_3)$, and therefore the term of $[(n - n') / (n_2 - n')] G^E(n_2, n_1, n_3)$ in above equation is obviously geometrically equal to the line segment cn .

The plotting procedure to test the principle of congruence for the ternary mixtures is described as follows:

Firstly, the excess functions of a reference binary system are plotted against the average number of carbon. n' is then calculated by eq. (10-2.15) and is found on the n -axis. Sequentially, n_2 and n are found on the n -axis. Two vertical lines nB , and $n_2 A$ then are drawn and intersected with the reference curve at points B , and A . The intersection of Bn and An' , then determines C . Bc should be $G^E(n,$

Fig. 10-5 GRAPHICAL METHOD FOR TERNARY MIXTURES

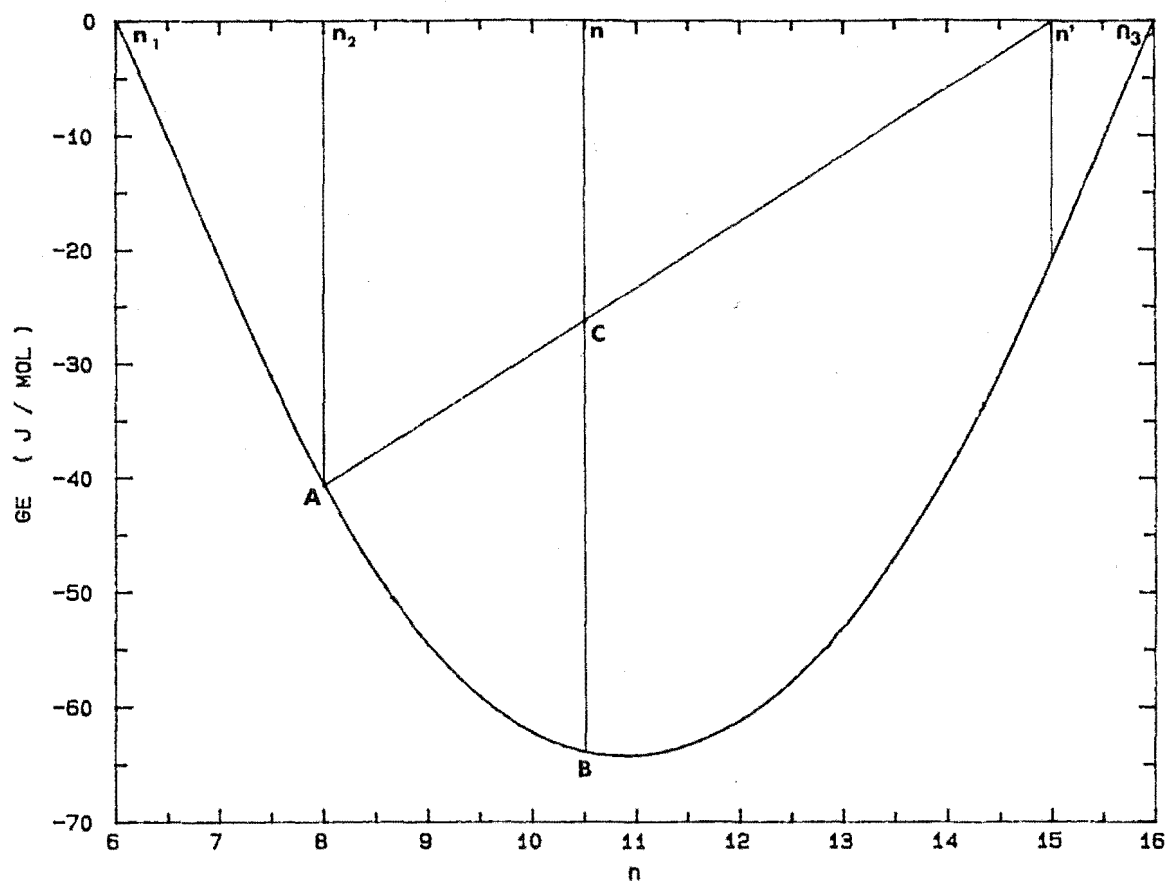
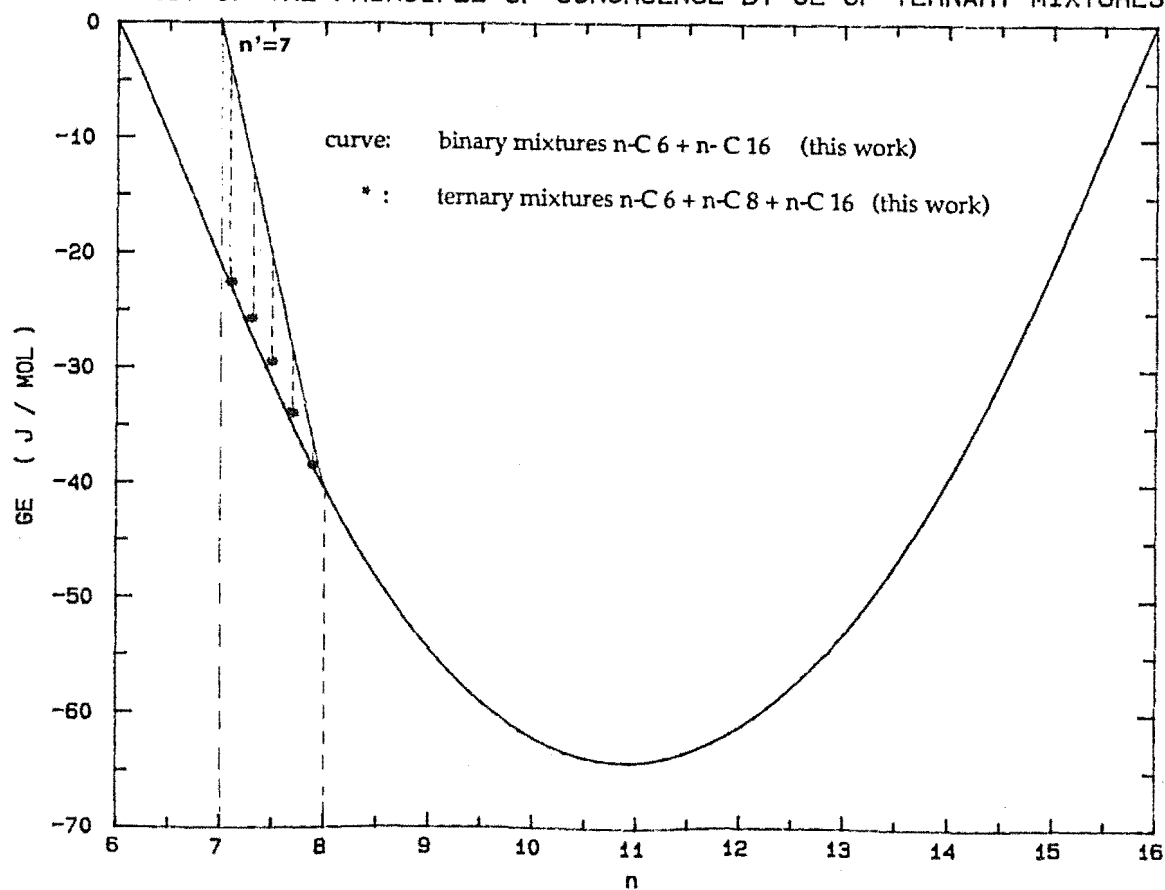


Fig. 10-6
TEST OF THE PRINCIPLE OF CONGRUENCE BY GE OF TERNARY MIXTURES



n_1, n_2, n_3), if the principle of congruence is obeyed for this ternary system.

For the ternary mixtures investigated in this work, we chose the binary mixtures of n-hexane + n-hexadecane as a reference, and n-octane as the component 2. In order to show the results of the test clearly, we plot each graph for a constant n' . Equation (10-2.4) may be used to calculate the mole fraction of component 1 for a required constant n' at various mole fractions of component 2 as long as we exchange subscripts 1 and 2:

$$x_1 = (n' - n_3)(1 - x_2) / (n_1 - n_3) \quad \text{..... (10-2.20)}$$

with $n_1 = 16, n_3 = 6$ then eq. (10-2.20) becomes

$$x_1 = (16/10 - n'/10)(1 - x_2) \quad \text{..... (10-2.21)}$$

using eq. (10-21), x_1 is calculated for the given n' and x_2 , then the average carbon number is obtained by eq. (10-2.6). The G^E of ternary mixtures at given composition is computed with the equations described in section 5-3.2 and the optimized parameters listed in section 6-4. All the calculated results are listed in table 10-2. Figure 10-6 to 10-10 show the plots for $n' = 7, 9, 11, 13, 15$, respectively. Δ' are less than 2 J mol^{-1} for all plotted points, within the maximum experimental errors. These tests confirm that the principle of congruence is valid for the ternary mixtures investigated in this work in the whole composition range.

10-3 NULL TESTS

According to the principle of congruence, if an n-alkane with the number of carbon n_i is mixed with a pseudo n-alkane with the same average number of carbon, then all excess functions should be zero.

A most convenient property of a ternary mixture for the null test is the logarithm of the activity coefficient, because it is independent of any information on mixing two pure liquids to form the pseudo n-alkane. Let γ_i denote the activity coefficient of component i in a ternary mixture which has the carbon number n_i . Obviously $\ln \gamma_i$ is equal to 0 for all the ternary mixtures which have an average number of carbon n_i , if the principle of congruence is valid. It

Fig.10-7
TEST OF THE PRINCIPLE OF CONGRUENCE BY GE OF TERNARY MIXTURES

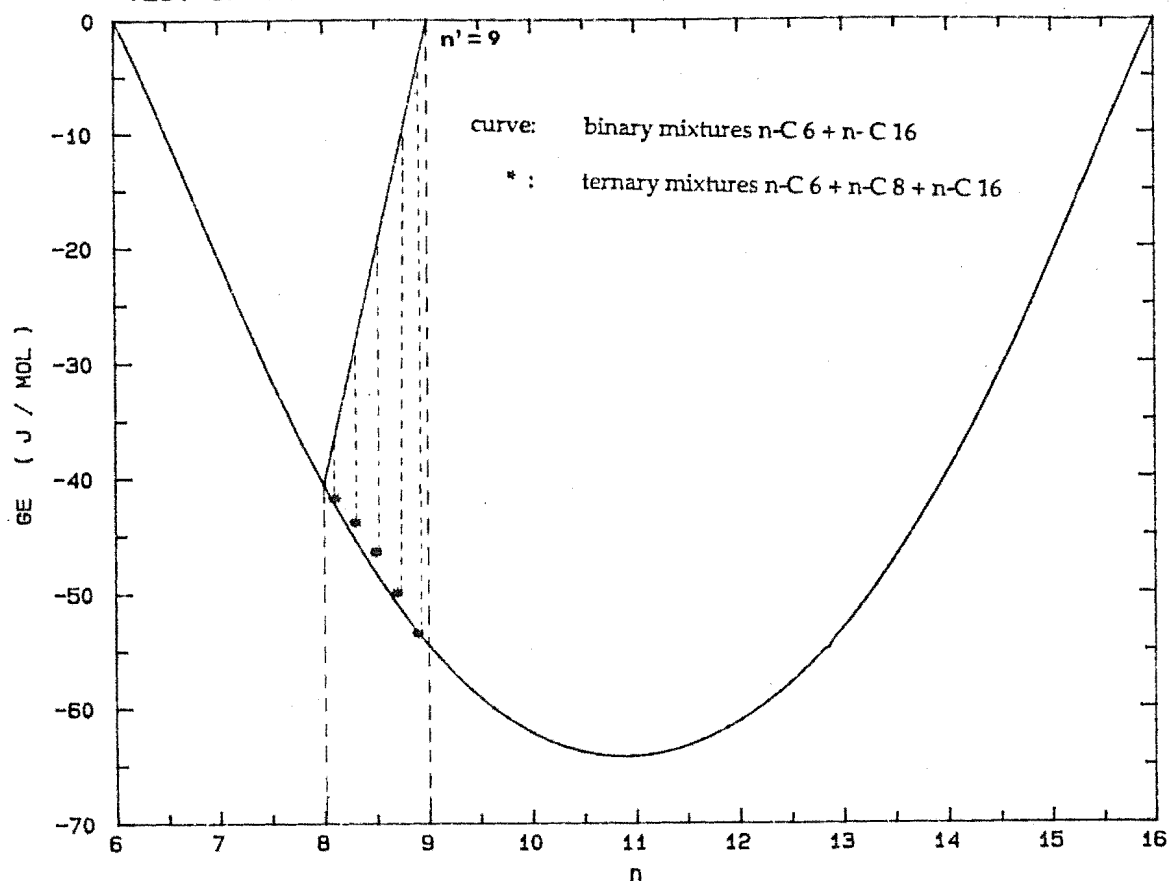


Fig.10-8
TEST OF THE PRINCIPLE OF CONGRUENCE BY GE OF TERNARY MIXTURES

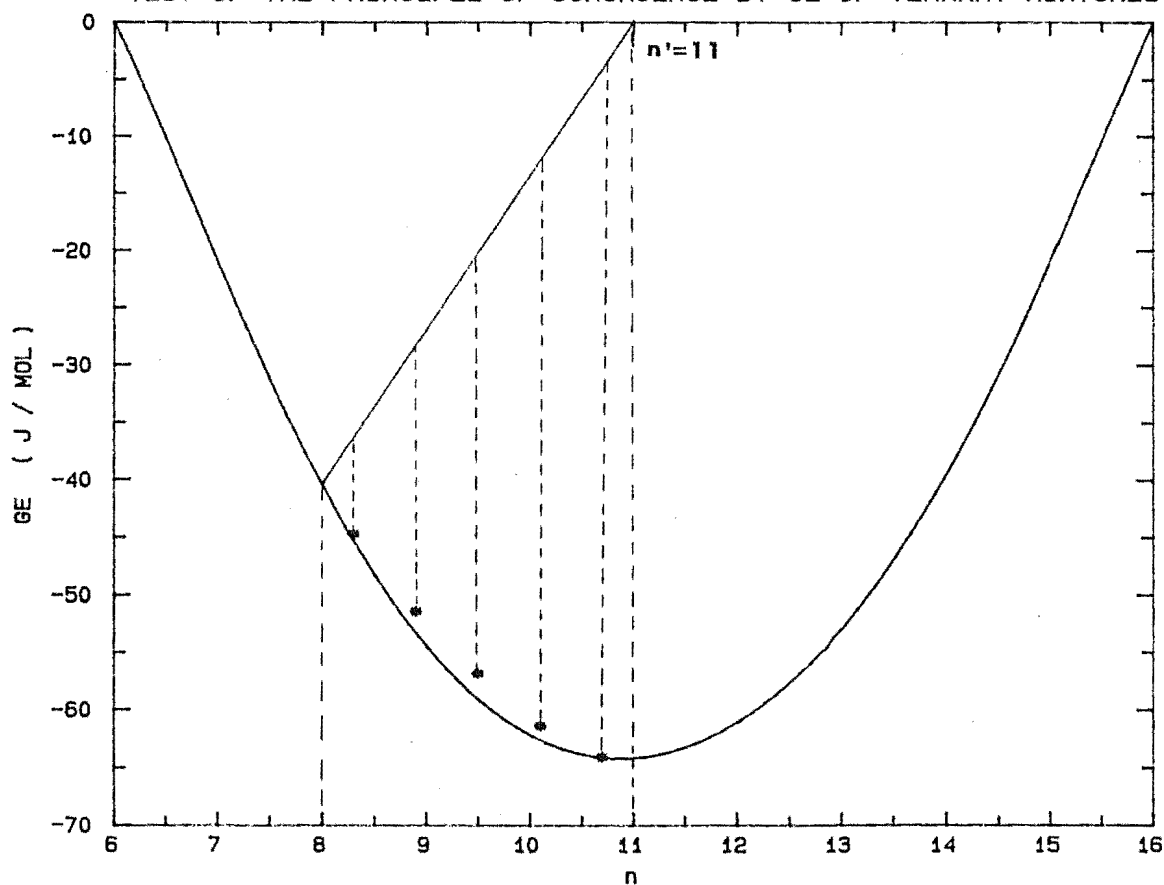


Fig. 10-9

TEST OF THE PRINCIPLE OF CONGRUENCE BY GE OF TERNARY MIXTURES

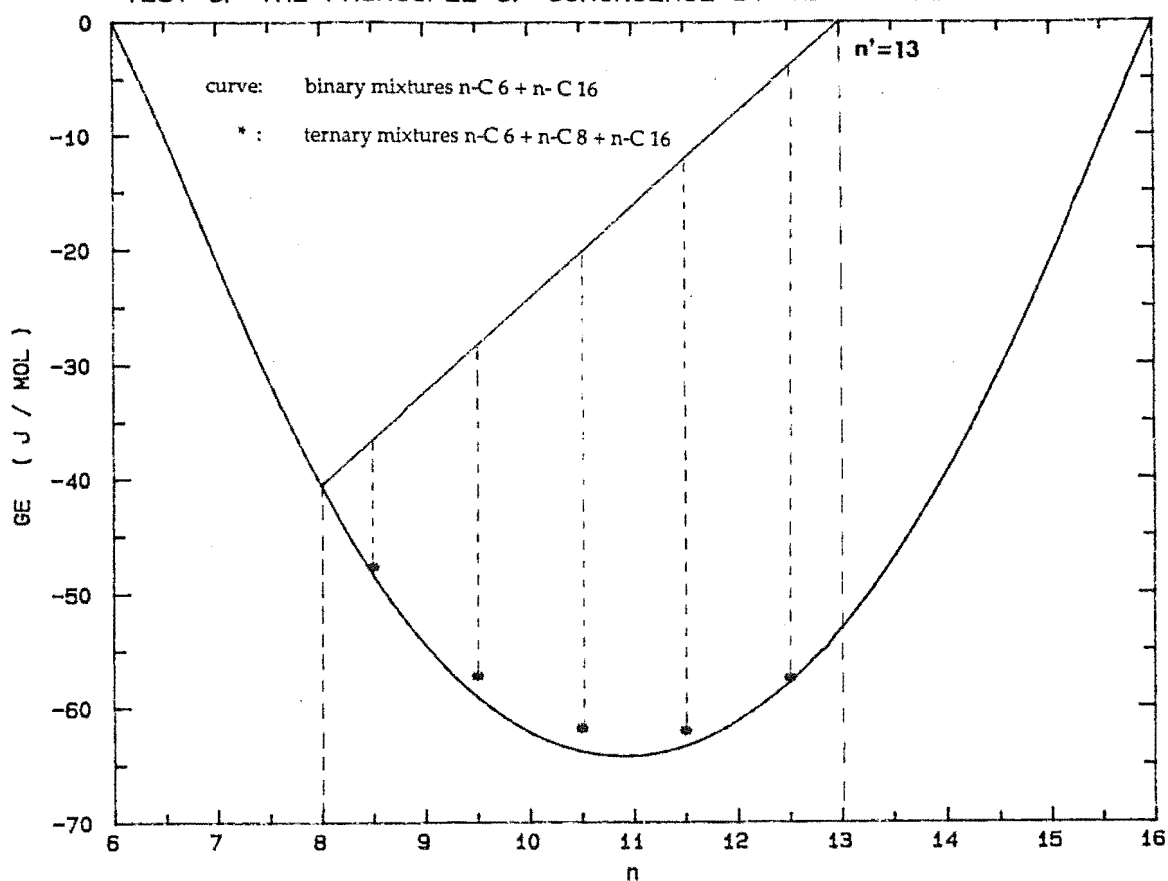


Fig. 10-10

TEST OF THE PRINCIPLE OF CONGRUENCE BY GE OF TERNARY MIXTURES

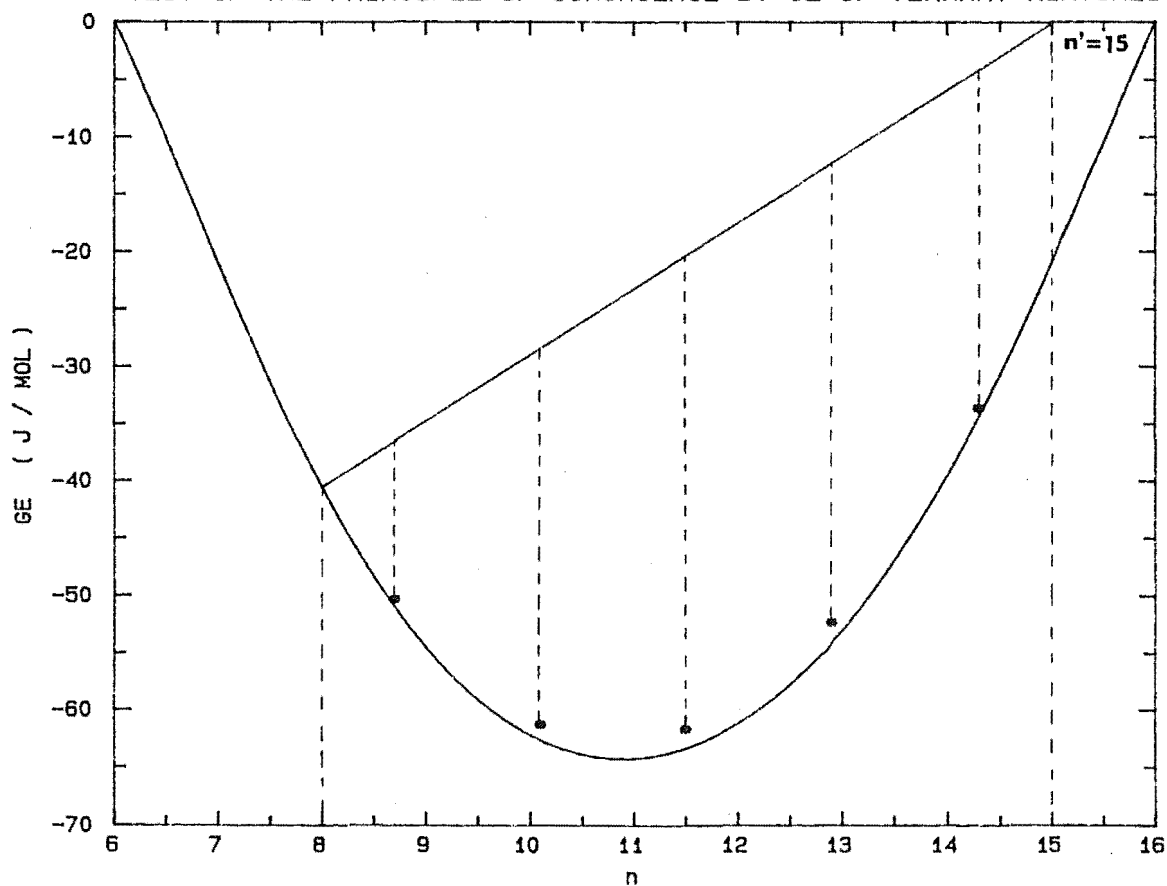


Table 10-2 Calculated G^E of Ternary Mixtures for Ternary Graphical Test

x_1	x_2	x_3	n	$G^E_{(ternary)}(\text{Jmol}^{-1})$
$n'=15$				
0.09	0.1	0.81	14.3	-29.5
0.07	0.3	0.63	12.9	-40.0
0.05	0.5	0.45	11.5	-41.3
0.03	0.7	0.27	11.1	-32.8
0.01	0.9	0.09	8.7	-13.8
$n'=13$				
0.27	0.1	0.63	12.5	-53.4
0.21	0.3	0.49	11.5	-49.8
0.15	0.5	0.35	10.5	-41.6
0.09	0.7	0.21	9.5	-28.9
0.03	0.9	0.07	8.5	-11.2
$n'=11$				
0.45	0.1	0.45	10.7	-60.1
0.35	0.3	0.35	10.2	-49.3
0.25	0.5	0.25	9.5	-36.6
0.15	0.7	0.15	8.9	-23.1
0.05	0.9	0.05	8.3	-8.33
$n'=9$				
0.63	0.1	0.27	8.9	-49.3
0.49	0.3	0.21	8.7	-37.7
0.35	0.5	0.15	8.5	-26.1
0.21	0.7	0.09	8.3	-15.4
0.07	0.9	0.03	8.1	-5.3
$n'=7$				
0.81	0.1	0.09	7.1	-18.5
0.63	0.3	0.07	7.3	-13.7
0.45	0.5	0.05	7.5	-9.4
0.27	0.7	0.03	7.7	-5.7
0.09	0.9	0.01	7.9	-2.1

may be expressed more mathematically that in a three dimensional Cartesian coordinate expressing the dependence of $\ln \gamma_i$ on the mole fractions for ternary mixtures, there exists a curve on which the average number of carbon is constant and equal to n_i , and the values of $\ln \gamma_i$ on this curve are zero if the principle of congruence is valid for these ternary mixtures.

In principle, an equation expressing mole fractions with constant zero value of $\ln \gamma_i$ may be obtained by substitution of $\ln \gamma_i = 0$ into the equations described in section 5-3.2. The derived curve then may be compared with the curve $n = n_i$ in the three dimensional Cartesian coordinate. The departure of these two curves denotes the deviations from the principle of congruence.

More simply, one may calculate the values of $\ln \gamma_i$ for given individual points on the curve $n = n_i$ to investigate the deviations from the zero value. We chose n-octane as component i (i.e. $i=2$). The calculated values of $\ln \gamma_2$ for $n = n_2$ at various compositions are listed in table 10-3. The deviations of $\ln \gamma_2$ from the zero are shown in figure 10-11. these deviations seem to be lower in the higher mole fraction of n-octane and up to about 0.002 at $x(\text{n-octane}) \approx 0.2$. It could be caused by a small systematic experimental errors, or the errors introduced from the data reduction, or departure from the principle of the congruence.

Following the procedure described in the last section, the G^E on mixing two n-alkanes to form a pseudo n-alkane which is congruent with component i and the G^E for ternary mixture are calculated. Then G^E (n-octane + pseudo) is obtained from eq. (10-2.3) and listed in the last column in table 10-3. The deviations from zero are shown in figure 10-12, which is quite symmetric against the mole fraction of n-octane with a maximum value of 1.7 J mol^{-1} . This is less than the maximum error of experiments.

10-4 ANALYTICAL TEST USING B-M EQUATION FOR G^E OF BINARY MIXTURES

As mentioned in section 9-7, the Bellemans and Mat equation (B-M equation) may be expressed as

Table 10-3 Calculated $\ln\gamma_2$ for Null Test

x_1	x_2	x_3	γ_2	$\ln\gamma_2 (10^{-3})$	$G^E(\text{c-8+pseudo})$ (J mol ⁻¹)
0.72	0.1	0.18	1.0013	1.3	0.1
0.64	0.2	0.16	1.0019	1.9	0.6
0.56	0.3	0.14	1.0018	1.8	1.1
0.48	0.4	0.12	1.0014	1.4	1.5
0.40	0.5	0.10	1.0008	0.8	1.7
0.32	0.6	0.08	1.0003	0.3	1.6
0.24	0.7	0.06	1.0000	0	1.3
0.16	0.8	0.04	0.9999	0.1	0.8
0.08	0.9	0.02	0.9999	0.1	0.3

Fig. 10-11

NULL TEST OF THE PRINCIPLE OF CONGRUENCE BY $\ln \gamma_2$ OF TERNARY MIXTURES

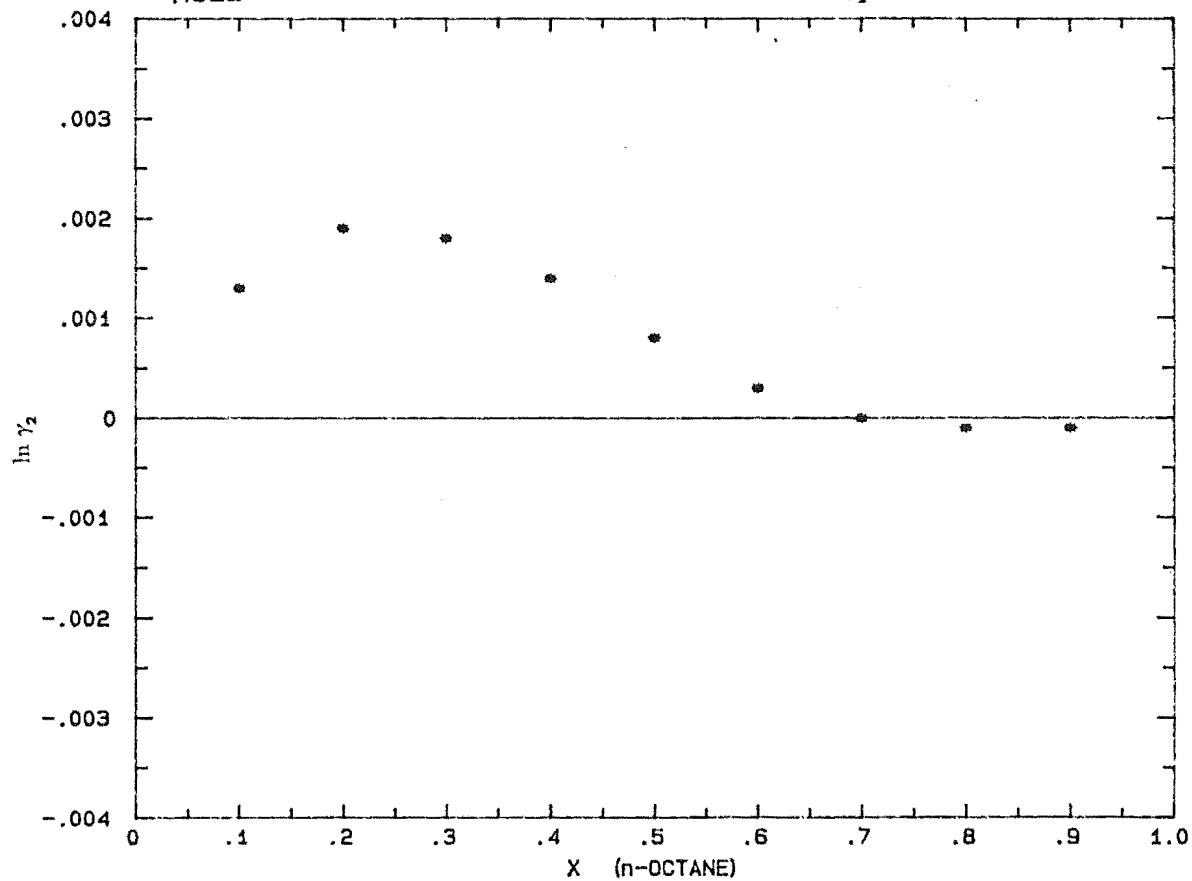
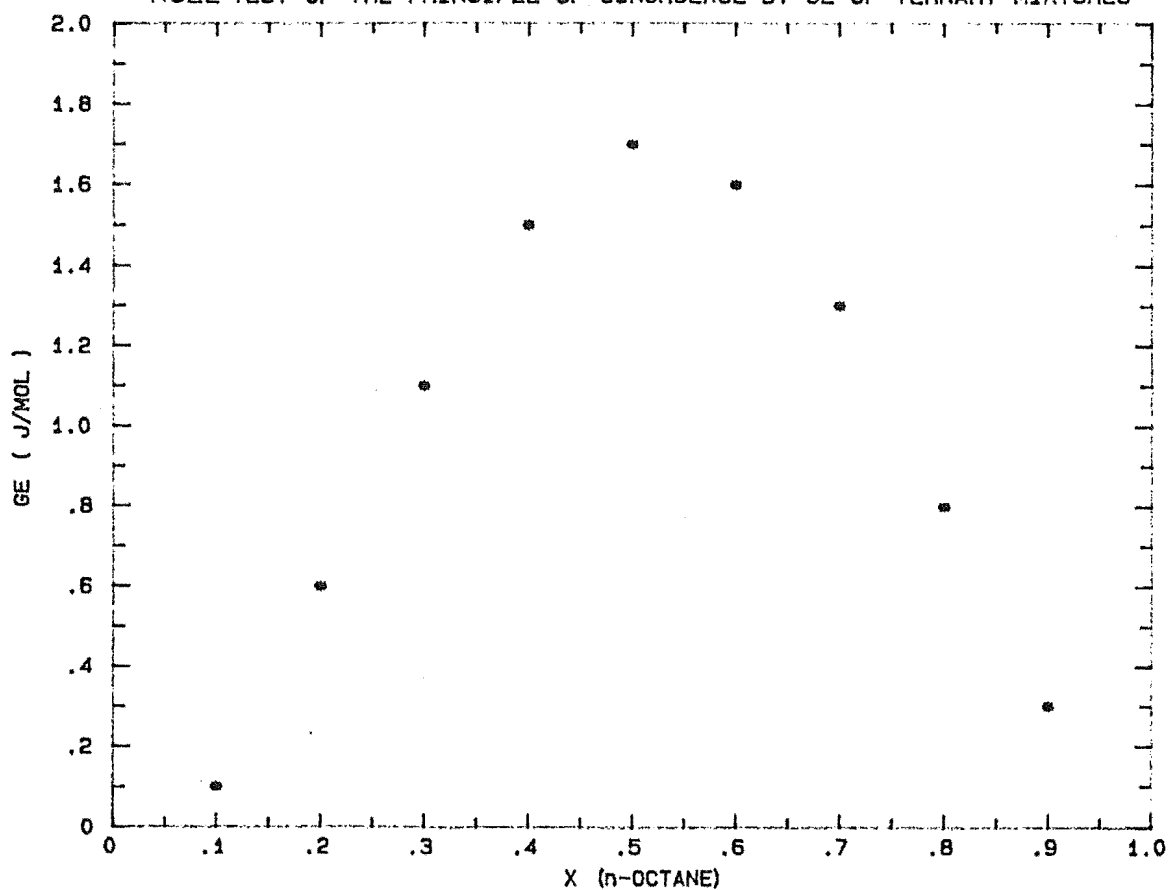


Fig. 10-12

NULL TEST OF THE PRINCIPLE OF CONGRUENCE BY GE OF TERNARY MIXTURES



$$G^E / RT = -Q_0 + g_{-1} Q_1 + g_{-2} Q_2 \quad \text{.....} \quad (10-4.1)$$

$$Q_0 = \ln n - x_1 \ln n_1 - x_2 \ln n_2 \quad \text{.....} \quad (10-4.2)$$

$$Q_1 = 1/n - x_1/n_1 - x_2/n_2 \quad \text{.....} \quad (10-4.3)$$

$$Q_2 = 1/n^2 - x_1/n_1^2 - x_2/n_2^2 \quad \text{.....} \quad (10-4.4)$$

Rearranging eq. (4-1), we have

$$(G^E / RT + Q_0) / Q_1 = g_{-1} + g_{-2} Q_2 / Q_1 \quad \text{.....} \quad (10-4.5)$$

A plot of the left hand side of eq. (10-4.5) against Q_2 / Q_1 , yields a straight line, if the B-M eq. is valid.

The experimental data of n-hexane + n-decane, + n-undecane, + n-dodecane reported by Masher and Ott (1980, 1981) and of n-hexane + n-octane, + n-hexadecane, and n-hexane + n-octane determined in this work were fitted to eq. (10-4.5) with the linear least squares methods and the results of regression are listed in table 10-4. In table 10-4, Column 3, 4, 5, 6 give the optimal parameters in eq. (10-4.5) and their errors, respectively. Column 7 gives the standard errors (R^*) of $(G^E / RT + Q_0) / Q_1$, and column 9 gives the correlation coefficients (CR).

The standard errors in excess Gibbs function (δG^E) were estimated by

$$\delta G^E / RT = R^* Q_1(\text{average}) \quad \text{.....} \quad (10-4.6)$$

and listed in column 8 of table 10-4, where $Q_1(\text{average})$ is the average value over the range of mole fractions for each system.

The results of regression of B-M equation for the individual binary mixtures of n-hexane + n-octane, + n-undecane, + n-dodecane, + n-hexadecane, and n-octane + n-hexadecane are listed in rows 1 to 6 of table 10-4. The results show that the B-M equation gives an excellent representation of the experimental G^E (within the experimental errors) for the each individual system and the parameters g_{-1} and g_{-2} are quite universal for the system 2 to 5, but the differences in parameters between n-octane + n-hexadecane, n-hexane + n-octane, and the rest systems are considerable. This is shown more clearly in figure 10-13, where the straight line 2 and 3 represent the B-M eq. (10-4.5) for n-octane + n-hexadecane, and n-hexane + n-octane. The straight line 1 is for systems 2 to 5 altogether.

Table 10-4 Results of Regression of B-M equation for Binary Mixtures

System	No	g_{-1}	g_{-2}	δg_{-1}	δg_{-1}	R^*	δG^E (J mol ⁻¹)	cR
n-c6 + n-c8	1	-1.30	-5.26	0.058	0.042	0.0041	0	0.997
n-c6 + n-c10	2	-5.62	5.47	0.194	0.164	0.0247	0.5	0.973
n-c6 + n-c11	3	-5.60	5.59	0.095	0.083	0.0141	0.4	0.993
n-c6 + n-c12	4	-5.63	5.70	0.073	0.067	0.0123	0.4	0.996
n-c6 + n-c16	5	-5.45	5.16	0.075	0.072	0.0166	1.0	0.992
n-c8 + n-c16	6	-6.11	7.35	0.012	0.011	0.0023	0.1	1.00
system 1 to 6		-5.14	4.05	0.097	0.034	0.1300	3.5	0.884
system 1, 5, 6		-4.94	3.21	0.081	0.039	0.1014	3.1	0.915

Fig. 10-13
PLOT OF GE OF BINARY n-ALKANE MIXTURES USING B-M EQ.

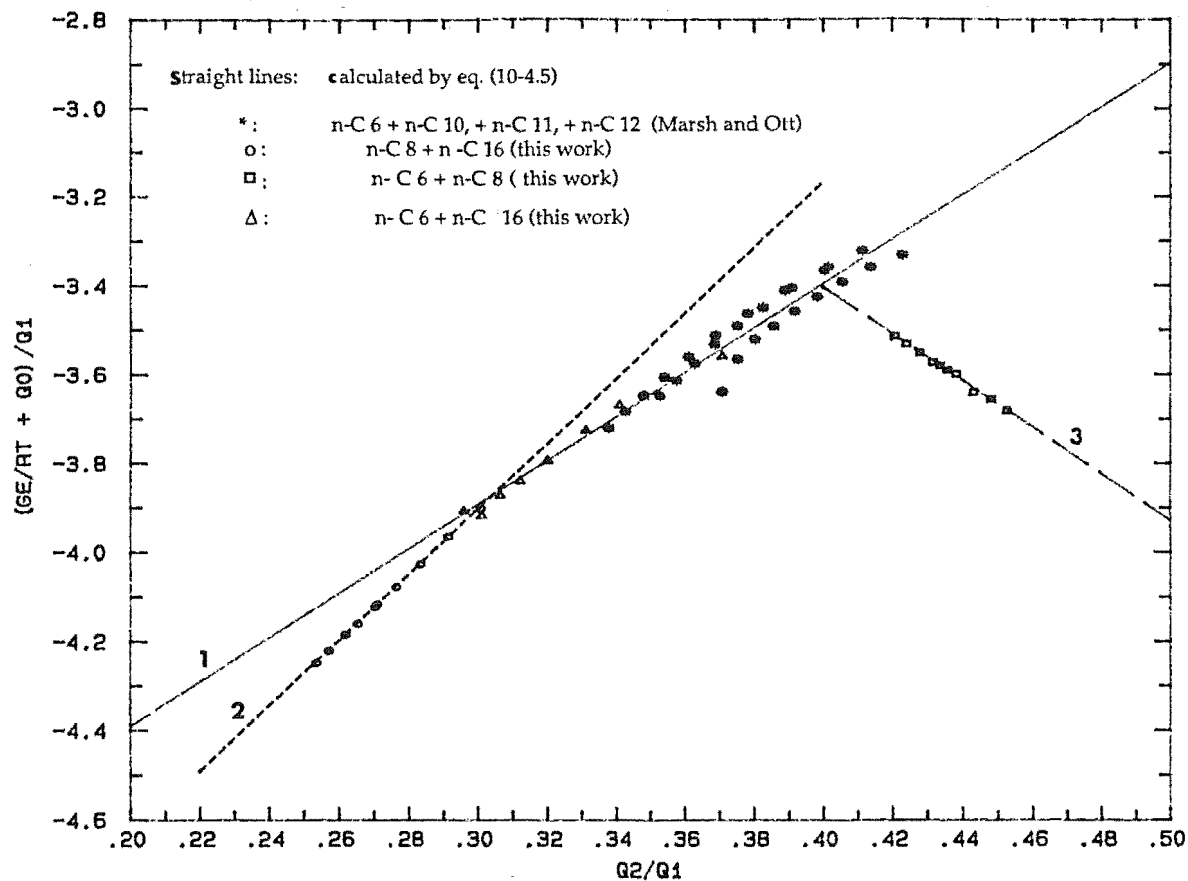
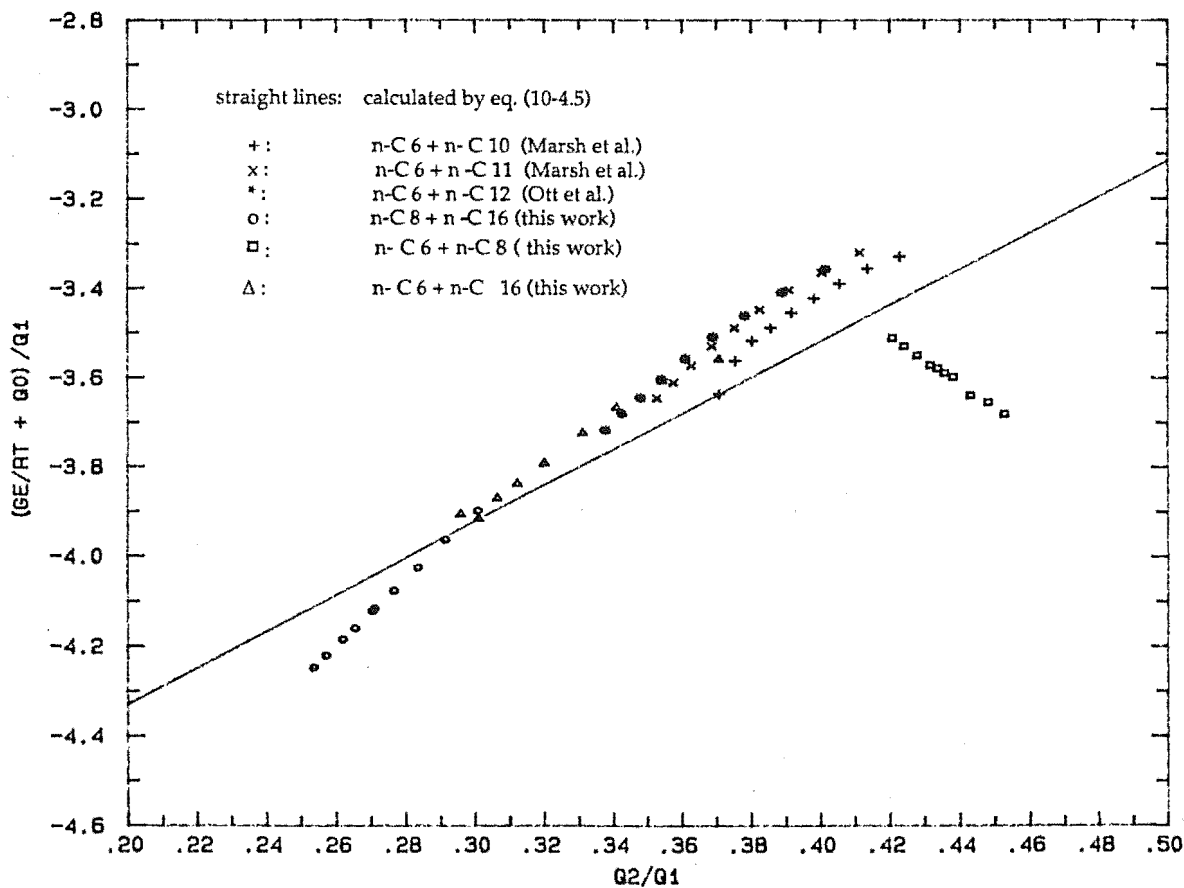


Fig. 10-14
PLOT OF BINARY n-ALKANE MIXTURES USING B-M EQ.



Applying the B-M equation to all 6 systems, the results of the regression are shown in row 7 of table 10-4 and illustrated more clearly in figure 10-14. The estimated standard error in G^E is about 3.5 J mol^{-1} , larger than the maximum experimental error.

Row 8 of table 10-4 shows the results of regression for the three binary systems investigated in this work. The estimated standard error of G^E is about 3.1 J mol^{-1} , which is also larger than the maximum errors in our experiments. Therefore it may be predicated that the B-M equation would not be successful to represent the excess Gibbs functions of mixtures obtained from the R-K equation with the parameters optimized from ternary P-x experimental data. It is necessary to investigate the ability of the B-M equation to directly express the P-x data instead of the indirect representation of G^E before any attempt is made to modify the B-M equation.

10-5. ANALYTICAL TEST USING B-M EQUATION FOR G^E OF TERNARY MIXTURES

The B-M equation can easily be extended to ternary systems in the form

$$Q = G^E/RT = -\ln n + x_1 \ln n_1 + x_2 \ln n_2 + x_3 \ln n_3 \\ + g_{-1} [1/n - x_1/n_1 - x_2/n_2 - x_3/n_3] + g_{-2} [1/n^2 - x_1/n_1^2 - x_2/n_2^2 - x_3/n_3^2] \\ \dots\dots\dots (10-5.1)$$

and

$$\ln \gamma_1 = [Q - x_2 (\partial Q / \partial x_2)_{x_3} - x_3 (\partial Q / \partial x_3)_{x_2}] \dots\dots\dots (10-5.2)$$

where

$$n = x_1 n_1 + x_2 n_2 + x_3 n_3, \quad (\partial n / \partial x_2)_{x_3} = -n_1 + n_2, \quad (\partial n / \partial x_3)_{x_2} = -n_1 + n_3$$

Taking the derivative of eq. (10-5.1) with respect to x_2 and x_3 , yields

$$(\partial Q / \partial x_2)_{x_3} = (n_1 - n_2) / n - \ln n_1 + \ln n_2 + g_{-1} [(n_1 - n_2) / n^2 + 1/n_1 - 1/n_2] \\ + g_{-2} [2(n_1 - n_2) / n^3 + 1/n_1^2 - 1/n_2^2] \dots\dots\dots (10-5.3)$$

$$-x_2 (\partial Q / \partial x_2)_{x_3} = x_2 (n_2 - n_1) / n + x_2 \ln n_1 - x_2 \ln n_2 + g_{-1} [x_2 (n_2 - n_1) / n^2 \\ - x_2 / n_1 + x_2 / n_2] + g_{-2} [2 x_2 (n_2 - n_1) / n^3 - x_2 / n_1^2 + x_2 / n_2^2] \\ \dots\dots\dots (10-5.4a)$$

$$\begin{aligned}
-x_3 (\partial Q / \partial x_3)_{x_2} &= x_3 (n_3 - n_1) / n + x_3 \ln n_1 - x_3 \ln n_3 + g_{-1} [x_3 (n_3 - n_1) / n^2 \\
&\quad - x_3 / n_1 + x_3 / n_3] + g_{-2} [2 x_3 (n_3 - n_1) / n^3 - x_3 / n_1^2 + x_3 / n_3^2] \\
&\quad \dots\dots\dots (10-5.4b)
\end{aligned}$$

Substituting (10-5.3) and (10-5.4) into (10-5.2), we have

$$\begin{aligned}
\ln \gamma_1 &= \ln(n_1/n) + [x_2 (n_2 - n_1) + x_3 (n_3 - n_1)] / n + g_{-1} \{1/n - 1/n_1 \\
&\quad + [x_2 (n_2 - n_1) + x_3 (n_3 - n_1)] / n^2\} + g_{-2} \{1/n^2 - 1/n_1^2 \\
&\quad + 2 [x_2 (n_2 - n_1) + x_3 (n_3 - n_1)] / n^3\} \quad \dots\dots\dots (10-5.5)
\end{aligned}$$

Similarly, we can derive the expressions for $\ln \gamma_2$ and $\ln \gamma_3$:

$$\begin{aligned}
\ln \gamma_2 &= \ln(n_2/n) + [x_1 (n_1 - n_2) + x_3 (n_3 - n_2)] / n + g_{-1} \{1/n - 1/n_2 \\
&\quad + [x_1 (n_1 - n_2) + x_3 (n_3 - n_2)] / n^2\} + g_{-2} \{1/n^2 - 1/n_2^2 \\
&\quad + 2 [x_1 (n_1 - n_2) + x_3 (n_3 - n_2)] / n^3\} \quad \dots\dots\dots (10-5.6)
\end{aligned}$$

$$\begin{aligned}
\ln \gamma_3 &= \ln(n_3/n) + [x_1 (n_1 - n_3) + x_2 (n_2 - n_3)] / n + g_{-1} \{1/n - 1/n_3 \\
&\quad + [x_1 (n_1 - n_3) + x_2 (n_2 - n_3)] / n^2\} + g_{-2} \{1/n^2 - 1/n_3^2 \\
&\quad + 2 [x_1 (n_1 - n_3) + x_2 (n_2 - n_3)] / n^3\} \quad \dots\dots\dots (10-5.7)
\end{aligned}$$

With equations (10-5.5) to (10-5.7), and eq. (5-3.1) we can express the total vapour pressure as a function of mole fraction with the universal parameters g_{-1} and g_{-2} .

The experimental P-x data of n-hexane + n-octane + n-hexadecane measured in this work were fitted to equations (10-5.5) to (10-5.7) and eq. (5-3.1) by non-linear squares methods described in chapter 5. The computation programme PVLR5 was written for this fitting procedure. The results are shown in table 10-5 and 10-8.

Table 10-5 lists the optimal parameters g_{-i} and the estimated errors of the parameters (σg_{-i}), the standard deviation (R) and the number of experimental points (N). Table 10-8 lists the calculated activities in liquid phase (γ_i), the mole fractions of vapour phase (y_i), the excess Gibbs function (G^E), and the deviations between calculated and experimental vapour pressure(r). The excess Gibbs function obtained by B-M equation are higher (the maximum difference is about 7 J mol^{-1}) numerically than that obtained by R-K equation. The deviation (r) is

Table 10-5 The parameters of B-M Equation (eq. 10-4.1) for Ternary System (298.15 K)

i	g_i	σg_i	R (pa)	N
1	-4.893	0.0346	9.0	44
2	3.731	0.0933		

Table 10-6 The Parameters of Modified B-M Equation (eq. 10-6.3) for Ternary System (298.15 K)

i	g_i	σg_i	R (pa)	N
0	0.233	0.0488	6.5	44
1	1.782	0.426		
2	-5.70	0.605		

Table 10-7 The parameters of Modified B-M equation (eq. 10-6.3) for Ternary System and Binary Systems (298.15 K)

i	g_i	σg_i	R (pa)	N
0	0.270	0.034	6.7	81
1	1.460	0.303		
2	-5.264	0.439		

Table 10-8 Calculated Results of Ternary System by B-M Equation

x_1	x_2	γ_1	γ_2	γ_3	y_1	y_2	G^E (J mol ⁻¹)	r (pa)
0.1332	0.2760	0.9533	0.9765	0.9865	0.8330	0.1670	-51.9	-9.3
0.2214	0.2479	0.9624	0.9827	0.9807	0.9024	0.0976	-57.4	-11.0
0.3075	0.2206	0.9706	0.9880	0.9738	0.9353	0.0647	-60.4	-12.6
0.3931	0.1933	0.9780	0.9924	0.9660	0.9548	0.0452	-60.8	-3.6
0.4810	0.1652	0.9846	0.9959	0.9571	0.9681	0.0320	-58.7	-2.0
0.5023	0.1430	0.9849	0.9961	0.9566	0.9734	0.0266	-59.4	6.7
0.5911	0.1176	0.9906	0.9985	0.9463	0.9813	0.0187	-54.1	10.9
0.6904	0.0891	0.9953	0.9998	0.9345	0.9878	0.0122	-45.0	6.4
0.8008	0.0573	0.9986	0.9998	0.9222	0.9932	0.0068	-31.3	-6.2
0.9006	0.0286	0.9998	0.9990	0.9139	0.9970	0.0030	-16.2	-19.1
0.1069	0.4448	0.9680	0.9863	0.9762	0.7141	0.2859	-50.6	-3.2
0.1988	0.3990	0.9746	0.9905	0.9698	0.8383	0.1617	-52.7	-0.6
0.3086	0.3444	0.9818	0.9945	0.9611	0.9033	0.0967	-52.9	3.1
0.3979	0.2999	0.9868	0.9969	0.9535	0.9326	0.0674	-51.1	5.7
0.5220	0.2324	0.9922	0.9991	0.9428	0.9591	0.0409	-46.5	9.1
0.6133	0.1880	0.9955	0.9999	0.9342	0.9715	0.0285	-40.5	2.6
0.7080	0.1420	0.9979	1.0000	0.9257	0.9812	0.0188	-32.5	-6.1
0.8034	0.0956	0.9993	0.9995	0.9182	0.9888	0.0112	-22.9	-16.1
0.8947	0.0513	0.9999	0.9988	0.9130	0.9946	0.0054	-12.5	-13.1
0.4833	0.3554	0.9957	0.9999	0.9336	0.9344	0.0656	-32.8	5.3
0.5995	0.2755	0.9978	1.0000	0.9259	0.9580	0.0420	-27.1	5.1
0.6929	0.2113	0.9990	0.9997	0.9203	0.9717	0.0283	-21.7	10.6
0.8018	0.1364	0.9997	0.9991	0.9150	0.9840	0.0160	-14.5	13.8
0.8979	0.0703	1.0000	0.9987	0.9120	0.9926	0.0074	-7.6	10.4

Table 10-8. Continued.....

x_1	x_2	γ_1	γ_2	γ_3	y_1	y_2	G^E (J mol ⁻¹)	r (J mol ⁻¹)
0.1192	0.6096	0.9840	0.9956	0.9580	0.6716	0.3284	-40.3	0.8
0.2076	0.5484	0.9875	0.9973	0.9522	0.7984	0.2016	-39.8	-1.8
0.3138	0.4750	0.9912	0.9987	0.9450	0.8737	0.1263	-38.0	-0.2
0.3922	0.4207	0.9935	0.9994	0.9396	0.9071	0.0929	-35.8	0.6
0.4938	0.3504	0.9960	1.0000	0.9326	0.9366	0.0634	-31.9	-3.0
0.1097	0.1056	0.9292	0.9585	0.9962	0.9143	0.0857	-38.5	-6.0
0.2105	0.0937	0.9433	0.9692	0.9915	0.9586	0.0414	-52.5	-9.1
0.3085	0.0821	0.9562	0.9785	0.9849	0.9749	0.0251	-61.7	-4.2
0.4135	0.0696	0.9688	0.9869	0.9755	0.9840	0.0160	-66.6	0.3
0.4986	0.0595	0.9778	0.9923	0.9662	0.9886	0.0114	-66.5	8.0
0.5955	0.0480	0.9864	0.9968	0.9540	0.9923	0.0077	-62.1	15.2
0.6996	0.0357	0.9935	0.9994	0.9397	0.9951	0.0049	-52.2	12.2
0.7945	0.0244	0.9976	1.0000	0.9267	0.9971	0.0029	-38.8	1.4
0.2111	0.7018	0.9959	0.9999	0.9329	0.7599	0.2401	-17.3	0
0.3489	0.5792	0.9976	1.0000	0.9270	0.8637	0.1363	-15.6	-5.3
0.4187	0.5171	0.9982	0.9999	0.9242	0.8949	0.1051	-14.5	-2.2
0.5233	0.4241	0.9990	0.9997	0.9202	0.9284	0.0716	-12.5	-4.4
0.6494	0.3119	0.9999	0.9993	0.9161	0.9562	0.0438	-9.6	-10.4
0.7224	0.2470	0.9998	0.9990	0.9142	0.9684	0.0316	-7.8	-14.4
0.8302	0.1511	1.0000	0.9987	0.9122	0.9829	0.0171	-4.8	-16.1

up to 19.1 pa, beyond the range of experimental errors.

The F-test which has been discussed in section (5-2.3) was used to judge the adequacy of the B-M equation compared with the R-K equation. $F_a(v_1, v_2)$ was found from an F-table (Owen, 1962) and is 1.5 for degree of freedom of $v_1 = 42$, $v_2 = 41$ at the significance level $\alpha=0.10$.

$$R_1^2/R_2^2 = 9.0^2/6.3^2 = 2.04 > 1.5 \quad \text{.....} \quad (10-5.8)$$

According to eq. (5-2.33), the hypothesis $r_1^2 \leq r_2^2$ is rejected at significance level $\alpha = 0.10$, where, r_1, r_2 are the deviations for B-M and R-K equation respectively. Equation (10-5.8) denotes that B-M equation is significantly less adequate to representing the experimental p-x data than the R-K equation.

10-6 TEST OF THE PRINCIPLE OF CONGRUENCE BY MODIFIED

B-M EQUATION

Bellemans and Mat (1963) introduced a term in the logarithm of the carbon number into the expression for G^E in the consideration of the combinatorial entropy. The formulae for the combinatorial entropy ($S^E(\text{com})$) for athermal mixtures were proposed by Flory (1942), and derived more rigorously by Guggenheim (1952). Flory's expression, or the approximation of Guggenheim's derivation is

$$S^E(\text{com}) = \sum_i \ln(\phi_i/x_i) \quad \text{.....} \quad (10-6.1)$$

$$\text{where, } \phi_i/x_i = (x_i r_i) / \sum x_i r_i \quad \text{.....} \quad (10-6.2)$$

and the summation is over the range of all components. Although, the value of $S^E(\text{com})$ varies with different choices of r_i and with various modified formulae, it generally leads to a term in $\ln r$, where, r is the number of segments, contributing to the free energy of liquid. However it is not necessary to assign 1 to the coefficient of the logarithmic term, because there probably exist other

logarithmic terms for the contributions to total entropy, such as the free volume term in the Flory theory. Also the addition of a coefficient which is not equal to 1 before the logarithmic term does not destroy the thermodynamic consistency of the expressions for excess functions.

With these considerations, a modified B-M equation for ternary mixtures was obtained as follows

$$G^E / RT = -g_0 Q_0 + g_{-1} Q_1 + g_{-2} Q_2 \quad \text{.....} \quad (10-6.3)$$

$$Q_0 = \ln n - x_1 \ln n_1 - x_2 \ln n_2 - x_3 \ln n_3 \quad \text{.....} \quad (10-6.4)$$

$$Q_1 = 1/n - x_1/n_1 - x_2/n_2 - x_3/n_3 \quad \text{.....} \quad (10-6.5)$$

$$Q_2 = 1/n^2 - x_1/n_1^2 - x_2/n_2^2 - x_3/n_3^2 \quad \text{.....} \quad (10-6.6)$$

The experimental ternary p-x data were then fitted to the modified B-M equation. The computation programme PVL6 used for this fitting procedure is listed in appendix 3. The results are shown in table 10-6 and 10-9. The results are in excellent agreement with that obtained by the R-K equation. G^E for most of experimental points obtained from the modified equation are still higher numerically than those obtained from the R-K equation, but the differences for almost all points, except a few are less than 2 J mol^{-1} , within the error range of the experiments. The standard deviation is 6.5 Pa, slightly higher than that obtained in fitting R-K equation. The value of R_1^2/R_2^2 in this case is 1.06 and

$$F_{1-\alpha/2}(41,41) = 0.59 \quad F_{\alpha/2}(41,41) = 1.7 \text{ at } \alpha=0.10, \text{ and therefore,}$$

$$F_{\alpha/2}(41,41) > R_1^2/R_2^2 > F_{1-\alpha/2}(41,41) \quad \text{.....} \quad (10-6.7)$$

According to eq. (5-2.32), $r_1^2 = r_2^2$ is confirmed at significant level $\alpha = 0.10$. In the other words, there is no significant difference (at significant level $\alpha = 0.10$) in the adequacy of fit between modified B-M, and the R-K equations for representation of the experimental P-x data.

The same regression procedure was applied to the ternary plus binary mixtures. 81 P-x data points were fitted to the modified B-M equation. The results are listed in table 10-7 and 10-10, and show excellent agreement between the regressions through the modified B-M equation and the R-K equation; and the regressions of ternary data only and ternary plus binary data. For the binary system n-hexane + n-octane, the differences from the two equations are less than 2 J mol^{-1} , but the signs are opposite for some points. The values from the modified B-M equation are almost all negative. No conclusion about which

Table 10-9 Calculated Results of Ternary System by Modified B-M Equation

x_1	x_2	γ_1	γ_2	γ_3	y_1	y_2	G^E (J mol ⁻¹)	r (pa)
0.1332	0.2760	0.9553	0.9780	0.9896	0.8331	0.1669	-45.7	-3.3
0.2214	0.2479	0.9630	0.9833	0.9845	0.9024	0.0976	-51.6	-8.0
0.3075	0.2206	0.9703	0.9880	0.9784	0.9353	0.0647	-55.1	-14.1
0.3931	0.1933	0.9773	0.9921	0.9710	0.9548	0.0452	-56.4	-9.1
0.4810	0.1652	0.9838	0.9956	0.9621	0.9680	0.0320	-55.2	-9.4
0.5023	0.1430	0.9841	0.9958	0.9615	0.9734	0.0266	-55.9	-0.9
0.5911	0.1176	0.9901	0.9983	0.9507	0.9813	0.0187	-51.5	5.4
0.6904	0.0891	0.9954	0.9998	0.9376	0.9878	0.0122	-43.1	7.1
0.8008	0.0573	0.9991	0.9998	0.9237	0.9932	0.0068	-29.8	1.6
0.9006	0.0286	1.0002	0.9991	0.9164	0.9970	0.0030	-14.9	-12.3
0.1069	0.4448	0.9680	0.9865	0.9806	0.7140	0.2860	-45.4	-3.0
0.1988	0.3990	0.9741	0.9903	0.9746	0.8382	0.1618	-48.2	-2.8
0.3086	0.3444	0.9810	0.9942	0.9662	0.9032	0.0968	-49.3	-1.8
0.3979	0.2999	0.9861	0.9967	0.9584	0.9326	0.0674	-48.2	0
0.5220	0.2324	0.9919	0.9989	0.9469	0.9591	0.0409	-44.4	5.7
0.6133	0.1880	0.9955	0.9998	0.9372	0.9715	0.0285	-38.8	3.5
0.7080	0.1420	0.9983	1.0000	0.9275	0.9812	0.0188	-31.0	-0.4
0.8034	0.0956	0.9998	0.9995	0.9195	0.9888	0.0112	-21.5	-8.0
0.8947	0.0513	1.0002	0.9991	0.9164	0.9946	0.0054	-11.3	-7.6
0.4833	0.3554	0.9958	0.9999	0.9365	0.9344	0.0656	-31.4	6.3
0.5995	0.2755	0.9982	1.0000	0.9277	0.9580	0.0420	-25.9	-0.4
0.6929	0.2113	0.9995	0.9996	0.9216	0.9717	0.0283	-20.5	-3.6
0.8018	0.1364	1.0002	0.9992	0.9169	0.9840	0.0160	-13.3	-6.9
0.8979	0.0703	1.0002	0.9992	0.9171	0.9926	0.0074	-6.6	-6.8

Table 10-9. Continued.....

x_1	x_2	γ_1	γ_2	γ_3	y_1	y_2	G^E (J mol ⁻¹)	r (pa)
0.1192	0.6096	0.9832	0.9953	0.9630	0.6715	0.3285	-37.5	-1.4
0.2076	0.5484	0.9869	0.9970	0.9570	0.7984	0.2016	-37.4	-4.8
0.3138	0.4750	0.9908	0.9986	0.9493	0.8737	0.1263	-36.1	-2.9
0.3922	0.4207	0.9933	0.9994	0.9433	0.9071	0.0929	-34.2	-0.8
0.4938	0.3504	0.9961	1.0000	0.9354	0.9366	0.0634	-30.6	-1.7
0.1097	0.1056	0.9362	0.9638	0.9972	0.9145	0.0855	-33.0	-10.2
0.2105	0.0937	0.9471	0.9720	0.9936	0.9586	0.0414	-46.1	7.4
0.3085	0.0821	0.9577	0.9796	0.9881	0.9749	0.0251	-55.3	5.2
0.4135	0.0696	0.9687	0.9870	0.9799	0.9840	0.0160	-60.9	-0.4
0.4986	0.0595	0.9771	0.9920	0.9712	0.9886	0.0114	-61.8	1.1
0.5955	0.0480	0.9857	0.9965	0.9590	0.9923	0.0077	-58.7	6.8
0.6996	0.0357	0.9933	0.9994	0.9434	0.9951	0.0049	-49.9	9.6
0.7945	0.0244	0.9980	1.0000	0.9287	0.9971	0.0029	-37.2	7.3
0.2111	0.7018	0.9960	0.9999	0.9357	0.7599	0.2401	-16.6	0.5
0.3489	0.5792	0.9979	1.0000	0.9290	0.8637	0.1363	-15.0	-2.8
0.4187	0.5171	0.9987	0.9999	0.9258	0.8949	0.1051	-13.8	1.5
0.5233	0.4241	0.9995	0.9996	0.9215	0.9284	0.0716	-11.7	0.9
0.6494	0.3119	1.0001	0.9993	0.9177	0.9563	0.0437	-8.7	-4.3
0.7224	0.2470	1.0002	0.9991	0.9165	0.9684	0.0316	-6.8	-8.7
0.8302	0.1511	1.0002	0.9992	0.9169	0.9829	0.0171	-4.0	-12.3

Table 10-10 Calculated Results of Ternary Plus Binary System
by Modified B-M Equation

x_1	x_2	γ_1	γ_2	γ_3	y_1	y_2	G^E (J mol ⁻¹)	r (pa)
0.1332	0.2760	0.9555	0.9780	0.9894	0.8331	0.1669	-45.8	-2.8
0.2214	0.2479	0.9633	0.9833	0.9844	0.9024	0.0976	-51.6	-6.9
0.3075	0.2206	0.9706	0.9881	0.9783	0.9353	0.0647	-55.1	-12.5
0.3931	0.1933	0.9775	0.9922	0.9708	0.9548	0.0452	-56.2	-7.1
0.4810	0.1652	0.9840	0.9956	0.9619	0.9680	0.0320	-55.0	-7.1
0.5023	0.1430	0.9844	0.9958	0.9614	0.9734	0.0266	-55.7	1.4
0.5911	0.1176	0.9903	0.9984	0.9508	0.9813	0.0187	-51.2	7.5
0.6904	0.0891	0.9955	0.9998	0.9377	0.9878	0.0122	-42.8	8.7
0.8008	0.0573	0.9991	0.9998	0.9241	0.9932	0.0068	-29.5	2.2
0.9006	0.0286	1.0002	0.9991	0.9171	0.9970	0.0030	-14.8	-12.3
0.1069	0.4448	0.9682	0.9866	0.9804	0.7141	0.2859	-45.5	-2.5
0.1988	0.3990	0.9744	0.9904	0.9745	0.8383	0.1618	-48.2	-1.7
0.3086	0.3444	0.9812	0.9942	0.9661	0.9032	0.0968	-49.1	0.3
0.3979	0.2999	0.9863	0.9967	0.9583	0.9326	0.0674	-48.0	1.8
0.5220	0.2324	0.9920	0.9990	0.9469	0.9591	0.0409	-44.2	7.4
0.6133	0.1880	0.9957	0.9998	0.9374	0.9715	0.0285	-38.6	4.9
0.7080	0.1420	0.9983	1.0000	0.9278	0.9812	0.0188	-30.8	0.5
0.8034	0.0956	0.9998	0.9995	0.9200	0.9888	0.0112	-21.3	-7.6
0.8947	0.0513	1.0002	0.9991	0.9171	0.9946	0.0054	-11.2	-7.6
0.4833	0.3554	0.9959	0.9999	0.9367	0.9344	0.0656	-31.2	7.3
0.5995	0.2755	0.9983	1.0000	0.9281	0.9580	0.0420	-25.7	0.3
0.6929	0.2113	0.9995	0.9997	0.9221	0.9717	0.0283	-20.3	-3.1
0.8018	0.1364	1.0002	0.9992	0.9176	0.9840	0.0160	-13.1	-6.8
0.8979	0.0703	1.0002	0.9993	0.9178	0.9926	0.0074	-6.5	-6.8

Table 10-10. Continued.....

x_1	x_2	γ_1	γ_2	γ_3	y_1	y_2	G^E (J mol ⁻¹)	r (pa)
0.1192	0.6096	0.9834	0.9954	0.9629	0.6715	0.3285	-37.4	-0.7
0.2076	0.5484	0.9871	0.9971	0.9569	0.7984	0.2016	-37.3	-3.9
0.3138	0.4750	0.9910	0.9986	0.9493	0.8737	0.1263	-35.9	-1.8
0.3922	0.4207	0.9935	0.9994	0.9434	0.9071	0.0929	-34.0	0.3
0.4938	0.3504	0.9962	0.9999	0.9356	0.9366	0.0634	-30.4	-0.7
0.1097	0.1056	0.9362	0.9636	0.9972	0.9145	0.0855	-33.1	10.1
0.2105	0.0937	0.9472	0.9720	0.9935	0.9586	0.0414	-46.2	7.9
0.3085	0.0821	0.9579	0.9797	0.9880	0.9749	0.0251	-55.3	6.4
0.4135	0.0696	0.9689	0.9870	0.9798	0.9840	0.0160	-60.8	1.7
0.4986	0.0595	0.9774	0.9921	0.9710	0.9886	0.0114	-61.7	3.7
0.5955	0.0480	0.9860	0.9966	0.9588	0.9923	0.0077	-58.4	9.4
0.6996	0.0357	0.9935	0.9994	0.9435	0.9951	0.0049	-49.6	11.7
0.7945	0.0244	0.9981	1.0000	0.9290	0.9971	0.0029	-36.9	8.4
0.2111	0.7018	0.9961	0.9999	0.9359	0.7599	0.2401	-16.5	1.0
0.3489	0.5792	0.9980	1.0000	0.9293	0.8637	0.1363	-14.8	-2.4
0.4187	0.5171	0.9987	0.9999	0.9261	0.8949	0.1051	-13.7	2.0
0.5233	0.4241	0.9995	0.9996	0.9220	0.9284	0.0716	-11.6	1.2
0.6494	0.3119	1.0001	0.9993	0.9183	0.9563	0.0437	-8.6	-4.1
0.7224	0.2470	1.0002	0.9991	0.9172	0.9684	0.0316	-6.7	-8.6
0.8302	0.1511	1.0002	0.9992	0.9176	0.9829	0.0171	-3.9	-12.3

Table 10-10 Continued

x_1	γ_1	γ_2	y_1	G^E (J mol ⁻¹)	r (pa)
n-hexane (1)+n-hexadecane (2)					
0.1080	0.9258	0.9992	1	-22.5	11.3
0.2076	0.9378	0.9968	1	-39.4	10.2
0.3061	0.9497	0.9924	1	-52.3	-1.9
0.3949	0.9604	0.9864	1	-60.1	-14.0
0.4984	0.9722	0.9767	1	-64.2	-15.7
0.4996	0.9723	0.9765	1	-64.2	5.0
0.6196	0.9846	0.9610	1	-61.3	4.6
0.7055	0.9919	0.9473	1	-53.8	3.8
0.8013	0.9975	0.9310	1	-40.1	0.7
0.8940	1.0000	0.9187	1	-22.2	-2.6
n-hexane (1) + n- octane (2)					
0.1255	0.9985	0.9999	0.6025	-0.6	-6.5
0.2221	0.9992	0.9998	0.7499	-0.1	2.7
0.3290	0.9996	0.9996	0.8379	-1.0	-4.4
0.4270	0.9999	0.9994	0.8870	-0.9	-10.0
0.5274	1.0001	0.9992	0.9215	-0.7	-12.5
0.4795	1.0001	0.9993	0.9065	-0.8	-14.3
0.5867	1.0002	0.9992	0.9372	-0.6	-13.5
0.6979	1.0002	0.9991	0.9604	-0.3	-5.1
0.8055	1.0001	0.9994	0.9774	0	-2.1
0.8960	1.0001	0.9999	0.9890	0.1	- 8.7

Table 10-10. Continued

x_1	γ_1	γ_2	y_1	G^E (J mol ⁻¹)	r (pa)
n-octane (1) + n- hexadecane (2)					
0.1050	0.9531	0.9995	1	-13.6	1.8
0.2016	0.9605	0.9981	1	-23.9	-2.5
0.3169	0.9691	0.9950	1	-33.2	-3.4
0.3937	0.9746	0.9919	1	-37.4	-2.2
0.4895	0.9811	0.9867	1	-40.1	-2.6
0.5949	0.9875	0.9791	1	-39.8	-1.8
0.5024	0.9819	0.9859	1	-40.3	-1.1
0.6979	0.9928	0.9695	1	-35.7	-1.3
0.7963	0.9967	0.9584	1	-28.0	-6.4
0.8971	0.9992	0.9453	1	-16.2	-2.7
0.1186	0.9542	0.9994	1	-15.2	3.2
0.2868	0.9669	0.9960	1	-31.1	-2.1
0.3180	0.9692	0.9949	1	-33.2	-1.4
0.4857	0.9808	0.9869	1	-40.1	2.2
0.4980	0.9816	0.9862	1	-40.2	-1.5
0.6873	0.9923	0.9706	1	-36.3	-1.7
0.6921	0.9925	0.9701	1	-36.0	-2.5

equation is preferable to represent P-x data for this system may be drawn because our measurement is not accurate enough to do so. The standard deviation for this case is 6.7 Pa, slightly higher than that from the R-K equation, but very close to the value obtained from regression of ternary data only and $R_1^2/R_2^2 = 6.7^2/6.3^2 = 1.13$. The F-test was applied once more to compare the adequacies of the modified B-M equation and R-K equation for the ternary plus binary systems.

$F_{1-\alpha/2}(78,41) = 0.63$, and $F_{\alpha/2} = 1.6$ at $\alpha=0.10$, and $R_1^2/R_2^2 = 6.7^2/6.3^2 = 1.13$ therefore

$$F_{\alpha/2}(78,41) > R_1^2/R_2^2 > F_{1-\alpha/2}(78,41) \quad \text{.....} \quad (10-6.8)$$

It means that there is no significant difference (at the significant level $\alpha=0.10$) of the adequacies could be detected between the modified B-M and the R-K equations for the ternary plus binary systems.

In considering the fact that only three parameters are used in the modified equation while 12 parameters are required altogether in the R-K equation, the former equation is more powerful and preferable as compared with the latter. This is regarded as a good evidence of the validity of the principle of congruence for n-alkane systems.

Comparing the results of the original and the modified B-M equations (both obey the principle of congruence), one may find that an analytical formula obeying the principle of congruence for expressing the relation between the excess properties and the average carbon number is not always adequate to express experimental data, therefore a failure of such an equation in representation of experimental results does not mean the principle of congruence is not obeyed. In this respect, the graphical test seems more direct and less restrictive as compared with the analytical test.

10-7 THE SIGNIFICANCE OF g_0

As it has been described in last chapter, the lattice model assumes that the motion of molecules reduces merely to oscillation about the equilibrium position and the configurational entropy is obtained by counting the number of combinations of the segments of chain molecules at lattice points. As pointed out by Prigogine (1957), this assumption is rather questionable. This

over-estimation of order in the liquid by the lattice model was compensated by allowing the molecules to move in a "cell field" in the cell theory. Therefore, the configurational entropy is the sum of the contributions of combinations and "free volume". Moreover, according to Patterson's theory, there exists the molecular orientation correlation in n-alkane liquids, therefore the occupation of a lattice by a segment is not random for which some correction needs to be made.

We define g_0 as follows: $g_0 N$ molecules in N molecules are extremely ordered as described by lattice model and the rest $(1-g_0)N$ are regarded as mass points without shapes and dimensions. g_0 is a function of temperature and pressure as well. With r segments for each molecule, the $g_0 N$ molecules then have $g_0 N r$ segments altogether. therefore the total degree of order of the system is increased with r , even though g_0 is independent of r . The total configurational entropy may be derived by Flory's method (1942), with $g_0 N$ instead of N . With the assumption that g_0 is constant at given temperature and pressure for all n-alkane liquids, the configurational excess entropy on mixing of binary solutions now is given as

$$\begin{aligned} S^E/R &= -g_0 x_1 \ln[N_1 r_1 g_0 / (N_1 r_1 g_0 + N_2 r_2 g_0) x_1] - g_0 x_2 \ln[N_2 r_2 g_0 / (N_1 r_1 g_0 + N_2 r_2 g_0) x_2] \\ &= -g_0 x_1 \ln[r_1 / (r_1 x_1 + r_2 x_2)] - g_0 x_2 \ln[r_2 / (x_1 r_1 + x_2 r_2)] \\ &= -g_0 x_1 \ln[r_1 / r^m] - g_0 x_2 \ln[r_2 / r^m] \quad \dots\dots\dots (10-7.1) \end{aligned}$$

where, $r^m = x_1 r_1 + x_2 r_2$. Equation (10-7.1), obviously, leads to $g_0 \ln n$ in equation (10-6.3) to (10-6.6). According to the above discussion the configurational entropy expressed by eq. (10-7.1) should be equivalent to the sum of contributions of combinations (com) and free volumes (fv) in the Flory theory. With $g_0 = 0.27 \pm 0.034$ (optimized from P-x experimental data in this work), the configurational S^E are calculated and compared with the values calculated by Barbe and Patterson (1980) in table 10-11. Taking account of the errors both in Barbe's calculations and our own optimization of parameters, the results are fairly close to each other.

Table 10-11 Comparison of equimolar TS^E (Configuration) for n-alkane
Mixtures at 298.15 K (J mol⁻¹)

System	This Work	Barbe and Patterson		
		(com)	(fv)	Sum
n-hexadecane				
+ n-hexane	77±8.6	232	-166	65
+ n-heptane	56±6.3	168	-101	67
+n-octane	40±4.5	118	-63	55

10-8 GRAPHICAL TEST OF THE PRINCIPLE OF CONGRUENCE FOR H^E, V^E OF PSEUDO n-ALKANES + BRANCHED HEXANES

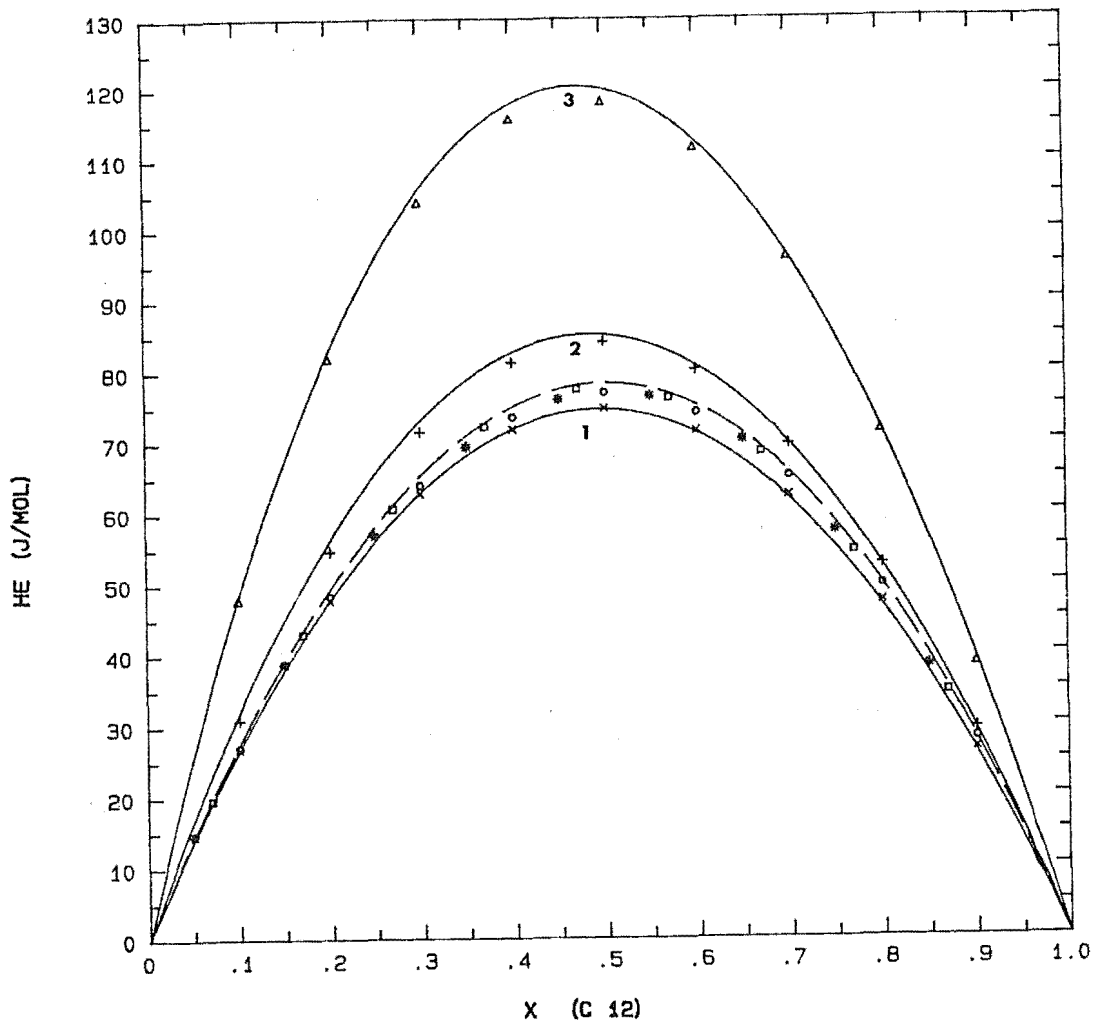
The graphical test of the principle of congruence has been applied to multiple component n-alkanes (Looi et al., 1974; Lim and Williamson, 1980). In these tests, a pseudo n-alkane was made by mixing two n-alkanes at first, then the excess enthalpies and volumes of mixing the pseudo n-alkane with another n-alkane were measured. The results were compared with those for a congruent binary mixture. Excellent agreements, usually with the difference of about 2 % were obtained in the previous work.

In order to extend this study to the ternary mixtures obtained by mixing a pseudo n-alkane with hexane isomers, we have measured the excess molar enthalpies of pseudo n-dodecane (10:14), [0.500 n-decane + 0.500 n-tetradecane] + 2-methylpentane, + 3-methylpentane, 2,3-dimethylpentane, 2,2-dimethylbutane, and of pseudo n-dodecane (11:13), ~~pseudo n-dodecane (8:16)~~ + 2-MP (see chapter 8); and the excess volumes of pseudo n-dodecane (10:14), [0.500 n-decane + 0.500 n-tetradecane] + the four hexane isomers (see chapter 7). The excess enthalpies and volumes of n-dodecane + hexane isomers have been reported by Hamam et al. (1984a). As has been discussed in section 8-4, and 7-6, the differences between our measurements and Hamam et al.'s are about 0.5 J mol⁻¹ for H^E and 5×10^{-3} cm³ mol⁻¹ for V^E .

Although Hamam et al.'s measurements are significantly smoother than ours, we believe that the agreements justify direct comparisons of our measurements with the corresponding binary data from Hamam et al.'s within ± 0.5 J mol⁻¹ for H^E , and $\pm 5 \times 10^{-3}$ cm³ mol⁻¹ for V^E . These comparisons are shown in figure 10-15 for H^E , and figure 10-16, and table 7-10 for V^E . The curves are from values calculated by equation (8-4.1) and equation (7-1.3) with the parameters optimized from this work for n-dodecane + 2-MP (dotted curve), and from Hamam et al for n-dodecane + the other three hexane isomers (solid curves). The points are the experimental values for the ternary mixtures.

The excess molar enthalpies of the ternary mixtures in this study are slightly lower than those of the congruent binary mixtures. The differences of about 2 % are similar to these observed results for the ternary n-alkane mixtures (Looi et al., 1974).

FIG. 10-15 EXCESS ENTHALPIES FOR n-DODECANE AND HEXANE ISOMERS



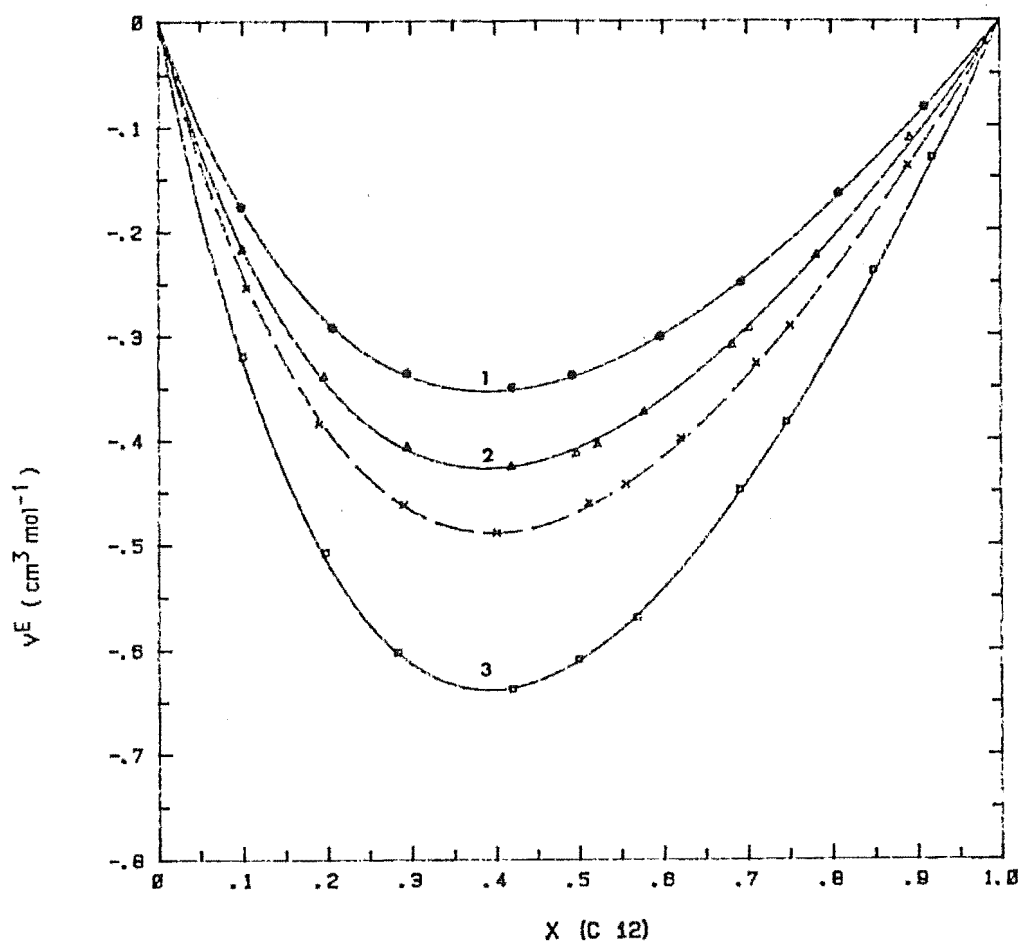
dotted curve: Equation (8-4.1) with parameters from table 8-3, system 2 for n-dodecane + 2-MP

solid curves: Equation (8-4.1) with parameters from table 8-3, for (1) n-dodecane + 3-MP (system 6), (2) n-dodecane + 2,3-DMB, (system 8), (3) n-dodecane + 2,2-DMB (system 10)

Experimental Results:

- o Pseudo n-dodecane (10:14) + 2-MP
- x Pseudo n-dodecane (10:14) + 3-MP
- + Pseudo n-dodecane (10:14) + 2,3-DMB
- Δ Pseudo n-dodecane (10:14) + 2,2-DMB
- \square Pseudo n-dodecane (8:16) + 2-MP
- * Pseudo n-dodecane (11:13) + 2-MP

FIG. 10-16 EXCESS VOLUMES FOR n-DODECANE AND HEXANE ISOMERS



dotted curve: Equation (7-1.3) with parameters from table 7-9, system 2 for n-dodecane + 2-MP

solid curve: Equation (7-1.3) with parameters from table 7-9, for (1) n-dodecane + 3-MP (system 4), (2) n-dodecane + 2,3-DMB (system 6), (3) n-dodecane + 2,2-DMB (system 8)

Experimental Results

- x Pseudo n-dodecane (10:14) +2-MP
- * Pseudo n-dodecane (10:14) +3-MP
- Δ Pseudo n-dodecane (10:14) +2,3-DMB
- pseudo n-dodecane (10:14) + 2,2-DMB

The excess volumes of the ternary mixtures investigated in this study obey the principle of congruence better than excess enthalpies. The differences of less than 1 % seem to be random.

Some suggestions are outlined as follows.

1. As described in chapter 10, the expression for the relation between G^E and composition for ternary mixtures n-hexane + n-octane + n-hexadecane obtained from this work may be used to calculate G^E of mixtures of various pseudo alkanes with n-hexane or n-octane, or n-hexadecane. An external test of the principle of congruence may be made by comparing the excess Gibbs functions of mixtures between a pseudo alkane and its congruent pure n-alkane with a common component. An internal test of the principle with the properties of mixtures for a ternary system also may be made by graphical methods and the modified B-M equation developed in chapter 10.

The external test with the ternary data obtained in this work may be extended to the range of carbon number from 6 to 16 as long as there are sufficient binary data available. Therefore we need to measure G^E of n-hexane + n-alkane (n-C 7, n-C 9, n-C 13, n-C 14, n-C 15) and of n-octane + n-alkane (from n-C 9 to n-C 15). Measurements of G^E of new ternary mixtures also are interesting because they may be used for internal tests in a new range of carbon number with the methods developed in chapter 10, and for a wider external test by comparing the ternary with ternary mixtures, and ternary with binary mixtures.

2. The apparatus and the experimental techniques need to be modified so that they may be used for accurate measurements of vapour pressures at various mole fractions for ternary mixtures containing two involatile components. This would not only extend the test of the principle of congruence to a wide range of carbon number but also test the principle through the directly measured quantity, vapour pressure, instead of derived quantities such as G^E , γ_i which are, more or less, dependent on the methods of data reduction.

3. As reviewed in chapter 5, G^E , γ_i for a mixture obtained from p-x data by Barker's method are dependent of the equation used to express the relation between G^E and mole fractions in the liquid phase. It is interesting to compare

the tests of the principle with the results from the different equations.

The direct method and the Mixon-Gumowski-Garpenter method are more rigorous than Barker's method and more suitable for obtaining G^E for graphical tests. Comparing the results from different data reduction methods could give us some enlightenment about deviations of the principle of congruence from the experimental data.

4. The vapour-liquid equilibrium of mixtures of a branched alkane or other compound with a pseudo n-alkane and its congruent pure n-alkane should be measured so that the external tests used for H^E and V^E for n-alkane + branched hexanes in this work may be applied to G^E and γ_i . These investigations might be more easily made by measurements of the activity coefficients of a volatile component at infinite dilution in pure n-alkane solvent and its congruent pseudo mixed n-alkane solvent with gas chromatography.

5. The methods for internal test of the principle of congruence developed in chapter 10 also may be used for H^E and V^E of ternary mixtures. Therefore it would be interesting to measure H^E and V^E of ternary n-alkane mixtures over the whole range of compositions.

6. Further comparisons of H^E and V^E of mixtures of pseudo n-alkane and its congruent pure n-alkane with one of various compounds such as branched n-alkanes, cyclohexane, alcohols would be interesting and require a series measurements of H^E and V^E of corresponding binary and ternary mixtures.

7. Hamam et al. (1984a) found that $\Delta H^E(0.5)$ defined as the difference between $H^E(0.5)$ for an equimolar mixture of an n-alkane with a hexane isomer, and $H^E(0.5)$ for an equimolar mixture of the same n-alkane with n-hexane, varied nearly linearly with the acentric factors of the n-alkanes. They pointed out that the plots of $\Delta H^E(0.5)$ against the acentric factors of n-alkanes could be used to interpolate values of $H^E(0.5)$ for binary mixtures of other n-alkanes with the hexane isomers. It would be interesting to examine the relation between ΔH^E

and ΔV^E and carbon number instead of the acentric factors in the whole range of mole fraction because it may facilitate the external test of the principle of congruence and the discussions and explanations of the principle of congruence or of the deviations of the principle from the real values of properties of mixing.

8. Flory's theory has been extensively used in interpretation of the experimental results of binary H^E , V^E , but less attentions have been made for G^E of binary mixtures. Flory's theory could be applied to our measurements of G^E for the binary n-alkane mixtures. It would be also interesting to apply the cell-hole and perturbation theories of the liquid state to our experimental results for binary and ternary mixtures and in the discussion of the principle of congruence.

REFERENCES

- Abbott, M. M. et al., 1975. AICHE. J., 21: 73.
- Abbott, M. M. and Van Ness, H. C. , 1977. Fluid Phases Equilibria, 1: 3.
- Abbott, M.M., 1986. Fluid Phase Equilibria, 29: 193.
- Adams, W. A. et al., 1974. Can. J. Chem. Eng., 52: 121.
- Ahmed, A. et al., 1977. J. Chem. Thermodyn., 9: 1087.
- Aim, K., 1978. Fluid Phase Equilibria., 2 : 119.
- Alders, L., 1959. Liquid-Liquid Extraction, 2nd edn. Elsevier, Amsterdam.
- Anderson, T. F. et al., 1978. AIChE. J., 24: 20.
- Anderssen, R. S. and Osborne, M. R., 1969." Least Squares Methods In Data Analysis", University Of Queensland Press.
- API Project 44, 1953. "Selected Values of Physical and Thermodynamic Properties of Hadrocarbons and Related Compounds", Carnegie Press.
- Ashworth, A. J. and Everett, D. H., 1960. Trans. Faraday Soc., 56: 1609.
- Awwad, A. M. and Allos, E. I., 1985. Fluid Phase Equilibria. 22: 353.
- Barbe, M. and Patterson, D., 1980. J. Solution Chem., 9: 753.
- Barker, J. A., 1953. Australian J. Chem., 6: 207.
- Barker, J. A., 1963. " Lattice Theories of the Liquid State", Pergamon.
- Battino, R. et al., 1971. An Chem., 43: 806.
- Battino, R., 1971. Chem. Rev., 71: 5.
- Bauer, N. and Lewin, S., 1971. "Physical Methods of Chemistry", Vol. I, Part 4, Chap. 2, Interscience, New York.
- Beath, L. A. et al., 1969. J. Chem. Thermodyn., 1: 293.
- Bell, T. N. et al., 1968. J. Phys. Chem., 72 (13) : 4693.
- Bellemans, A. and Mat, P., 1963. Mol. Phys., 6: 637.
- Bhattacharyya, S. N. and Patterson, D., 1980. J. Solution Chem., 9: 247.

- Bhattacharyya, S. N. et al., 1985. *Fluid Phases Equilibria*, 20: 27.
- Booth, C., 1975. *Polym. Handb.*, 4: 323.
- Bottomley, G. A. and Scott, R. L., 1974. *J. Chem. Thermodyn.*, 6: 973.
- Brennan, J. S. et al., 1978. *J. Chem. Thermodyn.*, 10: 169.
- Bronsted, J. N. and Koefoed, J., 1946. *Kgl. Dan. Vidensk. Selsk., Mat. Fys. Medd.*, 22(17): 1.
- Brown, I. and Lane, J. E., 1976. *Pure and Applied Chemistry*, 45 (1) : 7.
- Chai, Z. K., 1987. *Chinese Science, B*, 8: 809.
- Chareyron, R. and Clechet, P., 1971. *Bull. Soc. Chim. Fr.*, 2853.
- Conder, J. R., 1968. *Adv. Analyt. Chem. Instrumen.*, "Progress In Gas Chromatography", 6:209.
- Conder, J. R. and Purnell, J. H., 1969. *Trans. Faraday Soc.*, 65: 824; 839.
- Conder, J. R. and Young, C. L., 1979. "Physicochemical Measurement By Gas Chromatography", John Wiley & Sons.
- Cruickshank, M. L. et al., 1966. *Proc. Roy. Soc.*, A295, 271.
- Desmyter, A. and Van der Waals, J. H., 1958. *Rec. Trav. Chim.*, 77: 53.
- Dickinson, E. et al., 1975. *J Chem. Thermodyn.*, 7: 731.
- Dieisi, D. P. et al., 1978. *J. Chem. Eng. Data*. 23 : 242.
- Dixon, B. T. and McGlashan, M. L., 1965. *Nature, London*, 206: 710.
- Dohnal, V. and Fenclova, D., 1985. *Fluid. Phase Equilibria*, 19: 1.
- Dohanal, V. and Fenclova, D., 1985. *Fluid Phase Equilibria*, 21: 211.
- Dymond, J. H., 1986, *Fluid Phase Equilibria*, 27:1.
- Edgington, E. S., 1961. *J. Am. Stat. Assoc.*, 56: 156.
- Eichinger, B. E. and Flory, P. J., 1968. *Trans. Faraday Soc.* 64: 2035.
- Eubank, P. T. et al., 1980. 2nd Int. Conf. on Phase Equilibria and Fluid Properties in Chemical Industry, DECHEMA, Frankfurt, Part 2, pp. 675.
- Ewing, M. B., et al., 1970. *J. Chem. Thermodyn.* 2: 751.

- Fabries, J. F. and Renon, H., 1975. *AICHE. J.*, 21: 735.
- Fenby, D. V. et al., 1980. *Aust. J. Chem.*, 33: 1927.
- Fisher, R. A., 1922. *Phil. Trans. Royal Soc., London, A* 222: 309.
- Flory, P. J., 1942. *J. Chem. Phys.*, 10: 51.
- Flory, P. J. et al., 1964. *J. Am. Chem. Soc.*, 86: 3507; 3515.
- Flory, P. J., 1965. *J. Am. Chem. Soc.*, 87: 1833.
- Frabnluka, I. and Holub, R., 1983. *Collect Crzech Chem. Commun.*, 48: 199.
- Francois, J. et al., 1971. *C. R. Acad. Sci. Paris, Ser. C*, 273: 1577.
- Franks, F. and Smith, H. T., 1967. *Trns. Faraday Soc.*, 63: 2586.
- Garcia, M. et al., 1984. *J. Chem. Thermodyn.*, 16: 603.
- Gautreaux, M. F. and Coates, J., 1955. *AICHE. J.*, 1: 496.
- Geffcken, W. et al., 1937. *Z. Phys. Chem., Abt. B* 35: 317.
- Gibbs, R. E. and Van Ness, H. C., 1972. *Ind. Eng. Chem. Fundam.*, 11: 410.
- Gibulka, I. and Holub, R., 1978. *Chem. Listy*, 72: 457.
- Gierycz, P. et al, 1985. *Fluid Phase Equilibria*, 22: 107.
- Goates, J. R. et al., 1977. *J. Chem. Thermodyn.*, 9: 249.
- Goates, J. R. et al., 1979. *J. Chem. Thermodyn.*, 11: 497.
- Goates, J. R. et al., 1981. *J. Chem. Thermodyn.*, 13: 907.
- GoMez-Ibanez, J. D. and Wang, F. T.; 1971. *J. Chem. Thermodyn.* 3: 811.
- Goral, M. and Janaszewski, B., 1977. *Z. Phy. Chemie., Leipzig*, 258: 417.
- Goral, M., 1977. *Z. Phy. Chemie., Leipzig*, 258: 1040.
- Goral, M. et al., 1985. *Fluid Phase Equilibria*, 23: 89.
- Green, J. R. and Margerison, D., 1978. " Statistical Treatment of Experimental Data", Elsevier, Amsterdam
- Grolier, J.-P. E. et al., 1974. *J. Chem. thermodyn.*, 6: 895.
- Guggenheim, E. A., 1948. *Trans. Faraday Soc.* 44: 1007.

- Guggenheim, E. A., 1952. "Mixtures", Oxford, London.
- Hala, H. et al., 1967. "Vapour-Liquid Equilibrium", Pergamon, Oxford.
- Hales, J. L., 1970. J. Phys. E. Sci. Instrum. 3: 855.
- Hamam, S. E. M. et al., 1977. Ind. Eng. Chem. Process. Des. Develop., 16: 51.
- Hamam, S. E. M. et al., 1984a. J Chem. Thermodyn., 16: 537.
- Hamam, S. E. M., 1984b. Fluid Phase Equilibria. 18: 147.
- Hamam, S. E. M., and Benson G. C., 1986. J. Chem., 33: 1927.
- Handa, Y. P. et al., 1977. J. Chem. Eng. Data. 22: 218.
- Handa, Y. P. and Benson, G. C., 1979. Fluid Phase Equilibria, 3: 185.
- Harris, K. R. and Dunlop, P. J., 1967. J. Phys. Chem., 71: 483.
- Heintz, A. and Lichtenthaler, R. N., 1979. Ber. Bunsenges. Phys. Chem. 83: 853.
- Heintz, A. and Lichtenthaler, R. N., 1980. Ber. Bunsenges. Phys. Chem., 84: 890.
- Heintz, A. and Lichtenthaler, R. N., 1982. Angew. Chem. Int. Ed. Engl., 21: 184.
- Hijmans, J., 1958. Mol. Phys., 1: 307.
- Hijmans, J., 1961. Physica, 27: 433.
- Holleman, Th. and Hijmans, J., 1962, Physica, 28: 604.
- Holleman, Th. 1963. Physica, 29: 585.
- Holleman, Th., and Hijmans, J., 1965, Physica, 31: 64.
- Hutchings, R. S. and Van Hook, W. A., 1985. Fluid Phase Equilibria., 21: 165.
- Janssens, J.-M. and Ruel, M., 1972. Can. J. Chem. Eng., 50: 591.
- Kemeny, S. et al., 1982. AIChE. J., 28: 20.
- Kerker, M. 1969. "The Scattering of light", Academic Press, Chap. 9, pp. 487.
- Kershaw, R. W. and Malcolm, G. N., 1968. Tras. Faraday Soc., 64: 323.
- Kimura, F. et al., 1983a. Fluid Phase Equilibria, 11: 245.
- Kimura, F. and Benson, G. C., 1983b. J. Chem. Eng. Data. 28: 387.
- Kiyohara, O. and Benson G. C., 1973. Can. J. Chem., 51: 2489.

- Klaus, R. L. and Van Ness, H. C., 1967. *AICHE. J.*, 13: 1132.
- Koh, S. P. and Williamson, A.G., 1980. *Chem. Eng. J.*, 19: 85.
- Kolasinskan, G. and Oracz, P., 1979. *Z. Phy. Chemie., Leipzig*, 260: 169.
- Kratky, O. et al., 1969. *Z. Angew Phys.*, 27: 273.
- Kumaran, M. K. and McGlashan, M. L., 1977. *J. Chem. Thermodyn.*, 9: 259.
- Kumaran, M. K. and Benson, G. C., 1984. *J. Chem. Thermodyn.*, 16: 183.
- Lacombe, R. H. and Sanchez, I. C., 1976. *J. Phys. Chem.*, 80: 2568.
- Lacmann, R. and Synowietz, C., "Densities Of Liquid Systems", *Landolt-Bornstein New Series*, Vol. IV/1a, Springer-Verlag, Berlin, pp.714.
- Lam, V. T. et al., 1974. *J. Chem. Soc., Faraday Trans. 2*, 70: 1465.
- Lane, C. F. and Kramer, G. W., 1977. *Aldrichimica Acta*, 10: 11.
- Laugier, S. and Richon, D., 1986. *Rev. Sci. Instrum.*, 57: 469.
- Letcher, T. M., 1975. *Chemsa*, 1: 226.
- Letcher, T. M., 1978. "Chemical Thermodynamics (special periodical report)", Vol. 2, Chap. 2. The Chemical Society, London, pp46.
- Li, T. P., 1981. "Mathematic Treatment of Experimental Data", Science, Beijing.
- Lim, C. B. and Williamson A. G., 1980. *J. Chem. Thermodyn.*, 12: 65.
- Linnik, J. W., 1961. "Die Methode Der Kleinsten Quadrte In Moderner Darstellung", VEB Dentsche Verlag Der Wissenchaften, Berlin.
- Ljunglin, J. J. and Van Ness, H. C., 1962. *Chem. Eng. Sci.*, 17: 531.
- Loeche, J. R. et al., 1983. *J. Chem. Eng. Data*, 28 : 405.
- Longuet-Higgins, H. C., 1953. *Discuss, Faraday Soc.*, 15: 73.
- Looi, C. K. et al., 1974. *J. Chem. Thermodyn.*, 6: 1171.
- Maher, P. J. and Smith, B. D., 1979. *J. Chem. Eng. Data*, 24: 16.
- Malanowski, S., 1982a. *Fluid Phase Equilibria*, 8: 197.
- Malanowski, S., 1982b. *Fluid Phase Equilibria*, 9: 311.
- Margules, H., 1895. *Sitzungber, Wien Akad.*, 104: 1243.

- Marsh, K. N., 1968. *Trans. Faraday Soc.*, 64: 883.
- Marsh, K. N., 1977. *J. Chem. Thermodyn.*, 9: 719.
- Marsh, K. N. 1978. "Chemical Thermodynamics (special periodical report)", Vol. 2, Chap. 1. The Chemical Society, London, pp1.
- Marsh, K. N. et al., 1980a. *J. Chem. Thermodyn.*, 12: 343.
- Marsh, K. N. et al., 1980b. *J. Chem. Thermodyn.*, 12: 897.
- Martin, M. L. and Murray, R. S., 1972. *J. Chem. Thermodyn.*, 4: 723.
- Mcbain, J. W., and Bakr, A. M., 1926. *J. Am. Chem. Soc.*, 48: 690.
- Mcdermott, C. and Ellis, S. R. M., 1965. *Chem. Eng. Sci.*, 20: 545.
- McGlashan, M. L. , and Williamson, A. G., 1961. *Trans. Faraday Soc.*, 57: 588.
- McGlashan, M. L. and Potter, D. J. B., 1962. *Proc. Roy. Soc. A*, 267: 478.
- McGlashan, M. L., 1978. "Chemical Thermodynamics (special periodical report)", Vol. 2, Chap. 1. The Chemical Society, London.
- Meixner, O. and Lichtenthaler, R. N., 1979. *Ber. Bunsenges. Phys. Chem.* 83: 567.
- Mentzer, et al., 1982. *J. Chem. Thermodynamics*, 14 : 817.
- Mixon, F. O., Gumowski, B. and Carpenter, B. H., 1965. *Ind. Eng. Chem. Fundam.*, 4: 455.
- Millero, F. J., 1967. *Rev. Sci. Instrum.*, 38: 1441.
- Munjal, S. et al., 1983. *Fluid Phase Equilibria*, 12: 29.
- Munster, A., 1969. "Statistical Thermodynamics", Springer-Verlag Academic Press.
- Myers, D. and Scott R. L., 1963. *Ind. Eng. Chem.*, 55: 43.
- Myers, R. S. and Clever, H. L., 1970. *J. Chem. Thermodynamics*, 2: 53.
- Nagata, I. and Ohta, T., 1974. *Ind. Eng. Chem. Des. Develop.*, 13: 304.
- Nagahama, K. et al., 1971. *J. Chem. Eng. Japan*, 4: 1.
- Nicholas, J. V. and White, D. R., 1982. "Traceable Temperature", P.D. Hasselbarg, Wellington, 83pp.
- Nissema, A., 1970. *Ann. Acad. Sci. Fenn. Ser. A2*, 153: 16.

- Nitta, T. and Katayama, T., 1973. J. Chem. Eng. Japan., 6: 224.
- Olson, J. D., 1983. Fluid Phase Equilibria, 14: 383.
- Orwoll, R. A. and Flory, P. J., 1967. J. Am. Chem. Soc. 89(26): 6822.
- Ott, J. B. et al., 1980. Aust. J. Chem., 33: 1921.
- Ott, J. B. et al., 1981. J. Chem Thermody., 13: 371.
- Owen, D. B., 1962. "Handbook Of Statistical Tables", Addison-Wesley.
- Patterson, D., 1979. Appl. Chem., 47: 305.
- Pena, M. D. and Fernandez-Martin, F., 1964. An. R. Soc. Esp. Fis. Quim. Ser. B., 60: 9.
- Peng, D. Y. and Robinson, D. B., 1976. Ind. Eng. Chem. Fundam., 15: 59.
- Peneloux, A. et al., 1975. J. Chim. Phys., 72: 1107.
- Pflug, H. D. and Benson, G. C., 1968. can. J. Chem. , 46: 287.
- Picker, P. et. al., 1974. J. Solution Chem., 3: 377.
- Plank, C. A. et al., 1981. Fluid Phase Equilibria, 6: 39.
- Pope, A. E. et al., 1967. Can. J. Chem., 45: 2665.
- Powell, R. J., and Swinton, F. L., 1968. J. Chem. Eng. Data, 13: 260.
- Prigogine, I. 1957. "The Molecular Theory of Solutions", North Holland Publishing Company, Amsterdam.
- Rao, D. N. and Naidu, P. R., 1981. J. Chem. Thermodyn., 13: 691.
- Redlich, O. and Kister, A. T., 1948. Ind. Eng. Chem., 40: 345.
- Redojkovic, N. et al., 1976. J. Chem. Thermodyn., 8: 1111.
- Riddick, J. A. and Bunger, W. B., 1970. "Techniques of Chemistry, Vol 2, Organic Solvents". 3rd ed. Edited by Arnold Weissberger. Wiley-Interscience, New York.
- Rogalski, M. and Malanowski, S., 1980. Fluid Phase Equilibria, 5: 97.
- Rogers, B. L. and Prausnitz, J. M., 1970. Ind. Eng. Chem. Fundam., 9: 174.
- Ronc, M. and Ratcliff, G. R., 1976. Can. J. Chem. Eng., 54 : 326.
- Sanni, S. A. et al., 1971. J. Chem. Eng. Data, 16: 424.

- Schneider, G. M., 1975. "Experimental Thermodynamics", Vol. 2. Butterworths, London, Chap. 16, (Part 2), pp. 787.
- Scott, R. L., and Fenby, D. V., 1969. *Ann Rev. Phys. Chem.*, 20: 111.
- Shen, W. G., 1981. Master Thesis, Lanzhou University.
- Shen, W. G. et al., 1983. *J. Chem. Ind. Eng. (China)*, (1): 45.
- Singh, J. and Benson, G. C., 1968. *Can. J. Chem.*, 46 : 1249.
- Smith, B. D. et al., 1982. *J. Phys. Chem. Ref. Data*, 11: 1151.
- Smith, V. C. and Robinson, R. L., 1970. *J. Chem. Eng. Data*, 15: 391.
- Sorensen, J. M. et al., 1979a. *Fluid Phase Equilibria*. 2: 297.
- Sorensen, J. M. et al., 1979b. *Fluid Phase Equilibria*. 3: 47.
- Stabinger, H. et al., 1967. *Monatsh. Chem.*, 98: 436.
- Stokes, R. H. et al., 1969. *J. Chem. Thermodyn.*, 1: 211.
- Stokes, R. H. et al., 1970. *J. Chem. Thermodyn.*, 2: 43.
- Stokes, R. H. and K. N. Marsh, 1972. *Ann. Rev. Phys. Chem.*, 23: 65.
- Stokes, R. H., 1974. *J. Solution Chem.*, 3: 673.
- Stookey, D. J. et al., 1973. *J. Chem. Thermodyn.*, 5: 741.
- Suri, S. K. and Ramakrishna, V., 1969. *India J. Chem.*, 7: 490.
- Swinton, F. L., 1976. *Ann. Rev. Phys. Chem.*, 27: 153.
- Tamir, A. et al., 1981. *Fluid Phase Equilibria*. 6: 237.
- Takenaka, M. et al., 1980. *J. Chem. Thermodyn.*, 12: 849.
- Tanaka, R. et al., 1975. *Can. J. Chem.*, 53: 2262.
- Tao, L. C., 1961. *Ind. Eng. Chem.*, 53: 307.
- Tomlins, R. P. and K. N. Marsh, 1976. *J. Chem. Thermodyn.*, 8: 1185.
- TRC Thermodynamic Tables. 1985. Thermodynamics Research centre, The Texas A & M University, System College Station.
- Van Hook, W. A., 1985. *Fluid Phase Equilibria*, 22: 55.

Van Laar, J. J., 1913. Z. Physik. Chem., 72: 723.

Van Ness, H. C., 1964. "Classical Thermodynamics of Non- Electrolyte Solution", Pergamon Press.

Van Ness, H. C. and Abbott, M. M., 1978. Ind. Eng. Chem. Fundam. 17: 66.

Varma, K. T. R. et al., 1976. J. Chem. Thermodyn., 8: 657.

Watson, I. D. et al., 1968. Trans. Faraday Sco., 64: 1763.

Weast, 1975. " Handbook of Chemistry and Physics", 56th edition, CRC.

Weeks, I. A. and Benson, G. C., 1973. J. Chem. Thermodyn., 5: 107.

Weclawski, J. and Bylicki, A, 1983. Fluid Phase Equilibria, 12 : 143.

Wieczorek, S. A. and Zywocinski, A., 1983. J. Chem. Thermodyn., 15: 327.

Williamson, A. G., 1957. Ph.D Thesis, Reading University.

Williamson, A. G., 1975. "Experimental Thermodynamics", Butterworths, London, Vol. 2, Chap. 16(Part 1), pp. 749.

Wilson, G. M., 1964. J. Am. Chem. Soc., 86: 127.

Wohl, K., 1953. Chem. Eng. Progr., 49: 218.

Young, C. L., 1968. Chromatog. Rev., 10: 129.

Young, C. L., 1978. Chemical Thermodynamics. Vol. 2, The Chemical Society, London, Chap. 3, pp. 71.

Zheng, G. K. et al., 1984. J. Chem. Thermodyn., 16: 943.

APPENDIX 1

The heat capacity at constant pressure, C_p , can be estimated by

$$C_p = (E + Q) / (dT/dt)$$

Where, E and Q are the power supplied by heating elements and the power lost from the air bath to the ambient, respectively. At the temperature of the bath which is 14 K higher than that of ambient, E= 100 watts, Q= -32 watts, dT/dt = the slope of the tangent of curve at $t=0$ in the figure 3-6.

APPENDIX 2

The Redlich-Kister equation for a ternary system is

$$G^E / RT = Q^{12} + Q^{13} + Q^{23} + Q^{123} \quad \text{..... (A2-1)}$$

The binary terms, Q^{ij} , may be expressed as

$$Q^{ij} = x_i x_j (x_i + x_j) \sum_{L=0}^m A_L (1 - 2x_i^*)^L \quad \text{..... (A2-2)}$$

where, $x_i^* = x_i / (x_i + x_j)$. The ternary term is

$$Q^{123} = x_1 x_2 x_3 [c_0 + c_1 (3x_1 - 1) + c_2 (3x_2 - 1)] \quad \text{..... (A2-3)}$$

The activity of each component in liquid phase can be derived from the expression of G^E vs mole fraction by using equation

$$\gamma_i^{ij} = [Q^{ij} - \sum_{k \neq i} x_k \left(\frac{\partial Q^{ij}}{\partial x_k} \right)_{x_{L \neq k, i}}] \quad \text{..... (A2-4)}$$

With x_1 constant,

$$\begin{aligned} x_1 (\partial Q^{12} / \partial x_2)_{x_1} &= x_1 x_2^2 \sum_{L=0}^m A_L (1 - 2x_1^*)^L + (x_1 + x_2) x_1 x_2 \sum_{L=0}^m A_L (1 - 2x_1^*)^L \\ &\quad + (x_1 + x_2) x_1 x_2^2 [2x_1 / (x_1 + x_2)^2] \sum_{L=0}^m A_L L (1 - 2x_1^*)^{L-1} \end{aligned}$$

Let:

$$\{L; i/ij\} = \sum_{L=0}^m A_L (1 - 2x_i^*)^L = \sum_{L=0}^m A_L [1 - 2x_i / (x_i + x_j)]^L \quad \text{..... (A2-5A)}$$

$$\{L-1; i/ij\} = \sum_{L=0}^m A_L L (1 - 2x_i^*)^{L-1} = \sum_{L=0}^m A_L L [1 - 2x_i / (x_i + x_j)]^{L-1} \quad \text{..... (A2-5B)}$$

then

$$\begin{aligned} x_2 (\partial Q^{12} / \partial x_2)_{x_1} &= x_2^2 x_1 \{L; 1/12\} + (x_1 + x_2) x_1 x_2 \{L; 1/12\} + \\ &\quad + (x_1 + x_2) x_1 x_2^2 [2x_1 / (x_1 + x_2)^2] \{L-1; 1/12\} \quad \text{..... (A2-6)} \end{aligned}$$

With x_2 constant

$$\begin{aligned} x_1 (\partial Q^{12} / \partial x_1)_{x_2} &= x_1^2 x_2 \{L; 1/12\} + (x_1 + x_2) x_1 x_2 \{L; 1/12\} + (x_1 + x_2) x_1^2 x_2 \\ &\quad [-2 / (x_1 + x_2) + 2x_1 / (x_1 + x_2)^2] \{L-1; 1/12\} \quad \text{..... (A2-7)} \end{aligned}$$

Substitutions of eq. (A2-6) and (A2-7) into (A2-4), yield:

$$\begin{aligned} \ln \gamma_3^{12} &= Q^{12} - x_2(\partial Q^{12}/\partial x_2)_{x_1} - x_1(\partial Q^{12}/\partial x_1)_{x_2} = -[x_1^2 x_2 + x_2^2 x_1 + (x_1 + x_2) x_1 x_2] \{L; \\ &1/12\} + \\ &+ [2 x_1^2 x_2 - (2 x_1^3 x_2 + 2 x_1^2 x_2^2) / (x_1 + x_2)] \{L-1; 1/12\} \quad \text{..... (A2-8)} \\ &= -2 (x_1 + x_2) x_1 x_2 \{L; 1/12\} \end{aligned}$$

With x_3 constant; then $x_1 = \text{constant} - x_2$:

$$\begin{aligned} x_2(\partial Q^{12}/\partial x_2)_{x_3} &= (x_1 + x_2) x_1 x_2 \{L; 1/12\} - (x_1 + x_2) x_2^2 \{L; 1/12\} + 2 x_1 x_2^2 \{L-1; 1/12\} \\ &\quad \text{..... (A2-9)} \end{aligned}$$

With x_2 constant; then $x_1 = \text{constant} - x_3$:

$$\begin{aligned} x_3(\partial Q^{12}/\partial x_3)_{x_2} &= -x_1 x_2 x_3 \{L; 1/12\} - (x_1 + x_2) x_2 x_3 \{L; 1/12\} + x_1 x_2 x_3 \\ &\quad [2 - 2x_1 / (x_1 + x_2)] \{L-1; 1/12\} \quad \text{..... (A2-10)} \end{aligned}$$

Substitutions of (A2-9) and (A2-10) into (A2-4), yield:

$$\begin{aligned} \ln \gamma_1^{12} &= Q^{12} - x_2(\partial Q^{12}/\partial x_2)_{x_3} - x_3(\partial Q^{12}/\partial x_3)_{x_2} = [(x_1 + x_2) x_2^2 + x_1 x_2 x_3 + (x_1 + x_2) \\ &x_2 x_3] \\ &\quad \{L; 1/12\} - \{ 2 x_1 x_2^2 + 2 x_1 x_2 x_3 [1 - x_1 / (x_1 + x_2)] \} \{L-1; 1/12\} \\ &= (x_2^2 + 2 x_1 x_2 x_3) \{L; 1/12\} - 2 x_1 x_2^2 / (x_1 + x_2) \{L-1; 1/12\} \quad \text{..... (A2-11)} \end{aligned}$$

With x_3 constant; then $x_2 = \text{constant} - x_1$:

$$\begin{aligned} x_1(\partial Q^{12}/\partial x_1)_{x_3} &= (x_1 + x_2) x_1 x_2 \{L; 1/12\} - (x_1 + x_2) x_1^2 \{L; 1/12\} - 2 x_1^2 x_2 \{L-1; 1/12\} \\ &\quad \text{..... (A2-12)} \end{aligned}$$

With x_1 constant; then $x_2 = \text{constant} - x_3$:

$$\begin{aligned} x_3(\partial Q^{12}/\partial x_3)_{x_1} &= -x_1 x_2 x_3 \{L; 1/12\} - (x_1 + x_2) x_1 x_3 \{L; 1/12\} - x_1 x_2 x_3 \\ &\quad [2x_1 / (x_1 + x_2)] \{L-1; 1/12\} \quad \text{..... (A2-13)} \end{aligned}$$

Substitutions of (A2-12) and (A2-13) into eq. (A2-4), yeild:

$$\begin{aligned} \ln \gamma_2^{12} &= Q^{12} - x_1(\partial Q^{12}/\partial x_2)_{x_3} - x_3(\partial Q^{12}/\partial x_3)_{x_1} = [(x_1 + x_2) x_1^2 + x_1 x_2 x_3 + (x_1 + x_2) \\ &x_1 x_3] \\ &\quad \{L; 1/12\} + 2 [x_1^2 x_2 + x_1^2 x_2 x_3 / (x_1 + x_2)] \{L-1; 1/12\} \\ &= (x_1^2 + 2 x_1 x_2 x_3) \{L; 1/12\} + 2 x_1^2 x_2 / (x_1 + x_2) \{L-1; 1/12\} \quad \text{..... (A2-14)} \end{aligned}$$

The expressions for $\ln \gamma_i^{13}$ and $\ln \gamma_i^{23}$ are obtained by cyclic rotation of suffices:

$$\ln \gamma_1^{13} = (x_3^2 + 2x_1x_2x_3) \{L; 1/13\} - 2x_1x_3^2 / (x_1 + x_3) \{L-1; 1/13\} \quad \dots (A2-15)$$

$$\ln \gamma_1^{23} = -2(x_2 + x_3)x_2x_3 \{L; 2/23\} \quad \dots (A2-16)$$

$$\ln \gamma_2^{13} = -2(x_1 + x_3)x_1x_3 \{L; 1/13\} \quad \dots (A2-17)$$

$$\ln \gamma_2^{23} = (x_3^2 + 2x_1x_2x_3) \{L; 2/23\} - 2x_2x_3^2 / (x_2 + x_3) \{L-1; 2/23\} \quad \dots (A2-18)$$

$$\ln \gamma_3^{23} = (x_2^2 + 2x_1x_2x_3) \{L; 2/23\} + 2x_2^2x_3 / (x_2 + x_3) \{L-1; 2/23\} \quad \dots (A2-19)$$

$$\ln \gamma_3^{13} = (x_1^2 + 2x_1x_2x_3) \{L; 1/13\} + 2x_1^2x_3 / (x_1 + x_3) \{L-1; 1/13\} \quad \dots (A2-20)$$

The similar derivation can be made for the ternary terms.

With x_3 constant; then $x_1 = \text{constant} - x_2$:

$$x_2 (\partial Q^{123} / \partial x_2)_{x_3} = x_2 (x_3 x_1 - x_2 x_3) [c_0 + c_1(3x_1 - 1) + c_2(3x_2 - 1)] + x_1 x_2^2 x_3 [-3c_1 + 3c_2] \quad \dots (A2-21)$$

with x_2 constant, $x_1 = \text{constant} - x_3$:

$$x_3 (\partial Q^{123} / \partial x_3)_{x_2} = x_3 (x_1 x_2 - x_2 x_3) [c_0 + c_1(3x_1 - 1) + c_2(3x_2 - 1)] + x_1 x_2 x_3^2 (-3c_1) \quad \dots (A2-22)$$

Substitutions of eq. (A2-21), (A2-22) into eq. (A2-4), yield:

$$\begin{aligned} \ln \gamma_1^{123} &= Q^{123} - x_2 (\partial Q^{123} / \partial x_2)_{x_3} - x_3 (\partial Q^{123} / \partial x_3)_{x_2} = [-x_1 x_2 x_3 + x_2^2 x_3 + x_2 x_3^2] \\ &\quad [c_0 + c_1(3x_1 - 1) + c_2(3x_2 - 1)] - x_1 x_2^2 x_3 [-3c_1 + 3c_2] - x_1 x_2 x_3^2 (-3c_1) \\ &= c_0 (x_2 x_3 - 2x_1 x_2 x_3) + c_1 [(3x_1 - 1)(x_2 x_3 - 2x_1 x_2 x_3) + 3x_1 x_2 x_3 (x_2 + x_3)] + \\ &\quad + c_2 [(3x_2 - 1)(x_2 x_3 - 2x_1 x_2 x_3) - 3x_1 x_2^2 x_3] \quad \dots (A2-23) \end{aligned}$$

With similar procedures, we have:

$$\begin{aligned} \ln \gamma_2^{123} &= c_0 (x_1 x_3 - 2x_1 x_2 x_3) + c_1 [(3x_1 - 1)(x_1 x_3 - 2x_1 x_2 x_3) - 3x_1^2 x_2 x_3] + \\ &\quad + c_2 [(3x_2 - 1)(x_1 x_3 - 2x_1 x_2 x_3) + 3x_1 x_2 x_3 (x_1 + x_3)] \quad \dots (A2-24) \end{aligned}$$

$$\begin{aligned} \ln \gamma_3^{123} &= c_0 (x_1 x_2 - 2x_1 x_2 x_3) + c_1 [(3x_1 - 1)(x_1 x_2 - 2x_1 x_2 x_3) - 3x_1^2 x_2 x_3] + \\ &\quad + c_2 [(3x_2 - 1)(x_1 x_2 - 2x_1 x_2 x_3) + 3x_1 x_2^2 x_3] \quad \dots (A2-25) \end{aligned}$$

APPENDIX 3 COMPUTER PROGRAMMES

A3-1 DVEC AND DVES

DVEC and DVES were written to calculate the excess molar volumes of mixtures from period of oscillation measured by the vibrating tube densimeter. DVEC is used when the measurements are carried with a mixing cell while DVES is used in the case of " pressure Lok"- syringe.

DATA INPUT

POIR: The barometer reading

POMI: Pressure correction for moist air

MOLW: Molar weight

A,B,C: The coefficients of Antoine eq.

D: Density of sample

D0: Density of sample at room temperature

VTOT: Total volume of mixing cell

VSPA1 and Vspa: Volumes of the space above the liquid in syringe after suck of first and second components.

T: Period of oscillation

M: Weight of sample

1, 2, mix, air, w: Component 1, 2, mixture, air, water

DATA OUTPUT

X1, X2,: Mole fraction

VE: Excess molar volume of mixture

D1, D2, DMIX: Density of component 1, 2, mixture.


```

1 REM          DVEC (MIXING CELL)

45  READ MOLW1,MOLW2,A1,B1,C1,A2,B2,C2,D10,D20,
    P0AIR,PMOI,T,T1,T2,TAIR,TW
120 PRINT "M1=?"
130 INPUT M1
140 PRINT "M2=?"
150 INPUT M2
160 PRINT "VTOT=?"
170 INPUT VTOT
180 PRINT "TMIX=?"
190 INPUT TMIX
500 DAIR=1.2929*(273.13/298.15)*(P0AIR-PMOI)*.001/1013.25
520 DAIR0=1.2929*(273.13/(T+273.15))*(P0AIR-PMOI)*.001/1013.25
550 D1=.997044+(.997044-DAIR)*(T1**2-TW**2)/(TW**2-TAIR**2)
600 D2=.997044+(.997044-DAIR)*(T2**2-TW**2)/(TW**2-TAIR**2)
650 DMIX=.997044+(.997044-DAIR)*(TMIX**2-TW**2)/(TW**2-TAIR**2)
700 VSPA=VTOT-M1/D10-M2/D20
800 W1=(1-DAIR0/8.4)*M1
900 W2=(1-DAIR0/8.4)*M2
1000 N10=W1/MOLW1
1100 N20=W2/MOLW2
1200 X10=N10/(N10+N20)
1300 X20=1-X10
1310 VSPA1=VSPA
1400 P1=(EXP(2.3025851*(A1-B1/(T+C1))))*133.32237
1500 P2=(EXP(2.3025851*(A2-B2/(T+C2))))*133.32237
1600 DALTRAN1=(P1*X10*VSPA1*.000001)/(8.31441*(T+273.15))
1700 DALTRAN2=(P2*X20*VSPA1*.000001)/(8.31441*(T+273.15))
1800 N1=N10-DALTRAN1
1900 N2=N20-DALTRAN2
2000 X1=N1/(N1+N2)
2100 X2=1-X1
2200 VE=X1*MOLW1*(1/DMIX-1/D1)+X2*MOLW2*(1/DMIX-1/D2)
2400 VSPA1=VSPA-VE*(N1+N2)
2500 S=ABS(VSPA1-VSPA)
2503 PRINT "VE=",VE;"S=",S
2600 IF S <.08 GOTO 2700
2620 X10=X1
2630 X20=X2
2640 GOTO 1600
2700 PRINT "X1=",X1;"X2=",X2;"VE=",VE;"D1=",D1;"D2=",D2;"DMIX=",DMIX
2800 GOTO 120
2900 DATA 84.1068,78.1134,6.84498,1203.526,222.863,6.90565,1211.033,220.79
3000 DATA .7736,.8734,1018.5,8.74,21,1.834013,1.881863,1.409476,1.939548
3100 END

```

```
40 READ MOLW1,MOLW2,A1,B1,C1,A2,B2,C2,D10,D20,P0AIR,PMOI,T,
   T1,T2,TAIR,TW
120 PRINT "M1=?"
130 INPUT M1
140 PRINT "M2=?"
150 INPUT M2
153 PRINT "VSPA1="
155 INPUT VSPA1
160 PRINT "VSPA=?"
170 INPUT VSPA
180 PRINT "TMIX=?"
190 INPUT TMIX
500 DAIR=1.2929*(273.13/298.15)*(P0AIR-PMOI)*.001/1013.25
520 DAIR0=1.2929*(273.13/(T+273.15))*(P0AIR-PMOI)*.001/1013.25
550 D1=.997044+(.997044-DAIR)*(T1**2-TW**2)/(TW**2-TAIR**2)
600 D2=.997044+(.997044-DAIR)*(T2**2-TW**2)/(TW**2-TAIR**2)
650 DMIX=.997044+(.997044-DAIR)*(TMIX**2-TW**2)/(TW**2-TAIR**2)
910 W1=(1-DAIR0/8.4)*M1+M1*DAIR0/D10
920 W2=(1-DAIR0/8.4)*M2+M2*DAIR0/D20
923 PRINT "W1=",W1;"W2=",W2
1000 N10=W1/MOLW1
1100 N20=W2/MOLW2
1200 X10=N10/(N10+N20)
1300 X20=1-X10
1400 P1=(EXP(2.3025851*(A1-B1/(T+C1))))*133.32237
1500 P2=(EXP(2.3025851*(A2-B2/(T+C2))))*133.32237
1600 DALTAN1=(P1*X10*VSPA*.000001)/(8.31441*(T+273.15))
1700 DALTAN2=(P2*X20*VSPA*.000001)/(8.31441*(T+273.15))
1705 W1=(1-DAIR0/8.4)*M1+W1*DAIR0/D10+P1*DAIR0*VSPA1/(P0AIR*100)
1710 W2=(1-DAIR0/8.4)*M2+W2*DAIR0/D20+(P1*X10+P2*X20)*VSPA*
   DAIR0/(P0AIR*100)
1720 N10=W1/MOLW1
1725 N20=W2/MOLW2
1800 N1=N10-DALTAN1
1900 N2=N20-DALTAN2
2000 X1=N1/(N1+N2)
2100 X2=1-X1
2110 Q1=ABS(X1-X10)
2111 PRINT "Q1=",Q1
2115 IF Q1 <.00001 GOTO 2200
2120 X10=X1
2130 GOTO 1400
2200 VE=X1*MOLW1*(1/DMIX-1/D1)+X2*MOLW2*(1/DMIX-1/D2)
2700 PRINT "X1=",X1;"X2=",X2;"VE=",VE;"D1=",D1;"D2=",D2;"DMIX=",DMIX
2900 GOTO 120
2950 DATA 170.341,86.178,6.98059,1625.928,180.311,6.75483,1081.176,229.343
2980 DATA .748,.647,1020.4,5.87,22,1.820102,1.770075,1.4095,1.93957
3000 END
```

A3-2 HE

Programme HE was written to calculate molar enthalpies from the calorimeter measurements.

DATA INPUT

VD: Volume of liquid in the calorimeter

D: Density of liquid (g cm^{-3})

MW: Molar weight (g cm^{-3})

CP2: Heat capacity of liquid 2 ($\text{J mol}^{-1} \text{K}^{-1}$)

TCORR: Temperature correction found by stirrer on/off measurements (K).

F: Number of experimental points

1,2 refer to component 1 (in calorimeter), and 2 (in bulb)

E: Voltage across the heater (V)

I: Heater current

V2: Accumulated volume of liquid 2 injected into the calorimeter (cm^3)

T: Accumulated time when the heater was on

DATA OUTPUT

X2: Mole fraction

HE: Excess molar enthalpy of mixtures

1 REM

HE

```
5 OPEN "DATA" FOR OUTPUT AS FILE #1
6 PRINT #1, "X2","HE"
10 READ V1, D1,D2,MW1,MW2,CP2,TCORR,F
20 N=0
30 N=N+1
31 PRINT "E="
32 INPUT E
33 PRINT "I"
34 INPUT I
40 PRINT "V2="
50 INPUT V2
53 PRINT "T="
55 INPUT T
57 N2=D2*V2/MW2
59 N1=D1*V1/MW1
60 X2=N2/(N1+N2)
61 X1=1-X2
72 QH=QH+E*I*T
74 QM=QH/(N1+N2)
73 QS=(0.7*N2*CP2*TCORR)/(N1+N2)
75 HE=QM-QS
77 PRINT "X2=";X2,"HE=";HE
78 PRINT #1,
80 PRINT #1, 82 PRINT #1, X2,HE
85 IF N<F THEN 20
80 DATA 30.48,.6209,.7449,86.178,226.45,485,.03,23
90 END
```

A3--3 CHVE

The programme CHVE was written to fit the experimental excess molar volumes and enthalpies of mixing to the polynomial expression:

$$X^E = A_1 x(1-x) + A_2 x(1-x)(1-2x) + A_3 x(1-x)(1-2x)^2 + \dots$$

The number of parameters was determined by minimizing DS2.

Data are input with data statements in following sequence:

W: Number of experimental points

S: Initial number of parameters

Matrix X2(W,1): Molar fraction of component 2

Matrix Y (W,1): Values of measurements of excess molar functions

The computed results are output in the following sequence:

Matrix A: Parameters

YC: Calculated values of excess molar functions

$$DS2 = [\sum R^2 / (w-S)]^{1/2}$$

Where, S is the number of parameters determined by minimizing DS2.

```

1 REM      CHVE (LEAST SQUARES FITTING FOR HE,VE)

2 OPEN "DAT" FOR OUTPUT AS FILE #1
3 PRINT #1,"W=THE NUMBER OF EXPERIMENTAL POINTS;S=THE
  NUMBER OF THE PARAMETERS"
4 PRINT #1,"Y,H(V)E =EXPERIMENTAL DATA OF EXCESS
  FUNCTION;YC=CALCULATED RESULTS"
5 PRINT #1,"A=OPTIMIZED PARAMETERS, R=YC-Y, DS1=SQR[(SUM OF
  R**2)/(W-1)]"
6 PRINT #1, "DS2=SQR[(SUM OF R**2)/(W-S)], X2=MOLE FRACTION OF
  COMPONENT 2"
7 PRINT #1,"THE EQUATION:YC=(X1*X2)* [A1+A2*(1-2*X2)
  +A3*(1-2*X2)**2+A4"
8 PRINT #1, " (1-2*X2)**3+A5*(1-2*X2)**4+ .....]"
9 PRINT #1,"YOU SHOULD INPUT W, INITIAL VALUE OF S
  (USUALLY IS 0), X2, Y"
10 PRINT #1,"BEFORE YOU RUN THIS PROGRAM"
11 READ W,S
12 DIM REAL Y(W,1), YP(W,1)
13 MAT READ X2(W,1),Y(W,1)
14 PRINT #1,"X2:"
15 MAT PRINT #1, X2
16 PRINT #1, "HE(VE)[EXP]:"
17 MAT PRINT #1, Y
18 PRINT #1, "-----**-----***-----**-----"
23 DS2=0
24 DT=DS2
28 S=S+1
30 DIM REAL GARM(S,W)
50 FOR I=1 TO W
60 FOR J=1 TO S
70 GARM(J,I)=X2(I,1)*(1-X2(I,1))*(1-2*X2(I,1))**(J-1)
90 NEXT J
100 NEXT I
110 DIM REAL TGARM(W,S),Y2(S,S),Y3(S,S),Y4(S,W),A(S,1)
120 MAT TGARM=TRN(GARM)
130 MAT Y2=GARM*TGARM
140 MAT Y3=INV(Y2)
150 MAT Y4=Y3*GARM
160 MAT A=Y4*Y
164 MAT PRINT A
165 PRINT #1, "A:"
166 MAT PRINT #1, A
167 PRINT #1, "*****"
173 DS=0
174 FOR I=1 TO W
175 YC=0
180 FOR J=1 TO S
190 YC=YC+X2(I,1)*(1-X2(I,1))*(A(J,1)*(1-2*X2(I,1))**(J-1))
200 NEXT J
203 R=YC-Y(I,1)

```

```
204 DS=DS+R**2
205 PRINT YC
208 PRINT #1,"X2=";X2(I,1),"YC=";YC,"Y=";Y(I,1),"R=";R
220 NEXT I
221 DS1=SQR(DS/(W-1))
222 PRINT "DS1=",DS1
223 PRINT #1,"DS1=",DS1
250 DS2=SQR(DS/(W-S))
252 PRINT "DS2=",DS2
255 PRINT #1,"DS2=",DS2
257 PRINT #1,"-----***-----**-----***-----"
260 IF DT=O GOTO 24
270 IF DS2<DT GOTO 24
280 PRINT "END"
283 PRINT #1,"END"
290 DATA 21,1
300 DATA 0,.05,.1,.15,.2,.25,.3,.35,.4,.45,.5,.55,.6,.65,.7,.75,.8,.85,.9,.95,1
310 DATA 0,.05,.12,.2,.27,.35,.41,.45,.46,.46,.43,.37,.29,.21,.1,.02,-.07,-.12
320 DATA -.14,-.1,0
```

A3-4 PVLR2 AND PVLR3

Programme PVLR2 and PVLR3 were written to fit the experimental data to R-K equation to obtain the optimal parameters, the residuals, calculated mole fractions in liquid and vapour phases, activity coefficients in liquid phases, excess molar Gibbs functions, standard deviations, and covariance matrix of optimal parameters. PVLR2 is used for binary mixtures, while PVLR3 is used for ternary mixtures.

DATA INPUT

Data are input with data statements in the following sequence for PVLR2:

MM: Initial number of parameters (Usually is 1). The final number of optimal parameters are determined by minimizing DS2.

ME: Options of error analysis of optimal parameters. ME=2: no error analysis is required, ME=1: error analysis with input of experimental error matrix is required. ME=3: error analysis is required with the assumption that the errors are the same for the experimental points.

N: Number of experimental points.

EE: If the difference of optimized parameters between two iterations is less than EE, the iteration procedure stops.

Data are input with data statements in the following sequence for PVLR3:

ME: See PVLR2.

M1, M2, M3: The number of parameters for each of three ternary mixtures

N: See PVLR2

Data input with file "DINM4" for PVLR2:

Matrix P: Measured total vapour pressures

Matrix N1: Mole numbers of component 1

Matrix N2: Mole numbers of component 2

Matrix VV: Volumes of vapour space above the liquid sample in vapour pressure cell.

P10: Vapour pressure of pure component 1

P20: Vapour pressure of pure component 2

RR: Gas constant

T: Temperature in the vapour pressure cell

VL1, VL2: Mole volumes of liquid component 1, and component 2

B1,B2,B12, Second Virial coefficients of component 1,2 and interaction second Virial coefficient

Data are input with a file "3DIN" for PVLR3:

Matrixes P, Ni, VV: See PVLR2, i denotes component i

Data input with a file "DIN1" for PVLR3:

Pi0, T, E, VLi, Bi: See PVLR2, i denotes component i

Data are output with a file "GE2OUT" for PVLR2, and "GE3OUT" for pvlr3:

Matrix A: Optimal parameters

X1: Mole fraction of component 1 in liquid phase

X2: Mole fraction of component 2 in liquid phase

X3: Mole fraction of component 3 in liquid phase

GAM1: Activity coefficient of component 1 in liquid phase

GAM2: Activity coefficient of component 2 in liquid phase

GAM3: Activity coefficient of component 3 in liquid phase

Y1: Mole fraction of component 1 in vapour phase

Y2: Mole fraction of component 2 in vapour phase

Y3: Mole fraction of component 3 in vapour phase

PC: Calculated total vapour pressure

R: Residuals of vapour pressure = $P_{\text{exp}} - P_{\text{cal}}$

ZAR2: Standard deviation

Matrix WP: Error matrix of optimal parameters

WP(I,I): The diagonal elements of the error matrix WP

```

1 REM   PVLR2 (P-X FITTING M PARAMETERS RK EQ., BINARY
MIXTURES)

```

```

10 READ MM, ME, N, EE
15 OPEN "GE2OUT4" FOR OUTPUT AS FILE #2
14 ZAR22=0
16 M=MM-1
17 M=M+1
18 PRINT "M=";M
19 PRINT #2, "M=";M
20 DIM Z1(M,N), Z2(M,N), Z3(M,M), Z4(M,M), Z5(M,N), R(N,1), DA(M,1), A(M,1)
23 DIM GAM1(N), GAM2(N), PPA(N,M)
30 DIM X1(N), D(M), E(M), Y1(N), PC(N), P(N), GED(N), N1(N), N2(N), VV(N)
40 OPEN "DINM4" FOR INPUT AS FILE #1
60 MAT INPUT #1, P; N1; N2; VV;
65 INPUT #1, P10; P20; R; T; E; VL1; VL2; B1; B2; B12
70 CLOSE #1
80 A(M,1)=0
125 S=0
127 S=S+1
128 PRINT #2,
130 PRINT "S="; S; 131 PRINT #2, "S="; S
132 PRINT #2, "A:"
134 MAT PRINT #2, A;
138 IF ME=3 THEN 185
139 IF ME=2 THEN 185
140 DIM WP(N,N), VC(M,M), Z5(N,M)
150 OPEN "DWP" FOR INPUT AS FILE #1
160 FOR I=1 TO N
170 INPUT #1, WP(I,I)
180 NEXT I
183 CLOSE #1
185 FOR I=1 TO N

190 GOSUB 1000

200 GOSUB 2000

205 NEXT I
210 IF ME=2 THEN 380
220 IF ME=3 THEN 380
300 MAT Z1=TRN(PPA)
310 MAT Z2=Z1*WP
320 MAT Z3=Z2*PPA
330 MAT VC=INV(Z3)
340 MAT Z2=VC*Z1

```

```

350 MAT Z1=Z2*WP
360 MAT DA=Z1*R
370 GOTO 430
380 MAT Z1=TRN(PPA)
390 MAT Z3= Z1*PPA
400 MAT Z4=INV(Z3)
410 MAT Z2= Z4*Z1
420 MAT DA=Z2*R
430 FOR I=1 TO M
445 IF ABS(DA(I,1))>EE THEN 485
450 NEXT I
482 GOTO 619
485 MAT A=A+DA
488 GOTO 127

619 PRINT #2,
620 PRINT " RESULTS:"
623 PRINT #2,"-----"
625 PRINT #2, "RESULTS:"
627 PRINT #2,
628 PRINT "A="
630 MAT PRINT A;
640 PRINT #2,"A:"
650 MAT PRINT #2, A;
655 PRINT #2, " ..... "
657 PRINT #2,
658 RT=0
659 RTS=0
660 FOR I=1 TO N
661 RT=RT+ABS(R(I,1))
662 RTS=RTS+R(I,1)**2
670 PRINT #2,"X1=";X1(I);"GAM1=";GAM1(I);"GAM2=";GAM2(I);
680 PRINT #2, "Y1=";Y1(I);"PC=";PC(I);
690 PRINT #2, "GE=";GED(I);"R="; R(I,1)
695 PRINT #2,
700 NEXT I
701 AVR=RT/N
702 ZAR1=(RTS/N)^.5
703 ZAR2=(RTS/(N-M))^.5
704 PRINT #2,
706 PRINT #2,"AVR=";AVR;"ZAR1=";ZAR1;"ZAR2=";ZAR2
708 PRINT #2,
709 PRINT #2,
710 IF M>MM THEN 770
720 ZAR22=ZAR2
722 PRINT "ZAR22=";ZAR22
730 GOTO 17

770 PRINT #2,
772 PRINT #2,
779 IF ME=2 THEN 807
780 GOSUB 3490

```

```

785 GOSUB 3000
790 IF ABS(ZAR2)>ABS(ZAR22) THEN 807
793 ZAR22=ZAR2
795 GOTO 17
807 PRINT #2,
809 PRINT "END"
810 PRINT #2, "END"
820 GOTO 4000

1000 X1(I)=N1(I)/(N1(I)+N2(I))
1043 X2=1-X1(I)
1044 PRINT "X1=";X1(I);"P=";P(I)
1050 LNGAM1=0
1053 LNGAM2=0
1060 FOR J=1 TO M
1061 IF J>1 THEN 1070
1063 D(1)=X2**2
1065 E(1)=X1(I)**2
1067 GOTO 1090
1070 D(J)=X2**2*(-(2*X1(I)-1))**(J-1)-2*(J-1)*X1(I)*X2**2*(-(2*X1(I)-1))**(J-2)
1080 E(J)=X1(I)**2*(2*X2-1)**(J-1)+2*(J-1)*X2*X1(I)**2*(2*X2-1)**(J-2)
1090 LNGAM1=LNGAM1+A(J,1)*D(J)
1100 LNGAM2=LNGAM2+A(J,1)*E(J)
1330 NEXT J
1340 GAM1(I)=EXP(LNGAM1)
1350 GAM2(I)=EXP(LNGAM2)
1368 F=0
1370 IF B12<>0 THEN 1375
1371 DA12=0
1372 GOTO 1376
1375 DA12=2*B12-B1-B2
1376 F=F+1
1400 FA1=EXP(((VL1-B1)*(P(I)-P10)-P(I)*DA12*Y2**2)/(R*T))
1410 FA2=EXP(((VL2-B2)*(P(I)-P20)-P(I)*DA12*Y1(I)**2)/(R*T))
1500 P1D=X1(I)*P10*FA1
1510 P2D=X2*P20*FA2
1513 PC(I)=GAM1(I)*P1D+GAM2(I)*P2D
1515 Y1(I)=GAM1(I)*P1D/PC(I)
1517 Y2=1-Y1(I)
1519 IF F<3 THEN 1370
1560 N1L=N1(I)-P1D*GAM1(I)*VV(I)/(R*T)
1570 N2L=N2(I)-P2D*GAM2(I)*VV(I)/(R*T)
1590 NL=N1L+N2L
1600 X1=N1L/NL
1610 X2=N2L/NL
1630 DX1=X1-X1(I)
1650 PRINT "DX1=";DX1;
1660 IF ABS(DX1)>E THEN 1800
1700 R(I,1)=P(I)-PC(I)
1702 PRINT "R=";R(I,1)
1705 PRINT #2, "R="; R(I,1),
1733 GED(I)=R*T*(X1(I)*LOG(GAM1(I))+X2*LOG(GAM2(I)))

```

```

1780 RETURN
1800 X1(I)=X1
1830 GOTO 1043
1850 RETURN
1900 FA1=1
1910 FA2=1
1930 GOTO 1500
1940 RETURN
1980 P1D=P10*X1(I)
1982 P2D=P20*X2
1983 PC(I)=P1D*GAM1(I)+P2D*GAM2(I)
1985 Y1(I)=GAM1(I)*P1D/PC(I)
1987 GOTO 1700
1990 RETURN

2000 FOR J=1 TO M
2020 PPA(I,J)=P1D*GAM1(I)*D(J)+P2D*GAM2(I)*E(J)
2030 NEXT J
2100 RETURN

3000 SS=0
3001 DIM DGE(N)
3005 PRINT #2,
3007 PRINT #2, " DGE="
3010 FOR I=1 TO N
3020 DGE(I)=0
3040 FOR J=0 TO M-1
3050 DGE (I) =DGE(I)+(RR*T*X1(I)*(1-X1(I))*
      (1-2*X1(I))*J*VC(J+1,J+1)**(1/2))**2
3051 DGE (I)= DGE(I)**(1/2)
3060 NEXT J
3063 PRINT #2,
3070 PRINT #2,DGE(I)
3100 NEXT I
3107 PRINT #2,
3108 PRINT #2,
3110 RETURN

3490 IF ME=3 THEN 3540
3510 MAT Z5=PPA*VC
3515 MAT Z1=TRN(PPA)
3520 MAT WP=Z5*Z1
3530 GOTO 3580
3540 DIM WP(N,N),VC(M,M), Z5(N,M)
3550 MAT VC=(ZAR2)*Z4
3560 MAT Z5=PPA*VC
3565 MAT Z1=TRN(PPA)
3570 MAT WP=Z5*Z1
3571 PRINT #2,
3573 PRINT #2,
3574 PRINT #2,"~~~~~"
3576 PRINT #2,

```

```
3577 PRINT #2,"ERROR MATRIX:"  
3578 PRINT #2,  
3580 PRINT #2,"VC=:"  
3589 PRINT #2,  
3590 MAT PRINT #2, VC;
```

```
3591 PRINT #2,  
3592 PRINT #2,  
3593 PRINT " DO YOU LIKE ALL THE INFORMATION ABOUT WP  
        (NO:1,YES:2)?"
```

```
3594 INPUT O  
3595 IF O=1 THEN 3613  
3600 PRINT #2, "WP:"
```

```
3610 MAT PRINT #2, WP;  
3613 PRINT #2, "WP(I,I):"  
3614 PRINT #2,  
3616 FOR I=1 TO N  
3617 PRINT #2,WP(I,I),  
3618 NEXT I  
3619 RETURN
```

```
3990 DATA 1,3,10,10E-7
```

```
4000 END
```

```

1 REM   PVL3 [P-X FITTING (M1+M2+M3)+M PARAMETERS R-K
        EQ. TERNARY MIXTURES]
2 REM   M1,M2,M3: FROM THREE BINARY MIXTURES, M: OPTIMIZED
        TERNARY PARAMETERS IN THIS PROGRAM.

3 READ ME, M, M1, M2, M3, N, EE
4 FOR J=1 TO M1
5 READ B1(J)
6 NEXT J
7 FOR J=1 TO M2
8 READ B2(J)
9 NEXT J
10 FOR J=1 TO M3
11 READ B3(J)
12 NEXT J
13 PRINT "M";M,"M1";M1,"M2";M2,"M3";M3,"EE";EE
19 OPEN "GE3OUT" FOR OUTPUT AS FILE #2
20 DIM Z1(M,N),Z2(M,N),Z3(M,M),Z4(M,M),Z5(M,N),DA(M,1),R(N,1),A(M,1)
23 DIM GAM1(N),GAM2(N),GAM3(N),PPA(N,M)
30 DIM X1(N),X2(N),D1(M1),D2(M2),D3(M3),D4(M),E1(M1),E2(M2),E3(M3),E4(M)
33 DIM N1(N),N2(N),N3(N),VV(N)
35 DIM F1(M1),F2(M2),F3(M3),F4(M),Y1(N),Y2(N),PC(N),P(N),GED(N),GETO(N)
40 OPEN "3DIN" FOR INPUT AS FILE #1
52 MAT INPUT #1, A;P;N1;N2;N3;VV
53 MAT PRINT #2,A;P;N1;N2;N3;VV
58 CLOSE #1
60 OPEN "3DIN1" FOR INPUT AS FILE #1
65 INPUT #1, P10,P20,P30,T,E,VL1,VL2,VL3,B1,B2,B3,B12,B13,B23
66 PRINT #2, P10,P20,P30,T,E,VL1,VL2,VL3,B1,B2,B3,B12,B13,B23
68 CLOSE #1
120 RR=8.3144
125 S=0
127 S=S+1
128 PRINT "S=";S
129 PRINT #2,
131 PRINT #2, "S=";S
132 PRINT #2, "A:"
134 MAT PRINT #2, A;
138 IF ME=3 THEN 185
139 IF ME=2 THEN 185
140 DIM WP(N,N),VC(M,M),Z5(N,M)
150 OPEN "DWP" FOR INPUT AS FILE #1
160 FOR I=1 TO N
170 INPUT #1, WP(I,I)
180 NEXT I

183 CLOSE #1
185 FOR I=1 TO N
190 GOSUB 1000

```

```

200 GOSUB 2000
205 NEXT I
210 IF ME=2 THEN 380
220 IF ME=3 THEN 380
300 MAT Z1=TRN(PPA)
310 MAT Z2=Z1*WP
320 MAT Z3=Z2*PPA
330 MAT VC=INV(Z3)
340 MAT Z2=VC*Z1
350 MAT Z1=Z2*WP
360 MAT DA=Z1*R
370 GOTO 430
380 MAT Z1=TRN(PPA)
390 MAT Z3= Z1*PPA
400 MAT Z4=INV(Z3)
410 MAT Z2= Z4*Z1
420 MAT DA=Z2*R
430 FOR I=1 TO M
440 IF ABS(DA(I,1))>EE THEN 485
450 NEXT I
460 GOTO 620
485 MAT A=A+DA
488 GOTO 127

620 PRINT " RESULTS:"
623 PRINT #2,"-----"
625 PRINT #2, "RESULTS:"
627 PRINT #2,
628 PRINT "A=:"
630 MAT PRINT A;
640 PRINT #2,"A:"
650 MAT PRINT #2, A;
655 PRINT #2, " ..... "
657 PRINT #2,
658 RT=0
659 RTS=0
660 FOR I=1 TO N
662 RT=RT+ABS(R(I,1))
664 RTS=RTS+R(I,1)**2
670 PRINT #2,"X1=";X1(I);"X2=";X2(I);"GAM1=";GAM1(I);"GAM2=";GAM2(I);
680 PRINT #2, "GAM3=";GAM3(I);"Y1=";Y1(I);"Y2=";Y2(I);"PC=";PC(I);
690 PRINT #2, "GE=";GED(I);"GETO=";GETO(I);"R="; R(I,1)
695 PRINT #2,
697 NEXT I
698 AVR=RT/N
699 ZAR1=((RTS)/N)^.5
700 ZAR2=((RTS)/(N-M))^.5
701 PRINT #2,"AVR=";AVR;"ZAR1=";ZAR1;"ZAR2=";ZAR2
702 PRINT #2,
480 IF ME=2 THEN 820
770 GOSUB 3490
780 GOSUB 3000

```



```

820 PRINT "END"
830 PRINT #2, "END"
840 GOTO 4000

```

```

1000 REM
1010 X1(I)=N1(I)/(N1(I)+N2(I)+N3(I))
1020 X2(I)=N2(I)/(N1(I)+N2(I)+N3(I))
1040 X3=1-X1(I)-X2(I)
1044 PRINT "X1=";X1(I);"X2=";X2(I);"X3=";X3;"P=";P(I)
1045 X123=X1(I)*X2(I)*X3
1050 X12=X1(I)+X2(I)
1052 X13=X1(I)+X3
1055 X23=X2(I)+X3
1060 X1D1=2*X1(I)/X12-1
1065 X2D1=2*X2(I)/X12-1
1068 X1D2=2*X1(I)/X13-1
1070 X3D2=2*X3/X13-1
1073 X2D3=2*X2(I)/X23-1
1075 X3D3=2*X3/X23-1
1077 D1(1)=X2(I)**2+2*X123
1078 E1(1)=X1(I)**2+2*X123
1079 F1(1)=-2*X12*X1(I)*X2(I)
1080 FOR J=2 TO M1
1085 D1(J)=(X2(I)**2+2*X123)*(-X1D1)**(J-1)-2*(J-1)*X1(I)*X2(I)**2&
      *(-X1D1)**(J-2)/X12
1090 E1(J)=(X1(I)**2+2*X123)*X2D1**(J-1)+2*(J-1)*X2(I)*X1(I)**2&
      *X2D1**(J-2)/X12
1092 F1(J)=-2*X12*X1(I)*X2(I)*(-X1D1)**(J-1)
1095 NEXT J
1097 D2(1)=X3**2+2*X123
1098 E2(1)=-2*X13*X1(I)*X3
1099 F2(1)=X1(I)**2+2*X123
1100 FOR J=2 TO M2
1105 D2(J)=(X3**2+2*X123)*(-X1D2)**(J-1)-2*(J-1)*X1(I)*X3**2*(-X1D2)**(J-2)/X13
1106 E2(J)=-2*X13*X1(I)*X3*(-X1D2)**(J-1)
1110 F2(J)=(X1(I)**2+2*X123)*X3D2**(J-1)+2*(J-1)*X3*X1(I)**2*X3D2**(J-2)/X13
1115 NEXT J
1117 D3(1)=-2*X23*X2(I)*X3
1118 E3(1)=X3**2+2*X123
1119 F3(1)=X2(I)**2+2*X123
1125 FOR J=2 TO M3
1128 D3(J)=-2*X23*X2(I)*X3*(-X2D3)**(J-1)
1130 E3(J)=(X3**2+2*X123)*(-X2D3)**(J-1)-2*(J-1)*X2(I)*X3**2*(-X2D3)**(J-2)/X23
1135 F3(J)=(X2(I)**2+2*X123)*X3D3**(J-1)+2*(J-1)*X3*X2(I)**2*X3D3**(J-2)/X23
1138 NEXT J
1141 D4(1)=X2(I)*X3-2*X123
1142 D4(2)=(3*X1(I)-1)*(X2(I)*X3-2*X123)+3*X123*X23
1143 D4(3)=(X2(I)*X3-2*X123)*(3*X2(I)-1)-3*X1(I)*X2(I)**2*X3
1144 E4(1)=X1(I)*X3-2*X123
1145 E4(2)=(3*X1(I)-1)*(X1(I)*X3-2*X123)-3*X1(I)**2*X2(I)*X3
1146 E4(3)=(3*X2(I)-1)*(X1(I)*X3-2*X123)+3*X123*X13

```

```

1147 F4(1)=X1(I)*X2(I)-2*X123
1148 F4(2)=(3*X1(I)-1)*(X1(I)*X2(I)-2*X123)-3*X1(I)**2*X2(I)*X3
1149 F4(3)=(3*X2(I)-1)*(X1(I)*X2(I)-2*X123)-3*X1(I)*X2(I)**2*X3
1150 LNGAM1=0
1160 LNGAM2=0
1170 LNGAM3=0
1190 FOR J=1 TO M1
1200 LNGAM1=LNGAM1+B1(J)*D1(J)
1210 LNGAM2=LNGAM2+B1(J)*E1(J)
1215 LNGAM3=LNGAM3+B1(J)*F1(J)
1220 NEXT J
1225 FOR J=1 TO M2
1230 LNGAM1=LNGAM1+B2(J)*D2(J)
1235 LNGAM2=LNGAM2+B2(J)*E2(J)
1240 LNGAM3=LNGAM3+B2(J)*F2(J)
1250 NEXT J
1260 FOR J=1 TO M3
1265 LNGAM1=LNGAM1+B3(J)*D3(J)
1270 LNGAM2=LNGAM2+B3(J)*E3(J)
1280 LNGAM3=LNGAM3+B3(J)*F3(J)
1330 NEXT J
1341 FOR J=1 TO M
1342 LNGAM1=LNGAM1+A(J,1)*D4(J)
1343 LNGAM2=LNGAM2+A(J,1)*E4(J)
1344 LNGAM3=LNGAM3+A(J,1)*F4(J)
1346 NEXT J
1348 GAM1(I)=EXP(LNGAM1)
1350 GAM2(I)=EXP(LNGAM2)
1360 GAM3(I)=EXP(LNGAM3)
1367 IF B12<>0 THEN 1380
1368 IF B13<>0 THEN 1380
1369 IF B23<>0 THEN 1380
1377 SC1=SC2=SC3=0
1378 GOTO 1400
1380 DA12=2*B12-B1-B2
1383 DA13=2*B13-B1-B3
1385 DA23=2*B23-B2-B3
1388 SC1=Y2**2*DA12+Y3**2*DA13+Y2*Y3*DA12-Y2*Y3*DA23+Y2*Y3*DA13
1390 SC2=Y1**2*DA12+Y3**2*DA23+Y1*Y3*DA12-Y1*Y3*DA13+Y1*Y3*DA23
1392 SC3=Y1**2*DA13+Y2**2*DA23+Y1*Y2*DA23-Y1*Y2*DA12+Y1*Y2*DA13
1400 FA1=EXP(((VL1-B1)*(P(I)-P10)-P(I)*SC1)/(RR*T))
1410 FA2=EXP(((VL2-B2)*(P(I)-P20)-P(I)*SC2)/(RR*T))
1420 FA3=EXP(((VL3-B3)*(P(I)-P30)-P(I)*SC3)/(RR*T))
1500 P1D=X1(I)*P10*FA1
1510 P2D=X2(I)*P20*FA2
1520 P3D=X3*I*P30*FA3
1521 PC(I)=P1D*GAM1(I)*FA1+P2D*GAM2(I)*FA2+P3D*GAM3(I)*FA3
1523 Y1=GAM1(I)*P1D/PC(I)
1525 Y2=GAM2(I)*P2D/PC(I)
1527 Y3=1-Y1-Y2
1529 DY1=Y11-Y1
1530 DY2=Y22-Y2

```

```

1531 PRINT "DY1=";DY1;"DY2=";DY2
1532 IF ABS(DY1)>.0001 THEN 1540
1533 IF ABS(DY2)>.0001 THEN 1540
1534 GOTO 1555
1540 Y11=Y1
1542 Y22=Y2
1545 GOTO 1367

1555 N1L=N1(I)-P1D*GAM1(I)*VV(I)/(RR*T)
1570 N2L=N2(I)-P2D*GAM2(I)*VV(I)/(RR*T)
1580 N3L=N3(I)-P3D*GAM3(I)*VV(I)/(RR*T)
1590 NL=N1L+N2L+N3L
1600 X1=N1L/NL
1610 X2=N2L/NL
1630 DX1=X1-X1(I)
1640 DX2=X2-X2(I)
1650 PRINT "DX1=";DX1;"DX2=";DX2;
1660 IF ABS(DX1)>E THEN 1800
1670 IF ABS(DX2)>E THEN 1800
1690 PC(I)=P1D*GAM1(I)+P2D*GAM2(I)+P3D*GAM3(I)
1700 R(I,1)=P(I)-PC(I)
1702 PRINT "R=";R(I,1)
1705 PRINT #2, "R="; R(I,1),
1710 Y1(I)=GAM1(I)*P1D/PC(I)
1720 Y2(I)=GAM2(I)*P2D/PC(I)
1723 GED(I)=RR*T*(X1(I)*LOG(GAM1(I))+X2(I)*
      LOG(GAM2(I))+X3*LOG(GAM3(I)))
1725 GE1=0
1726 GE2=0
1727 GE3=0
1736 FOR J=1 TO M1
1738 GE1=GE1+X12*X1(I)*X2(I)*B1(J)*(-X1D1)**(J-1)
1739 NEXT J
1740 FOR J=1 TO M2
1741 GE2=GE2+X13*X1(I)*X3*B2(J)*(-X1D2)**(J-1)
1742 NEXT J
1743 FOR J=1 TO M3
1745 GE3=GE3+X23*X2(I)*X3*B3(J)*(-X2D3)**(J-1)
1746 NEXT J
1750 GE4=X123*(A(1,1)+A(2,1)*(3*X1(I)-1)+A(3,1)*(3*X2(I)-1))
1765 GETO(I)=(GE1+GE2+GE3+GE4)*RR*T
1780 RETURN
1800 X1(I)=X1
1810 X2(I)=X2
1830 GOTO 1040
1850 RETURN
1900 FA1=1
1910 FA2=1
1920 FA3=1
1930 GOTO 1500
1940 RETURN

```

```

2000 FOR J=1 TO M
2020 PPA(I,J)=P1D*GAM1(I)*D4(J)+P2D*GAM2(I)*E4(J)+P3D*GAM3(I)*F4(J)
2030 NEXT J
2100 RETURN

```

```

3000 PRINT #2,
3005 DIM DGE(N)
3100 PRINT #2,"DGE="
3105 FOR I=1 TO N
3110 SSS=RR*T*X1(I)*X2(I)*(1-X1(I)-X2(I))
3111 SS1=(3*X1(I)-1)*VC(2,2)**(1/2)
3112 SS2=(3*X2(I)-1)*VC(3,3)**(1/2)
3115 DGE(I)=(VC(1,1)+SS1**2+SS2**2)**(1/2)
3120 DGE(I)=SSS*DGE(I)
3130 PRINT#2, DGE(I)
3140 NEXT I
3150 RETURN

```

```

3490 IF ME=3 THEN 3540
3510 MAT Z5=PPA*Z4
3520 MAT WP=Z5*Z1
3530 GOTO 3580
3540 DIM WP(N,N),VC(M,M), Z5(N,M)
3550 MAT VC=(ZAR2)*Z4
3560 MAT Z5=PPA*VC
3565 MAT Z1=TRN(PPA)
3570 MAT WP=Z5*Z1
3571 PRINT #2,
3572 PRINT #2,
3573 PRINT #2, " ~~~~~"

```

```

3575 PRINT #2, "RESULTS:"
3576 PRINT #2,
3577 PRINT #2, "ERROR MATRIX:"
3580 PRINT #2, "VC=:"
3590 MAT PRINT #2, VC;

```

```

3591 PRINT #2,

```

```

3592 PRINT #2,
3593 PRINT " DO YOU LIKE ALL THE INFORMATION ABOUT WP
      (NO:1,YES:2)?"
3594 INPUT O
3595 IF O=1 THEN 3613
3600 PRINT #2, "WP:"
3610 MAT PRINT #2, WP;
3613 PRINT #2, "WP(I,I):"
3614 PRINT #2,
3616 FOR I=1 TO N
3617 PRINT #2,WP(I,I),
3618 PRINT #2,

```

3619 NEXT I
3620 RETURN

3985 DATA 3,3,2,5,2,44,.00001,.00143229,-.00399029,-.103621,.0045545
3990 DATA -.00209169,-.00707403,.027154,-.0639962,.00434808

4000 END

A3-5 PVLR4

Programme PVLR4 was written to calculate GE of ternary mixtures from R-K equation using known parameters and mole fractions.

Data are input with data statements in the following sequence:

M: Number of ternary parameters

M1, M2, M3: Number of parameters for each of three binary mixtures

B1(J): Parameters for the first binary mixture

B2(J): Parameters for the second binary mixture

B3(J): Parameters for the third binary mixture

Data are input with a file "DIN3":

Matrix A: Ternary parameters

Matrix X1: Mole fractions of component 1

Matrix X2: Mole fractions of component 2

Data are input with a file "3DN1": See PVLR3

Data are output with a file "GECOUT4":

X_i : Mole fraction of component i in liquid phase

GAM_i : Activity coefficient of component i in liquid phase

Y_i : Mole fraction of component i in vapour phase

GE: Molar excess Gibbs function

1 REM PVL4 (CALCULATION OF GE FROM OPTIMAL PARAMETERS
AND MOLE FRACTIONS OF MIXTURES)

```

3 READ M,M1,M2,M3, N
4 FOR J=1 TO M1
5 READ B1(J)
6 NEXT J
7 FOR J=1 TO M2
8 READ B2(J)
9 NEXT J
10 FOR J=1 TO M3
11 READ B3(J)
12 NEXT J
13 PRINT "M";M,"M1";M1,"M2";M2,"M3",M3
19 OPEN "GECOUT4" FOR OUTPUT AS FILE #2
23 DIM A(M,1),GAM1(N),GAM2(N),GAM3(N),PPA(N,M)
30 DIM X1(N),X2(N),D1(M1),D2(M2),D3(M3),D4(M),E1(M1),E2(M2),E3(M3),E4(M)
35 DIM F1(M1),F2(M2),F3(M3),F4(M),Y1(N),Y2(N),PC(N),P(N),GED(N),GETO(N)
40 OPEN "CDIN3" FOR INPUT AS FILE #1
52 MAT INPUT #1, A;X1;X2
53 MAT PRINT #2,A;X1;X2
58 CLOSE #1
60 OPEN "3DIN1" FOR INPUT AS FILE #1
65 INPUT #1, P10,P20,P30,T,VL1,VL2,VL3,B1,B2,B3,B12,B13,B23
66 PRINT #2, P10,P20,P30,T,VL1,VL2,VL3,B1,B2,B3,B12,B13,B23
68 CLOSE #1
120 RR=8.3144
185 FOR I=1 TO N

190 GOSUB 1000

575 PRINT #2, "RESULTS:"
576 PRINT #2,
670 PRINT #2,"X1=";X1(I);"X2=";X2(I);"GAM1=";GAM1(I);"GAM2=";GAM2(I);
680 PRINT #2, "GAM3=";GAM3(I);"Y1=";Y1(I);"Y2=";Y2(I);"PC=";PC(I);
690 PRINT #2, "GE=";GED(I);"GETO=";GETO(I)
695 PRINT #2,
697 NEXT I
820 PRINT "END"
830 PRINT #2, "END"
840 GOTO 3000

1000 REM
1040 X3=1-X1(I)-X2(I)
1044 PRINT "X1=";X1(I);"X2=";X2(I);"X3=";X3
1045 X123=X1(I)*X2(I)*X3
1050 X12=X1(I)+X2(I)

```

```

1052 X13=X1(I)+X3
1055 X23=X2(I)+X3
1060 X1D1=2*X1(I)/X12-1
1065 X2D1=2*X2(I)/X12-1
1068 X1D2=2*X1(I)/X13-1
1070 X3D2=2*X3/X13-1
1073 X2D3=2*X2(I)/X23-1
1075 X3D3=2*X3/X23-1
1076 D1(1)=X2(I)**2+2*X123
1077 E1(1)=X1(I)**2+2*X123
1078 F1(1)=-2*X12*X1(I)*X2(I)
1080 FOR J=2 TO M1
1085 D1(J)=(X2(I)**2+2*X123)*(-X1D1)**(J-1)-2*(J-1)*X1(I)*X2(I)**2&
      *(-X1D1)**(J-2)/X12
1090 E1(J)=(X1(I)**2+2*X123)*X2D1**(J-1)+2*(J-1)*X2(I)*X1(I)**2&
      *X2D1**(J-2)/X12
1092 F1(J)=-2*X12*X1(I)*X2(I)*(-X1D1)**(J-1)
1095 NEXT J
1097 D2(1)=X3**2+2*X123
1098 E2(1)=-2*X13*X1(I)*X3
1099 F2(1)=X1(I)**2+2*X123
1100 FOR J=2 TO M2
1105 D2(J)=(X3**2+2*X123)*(-X1D2)**(J-1)-2*(J-1)*X1(I)*X3**2*(-X1D2)**(J-2)/X13
1106 E2(J)=-2*X13*X1(I)*X3*(-X1D2)**(J-1)
1110 F2(J)=(X1(I)**2+2*X123)*X3D2**(J-1)+2*(J-1)*X3*X1(I)**2*X3D2**(J-2)/X13
1115 NEXT J
1117 D3(1)=-2*X23*X2(I)*X3
1118 E3(1)=X3**2+2*X123
1119 F3(1)=X2(I)**2+2*X123
1125 FOR J=2 TO M3
1128 D3(J)=-2*X23*X2(I)*X3*(-X2D3)**(J-1)
1135 E3(J)=(X3**2+2*X123)*(-X2D3)**(J-1)-2*(J-1)*X2(I)*X3**2*(-X2D3)**(J-2)/X23
1136 F3(J)=(X2(I)**2+2*X123)*X3D3**(J-1)+2*(J-1)*X3*X2(I)**2*X3D3**(J-2)/X23
1138 NEXT J
1141 D4(1)=X2(I)*X3-2*X123
1142 D4(2)=(3*X1(I)-1)*(X2(I)*X3-2*X123)+3*X123*X23
1143 D4(3)=(X2(I)*X3-2*X123)*(3*X2(I)-1)-3*X1(I)*X2(I)**2*X3
1144 E4(1)=X1(I)*X3-2*X123
1145 E4(2)=(3*X1(I)-1)*(X1(I)*X3-2*X123)-3*X1(I)**2*X2(I)*X3
1146 E4(3)=(3*X2(I)-1)*(X1(I)*X3-2*X123)+3*X123*X13
1147 F4(1)=X1(I)*X2(I)-2*X123
1148 F4(2)=(3*X1(I)-1)*(X1(I)*X2(I)-2*X123)-3*X1(I)**2*X2(I)*X3
1149 F4(3)=(3*X2(I)-1)*(X1(I)*X2(I)-2*X123)-3*X1(I)*X2(I)**2*X3
1150 LNGAM1=0
1160 LNGAM2=0
1170 LNGAM3=0
1190 FOR J=1 TO M1
1200 LNGAM1=LNGAM1+B1(J)*D1(J)
1210 LNGAM2=LNGAM2+B1(J)*E1(J)
1215 LNGAM3=LNGAM3+B1(J)*F1(J)
1220 NEXT J
1225 FOR J=1 TO M2

```



```

1230 LNGAM1=LNGAM1+B2(J)*D2(J)
1235 LNGAM2=LNGAM2+B2(J)*E2(J)
1240 LNGAM3=LNGAM3+B2(J)*F2(J)
1250 NEXT J
1260 FOR J=1 TO M3
1265 LNGAM1=LNGAM1+B3(J)*D3(J)
1270 LNGAM2=LNGAM2+B3(J)*E3(J)
1280 LNGAM3=LNGAM3+B3(J)*F3(J)
1330 NEXT J
1341 FOR J=1 TO M
1342 LNGAM1=LNGAM1+A(J,1)*D4(J)
1343 LNGAM2=LNGAM2+A(J,1)*E4(J)
1344 LNGAM3=LNGAM3+A(J,1)*F4(J)
1346 NEXT J
1348 GAM1(I)=EXP(LNGAM1)
1350 GAM2(I)=EXP(LNGAM2)
1360 GAM3(I)=EXP(LNGAM3)
1367 IF B12<>0 THEN 1380
1368 IF B13<>0 THEN 1380
1369 IF B23<>0 THEN 1380
1377 SC1=SC2=SC3=0
1378 GOTO 1400
1380 DA12=2*B12-B1-B2
1383 DA13=2*B13-B1-B3
1385 DA23=2*B23-B2-B3
1388 SC1=Y2**2*DA12+Y3**2*DA13+Y2*Y3*DA12-Y2*Y3*DA23+Y2*Y3*DA13
1390 SC2=Y1**2*DA12+Y3**2*DA23+Y1*Y3*DA12-Y1*Y3*DA13+Y1*Y3*DA23
1392 SC3=Y1**2*DA13+Y2**2*DA23+Y1*Y2*DA23-Y1*Y2*DA12+Y1*Y2*DA13
1400 FA1=EXP(((VL1-B1)*(P(I)-P10)-P(I)*SC1)/(RR*T))
1410 FA2=EXP(((VL2-B2)*(P(I)-P20)-P(I)*SC2)/(RR*T))
1420 FA3=EXP(((VL3-B3)*(P(I)-P30)-P(I)*SC3)/(RR*T))
1500 P1D=X1(I)*P10*FA1
1510 P2D=X2(I)*P20*FA2
1520 P3D=X3*I*P30*FA3
1521 PC(I)=P1D*GAM1(I)*FA1+P2D*GAM2(I)*FA2+P3D*GAM3(I)*FA3
1523 Y1=GAM1(I)*P1D/PC(I)
1525 Y2=GAM2(I)*P2D/PC(I)
1527 Y3=1-Y1-Y2
1529 DY1=Y11-Y1
1530 DY2=Y22-Y2

1531 PRINT "DY1=";DY1;"DY2=";DY2
1532 IF ABS(DY1)>.0001 THEN 1540
1533 IF ABS(DY2)>.0001 THEN 1540
1534 GOTO 1690
1540 Y11=Y1
1542 Y22=Y2
1545 GOTO 1367
1690 PC(I)=P1D*GAM1(I)+P2D*GAM2(I)+P3D*GAM3(I)
1710 Y1(I)=GAM1(I)*P1D/PC(I)
1720 Y2(I)=GAM2(I)*P2D/PC(I)
1723 GED(I)=RR*T*(X1(I)*LOG(GAM1(I))+X2(I)

```

```
      *LOG(GAM2(I))+X3*LOG(GAM3(I)))
1725 GE1=0
1726 GE2=0
1727 GE3=0
1736 FOR J=1 TO M1
1738 GE1=GE1+X12*X1(I)*X2(I)*B1(J)*(-X1D1)**(J-1)
1739 NEXT J
1740 FOR J=1 TO M2
1741 GE2=GE2+X13*X1(I)*X3*B2(J)*(-X1D2)**(J-1)
1742 NEXT J
1743 FOR J=1 TO M3
1745 GE3=GE3+X23*X2(I)*X3*B3(J)*(-X2D3)**(J-1)
1746 NEXT J
1750 GE4=X123*(A(1,1)+A(2,1)*(3*X1(I)-1)+A(3,1)*(3*X2(I)-1))
1765 GETO(I)=(GE1+GE2+GE3+GE4)*RR*T
1780 RETURN

2200 DATA 3,2,5,2,9,.00143229,-.00399029,-.103621,.0045545,-.00209169
2205 DATA -.00707403,.027154,-.0639962,.00434808

3000 END
```

A3-6 PVLR5 AND PVLR6

Programme PVLR5 and PVLR6 were written to fit the experimental data to the B-M equation and modified B-M equation, respectively. Only PVLR6 is listed in this appendix.

Data are input with data statements as the following sequence:

ME: See PVLR2

M: See PVLR3

NN1,NN2,NN3: Carbon number of component 1,2,3

N: See PVLR2

EE: See PVLR2

Data are input with file "6DIN1":

Matrix A, X1, X2: See PVLR4.

Data out with a file "GE6OUT": See "GE3OUT" of PVLR3,

1 REM PVLR6 (P-X FITTING, MODIFIED B-M EQUATION)

```

3 READ ME, M, NN1, NN2, NN3, N, EE
4 PRINT NN1, NN2, NN3, N, EE
19 OPEN "GE6OUT" FOR OUTPUT AS FILE #2
20 DIM Z1(M,N), Z2(M,N), Z3(M,M), Z4(M,M), Z5(M,N), DA(M,1), R(N,1), A(M,1)
23 DIM GAM1(N), GAM2(N), GAM3(N), PPA(N,M)
30 DIM X1(N), X2(N), D1(M1)
35 DIM Y1(N), Y2(N), PC(N), P(N), GED(N), GETO(N)
40 OPEN "6DIN1" FOR INPUT AS FILE #1
52 MAT INPUT #1, A; P; X1; X2
53 MAT PRINT #2, A; P; X1; X2
58 CLOSE #1
60 OPEN "3DIN1" FOR INPUT AS FILE #1
65 INPUT #1, P10, P20, P30, T, E, VL1, VL2, VL3, B1, B2, B3, B12, B13, B23
66 PRINT #2, P10, P20, P30, T, E, VL1, VL2, VL3, B1, B2, B3, B12, B13, B23
68 CLOSE #1
120 RR=8.3144
125 S=O
127 S=S+1
128 PRINT "S="; S
129 PRINT #2,
131 PRINT #2, "S="; S
132 PRINT #2, "A:"
134 MAT PRINT #2, A;
138 IF ME=3 THEN 185
139 IF ME=2 THEN 185
140 DIM WP(N,N), VC(M,M), Z5(N,M)
150 OPEN "DWP" FOR INPUT AS FILE #1
160 FOR I=1 TO N
170 INPUT #1, WP(I,I)
180 NEXT I
183 CLOSE #1
185 FOR I=1 TO N

190 GOSUB 1000

200 GOSUB 2000

205 NEXT I
210 IF ME=2 THEN 380
220 IF ME=3 THEN 380
300 MAT Z1=TRN(PPA)

```

```

310 MAT Z2=Z1*WP
320 MAT Z3=Z2*PPA
330 MAT VC=INV(Z3)
340 MAT Z2=VC*Z1
350 MAT Z1=Z2*WP
360 MAT DA=Z1*R
370 GOTO 430
380 MAT Z1=TRN(PPA)
390 MAT Z3= Z1*PPA
400 MAT Z4=INV(Z3)
410 MAT Z2= Z4*Z1
420 MAT DA=Z2*R
430 FOR I=1 TO M
440 IF ABS(DA(I,1))>EE THEN 485
450 NEXT I
460 GOTO 620
485 MAT A=A+DA
488 GOTO 127

620 PRINT " RESULTS:"
623 PRINT #2,"-----"
625 PRINT #2, "RESULTS:"
627 PRINT #2,
628 PRINT "A:."
630 MAT PRINT A;
640 PRINT #2,"A:"
650 MAT PRINT #2, A;
655 PRINT #2, " ..... "
657 PRINT #2,
658 RT=0
659 RTS=0
660 FOR I=1 TO N
662 RT=RT+ABS(R(I,1))
664 RTS=RTS+R(I,1)**2
670 PRINT #2,"X1=";X1(I);"X2=";X2(I);"GAM1=";GAM1(I);"GAM2=";GAM2(I);
680 PRINT #2, "GAM3=";GAM3(I);"Y1=";Y1(I);"Y2=";Y2(I);"PC=";PC(I);
690 PRINT #2, "GE=";GED(I);"GETO=";GETO(I);"R="; R(I,1)
695 PRINT #2,
697 NEXT I
698 AVR=RT/N
699 ZAR1=((RTS)/N)^.5
700 ZAR2=((RTS)/(N-M))^.5
701 PRINT #2,"AVR=";AVR;"ZAR1=";ZAR1;"ZAR2=";ZAR2
702 PRINT #2,
480 IF ME=2 THEN 820
770 GOSUB 3490
820 PRINT "END"
830 PRINT #2,
"END"
840 GOTO 4000

1000 REM

```

```

1040 X3=1-X1(I)-X2(I)
1044 PRINT "X1=";X1(I);"X2=";X2(I);"X3=";X3;"P=";P(I)
1050 NN=NN1*X1(I)+NN2*X2(I)+NN3*X3
1051 PRINT "NN=";NN
1055 D1=LOG(NN1/NN)+(1/NN)*(X2(I)*(NN2-NN1)+X3*(NN3-NN1))
1060 D2=LOG(NN2/NN)+(1/NN)*(X1(I)*(NN1-NN2)+X3*(NN3-NN2))
1070 D3=LOG(NN3/NN)+(1/NN)*(X1(I)*(NN1-NN3)+X2(I)*(NN2-NN3))
1075 E1=(1/NN**2)*(X2(I)*(NN2-NN1)+X3*(NN3-NN1))+1/NN-1/NN1
1080 E2=(1/NN**2)*(X1(I)*(NN1-NN2)+X3*(NN3-NN2))+1/NN-1/NN2
1085 E3=(1/NN**2)*(X2(I)*(NN2-NN3)+X1(I)*(NN1-NN3))+1/NN-1/NN3
1090 F1=(2/NN**3)*(X2(I)*(NN2-NN1)+X3*(NN3-NN1))+1/NN**2-1/NN1**2
1100 F2=(2/NN**3)*(X1(I)*(NN1-NN2)+X3*(NN3-NN2))+1/NN**2-1/NN2**2
1125 F3=(2/NN**3)*(X2(I)*(NN2-NN3)+X1(I)*(NN1-NN3))+
      1/NN**2-1/NN3**2
1200 LNGAM1=A(1,1)*D1+A(2,1)*E1+A(3,1)*F1
1210 LNGAM2=A(1,1)*D2+A(2,1)*E2+A(3,1)*F2
1215 LNGAM3=A(1,1)*D3+A(2,1)*E3+A(3,1)*F3
1216 PRINT "D1=";D1,"D2=";D2,"D3=";D3,"E1=";E1,"E2=";E2,"E3=";E3,"F1=";F1
1217 PRINT "F2=";F2,"F3=";F3,"LNGAM1=";LNGAM1,"LNGAM2=";
      LNGAM2,"LNGAM3=";LNGAM3
1345 GAM1(I)=EXP(LNGAM1)
1350 GAM2(I)=EXP(LNGAM2)
1360 GAM3(I)=EXP(LNGAM3)
1367 IF B12<>0 THEN 1380
1368 IF B13<>0 THEN 1380
1369 IF B23<>0 THEN 1380
1377 SC1=SC2=SC3=0
1378 GOTO 1400
1380 DA12=2*B12-B1-B2
1383 DA13=2*B13-B1-B3
1385 DA23=2*B23-B2-B3
1388 SC1=Y2**2*DA12+Y3**2*DA13+Y2*Y3*DA12-Y2*Y3*DA23+Y2*Y3*DA13
1390 SC2=Y1**2*DA12+Y3**2*DA23+Y1*Y3*DA12-Y1*Y3*DA13+Y1*Y3*DA23
1392 SC3=Y1**2*DA13+Y2**2*DA23+Y1*Y2*DA23-Y1*Y2*DA12+Y1*Y2*DA13
1400 FA1=EXP(((VL1-B1)*(P(I)-P10)-P(I)*SC1)/(RR*T))
1410 FA2=EXP(((VL2-B2)*(P(I)-P20)-P(I)*SC2)/(RR*T))
1420 FA3=EXP(((VL3-B3)*(P(I)-P30)-P(I)*SC3)/(RR*T))
1500 P1D=X1(I)*P10*FA1
1510 P2D=X2(I)*P20*FA2
1520 P3D=X3*I*P30*FA3
1690 PC(I)=P1D*GAM1(I)+P2D*GAM2(I)+P3D*GAM3(I)
1700 R(I,1)=P(I)-PC(I)
1702 PRINT "R=";R(I,1)
1705 PRINT #2, "R="; R(I,1),
1710 Y1(I)=GAM1(I)*P1D/PC(I)
1720 Y2(I)=GAM2(I)*P2D/PC(I)
1723 GED(I)=RR*T*(X1(I)*LOG(GAM1(I))+X2(I)*LOG(GAM2(I))
      +X3*LOG(GAM3(I)))
1738 GE1=-LOG(NN)+X1(I)*LOG(NN1)+X2(I)*LOG(NN2)+X3*LOG(NN3)
1740 GE2=1/NN-X1(I)/NN1-X2(I)/NN2-X3/NN3
1750 GE3=1/NN**2-X1(I)/NN1**2-X2(I)/NN2**2-X3/NN3**2
1765 GETO(I)=(A(1,1)*GE1+A(2,1)*GE2+A(3,1)*GE3)*RR*T

```

1780 RETURN

2000 REM

2003 PPA(I,1)=P1D*GAM1(I)*D1+P2D*GAM2(I)*D2+P3D*GAM3(I)*D3

2005 PPA(I,2)=P1D*GAM1(I)*E1+P2D*GAM2(I)*E2+P3D*GAM3(I)*E3

2010 PPA(I,3)=P1D*GAM1(I)*F1+P2D*GAM2(I)*F2+PD3*GAM3(I)*F3

2020 PRINT "PPA(I,1)";PPA(I,1),"PPA(I,2)";PPA(I,2)

2100 RETURN

3490 IF ME=3 THEN 3540

3510 MAT Z5=PPA*Z4

3520 MAT WP=Z5*Z1

3530 GOTO 3580

3540 DIM WP(N,N),VC(M,M), Z5(N,M)

3550 MAT VC=(ZAR2)*Z4

3560 MAT Z5=PPA*VC

3565 MAT Z1=TRN(PPA)

3570 MAT WP=Z5*Z1

3571 PRINT #2,

3572 PRINT #2,

3573 PRINT #2, " ~~~~~"

3575 PRINT #2, "RESULTS:"

3576 PRINT #2,

3577 PRINT #2, "ERROR MATRIX:"

3580 PRINT #2, "VC=:"

3590 MAT PRINT #2, VC;

3591 PRINT #2,

3592 PRINT #2,

3593 PRINT " DO YOU LIKE ALL THE INFORMATION ABOUT WP
(NO:1,YES:2)?"

3594 INPUT O

3595 IF O=1 THEN 3613

3600 PRINT #2, "WP:"

3610 MAT PRINT #2, WP;

3613 PRINT #2, "WP(I,I):"

3614 PRINT #2,

3616 FOR I=1 TO N3617 PRINT #2,WP(I,I),

3618 PRINT #2,

3619 NEXT I

3620 RETURN

3985 DATA 3,3,6,8,16,81,.0001

4000 END